

UC Riverside

UC Riverside Electronic Theses and Dissertations

Title

Impacts of Nanomaterials on Microbial Communities in Engineered Systems

Permalink

<https://escholarship.org/uc/item/6056t0vt>

Author

Taylor, Alicia

Publication Date

2015

Peer reviewed|Thesis/dissertation

UNIVERSITY OF CALIFORNIA
RIVERSIDE

Impacts of Nanomaterials on Microbial Communities in Engineered Systems

A Dissertation submitted in partial satisfaction
of the requirements for the degree of

Doctor of Philosophy

in

Environmental Toxicology

by

Alicia Ann Taylor

June 2015

Dissertation Committee:
Dr. Sharon Walker, Chairperson
Dr. Mark Matsumoto
Dr. Haizhou Liu

Copyright by
Alicia Ann Taylor
2015

The Dissertation of Alicia Ann Taylor is approved:

Committee Chairperson

University of California, Riverside

Acknowledgements

I would first like to thank my committee members: Professor Mark Matsumoto and Professor Haizhou Liu (Chemical and Environmental Engineering, UCR). I used many of Dr. Matsumoto's water quality and septic systems books that were instrumental in developing this dissertation and received valuable feedback from Dr. Matsumoto on many drafts of my septic tank manuscript. Dr. Liu provided access to a very important piece of equipment for this work (ICP-MS), and was always available to discuss metal chemistry with me. Many people were involved in the work presented in this dissertation and were integral in making this project possible.

Many thanks also go out to collaborators on various projects. Doctors Sijie Lin, Dr. Zhaoxia (Ivy) Li, Dr. Cong Hyun, part of the University of California Center for Environmental Implications of Technology (UC-CEIN) answered my endless questions on nanoparticle material science. Without them, Chapter 4 of this dissertation would not have been possible. Dr. Nichola Kinsinger spent countless hours trouble shooting and fine tuning the ICP-MS. Dr. M. Yusuf Khan and Dr. Jennifer Helbley were helpful when I wanted to try something new with aerosolized nanoparticles and hair dryers.

While abroad in Israel, I made new friends and colleagues, Dr. Zeev Ronen, Noa Balaban, Almog Gafni, Jan Diitrich, Tomas Weiss, and Alice Yang. I also saw old friends in Israel, Meirav Cohen, Boaz, Jenia Gutman, and Itai. All of these people made my research possible, and provided friendship in a new country. My experience would not be the same without them.

My most sincere appreciation also goes out to all of those that helped me in the laboratory during this dissertation work: my first friend in Riverside, Cristina Pablos Carro, Jose Valle, Aaron Coyoca, William Wellman, Timothy Chow, Christina Gerges, Brian Cruz, and Clarisse Rangel-Ottero. A very big and special thank you goes to Risa Guysi. Words cannot describe how grateful I am for having her in my life and all of her help in the lab. I would also like to thank current and former labmates for their help and/or support: Jessamine Quijano, Indranil Chowdhury, Travis Waller, Drew Story, and Chen Chen.

Ian Marcus, my best friend, deserves the biggest thanks. His positive attitude and belief in me made grad school possible. He has been with me through every step of the way and I cannot thank him enough. His parents have also taken really good care of me throughout the years and for this I am very grateful. I also want to thank my friends in Riverside that have provided fun and support away from the lab: Lindley Maryoung, Anita Küpper, Aileen Maldonado, Ryan Neff, Pavan Gollapudi, Neeti Riar, Garrett, Christy, Kaylee, and Ronen Milliron, Daryl Bulloch, Minyoung Yun, Michael Giodano, Dan Short, Alexander Dudchenko, Wenyan Duan, and Ninad Kothari.

Special thanks also go to my parents. Every time my mom visited me in California, she made me weeks and weeks of food. My dad helped me more here and has done a lot of repairs on the house I rent. Most importantly, he helped me build my garden.

Finally, I would like to thank my Ph.D. advisor Professor Sharon Walker. Dr. Walker has been a wonderful mentor. I wanted a female role model so that I could learn

to juggle a daunting career path, family, and personal life, and still find time for all of the other many mentoring roles by watching Dr. Walker flawlessly achieve. I have learned so much about how to be a fair and motivating mentor from Dr. Walker. She has always been enthusiastic about my ideas and projects. I am glad I have had this wonderful experience and opportunity to work with Dr. Walker.

Chapter 2 of this dissertation has been reprinted in full (adapted) with permission from [Taylor, A.A., I.M. Marcus, R.L. Guysi, and S.L. Walker (2015) Metal Oxide Nanoparticles Induce Minimal Phenotypic Changes in a Model Colon Gut Microbiota. Environmental Engineering Science] Copyright (2015) Mary Liebert, Inc. Chapter 3 is currently in review (2015) at Environmental Science: Water Research & Technology. Chapter 4 of this dissertation has been reprinted (adapted) in full with permission from [Lin, S., Taylor, A.A., Ji, Z., Chang, C.H., Kinsinger, N.M., Ueng, W., Walker, S.L. and Nel, A.E. (2015) Understanding the Transformation, Speciation, and Hazard Potential of Copper Particles in a Model Septic Tank System using Zebrafish to Monitor the Effluent. *ACS Nano*] Copyright (2015) American Chemical Society. Appendix A of this dissertation, in full, is a reprint of the material as it appears in “Deposition and disinfection of *Escherichia coli* O157: H7 on naturally occurring photoactive materials in a parallel plate” published in Environmental Science: Processes & Impacts, volume 16(2), pages 194-202, 2014. It is reproduced with permission by The Royal Society of Chemistry. Appendix B of this dissertation, in full, is a reprint of the material as it appears in “D-Amino acids inhibit initial bacterial adhesion: thermodynamic evidence” published in Biotechnology & Bioengineering, 2014, DOI:10.1002/bit.25479 (published online before

inclusion in an issue). It is reproduced with permission by John Wiley & Sons, Inc. (License Number 3544460801626).

This work was funded through a National Research Service Award Institutional Training Grant (T32 ES018827). Special thanks to Professors Yinsheng Wang and David Eastmond for providing me with this funding opportunity for two academic years. The UC-CEIN (University of California Center for Environmental Implications of Nanotechnology) also provided funding and support; the UC-CEIN material is based upon work supported by the NSF and the EPA under Cooperative Agreement Number DBI 0830117. Other funding sources include National Science Foundation Grant No. CBET-0954130. USDA CSREES NRI water and watershed grant (no. 2008-01768), CNAS Dean's Distinguished Fellowship, and UCR Graduate Student Association Travel grants.

Dedication

This dissertation is dedicated to my parents, Diane and Jeffrey Taylor for their love, support, understanding, and encouragement. I am very lucky to have these two wonderful people in my life.

ABSTRACT OF THE DISSERTATION

Impacts of Nanomaterials on Microbial Communities in Engineered Systems

by

Alicia Ann Taylor

Doctor of Philosophy, Graduate Program in Environmental Toxicology

University of California, Riverside, June 2015

Dr. Sharon Walker, Chairperson

The overall goal of this dissertation was to determine the effects of an emerging contaminant, nanomaterials, on microbial communities in engineered systems. Specifically, communities within a simulated human colon and model septic system were studied. Microbial communities in their natural environments represent realistic scenarios for toxicity testing versus assays with enriched growth media and single cell cultures; the two engineered systems used in this work approach “real” scenarios communities would experience.

This dissertation work has allowed for the following observations. The simulation of metal oxide nanomaterials ingestion with the model colon demonstrated these particles do significantly alter the phenotype of the gut microbial community within the model colon reactor. Next, dosing experiments with copper materials in the septic system

established that the effluent had pulses of improper waste treatment and that incomplete organic breakdown was likely occurring. However, even with weekly fluctuations in water quality caused by the particles, data suggest that 100% of the time, water quality parameters and microbial composition were recovering towards baseline conditions. This indicates the system could maintain baseline conditions after perturbances, regardless of the particle type.

Finally, effluent containing copper emitted from the septic system was tested in a high throughput toxicity screening assay with zebrafish embryos. While “as-received” nanoscale copper materials caused the greatest embryo hatching interference, all three “processed” copper materials emitted from the model septic system demonstrated a decline in embryo toxicity, regardless of particle composition/size. Thus, the zebrafish screening in combination with the septic system, provide a novel way to study hazard potentials of commercial Cu-based particulates during partitioning, transformation, and speciation.

This collection of studies provides critical insights into the importance of understanding microbial communities more holistically and in realistic environments. These studies demonstrate the need to update toxicity tests such that they more accurately reflect real exposure scenarios simulating environmental conditions. This research also confirms the invalidity of using “as received” nanoparticles; toxicity tests must use particles reflective of those materials transformed in the environment. Future directions for toxicological studies need new useful testing combinations that provide additional information for complex matrices and microbial communities.

Table of Contents

Chapter 1: Introduction	1
Motivation and Background	2
Aim and Scope	5
Hypotheses and Specific Objectives	7
Experimental Approach	10
Manuscripts Resulted from Research	13
References	16
Chapter 2: Metal Oxide Nanoparticles Induce Minimal Phenotypic Changes in a Model Colon Gut Microbiota	23
Abstract	24
Introduction	25
Experimental Protocol	28
Results	32
Discussion	39
Conclusions	48
References	50
Supplemental Information	63

Chapter 3: Effects of Copper Particles on a Model Septic System's Function and Microbial Community	76
Abstract	77
Introduction	79
Materials and Methods	82
Results	87
Discussion	101
Conclusion and Environmental Implications	111
References	113
Supplemental Information	124
Chapter 4: Understanding the Transformation, Speciation, and Hazard Potential of Copper Particles in a Model Septic Tank System Using Zebrafish to Monitor the Effluent	149
Abstract	150
Introduction	151
Materials and Methods	154
Results	159
Discussion	177
Conclusion	181
References	183
Supplemental Information	189

Chapter 5: Summary and General Conclusions	202
Appendix A: Deposition and Disinfection of <i>Escherichia coli</i> O157:H7 on Naturally Occurring Photoactive Materials in a Parallel Plate Chamber	209
Abstract	210
Introduction	212
Materials and Methods	215
Results and Discussion	220
References	237
Supporting Information	244
Appendix B: D-Amino Acids Inhibit Initial Bacterial Adhesion: Thermodynamic Evidence	258
Abstract	259
Introduction	260
Materials and Methods	263
Results	270
Discussion	282
Conclusions	288
References	289
Supplemental Information	294

List of Tables

Table 2.1. Cell size measurements as a function of nanoparticle exposure.	38
Table S3.1. Experimental sampling schedule.	132
Table S3.2. Raw experimental values.	135
Table 4.1. Physicochemical characterization of Cu particles.	162
Table A.1. Physicochemical characteristics of collector and bacteria.	223
Table A.2. O157:H7 Bacterial Transfer Rate Coefficients (k) for O157:H7 with Full or Partial EPS on Quartz, SRHA-, and α -Fe ₂ O ₃ -coated surfaces.	252
Table A.3. DLVO interaction energies between <i>E. coli</i> O157:H7 and collector surfaces.	253
Table B.1. Results from the AFM force-distance curve over the range of D-Tyrosine concentrations.	281
Table B.2. Total interaction energy profiles as a function of separation distance between <i>E. coli</i> JM109 cells and quartz sand.	296

List of Figures

Figure 2.1. Short chain fatty acid (SCFA) analysis.	37
Figure 2.2. Protein and sugar content of EPS.	38
Figure 2.3. pH and conductivity in model colon.	39
Figure S1. Visual schematics of model colon system.	64
Figure S2. Butyric acid concentration.	68
Figure S3. Acetic acid concentration.	69
Figure S4. Hydrophobicity.	70
Figure S5. Electrophoretic mobility.	71
Figure S6. Average protein content	72
Figure S7. Average sugar content.	73
Figure 3.1. Changes in water quality parameters	100
Figure 3.2. Changes in microbial community phyla and biological oxygen demand.	101
Figure S3.1. Digital image of model laboratory-scale septic tank.	134
Figure S3.2. Changes in bacteria characterization parameters.	139
Figure S3.3. Changes in the water quality parameter total suspended solids.	143
Figure 4.1. Cu dissolution and hatching interference of as-received Cu particles.	164

Figure 4.2A. Combined use of a model septic tank and zebrafish. embryo high content screening to study the effects of Cu-containing effluents on embryo hatching.	167
Figure 4.2B. Combined use of a model septic tank and zebrafish. embryo high content screening to study the effects of Cu-containing effluents on embryo hatching.	168
Figure 4.3A. Characterization of septic tank effluents.	170
Figure 4.3B. Characterization of septic tank effluents.	171
Figure 4.3C. Characterization of septic tank effluents.	172
Figure 4.3D. Characterization of septic tank effluents.	173
Figure 4.4. Use of the methodology for diffusive gradients In thin-films (DGT) to quantify diffusible Cu ²⁺ in the effluents.	175
Figure 4.5A/B. The addition of humic acid (HA) decreased Cu toxicity.	176
Figure 4.5C/D. The addition of humic acid (HA) decreased Cu toxicity.	177
Figure S4.1A. Physicochemical analysis of Cu particles.	193
Figure S4.1B. Physicochemical analysis of Cu particles.	194
Figure S4.2A. Percent hatching of zebrafish embryos.	195
Figure S4.2B. Percent survival of zebrafish embryos.	196
Figure S4.3. XRD spectra.	197
Figure S4.4A. Water quality characteristics in the septic tank system	198
Figure S4.4B. Alkalinity.	199
Figure S4.4C. Hardness.	200

Figure A.1. Potentiometric titration of <i>E. coli</i> O1567:H7 with full and partial EPS.	224
Figure A.2. O157:H7 bacterial mass transfer coefficient (k).	225
Figure A.3. Survival of <i>E. coli</i> O157:H7 with coated and uncoated α -Fe ₂ O ₃ quartz slides as a function for attached and planktonic bacteria.	232
Figure A.4. Absorbance values of substrates from UV-visible Spectroscopy with and without α -Fe ₂ O ₃ coating on glass surface.	254
Figure A.5. Fourier transform infrared spectroscopy (FT-IR) of supernatant from partial and full EPS in <i>E. coli</i> O157: H7.	255
Figure B.1. Adhesion efficiency and desorption rate of <i>E. coli</i> onto a quartz collector surface, determined as a function of D-Tyrosine.	272
Figure B.2. The content of total EPS, polysaccharides, and proteins of the <i>E. coli</i> cells from LB media with different D-Tyrosine concentrations.	274
Figure B.3. The relative hydrophobicity and zeta potential values of <i>E. coli</i> cells as a function of D-Tyrosine concentration.	277
Figure B.4. Total interaction energy profiles as a function of separation distance for <i>E. coli</i> cells grown under a range of D-Tyrosine concentrations.	278
Figure B.5. Contribution of W^{AB} (a), W^{LW} (b) and W^{EL} (c) on the total interaction energy between <i>E. coli</i> cells and quartz sand exposed to different D-Tyrosine concentrations.	279
Figure B.6. Growth curves of <i>E. coli</i> cells from LB media with different D-Tyrosine concentrations.	297
Figure B.7. Adhesion and desorption efficiencies of <i>E. coli</i> onto and	298

off of a quartz collector surface, determined as a function of D-Tyrosine (a), and L-Tyrosine (b).

Figure B.8. The relative hydrophobicity and contact angles of *E. coli* cells as a function of D-Tyrosine concentration. 299

Figure B.9. AFM topographical (left) and deflective (right) images are shown for (a) *E. coli* JM109 cells and (b) SEM images of *E. coli* JM109 cells. 300

Chapter 1

Introduction

Chapter 1: Introduction

Motivation and Background

Toxicology did not arise as a formal discipline until the 1950s, as the effects of synthetically made chemicals on humans became a social concern.¹ Toxicity testing has been used to answer many types of issues, such as: chemical lethality to organisms at various concentrations, sub-lethal toxicity effects, organism sensitivities, and transformation of compounds in the environment.²⁻³ In fact, a considerable amount of legislation has been passed, and agencies formed to better regulate toxicity screening and risk assessment of chemicals.⁴ As a result, toxicity testing results have been used to predict environmental effects, compare various toxicants, and have served as guidance regulation purposes.¹

Many currently used methodologies for toxicity screenings were developed in the 1960s and 1970s and rely on high-dose studies in various animal subjects.⁵ For example, many acute and chronic toxicity tests using animal models have been used to study the absorption, distribution, metabolism, and excretion of chemicals.⁶ Animal models present numerous problems. Besides the need for large numbers of animals, these types of toxicity tests are incredibly expensive and time-consuming.⁵ Furthermore, extrapolating animal results to human risk is also difficult.⁵ Recent advances in numerous fields such as cell biology, tissue culture, genomics, bioinformatics, biomarkers, and molecular methods are changing the way that contaminants are examined.⁷ Specifically, a decrease in cost and time will occur as well as an increase in the amount of compounds that can be

tested.⁵ These new approaches will focus less on animal models and more on *in vitro*, *in silico* kinetic models, and high through-put assays using cell lines, which will preferably be human in origin.⁸ It is important to note that there are various cell-based toxicity tests in use. These include techniques that have been used for decades such as the Ames test, which is one of the most widely used bacterial acute testing method,⁹ the comet assay, which detects damaged DNA,¹⁰ and the HeLa cell line, the first continuous cancer cell line.¹¹

While both human and bacterial cell studies are often cheaper and faster than animal models, the downside is that single cell lines are also not a truly representative toxicity test, and are an “idealized” laboratory form of testing. This type of toxicity testing does not take into consideration many important factors such as role of metabolism, epigenetics, abnormal biological conditions, or other mechanisms.⁵ Therefore, relying solely on cell-based methods may not accurately portray the effects of chemicals. For example, the importance of an organism’s actual environment is crucial. Recently, the norovirus was cultured in a laboratory setting for the first time with the presence of bacteria from the gut.¹² The virus had never been grown before using traditional cell mono-culturing methods. Yet, with the presence of stimulatory carbohydrate molecules from enteric bacteria, the virus was grown using cell culture techniques. The norovirus behaves differently in the presence and absence of microbiota that represent the host’s intestines. This demonstrates that there are complex interactions occurring between either between an organism and a chemical, or an organism and its microbial communities. Toxicity testing must take into account various cellular

interactions, such as immune cell responses and the microbiota. Therefore, a more realistic form of toxicity testing should incorporate microbial communities. Characterization of these communities and their responses to pollutants can provide insight into important biomarkers that can be used to monitor environmental or human health.¹³

Because microbial communities constitute a large portion of the food web in aquatic environments and within the human body,¹⁴⁻¹⁷ risk assessment of contaminants should also include assessment of microbial communities. Studies usually rely on extrapolation of single species data or acute toxicity tests, which are likely to give erroneous results.¹⁸ Additionally, the toxic effects observed can also be skewed by the metabolic activity of a few resistant microbes.¹⁹ With the importance that the microbiome plays in human health,²⁰⁻²⁴ new toxicity testing will be crucial for understanding the dynamics between the microbiome, humans, disease, and chemicals. To date, numerous studies have included microbial communities in alternative toxicity screenings.²⁵⁻²⁸ Environmental and human-based applied microbial toxicity tests include biomass measurements, phenotypic changes, carbon and nitrogen transformations, changes in microbial diversity, and enzymatic tests.¹⁹ Due to the importance of microbial communities and their potential as a toxicity screening method, this work has focused on analyzing microbial communities in human and environmental systems (distal colon bioreactor and model septic system). Representative microbial communities were used within these systems to provide a realistic simulation of these environments for a more accurate portrayal of toxicity effects.

Microbial communities can also be used to investigate numerous compounds in a new sub-discipline of toxicology, nanotoxicology. Nanomaterials fall within the category of “contaminants of emerging concern” (CECs) which can also include pharmaceuticals and personal care products (PPCPs), pesticides, surfactants, and flame retardants.²⁹ Due to the increased use of nanoparticles in many common consumer goods and industrial applications,³⁰⁻³³ exposure to these materials will increase.³⁴ To date, safety evaluations and potential hazards are unknown for many nanomaterials, as well as the route of exposure.³⁴ Rapid analyses of these new materials with tools such as high-throughput screening³⁵ may be evaluated using microbial communities or with human cell line co-cultured with microbial communities rather than with traditional animal models.

Aim and Scope

The overall objective of this research was to determine the impact of various nanomaterials on two engineered systems (model colon bioreactor and septic system) and their microbial communities using alternative toxicity testing methods. Specifically, this work characterized the changes within the systems during baseline conditions and nanomaterial perturbances, and characterized changes to the microbial communities within these systems. Finally, the toxicity and fate of the nanomaterials emitted from the septic system effluent was assessed. This work used various metal-based nanomaterials at concentrations relevant to human and environmental exposures.^{31-32, 36-39} Nanomaterials were selected based on their broad use in many common consumer products^{30-33, 40-43} and due to their potential for human ingestion and release into the environment.^{31-32, 37-38, 44-46}

Studies have shown that nanomaterials may have negative health impacts for both humans and food webs, and nanomaterials are currently found in human food and water sources.^{31-32, 37-38, 44-46} The work presented here was conducted in collaboration with the University of California Center for Environmental Implications of Nanotechnology (UC-CEIN), which is a multi-disciplinary research community that addresses the responsible use and safe implementation of nanomaterials. This objective is met by studying nanomaterials in many capacities: evaluation of the material composition, toxicity using high throughput screening assays, fate transport and exposure, life cycle assessments, simulated ecosystem exposures, and molecular analyses. The nanomaterials used in this work were selected from the UC-CEIN's particle library, all which have undergone extensive characterization by Center partners. Additionally, the UC-CEIN has provided access to characterization tools and instrumentation otherwise not available that were used in this research. This dissertation addresses these topics in three core chapters: effects of metal oxide nanomaterials on a model colon microbial community (Chapter 2), copper-based particle effects on a septic system's function and microbial community (Chapter 3), and the toxicity, fate, and speciation of copper-based particles emitted in septic tank effluent (Chapter 4). The aims of this investigation were developed based upon the hypotheses and objectives presented in the subsequent section.

Hypotheses and Specific Objectives

To achieve the overall goal of this doctoral research, the following hypotheses and specific objectives were developed and are presented below (it should be noted that each specific objective has been addresses in a chapter within this dissertation).

Hypothesis 1: Exposure to metal oxide nanomaterials will cause measurable changes in the microbial community's phenotype within the model colon.

To test this hypothesis, a reproducible microbial community was developed from a healthy 26-year-old female for use within the model colon bioreactor. Bacterial phenotypic characteristics and biochemical properties of the model colon were monitored to determine changes induced by various metal oxide nanomaterials. Three nanomaterials at environmentally relevant concentrations simulating ingestion ($0.01 \mu\text{gL}^{-1}$ ZnO, $0.01 \mu\text{gL}^{-1}$ CeO₂, and 3mgL^{-1} TiO₂) were introduced into a model colon. These were selected based upon their broad use in consumer products and foods.^{31-32, 36-37, 39} Specifically, the following tests were used as an alternative toxicity screening: cell concentration, sugar and protein content of the extracellular polymeric substance (EPS), electrophoretic mobility (EPM, a surrogate for surface charge), cell hydrophobicity, cell size, short chain fatty acid (SCFA) production, pH, and conductivity. The purpose of this work was two-fold: (1) to identify if the nanomaterials were eliciting measurable changes in the microbial community and (2) if the changes could be identified by a combination of

phenotypic and biochemical assays (Chapter 2). This is important to human health because the gut microbiota plays a crucial role in overall human health.²⁰⁻²⁴

Hypothesis 2: Septic system function and operation, specifically turbidity, cell concentration, total suspended solids, and biological oxygen demand, will deviate from baseline conditions in the presence of various copper-based particles.

The overall goal of this investigation was to ascertain the influence of copper-based particles on the function and operation of a model septic system. A series of experiments were conducted as a two-fold approach: (1) phenotypic and genotypic characterization of the microbial community with the system during baseline and copper-exposure conditions, and (2) water quality measurements to evaluate the function of the septic system in treating the wastewater. The purpose of this work was to give insight as to whether copper-based particles may contribute to improper function in septic systems, and causing the release of untreated wastewater into the environment (Chapter 3). Copper nanoparticles are found in many common consumer goods⁴¹⁻⁴³; therefore, the disposal and subsequent environmental release and interactions between Cu-based nanoparticles and microbial communities may have detrimental impacts on wastewater treatment processes.^{31-32, 38, 44-45, 47-56} This study investigates the effects of three copper particles (micron- and nano-scale Cu particles, and nano-scale Cu(OH)₂-based fungicide) on the function and operation of a model septic tank. A concentration of 10 ppm was chosen based upon predicted concentrations of copper found in WWTPs (wastewater treatment

plants).^{31-32, 38} As only 40% of all septic tanks estimated to be properly functioning⁵⁷ it can be inferred that overall, septic tanks are indeed technically regulated, but the management and regular monitoring of septic tanks are not practically enforced, especially as compared to WWTPs.⁵⁷⁻⁶¹ To determine if the septic system performance deviated due to the presence of copper-based materials, the baseline conditions were first characterized and compared to known literature studies⁶²⁻⁶⁸ of septic systems. Specific experiments were designed to test the response of the septic system to the copper exposure.

Hypothesis 3: Effluent containing “aged” copper-based particles emitted from the secondary chamber of the septic system will be less toxic to zebrafish than “as-received” copper-based nanomaterials due to speciation and complexation with organic matter.

To test this hypothesis, six Cu-based particles, namely nano-sized Cu and CuO, micron-sized Cu and CuO, and nano Cu(OH)₂-based CuPRO and Kocide, a zebrafish high-throughput platform was used to compare the effects of the as-purchased materials as well as the “aged” materials through a model septic system. Zebrafish were selected due to their conventional cell culturing methods, cost and time efficiency, known genomics, and known embryotoxicity pathways.⁶⁹⁻⁷⁰ Copper-based nanomaterials may undergo speciation and transformation with engineered systems,^{50-52, 71} and these transformations within the anaerobic environment of the septic system lead to a decrease in toxicity through altered speciation. Thus, the use of zebrafish screening, in

combination with materials obtained from a real-life exposure scenario, provides a novel way to study the change in the hazard potential of commercial Cu-based particulates during partitioning, transformation, and speciation and is a new approach to combining traditional toxicity testing, such as high through-put screening with other interdisciplinary methods such as the use of a model septic system and microbial community characterization. The primary, and substantial, contribution to this collaborative study was the design and management of the experimental set-up (model septic system) with and without the nanoparticle perturbances, effluent characterization, and the measurement of and mass balance to determine the fate of copper within the system using ICP-MS (inductively coupled plasma mass spectrometry).

Experimental Approach

This dissertation is composed of five chapters including the Introduction (Chapter 1) and conclusion (Chapter 5). Following the Introduction, Chapter 2 describes the effects of three metal oxide nanomaterials at relevant concentrations ($0.01 \mu\text{gL}^{-1}$ ZnO, $0.01 \mu\text{gL}^{-1}$ CeO₂, and 3mgL^{-1} TiO₂) on the gut microbial community in a model colon bioreactor. Results indicated nanomaterials caused the microbial community's phenotype to partition into three distinct phases: initial conditions, a transition period, and a homeostatic phase, with the NP-exposed community displaying significant differences ($P < 0.05$) from the unexposed community in multiple phenotypic traits. Notably, phenotypes including short chain fatty acid (SCFA) production, hydrophobicity, sugar content of the extracellular polymeric substance, and electrophoretic mobility, which indicates changes in the

community's stability, were affected by the nanomaterials. The TiO₂ nanomaterial led to extended phenotypic transformations for hydrophobicity when compared to the other nanomaterials, likely due to its lack of dissociation and greater stability. This work aimed to quantify the phenotypic response to nanoparticle ingestion of a model microbial community within a model colon. This study is thoroughly described in Chapter 2 which is titled "Metal oxide nanoparticles induce phenotypic changes in a model colon gut microbiota".

Chapter 3, entitled "Effects of Copper Particles on a Model Septic System's Function and Microbial Community", investigated the effects of three copper particles (micron- and nano-scale Cu particles, and nano-scale Cu(OH)₂-based fungicide) on the function and operation of a model septic tank. Copper nanoparticles are found in many common consumer goods; therefore, the disposal and subsequent interactions between Cu-based nanoparticles and microbial communities may have detrimental impacts on wastewater treatment processes. Septic system analyses included water quality evaluation and microbial community characterization to detect changes in and relationships between the septic tank function and microbial community phenotype/genotype. During exposure to nano-scale Cu, biological oxygen demand (BOD) was reduced by at least 63%. Micron-scale Cu caused a reduction in the pH outside the optimum anaerobic fermentation range, indicating that the organic waste may have undergone incomplete degradation. The copper fungicide, Cu(OH)₂, caused an increase in total organic carbon, which corresponded to increased BOD during the majority of the Cu(OH)₂ exposure. Overall, results implied exposure to Cu particles caused disruption in septic tank

function. However, it was observed that the system was able to recover to typical operating conditions after three weeks post-exposure. These results suggested that during periods of Cu introduction, there is likely improper waste treatment and incomplete organic breakdown.

Chapter 4, entitled “Understanding the Partitioning, Transformation, Speciation, and Hazard Potential of Copper-based Particles through Integrating a Model Septic Tank and Zebrafish Embryo High-Throughput Screening”, explains the environmental hazard of commercial copper-based particles used for fungicidal or bactericidal applications. In order to study the hazard potential of six Cu-based particles, namely nano-sized Cu and CuO, micron-sized Cu and CuO, and nano Cu(OH)₂-based CuPRO and Kocide, a zebrafish high throughput platform was used to compare the effects of the as-purchased materials as well as the “processed” materials through a model septic system. While the nanoscale materials were clearly more potent than the micron-scale particulates in interfering embryo hatching, the “processed” nano Cu, CuPRO and micro Cu particles injected in the model septic system demonstrated a steep decline in embryo toxicity, regardless of particle composition and size. The decreased toxicity was accompanied by Cu transformation into inorganic [e.g., Cu(H₂PO₂)₂] and organic Cu species that did not interfere with embryo hatching. Moreover, we demonstrated that the addition of natural organic matters could lead to a dose-dependent decrease in Cu toxicity in the embryos. Thus, the use of zebrafish screening, in combination with materials obtained from a real-life exposure scenario, provided a novel way to study the change in the hazard potential of commercial Cu-based particulates during partitioning, transformation, and speciation.

This study was also novel in that it showed that “aged” nanomaterials have different toxicological effects on organisms than nanomaterials in their original, “as-received” state. This finding suggests that nanomaterials should be assessed using systems that will simulate environmental changes that the nanomaterials may undergo before contact and exposure to organisms.

Chapter 5, entitled “Summary and Conclusions” summarizes the findings from this PhD dissertation. Two of the three chapters of this work are currently undergoing the peer-review process with the anticipation of publication. Chapter three has been accepted in a peer-reviewed journal. All chapters are listed below.

Manuscripts Resulted from Research

The dissertation research and parallel projects conducted from 2011 to 2015 have resulted in the preparation of eight manuscripts. The first three manuscripts listed are the three chapters within this dissertation and include the supplemental information within the corresponding chapter. Each of the dissertation chapters are either currently in the peer-review process or have been accepted for publication. Additional projects were also completed during the same time frame and are also listed below. Manuscripts four and five are appendix A and B, respectively, and are already published.

Manuscript four and its supplemental information, titled “Deposition and disinfection of *Escherichia coli* O157:H7 on naturally occurring photoactive materials in a parallel plate chamber”, is available in Appendix A, and is worth noting for its relevance to studying iron oxide, which is present in many water systems and is known to

have toxic impacts to bacteria caused by reactive oxygen species.⁷² This paper was also highlighted by the journal as the cover article in January 2014. Manuscript five and its supplemental information, titled “D-Amino acids inhibit initial bacterial adhesion: thermodynamic evidence” complements the work completed in Appendix A and provides further insight into bacterial adhesion which is relevant for disinfection processes. Manuscript five is available in Appendix B.

1. Taylor, A.A., I.M. Marcus, Risa L. Guysi, and S.L. Walker. “Metal oxide nanoparticles induce phenotypic changes in a model colon gut microbiome” (in review, *Environmental Engineering Science*)
2. Taylor, A.A., and S.L. Walker. “Effects of various copper particles on a model septic system function and microbial community” (in review, *Environmental Science: Water Research & Technology*)
3. Lin, S., A.A. Taylor, Z. Ji, T. Waller, C.H. Chang, N.M. Kinsinger, W. Ueng, S.L. Walker, and A.E. Nel. “Understanding the transformation, speciation, and hazard potential of copper particles in a model septic tank system using zebrafish to monitor the effluent” (published online 01-27-2015) **DOI:** 10.1021/nn507216f
4. Taylor, A.A., I. Chowdhury, I. A. Gong, D.M. Cwiertny, and S.L. Walker. “Deposition and disinfection of *Escherichia coli* O157:H7 on naturally occurring photoactive materials in a parallel plate chamber” *Environ. Sci.: Processes Impacts* 2014:16:2 (194-202) (DOI: 10.1039/C3EM00527E).

5. Xing, S.F., X.F. Sun, A.A. Taylor, S.L. Walker, Y.F. Wang, and S.G. Wang. "D-Amino acids inhibit initial bacterial adhesion: thermodynamic evidence" *Biotechnology and Bioengineering* 2014: DOI: 10.1002/bit.25479

References

1. Buikema Jr, A. L.; Niederlehner, B. R.; Cairns Jr, J., Biological monitoring part IV—Toxicity testing. *Water Research* **1982**, *16* (3), 239-262.
2. Cairns Jr, J.; Dickson, K.; Maki, A., Introduction to a discussion of the use of aquatic toxicity tests for evaluation of the effects of toxic substances. *Estimating the hazard of chemical substances to aquatic life* **1978**, 15.
3. Sprague, J., The ABC's of pollutant bioassay using fish. *ASTM Spec. Tech. Publ.* **1973**, (528), 6-30.
4. Krewski, D.; Acosta, D.; Andersen, M.; Anderson, H.; Bailar, J. C.; Boekelheide, K.; Brent, R.; Charnley, G.; Cheung, V. G.; Green, S.; Kelsey, K. T.; Kerkvliet, N. I.; Li, A. A.; McCray, L.; Meyer, O.; Patterson, R. D.; Pennie, W.; Scala, R. A.; Solomon, G. M.; Stephens, M.; Yager, J.; Zeise, L.; Staff of Committee on Toxicity, T.; Assessment of Environmental, A., Toxicity Testing in the 21st Century: A Vision and a Strategy. *Journal of Toxicology and Environmental Health, Part B* **2010**, *13* (2-4), 51-138.
5. Holsapple, M. P.; Afshari, C. A.; Lehman-McKeeman, L. D., Forum Series: The “Vision” for Toxicity Testing in the 21st Century: Promises and Conundrums. *Toxicological Sciences* **2009**, *107* (2), 307-308.
6. Gad, S. C., *Animal models in toxicology*. CRC Press: 2006.
7. Andersen, M. E.; Krewski, D., Toxicity Testing in the 21st Century: Bringing the Vision to Life. *Toxicological Sciences* **2009**, *107* (2), 324-330.
8. Concil, N. N. R., Toxicity testing in the 21st century: a vision and a strategy. National Academy Press: Washington, D.C., 2007.
9. Kier, L. E.; Brusick, D. J.; Auletta, A. E.; Von Halle, E. S.; Brown, M. M.; Simmon, V. F.; Dunkel, V.; McCann, J.; Mortelmans, K.; Prival, M.; Rao, T. K.; Ray, V., The Salmonella typhimurium/mammalian microsomal assay: A report of the U.S. Environmental Protection Agency Gene-Tox Program. *Mutation Research/Reviews in Genetic Toxicology* **1986**, *168* (2), 69-240.
10. Fairbairn, D. W.; Olive, P. L.; O'Neill, K. L., The comet assay: a comprehensive review. *Mutation Research/Reviews in Genetic Toxicology* **1995**, *339* (1), 37-59.
11. Masters, J. R., HeLa cells 50 years on: the good, the bad and the ugly. *Nat Rev Cancer* **2002**, *2* (4), 315-319.

12. Jones, M. K.; Watanabe, M.; Zhu, S.; Graves, C. L.; Keyes, L. R.; Grau, K. R.; Gonzalez-Hernandez, M. B.; Iovine, N. M.; Wobus, C. E.; Vinjé, J.; Tibbetts, S. A.; Wallet, S. M.; Karst, S. M., Enteric bacteria promote human and mouse norovirus infection of B cells. *Science* **2014**, *346* (6210), 755-759.
13. Ford, T., Response of marine microbial communities to anthropogenic stress. *Journal of Aquatic Ecosystem Stress and Recovery* **2000**, *7* (1), 75-89.
14. Gerritsen, J.; Smidt, H.; Rijkers, G.; de Vos, W., Intestinal microbiota in human health and disease: the impact of probiotics. *Genes Nutr* **2011**, *6* (3), 209-240.
15. Li, M.; Wang, B.; Zhang, M.; Rantalainen, M.; Wang, S.; Zhou, H.; Zhang, Y.; Shen, J.; Pang, X.; Zhang, M.; Wei, H.; Chen, Y.; Lu, H.; Zuo, J.; Su, M.; Qiu, Y.; Jia, W.; Xiao, C.; Smith, L. M.; Yang, S.; Holmes, E.; Tang, H.; Zhao, G.; Nicholson, J. K.; Li, L.; Zhao, L., Symbiotic gut microbes modulate human metabolic phenotypes. *Proceedings of the National Academy of Sciences* **2008**, *105* (6), 2117-2122.
16. Neish, A. S., Microbes in Gastrointestinal Health and Disease. *Gastroenterology* **2009**, *136* (1), 65-80.
17. Sarmiento, H.; Montoya, J. M.; Vázquez-Domínguez, E.; Vaqué, D.; Gasol, J. M., Warming effects on marine microbial food web processes: how far can we go when it comes to predictions? *Philosophical Transactions of the Royal Society B: Biological Sciences* **2010**, *365* (1549), 2137-2149.
18. Brandt, K. K.; Jørgensen, N. O. G.; Nielsen, T. H.; Winding, A., Microbial community-level toxicity testing of linear alkylbenzene sulfonates in aquatic microcosms. *FEMS Microbiology Ecology* **2004**, *49* (2), 229-241.
19. van Beelen, P.; Doelman, P., Significance and application of microbial toxicity tests in assessing ecotoxicological risks of contaminants in soil and sediment. *Chemosphere* **1997**, *34* (3), 455-499.
20. A framework for human microbiome research. *Nature* **2012**, *486* (7402), 215-221.
21. Structure, function and diversity of the healthy human microbiome. *Nature* **2012**, *486* (7402), 207-214.
22. Cho, I.; Blaser, M. J., The human microbiome: at the interface of health and disease. *Nat Rev Genet* **2012**, *13* (4), 260-270.

23. Clemente, Jose C.; Ursell, Luke K.; Parfrey, Laura W.; Knight, R., The Impact of the Gut Microbiota on Human Health: An Integrative View. *Cell* **2012**, *148* (6), 1258-1270.
24. Consortium, T. H. M. J. R. S., A Catalog of Reference Genomes from the Human Microbiome. *Science* **2010**, *328* (5981), 994-999.
25. Lozupone, C. A.; Stombaugh, J. I.; Gordon, J. I.; Jansson, J. K.; Knight, R., Diversity, stability and resilience of the human gut microbiota. *Nature* **2012**, *489* (7415), 220-230.
26. Monachese, M.; Burton, J. P.; Reid, G., Bioremediation and Tolerance of Humans to Heavy Metals through Microbial Processes: a Potential Role for Probiotics? *Applied and Environmental Microbiology* **2012**, *78* (18), 6397-6404.
27. Reid, G.; Younes, J. A.; Van der Mei, H. C.; Gloor, G. B.; Knight, R.; Busscher, H. J., Microbiota restoration: natural and supplemented recovery of human microbial communities. *Nat Rev Micro* **2011**, *9* (1), 27-38.
28. Sun, G.-X.; Van de Wiele, T.; Alava, P.; Tack, F.; Du Laing, G., Arsenic in cooked rice: Effect of chemical, enzymatic and microbial processes on bioaccessibility and speciation in the human gastrointestinal tract. *Environmental Pollution* **2012**, *162* (0), 241-246.
29. Yan, S.; Subramanian, S.; Tyagi, R.; Surampalli, R.; Zhang, T., Emerging Contaminants of Environmental Concern: Source, Transport, Fate, and Treatment. *Practice Periodical of Hazardous, Toxic, and Radioactive Waste Management* **2010**, *14* (1), 2-20.
30. Kaida, T.; Kobayashi, K.; Adachi, M.; Suzuki, F., Optical characteristics of titanium oxide interference film and the film laminated with oxides and their applications for cosmetics. *Journal of cosmetic science* **2003**, *55* (2), 219-220.
31. Keller, A.; McFerran, S.; Lazareva, A.; Suh, S., Global life cycle releases of engineered nanomaterials. *J Nanopart Res* **2013**, *15* (6), 1-17.
32. Keller, A. A.; Lazareva, A., Predicted Releases of Engineered Nanomaterials: From Global to Regional to Local. *Environmental Science & Technology Letters* **2013**, *1* (1), 65-70.
33. Wolf, R.; Matz, H.; Orion, E.; Lipozencić, J., Sunscreens--the ultimate cosmetic. *Acta Dermatovenerol Croat* **2003**, *11* (3), 158-162.

34. Oberdörster, G.; Oberdörster, E.; Oberdörster, J., Nanotoxicology: An Emerging Discipline Evolving from Studies of Ultrafine Particles. *Environmental Health Perspectives* **2005**, *113* (7), 823-839.
35. Lin, S.; Zhao, Y.; Ji, Z.; Ear, J.; Chang, C. H.; Zhang, H.; Low-Kam, C.; Yamada, K.; Meng, H.; Wang, X.; Liu, R.; Pokhrel, S.; Mädler, L.; Damoiseaux, R.; Xia, T.; Godwin, H. A.; Lin, S.; Nel, A. E., Zebrafish High-Throughput Screening to Study the Impact of Dissolvable Metal Oxide Nanoparticles on the Hatching Enzyme, ZHE1. *Small* **2013**, *9* (9-10), 1776-1785.
36. Gottschalk, F.; Sonderer, T.; Scholz, R. W.; Nowack, B., Modeled Environmental Concentrations of Engineered Nanomaterials (TiO₂, ZnO, Ag, CNT, Fullerenes) for Different Regions. *Environmental Science & Technology* **2009**, *43* (24), 9216-9222.
37. Kiser, M. A.; Westerhoff, P.; Benn, T.; Wang, Y.; Pérez-Rivera, J.; Hristovski, K., Titanium Nanomaterial Removal and Release from Wastewater Treatment Plants. *Environmental Science & Technology* **2009**, *43* (17), 6757-6763.
38. Lazareva, A.; Keller, A. A., Estimating Potential Life Cycle Releases of Engineered Nanomaterials from Wastewater Treatment Plants. *ACS Sustainable Chemistry & Engineering* **2014**, *2* (7), 1656-1665.
39. Weir, A.; Westerhoff, P.; Fabricius, L.; Hristovski, K.; von Goetz, N., Titanium Dioxide Nanoparticles in Food and Personal Care Products. *Environmental Science & Technology* **2012**, *46* (4), 2242-2250.
40. Grosell, M.; Blanchard, J.; Brix, K.; Gerdes, R., Physiology is pivotal for interactions between salinity and acute copper toxicity to fish and invertebrates. *Aquatic toxicology* **2007**, *84* (2), 162-172.
41. Maynard, A.; Michelson, E., The nanotechnology consumer products inventory. *Woodrow Wilson International Center for Scholars, Washington, DC, accessed March* **2006**, 23.
42. Nasibulin, A.; Ahonen, P. P.; Richard, O.; Kauppinen, E.; Altman, I., Copper and Copper Oxide Nanoparticle Formation by Chemical Vapor Nucleation From Copper (II) Acetylacetonate. *J Nanopart Res* **2001**, *3* (5-6), 383-398.
43. Yang, J.-g.; Okamoto, T.; Ichino, R.; Bessho, T.; Satake, S.; Okido, M., A Simple Way for Preparing Antioxidation Nano-copper Powders. *Chemistry Letters* **2006**, *35* (6), 648-649.

44. Keller, A.; Vosti, W.; Wang, H.; Lazareva, A., Release of engineered nanomaterials from personal care products throughout their life cycle. *J Nanopart Res* **2014**, *16* (7), 1-10.
45. Kessler, R., Engineered Nanoparticles in Consumer Products: Understanding a New Ingredient. *Environmental Health Perspectives* **2011**, *119* (3), A120-A125.
46. Westerhoff, P.; Song, G.; Hristovski, K.; Kiser, M. A., Occurrence and removal of titanium at full scale wastewater treatment plants: implications for TiO₂ nanomaterials. *Journal of Environmental Monitoring* **2011**, *13* (5), 1195-1203.
47. Benn, T. M.; Westerhoff, P., Nanoparticle Silver Released into Water from Commercially Available Sock Fabrics. *Environmental Science & Technology* **2008**, *42* (11), 4133-4139.
48. Choi, O.; Deng, K. K.; Kim, N.-J.; Ross Jr, L.; Surampalli, R. Y.; Hu, Z., The inhibitory effects of silver nanoparticles, silver ions, and silver chloride colloids on microbial growth. *Water Research* **2008**, *42* (12), 3066-3074.
49. García, A.; Delgado, L.; Torà, J. A.; Casals, E.; González, E.; Puentes, V.; Font, X.; Carrera, J.; Sánchez, A., Effect of cerium dioxide, titanium dioxide, silver, and gold nanoparticles on the activity of microbial communities intended in wastewater treatment. *Journal of Hazardous Materials* **2012**, *199–200* (0), 64-72.
50. Jarvie, H. P.; Al-Obaidi, H.; King, S. M.; Bowes, M. J.; Lawrence, M. J.; Drake, A. F.; Green, M. A.; Dobson, P. J., Fate of Silica Nanoparticles in Simulated Primary Wastewater Treatment. *Environmental Science & Technology* **2009**, *43* (22), 8622-8628.
51. Kaegi, R.; Voegelin, A.; Sinnet, B.; Zuleeg, S.; Hagendorfer, H.; Burkhardt, M.; Siegrist, H., Behavior of Metallic Silver Nanoparticles in a Pilot Wastewater Treatment Plant. *Environmental Science & Technology* **2011**, *45* (9), 3902-3908.
52. Kiser, M. A.; Ryu, H.; Jang, H.; Hristovski, K.; Westerhoff, P., Biosorption of nanoparticles to heterotrophic wastewater biomass. *Water Research* **2010**, *44* (14), 4105-4114.
53. Limbach, L. K.; Bereiter, R.; Müller, E.; Krebs, R.; Gälli, R.; Stark, W. J., Removal of Oxide Nanoparticles in a Model Wastewater Treatment Plant: Influence of Agglomeration and Surfactants on Clearing Efficiency. *Environmental Science & Technology* **2008**, *42* (15), 5828-5833.

54. Mu, H.; Chen, Y.; Xiao, N., Effects of metal oxide nanoparticles (TiO₂, Al₂O₃, SiO₂ and ZnO) on waste activated sludge anaerobic digestion. *Bioresource Technology* **2011**, *102* (22), 10305-10311.
55. Sheng, Z.; Liu, Y., Effects of silver nanoparticles on wastewater biofilms. *Water Research* **2011**, *45* (18), 6039-6050.
56. Zheng, X.; Wu, R.; Chen, Y., Effects of ZnO Nanoparticles on Wastewater Biological Nitrogen and Phosphorus Removal. *Environmental Science & Technology* **2011**, *45* (7), 2826-2832.
57. 57. Canter, L. W.; Knox, R. C., *Septic tank system effects on ground water quality*. Lewis Publishers, Inc: 1985.
58. Federal Water Pollution Control Act Amendments of 1972. In PUBLIC LAW 92-500, Ed. 1972.
59. EPA, NPDES Permit Writers' Manual. EPA-833-B-96-003. Water, O. o., Ed. Washington, D.C., 1996.
60. EPA, Centralized Waste Treatment Effluent Limitations Guidelines and Pretreatment Standards (40 CFR 437). Water, O. o., Ed. Washington, D.C., 2001.
61. EPA, Protecting the Nation's Waters Through Effective NPDES Permits A Strategic Plan FY 2001 and Beyond. Water, O. o., Ed. Washington, D.C., 2001.
62. Beal, C. D.; Gardner, E. A.; Menzies, N. W., Process, performance, and pollution potential: A review of septic tank–soil absorption systems. *Soil Research* **2005**, *43* (7), 781-802.
63. Factor Affecting the Performance of Primary Treatment in Decentralized Wastewater Systems In *Decentralized Systems: Final Report*, Foundation, W. E. R., Ed. IWA Publishing: London, 2008.
64. Alternative Wastewater Treatment Design Manual, Appendix A Primary Treatment Units. Resources, I. D. o. N., Ed. 2007.
65. Septic Tank Effluent Values. Health, W. S. D. o., Ed. 2004.
66. Introduction to Anaerobic Digestion Study Guide. Resources, W. D. o. N., Ed. 1992.

67. Hickey, J. L. S.; Duncan, D. L., Performance of Single Family Septic Tank Systems in Alaska. *Journal (Water Pollution Control Federation)* **1966**, *38* (8), 1298-1309.
68. Zaveri, R. M.; Flora, J. R. V., Laboratory septic tank performance response to electrolytic stimulation. *Water Research* **2002**, *36* (18), 4513-4524.
69. Norton, W.; Bally-Cuif, L., Adult zebrafish as a model organism for behavioural genetics. *BMC Neuroscience* **2010**, *11* (1), 90.
70. Truong, L.; Harper, S.; Tanguay, R., Evaluation of Embryotoxicity Using the Zebrafish Model. In *Drug Safety Evaluation*, Gautier, J.-C., Ed. Humana Press: 2011; Vol. 691, pp 271-279.
71. Lowry, G. V.; Gregory, K. B.; Apte, S. C.; Lead, J. R., Transformations of Nanomaterials in the Environment. *Environmental Science & Technology* **2012**, *46* (13), 6893-6899.
72. Cabiscol, E.; Tamarit, J.; Ros, J., Oxidative stress in bacteria and protein damage by reactive oxygen species. *International Microbiology* **2010**, *3* (1), 3-8.

Chapter 2

Metal Oxide Nanoparticles Induce Phenotypic Changes in a Model Colon Gut Microbiota

Reproduced with Permission from *Environmental Engineering Science*, Copyright 2015, Mary Liebert, Inc.

Taylor. A.A., I.M. Marcus, R.L. Guysi, and S.L. Walker. (Just accepted).

Chapter 2: Metal Oxide Nanoparticles Induce Phenotypic Changes in a Model Colon Gut Microbiota

Abstract

Nanoparticles (NPs) are becoming prevalent in consumer goods including foods and cosmetics. Understanding the interactions between NPs and bacteria in an engineered model colon can indicate potential impacts of NP exposure on the gut, and therefore overall human health. Human microbiome health has important implications to overall individual health. This work aims to quantify the phenotypic response to NP ingestion of a model microbial community within a model colon. Three NPs at environmentally relevant concentrations ($0.01 \mu\text{gL}^{-1}$ ZnO, $0.01 \mu\text{gL}^{-1}$ CeO₂, and 3mgL^{-1} TiO₂) were individually introduced into a model colon to identify the subsequent impact on the gut microbial community. Results indicate NPs cause the microbial community's phenotype to partition into three distinct phases: initial conditions, a transition period, and a homeostatic phase, with the NP-exposed community displaying significant differences ($P < 0.05$) from the unexposed community in multiple phenotypic traits. Notably, phenotypes including short chain fatty acid (SCFA) production, hydrophobicity, sugar content of the extracellular polymeric substance, and electrophoretic mobility, which indicates changes in the community's stability, were affected by the NPs. TiO₂ NPs led to extended phenotypic transformations for hydrophobicity when compared to the other NPs, likely due to its lack of dissociation and greater stability. Overall, the NPs caused non-lethal, significant changes to the microbial community's phenotype, which may relate to overall health effects.

Introduction

Nanotechnology offers many positive benefits to human health, such as more efficient drug delivery, sensor development for toxic substances detection, and medical diagnostic techniques⁷³⁻⁷⁶; yet the increasing popularity of nanotechnology may lead to a rise in potential accidental exposures through ingestion or via environmental release of nanoparticles (NPs). It is estimated that 15,600 metric tons year⁻¹ of TiO₂ nanomaterials, 3,700 metric tons year⁻¹ of ZnO nanomaterials, and 300 metric tons year⁻¹ of CeO₂ nanomaterials enter water systems with the majority of these NPs discharged from wastewater treatment plants^{31, 77}.

TiO₂ NPs are used daily by consumers with products such as toothpastes, cosmetics, and sunscreens⁷⁸⁻⁷⁹ and may easily be ingested. CeO₂ NPs are introduced into water resources through the disposal of coatings, pigments, and paints³¹. Much like CeO₂ and TiO₂, ZnO NPs also can enter bodies of water through discarded coatings, pigments, and paints, but also from the disposal of cosmetics³¹⁻³². These three NPs were chosen based upon their potential for human exposures through their wide spread use in many consumer products, foods, and because of their potential to be in treated drinking water^{30-33, 36-37, 39, 44, 80-81}.

The NPs selected in this study all have been reported to have toxic, non-lethal effects on organisms. Recent work has shown TiO₂ NPs can cross the epithelial lining in an intestinal model cell line via transcytosis⁸². While TiO₂ did not cause cell death, there are implications of other non-lethal effects to the cells. CeO₂ NPs have caused negative effects in *Escherichia coli*, reduction in plant germination, and have caused membrane

damage in eukaryotic cells⁸³⁻⁸⁶. Additionally, research has also shown the CeO₂ NPs may have strain specific antimicrobial effects⁸⁷. CeO₂ particles are found in personal care products and humans may also risk exposure to CeO₂ nanoparticles through sunscreens and cosmetics⁸⁰⁻⁸¹. CeO₂ is also one of the most commonly utilized nanoparticles and are used in a wide variety of applications. The disposal of these products into water sources is a potential route of exposure for humans. ZnO NPs exhibit toxicity to eukaryotic cells, decreasing cell viability and proliferation, and disrupting membrane integrity⁸⁵. ZnO NPs have also shown antimicrobial effects on bacteria; these effects are size and concentration dependent, as well as species specific⁸⁸. However, it is important to note that many *in vivo* studies with higher level organisms often give mixed results on toxicity⁸⁹⁻⁹¹. Therefore, these three NPs were chosen to determine the potential toxicity on the gut microbiota, which is likely to occur through exposure routes such as accidental dosing and ingestion.

In vitro function of gut environments has previously been characterized by monitoring enzymatic activity⁹²⁻⁹³, short chain fatty acid (SCFA) production⁹²⁻⁹⁵, and by determining microbial community genotype^{92-93, 96-97}. Gut organisms play an important role with indispensable functions to the human host such as vitamin production, digestion, and immune system activity⁹⁸⁻¹⁰⁰.

The role of the gut microbiota is so prominent in human health that researchers have found links between gut microbes and numerous diseases¹⁰¹⁻¹⁰⁹. In fact, changes in diet alone can cause rapid transformations in the activity and structure of the gut microbiota¹¹⁰, indicating that the microbiota is sensitive with a quick reaction time to

changes in the human intestines. This work highlights the importance of studying the effects of environmental contaminants on the gut microbiota.

Understanding the gut microbiome and its importance to human health with techniques such as molecular methods¹¹¹⁻¹¹⁴ will give rise to more treatment and disease prevention options. However, more information is needed than just sequencing data to fully understand the complex and dynamic function of the gut microbiota. Monitoring changes in the community's characteristics over time, such as the physical-chemical features, may provide a more complete representation of the gut's function and role in human health. Here, phenotypic characterization techniques based upon colloidal (*e.g.*, cell) transport experiments provide valuable insight that may not typically be measured with a microbiota study. To date, this is the first paper analyzing the effects of environmentally relevant concentrations of nanoparticles and their effects on the physical-chemical components of the gut community.

Published work with this model colon design has shown that microbial communities in the gut, wastewater, and groundwater can undergo significant phenotypic and genotypic changes when a perturbation is introduced, such as a pathogen¹¹⁵. We hypothesize that as compared to pathogen induced disturbances, the model colon's microbial community will undergo similar phenotypic changes when the colon is dosed with environmentally relevant concentrations of three nanoparticles: TiO₂, CeO₂, and ZnO.

Experimental Protocol

Microbial community and model colon

The experimental parameters measured in this work were identical to Marcus *et al.* (2013) as was the preparation of the microbial community, the microbial medium representing digested food entering the large intestine ¹¹⁶, and the *in vitro* model colon reactor ^{94, 115}. The only exception was that the microbial community was donated by and developed ¹¹⁷ from a healthy 26-year-old female volunteer who had not received antibiotics in over eight months. Briefly, frozen stocks of the microbial community were stored at -80 °C and each week a stock community was thawed, inoculated into a 200 mL flask containing colon media ¹¹⁶, and incubated for 24 hrs before being pumped into the dialysis tube inside of the custom colon reactor.

A human colon was replicated by using a custom-built reactor ¹¹⁵, which represented conditions inside of a proximal colon ¹¹⁸. The model colon ran for consecutive five-day long experiments. Colon effluent, or waste, was collected three times a day during feedings for characterization experiments. The model colon was run for a minimum of two runs (two five-day long experiments) per experimental condition to ensure reproducible data. Additional details and images of the model colon set-up are located in the supplementary information (SI) in Figure S1.

Nanoparticle selection

Zinc oxide (ZnO, Meliorum Technologies, NY), titanium dioxide (TiO₂, Evonik Degussa Corporation, NJ) and cerium dioxide (CeO₂, Meliorum Technologies, NY) nanoparticles (NPs) were selected for this work. They have previously been characterized in another study with the primary particle size for each NP reported as 10 nm, 21 nm, and 10 nm, respectively¹¹⁹. Additional characteristics are listed in the Keller *et al.* study for the NPs, such as phase and structure, surface area, isoelectric point, purity, and electrophoretic mobility. Also, additional studies have been conducted using these identical NPs to study their transport, aggregation, and effects on soil microbial communities¹²⁰⁻¹²².

Environmentally relevant NP concentrations were chosen to emulate human exposures to NPs through both ingestion of food and drinking water at 0.01 µgL⁻¹ ZnO NP, 0.01 µgL⁻¹ CeO₂ NP, and 3 mgL⁻¹ TiO₂ NP^{31-32, 36-37, 39}. Recent work has also indicated that adults in the USA ingest 5 mg TiO₂ per day, half of which is in the nano-size range¹²³⁻¹²⁴. Exposure routes and reliable dosing information of NPs that are embedded in solid matrices is difficult to predict and is often a limitation of analytical techniques¹²⁵⁻¹²⁶. The exposure levels used in this study were predominately selected from literature values that give predictions on amount of NPs in water and food sources^{31-32, 36-37, 39}.

NPs were added in bulk to the colon media prior to autoclaving and without alteration to achieve the concentrations mentioned above; this eliminated any contamination issues that may have occurred by adding NPs to the colon reactor

independently of the food source. The addition of the NPs to the sterile food source also provided a realistic exposure scenario that can provide the possibility for representative NP transformations^{71, 127-132}. During the weeklong experiments the sterile colon media containing the NPs was continually stirred, and three times a day, 100 mL was added to the model colon by pumping the sterile colon media into the reactor. During each feeding, 100 mL of colon effluent was also removed for characterization experiments.

As a control, the model colon was run without NPs for two runs (two five-day long experiments) to determine the gut microbiota phenotype in the absence of NPs. All NP experiments were run for a minimum of two runs (two five-day long experiments) to ensure reproducibility and all colon experiments were run under dark conditions to eliminate light effects. Additional controls were conducted to test the electrophoretic mobility and hydrophobicity of the NPs as a function of the extreme range of pH in the gastrointestinal tract. The purpose of this was to account for possible transformations of NPs and their subsequent changes in physicochemical properties. These tests are listed in the SI and mentioned in the Discussion section.

Phenotypic characterization of microbial community

Changes in the gut microbiota phenotype were examined with the following analyses: cell concentration, sugar and protein content of the extracellular polymeric substance (EPS), electrophoretic mobility (EPM, an indicator of the relative surface charge), hydrophobicity, and cell size following published methods^{115, 133-134} (Marcus et al. 2012a;

Marcus et al. 2012b; Marcus et al. 2013)(Marcus *et al.* 2012a; Marcus *et al.* 2012b; Marcus *et al.* 2013)). Briefly, upon daily sampling, bacteria from the model colon were washed with centrifugation (3,700 x g) and then suspended in a 10 mM KCl solution prior to all phenotypic characterizations. All samples collected for all characterization methods were measured in three replicates twice a day at the same time points to eliminate additional variables. Additional details on these methods can be found in the SI.

Biochemical characterization of microbial community

Changes in short chain fatty acid (SCFA) production, pH, and conductivity of the gut environment were monitored to determine the effects of the NPs on the microbial community and gut environment. pH (Thermo Scientific™ Orion™ Model GD9156BNWP) and conductivity (YSI 3200 Conductivity Instrument Model # 3200 115V) of the colon effluent were measured twice a day at the same time points with three replicates each for all control and NP experiments. Conductivity is an indirect measurement of the metal ion dissociation from the NPs; measuring ionic content of the colon effluent gives approximations of changes in ionic strength¹³⁵. Samples for SCFA analysis were collected in three replicates twice a day at the same time points from the colon effluent and polyethylene glycol (PEG) solution and were stored at -20 ° until analysis with the "gas chromatography flame ionization detector (GC-FID) (Agilent, Santa Clara, CA) using previously published methods^{115, 136}. The total concentration of the SCFAs was determined based upon both the colon effluent and PEG samples. Butyric

acid and acetic acid were analyzed by integration under a fitted flame ionization detection curve. Propionic acid is not reported due to the inability to integrate under the curve and account for accurate measurements of this SCFA.

Statistical analyses

All data was tested for normality and equal variance and analyzed with a one-way analysis of variance (ANOVA) and a Student's t test in Excel (v.14.0, Microsoft, Redmond, WA) to determine the phenotypic variation of the microbial community. Results were considered significant if $P < 0.05$.

Results

All data presented in the results are based upon a minimum of two five-day-long experimental runs in the model colon. All data points collected are a culmination of a minimum of three replicates per measurement. Additional details are found in the SI regarding control experiments used in this study.

Phenotypic characterization

The extensive phenotypic testing of the microbial community was chosen based upon known human health indicators such as SCFA production, but also used common evaluation techniques, such as surface charge, hydrophobicity, cell concentration, and

EPS content, that are associated with environmental microbial community sampling^{133, 137-141}. These non-traditional testing methods were selected to further characterize the gut environment and microbial community and the changes that may occur during perturbances.

Data for cell hydrophobicity, electrophoretic mobility (EPM), and the sugar and protein content of the EPS partitioned into three statistically different phases ($P < 0.05$) throughout the five-day-long experiments. Tuesday and Wednesday (days 2-3) data were statistically the same ($P > 0.05$), and Thursday and Friday (days 4-5) data were also statistically the same ($P > 0.05$). Therefore, weekdays were grouped in the following manner as three significantly different time points: an initial phase on Monday (day 1), a transition phase on Tuesday and Wednesday (days 2-3), and a homeostatic phase on Thursday and Friday (days 4-5). Data for all of the phenotypic characterization tests are also displayed per daily values and can be found in the SI (Figures S2-S7).

For cell hydrophobicity, all three metal nanoparticles altered cellular hydrophobicity when compared to the control, ranging from a 0-10% increase during the course of the five-day experiments (Fig. 1). All day 1 values (for all three NPs and control) were statistically the same (1.5 ± 0.8 - 5.3% , $P > 0.05$). CeO₂ and ZnO showed significant increases in hydrophobicity ($P < 0.05$) between day 1 and days 2-3 (CeO₂ increased from $0.9 \pm 4.4\%$ to $19.0 \pm 5.3\%$, ZnO increased from $8.4 \pm 5.3\%$ to $15.0 \pm 8.2\%$) whereas all three metals lead to significant increases in cellular hydrophobicity from day 1 to days 4-5 (CeO₂ from $0.9 \pm 4.4\%$ to $34 \pm 16.8\%$, ZnO from $8.4 \pm 5.3\%$ to $31.0 \pm 14.1\%$, and TiO₂ from $4.5 \pm 0.6\%$ to $30 \pm 14.8\%$).

The electrophoretic mobility (EPM, an indicator of the relative surface charge) of the microbial community partitioned into three distinct phases. EPM became significantly less negative and was near neutral during the mid-week phase (days 2-3) for all three NPs when compared to the control (control = -1.1 ± 0.2 [$\mu\text{m/s}/(\text{V/cm})$]), NPs range from -0.7 ± 0.2 to -0.9 ± 0.3 [$\mu\text{m/s}/(\text{V/cm})$], Fig. 1). EPM then became significantly more negative during the homeostatic phase (days 4-5, control = -0.9 ± 0.6 [$\mu\text{m/s}/(\text{V/cm})$]), NPs range from -0.97 ± 0.5 to -1.2 ± 0.4 [$\mu\text{m/s}/(\text{V/cm})$] ($P < 0.05$).

The sugar and protein content of the extracellular polymeric substance (EPS) also partitioned into three significantly distinct data points (Fig. 2). The sugar content of the EPS significantly peaked mid-week during the transition phase (days 2-3, control = 3.6 ± 0.2 $\text{mg cell}^{-1} \times 10^{10}$, TiO_2 and CeO_2 $6-8.5 \pm 1.7-3.5$ $\text{mg cell}^{-1} \times 10^{10}$) for TiO_2 and CeO_2 NPs ($P < 0.05$) whereas protein content had no significant trends.

Cell concentration decreased from $4-5.5 \times 10^{10}$ cells/mL to $1-3 \times 10^{10}$ cells/mL during the course of the five-day-long experiments for all conditions (data not shown); no significance was noted between the control (without NPs) and the three metal NPs, indicating that NPs did not have an effect on cell concentration in the model colon.

There was no significant difference ($P > 0.05$) in cell size (radius) within the control experiments during the course of the five-day-long experiment (Table 1) indicating that in the absence of NPs cell size remains constant inside the model colon. However, significant changes ($P < 0.05$) were seen in cell size during exposure to all three metal NPs. Data did not partition into the three distinct phases seen with the other cell phenotypes. CeO_2 caused cells to decrease significantly for the entire duration of the

experiment when compared to the controls; specifically, cells were significantly smaller during the CeO₂ exposure on days 4 and 5 (control 0.60 ± 0.02 - 0.62 ± 0.02 μm , CeO₂ days 4 and 5 = 0.46 ± 0.02 - 0.47 ± 0.02 μm). Of the three NPs, CeO₂ caused the most significant deviations from the control cell size. TiO₂ NPs caused a decrease in cell radius on days 3 and 5, exhibiting a smaller cell size, 0.59 ± 0.01 and 0.55 ± 0.05 μm , when compared to the control. Of the three NPs, TiO₂ caused the least amount of changes in cell size. When compared to the control, ZnO caused significant ($P < 0.05$) decreases in cell size for days 1, 3, and 5 (0.49 ± 0.02 , 0.59 ± 0.05 , and 0.53 ± 0.04 μm). In summary, the phenotypic changes occurring to the gut microbiota indicates that overall, the nanoparticles elicit marginal changes in multiple phenotypes.

Biochemical characterization

Short chain fatty acid (SCFA) production remained relatively constant between the control and all nanoparticle conditions (Fig. 1). The only significant result occurred during exposure to CeO₂ and showed a decrease in butyric acid production ($P < 0.05$, control = 105.8 ± 13.9 mM, butyric acid = 78.0 ± 16.0 mM).

Changes in pH were monitored twice a day from the colon effluent. During the three individual NP exposures, the pH was significantly lower during the transition phase condition. The model colon expressed a lower pH for each NP when compared to the control for days 2-3 [$P < 0.05$ control pH = 7.2 ± 0.2 (day 2) and 6.6 ± 0.3 (day 3)]. Fig. 3 demonstrates comparisons among pH values for all experimental conditions. Day 1 pH

values for the controls and the TiO₂, CeO₂, and ZnO NPs all have a pH range between 6.8 - 7.2 ± 0.06-0.3, with no significance between the control and the three NP pH values (P = 0.07). For day 2, the pH was significantly lower for all three NPs (NP pH between 5.4 and 6.8 ± 0.2-0.7, control = 7.2 ± 0.2) when compared to the control pH. Day 3 showed a significantly lower pH in the presence of TiO₂ and CeO₂ (day 2 control pH = 6.6 ± 0.3, TiO₂ and CeO₂ pH < 4.5 ± 0.1-0.9). There were not significant differences between NP conditions and the control during days 4 and 5.

Increasing conductivity trends (Fig. 3) were noted for CeO₂ exposures, with only day 2 data significantly higher than the control (P=0.02, control = 5.9 ± 0.1 μS/cm, CeO₂ = 6.7 ± 0.5 μS/cm). ZnO on day 3 (P = 0.002) and day 5 (P = 0.008) had a lower conductivity for both days when compared to the control (control = 6.2 ± 0.1 μS/cm, ZnO = 5.0 ± 0.5 μS/cm). TiO₂ did not cause a statistical change in conductivity. Overall, biochemical characterization demonstrated that slight changes occurred within the model colon reactor due to the nanoparticles.

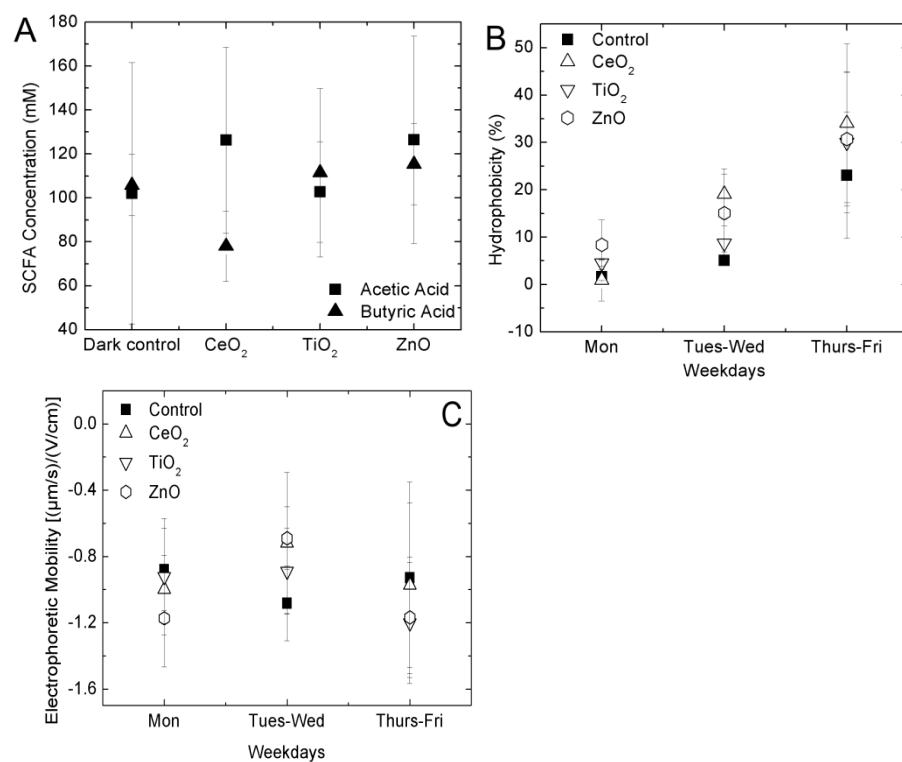


Figure 2.1.

Short chain fatty acid (SCA) analysis. (A) Comparison of the production of short chain fatty acids (SCFAs, acetic and butyric acids) over the five-day long experiments in the model colon in the presence and absence of TiO₂, CeO₂, and ZnO NPs. SCFA samples were collected twice a day for a minimum of two weeks and analyzed in triplicate with GC-FID. Each data point is an average a minimum of 60 values averaged that were collected over the course of two experimental weeks with samples in triplicate collected twice a day. (B) Hydrophobicity of the bacterial cells is displayed as a function of NP exposure in the model colon during the five-day long experiments. Hydrophobicity was measured twice a day in triplicates. (C) Electrophoretic mobility (EPM), an indicator of the relative surface charge, of the bacterial cells was measured in triplicate twice a day during the course of the five-day long experiments for a minimum of two weeks. All measurements were made on washed cells from the colon effluent. Error bars indicate standard deviation.

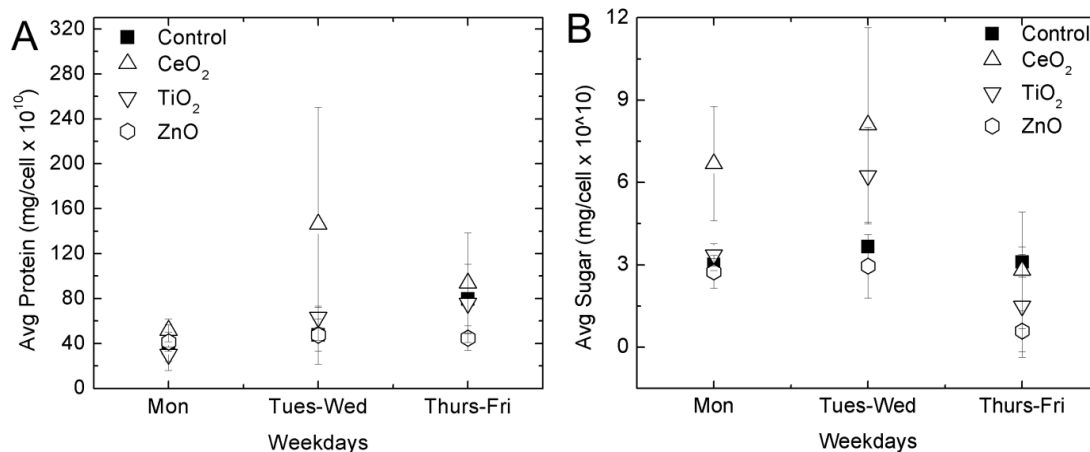


Figure 2.2

Protein and sugar content of EPS. The average protein (A) and sugar content (B) of the extracellular polymeric substance (EPS) was measured in triplicate once a day during the course of the five-day long experiments for a minimum of two weeks. EPS samples were collected once a day from the colon effluent and analyzed for sugar and protein content in triplicate. Error bars indicate standard deviation.

Table 2.1. Cell size measurements as a function of nanoparticle exposure.

	Day 1	Day 2	Day 3	Day 4	Day 5
Control	0.59 (0.05)	0.61 (0.02)	0.61 (0.020)	0.60 (0.02)	0.62 (0.02)
CeO ₂	0.53 ^b (0.03)	0.54 ^b (0.02)	0.54 ^b (0.02)	0.46 ^{a, b} (0.02)	0.47 ^{a, b} (0.02)
TiO ₂	0.63 (0.02)	0.62 (0.02)	0.59 ^{a, b} (0.01)	0.61 (0.03)	0.55 ^{a, b} (0.05)
ZnO	0.49 ^{a, b} (0.02)	0.53 ^b (0.02)	0.59 ^a (0.05)	0.56 (0.05)	0.53 ^b (0.04)

Cell size as bacteria radius (μm) was measured in triplicate twice a day during the course of the five-day long experiments for a minimum of two weeks. Values in parentheses indicate standard deviation. ^a indicates significant changes in cell size within individual weeks ($P < 0.05$) specific to NP treatments; ^b indicates significant changes in cell size ($P < 0.05$) as a function of NP treatment when compared to the control.

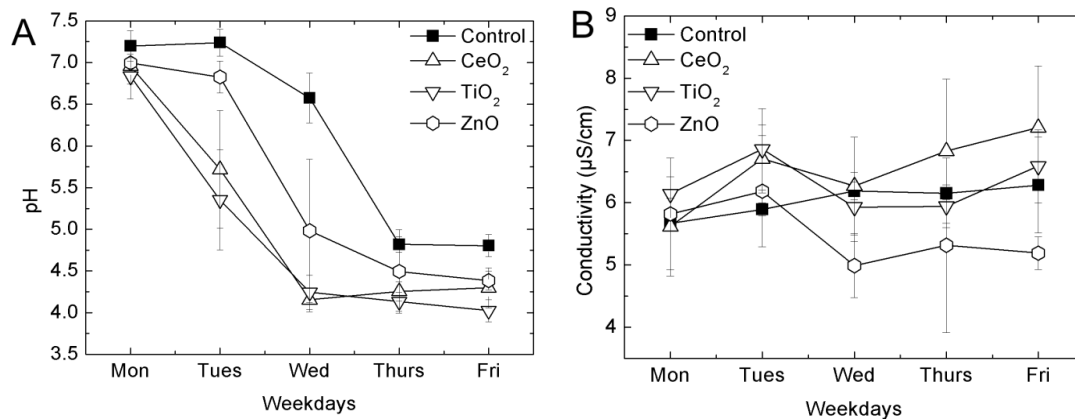


Figure 2.3.

pH and conductivity in model colon. (A) Change in pH during the course of the five-day long experiments for the control and the three NPs: TiO₂, CeO₂, and ZnO. pH measurements were taken from the colon and was measured in triplicate twice a day during the course of the five-day long experiments for a minimum of two weeks. (B) Change in conductivity (units) during the course of the five-day long experiments for the control and the three NPs: TiO₂, CeO₂, and ZnO. Conductivity measurements were taken from the colon effluent in triplicate twice a day for a minimum of two weeks, resulting in a minimum of 60 data points. Error bars indicate standard deviation.

Discussion

The techniques used in this work offer unique insight into alterations to the microbial metabolic processes inside of a model colon caused by NPs. An important consideration when studying the gut microbiota and interpreting results is that one human sample does not represent the high variability and diversity of gut microbiomes present in the human population. However, work has shown that even pure cultures of genetically identical bacteria can behave in radically different ways under the same experimental conditions¹⁴². This may explain some of the variation seen within the same conditions.

Here, the NPs added into the system clearly affected the phenotypic characteristics of the microbial community as well as the gut microenvironment. It is also important to note, that the system also exhibits small variation within the control conditions on a weekly basis, specifically, with the cell size (no significant difference during control conditions, $0.59 \pm 0.05 - 0.62 \pm 0.02 \mu\text{m}$) and the EPM (-0.90 ± 0.2 to $-1.1 \pm 0.2 [(\mu\text{m/s})/(\text{V/cm})]$). Therefore, the system may accurately reflect a human gut microbial community.

Phenotypic characterization

Changes in cellular hydrophobicity have been linked to the formation of biofilms^{134, 143}, which are aggregates of microorganisms. Over the course of the experiments, the cells experienced an increase in hydrophobicity in all NP conditions. Therefore, increases in hydrophobicity may limit the cell's surface area for interactions with the colon media and NP solution inside of the model colon, possibly reducing contact between cells and NPs.

Bacterial cells during the NP exposures that presented near-neutral EPM when compared to the control may be attributed to the NPs coating the surface of the cell and therefore changing its EPM¹⁴⁴. EPM has been linked to the attachment and stability of microorganisms, with higher absolute values of EPM linked with more stable, or mobile, microorganisms^{115, 145-146}. This suggests that the microbial community exposed to the NPs is the least stable during the mid-week transition phase, and is more stable in the initial and homeostatic phases. This indicates there is an increased chance for the

community to undergo attachment and form aggregates during less stable conditions. Additionally, this study had more near-neutral EPM values associated with the microbial community when compared to previous research with this system that used a microbial community that had more negative values and was donated from a healthy male ¹¹⁵. This demonstrates that microbial communities amongst individuals will also vary in the overall surface charge.

Sugar and protein content of the EPS were measured because they have been utilized as indicators of cellular conditions ¹⁴⁷. Increased amounts of sugar compared to the protein content of the EPS relate to cell aggregation and biofilm formation ¹⁴⁸, which may be a mechanism of the cell to limit exposure to NPs inside the model colon; less surface area of the cells may be exposed to the colon media/NP solution. Here, the sugar content relative to the protein increased mid-week, indicating a greater potential for the cells to undergo aggregation during the transition (mid-week) phase. However, the protein portion of the EPS did not show distinct trends; this indicates that this testing method may not be ideal for determining changes within a colon microbial community.

Establishing changes in the distribution of bacterial cell size can give an indication if NPs are causing phenotypic changes to the microbial community within the model colon; radius measurements indicate that morphological changes are occurring in bacteria width and length. Multiple changes in eukaryotic cellular morphology, which include changes in cell size such as cell rounding, nuclear membrane blebbing, chromatin condensation, and alterations in cytoplasmic organelles have been associated with cytotoxicity caused by quantum dots and single-walled carbon nanotubes (SWCNT) ¹⁴⁹⁻¹⁵⁰.

Decreases in bacteria cell size have been attributed to stress, with one example being starvation. Stressed cells undergo phenotypic changes in size to increase the likelihood of survival. This includes reductive division to increase cell numbers and increasing the production of hydrophobic molecules that favor aggregation¹⁵¹⁻¹⁵². However, it should be mentioned, that while community structure was not determined here with DNA sequencing, changes in the distribution of cell size may be attributed to changes in the microbial community structure¹⁵³⁻¹⁵⁵. Regardless, this measurement gives an indication that community's size distribution is changing over time in response to the NP exposures.

Biochemical characterization

Butyric acid is largely produced by the microbial breakdown of dietary fiber in the gut; increased levels of butyric acid inside the gut have been linked to protective measures against colorectal cancer such as cell proliferation reduction, decreases in tumor mass, and maintenance of a normal microbial population inside of the intestines^{140, 156-159}. A decrease in butyric acid inside the gut results in increased susceptibility to inflammation, but may also cause a decrease in the barrier function of the gut¹⁶⁰. This indicates that NPs could have a two-fold impact on the intestine by first affecting SCFA production, then leading to systemic circulation of the NPs via an inhibited intestinal barrier.

Under all conditions tested (control and the three individual NP exposures), the pH of the colonic fluid decreased with time. This decrease is a natural phenomenon of the microbial community as it ages and digests the nutrients it is supplied during the course

of the experiments ¹⁶¹⁻¹⁶². The presence of the NPs did not result in a significant difference from the control, with all experiments exhibiting the same gradual decline in pH. Therefore, it is likely that the addition of the NPs did not alter the pH, but induced a change in the microbes that may have altered the pH.

The pH did not partition into three distinct phases unlike the other data: hydrophobicity, sugar and protein content, and EPM. During the course of the experiments, the colon bioreactor mimicked conditions found inside of a proximal colon with an expected pH range between 5.5-7 ¹¹⁸ for control days 1-3, which demonstrates that the model colon is stable during this period. Control days 4-5 have a pH below 5.5; therefore the changes noted in the NP experiments during days 4-5 (homeostatic phase) cannot be exclusively credited to the presence of the NPs. While decreases in a complex media with a neutral pH has been attributed NP dissolution ¹⁶³, it is unlikely that this occurred in the model colon due to the similar trends between the control and the three NP trends. Changes in pH may also be caused by acidic metabolites and the available substrates within the intestines ¹⁶⁴. A study in the literature has shown that there are circadian fluctuations within the stomach and intestinal pH ^{162, 165}. Since pH did not show significant differences between the control and the NP exposures for 3 out of the 5 experimental days, overall, the decrease in pH within this system is a valid trend. ¹⁶¹⁻¹⁶²

Here, conductivity is used as an indirect measurement of the metal ion dissociation from the NPs; and gives approximations of changes in the ionic strength of the colon effluent ¹³⁵. Compared to the control, the increase in day 2 CeO₂ conductivity may be attributed to metal ion release from the NP at this specific pH, while the decrease

in conductivity for ZnO days 3 and 5 may be attributed to cellular uptake of ions, or ions being bound and made unavailable by the complex colon matrix ¹⁶³.

Additional controls with NPs were conducted to simulate the range of pH exposure that may occur, from ingestion of NPs in food and water at a neutral pH, to a low pH in a stomach environment, and finally to a pH of 5.5-7 in the proximal intestine. The purpose of these controls was to determine if changes in pH would affect the physicochemical properties of the NPs, and therefore have the possibility of altering the effects of NPs in the gut environment. As previous work has shown, changes in pH cause alterations in the physical-chemical behavior of NPs such as the surface charge, aggregation rate, and size ^{120, 166-167}. Similar results were noted in the additional NP controls used in this study (data not shown) and may indicate that NP behavior may change upon entering the low pH stomach environment, specifically the surface charge and size.

It is essential to note that interactions between NPs and bacteria in the intestines may be dependent upon numerous factors: the surface charge of the NPs and bacteria, the chemical composition and surface charge of the digested food, and variability in diet. These factors may ultimately correlate to effects seen in humans on an individual basis. In fact, similar work has demonstrated that exposing common NPs found in food to stomach-like conditions will change their surface chemistry from negative to neutral or positive, causing the NPs to interact with negatively charged mucus proteins in the gastrointestinal tract and in turn affecting the transport of NPs within the intestine ¹⁶⁸. The purpose of this work was to measure responses of the microbial community during

the NP exposures. Based upon previous research, it is anticipated that the NPs altered by stomach-like conditions would also cause changes in the gut environment ¹⁶⁸.

The changes measured in the microbial community when the model colon was dosed with environmentally relevant concentrations of NPs demonstrate that not only will the NPs only minimally affect phenotype, but the particles may also elicit other non-lethal effects. Such effects may include stress to the microbial community. This may imply that other undesired effects on the human gut occur due to the NPs and therefore some alterations in overall human health could occur. Other studies have indicated that intestinal exposure to metal NPs has numerous outcomes, such as alterations in the enteroendocrine secretory response of serotonin, and NPs having increased retention time within the gut from entrapment in the intestinal folds, which led to amplified changes to the intestinal physiology ¹⁶⁹⁻¹⁷⁰.

Additionally, ambient air particulate matter (<10 μm), which are particles three orders of magnitude larger than the model NPs investigated, have also been shown to cause changes inside of the mice intestine. Specifically, the colloidal material was observed to enhance gut permeability and cytokine secretion, altering short chain fatty acid production (decrease in butyric acid), and shifting the microbial community composition ¹⁷¹. This example provides evidence that additional and alternative exposure routes should be considered when designing NP studies. Particulate matter, which can contain particles on the nanoscale, has been shown to have adverse consequences on the gastrointestinal tract and is associated with increased risks for many diseases in which the gut microbiota also play a significant role ¹⁷¹⁻¹⁷⁶. Therefore, another route of exposure to

NPs in the gut may be through inhalation of ambient air, in addition to the ingestion exposure route and relevant doses accounted for in this study. The inhalation exposure route demonstrates that atypical exposure scenarios should be considered when designing future nanoparticle exposure experiments and is a relevant pathway for exposure given the current knowledge on ultrafine particle matter and its impacts on health (Bakand, 2012; Grassian, 2007).

Furthermore, NPs can undergo transformations in the environment or in consumer products such as speciation, dissolution, or aggregation that can alter the NP toxicity, reactivity, and physicochemical properties. These changes are not accurately represented with testing “as-received” particles^{71, 128-132}. Studying NPs in realistic scenarios is of the utmost importance. Here, the concern of a realistic exposure and subsequent transformation was addressed by dosing the sterile colon media with the NPs. The NPs remained in the colon media for the duration of the five-day-long experiments. Unfortunately, one disadvantage is the difficulty in characterizing NPs after introduction into complex media due to limitations in analytical techniques^{129, 132}. While the NP exposures were designed to mimic realistic scenarios that would involve NP transformation, it was beyond the scope of this particular paper to evaluate the degree of transformation occurring in the colon environment. However, complementary studies have used bacteria in both realistic settings and idealized laboratory studies to determine the effects of NP toxicity on organisms similarly without measuring the fate or transformation of the particles in the systems¹⁷⁷⁻¹⁷⁸.

Our initial hypothesis, that NPs induce phenotypic changes in a gut microbial community, was affirmed through significant measurable effects seen in the data. Tests that did support that NPs caused changes in the phenotype included hydrophobicity, EPM, sugar content of the EPS, cell size, conductivity, and SFCA (specifically butyric acid) production. Data for cell concentration and the protein content of the EPS demonstrated no significant results. Data was inconclusive for pH. With such a complex biological system, it is very likely that the phenotypic and biochemical changes observed are combinations of responses happening in parallel. The effects seen may be attributed to both changes induced by the NPs and natural phenomena associated with microbial community activity and other metabolic processes in a multifaceted environment such as the gut. Some examples of natural processes that could also influence the phenotypic and biochemical parameters are osmolarity, active metabolites, and electrolyte concentrations 179-180.

Additionally, not only the complexity of the microbiota, but also the intricacy of a living colon environment, is extremely difficult to predict and monitor. Since the human colon microbiota plays a large and diverse role in overall human health, particularly with immunity and disease development^{23, 181-182}, and can vary greatly per individual basis, having an understanding of how the microbiota is affected at the phenotypic level may provide crucial information to better characterize an unhealthy or stressed colon microbial community.

Conclusions

This work highlights the relevance of studying a complex matrix and microbial community *in situ* rather than individual microbial species *in vitro*. Diverse analyses, including techniques traditionally used for environmental microbial analysis such as phenotypic measurements, are also needed to further characterize changes in microbial communities. These tests can provide a depth of information that may complement microbial community sequencing data and other traditional colonic enzyme assays. Here, significant changes in hydrophobicity, EPM, sugar content of the EPS, cell size, conductivity, and SCFA demonstrated that representative NPs found in consumer products and water sources with the potential to be ingested can minimally impact the gut microbial community. The techniques used and presented herein offer a novel combination of indicators for identifying NP induced perturbances within the gut microbiota.

Acknowledgments

We would like to thank the following people for their help with this work: Brian C. Cruz, Christina E. Gerges, and Jose Valle de Leon. This work was funded by a National Research Service Award Institutional Training Grant (T32 ES018827) and through the UC-CEIN (University of California Center for Environmental Implications of Nanotechnology); this material is based upon work supported by the National Science

Foundation and the Environmental Protection Agency under Cooperative Agreement Number DBI 0830117. Any opinions, findings, and conclusions or recommendations expressed in this material are those of the author(s) and do not necessarily reflect the views of the National Science Foundation or the Environmental Protection Agency. This work has not been subjected to EPA review and no official endorsement should be inferred.

References

1. Aillon, K.L., Xie, Y., El-Gendy, N., Berkland, C.J. and Forrest, M.L. (2009) Effects of nanomaterial physicochemical properties on in vivo toxicity. *Advanced Drug Delivery Reviews* **61**, 457-466.
2. Albanese, A. and Chan, W.C.W. Effect of Gold Nanoparticle Aggregation on Cell Uptake and Toxicity. *ACS Nano* **5**, 5478-5489.
3. Ames, B. (1983) Dietary carcinogens and anticarcinogens: Oxygen radicals and degenerative diseases. *Science* **221**, 1256-1264.
4. Ananthakrishnan, A.N., McGinley, E.L., Binion, D.G. and Saeian, K. (2011) Ambient air pollution correlates with hospitalizations for inflammatory bowel disease: An ecologic analysis. *Inflammatory Bowel Diseases* **17**, 1138-1145.
5. Apajalahti, J.H.A., Särkilahti, L.K., Mäki, B.R.E., Heikkinen, J.P., Nurminen, P.H. and Holben, W.E. (1998) Effective Recovery of Bacterial DNA and Percent-Guanine-Plus-Cytosine-Based Analysis of Community Structure in the Gastrointestinal Tract of Broiler Chickens. *Applied and Environmental Microbiology* **64**, 4084-4088.
6. Armougom, F., Henry, M., Vialettes, B., Raccach, D. and Raoult, D. (2009) Monitoring bacterial community of human gut microbiota reveals an increase in *Lactobacillus* in obese patients and methanogens in anorexic patients. *PloS one* **4**, e7125.
7. Auffan, M., Rose, J., Orsiere, T., De Meo, M., Thill, A., Zeyons, O., Proux, O., Masion, A., Chaurand, P., Spalla, O., Botta, A., Wiesner, M.R. and Bottero, J.-Y. (2009) CeO₂ nanoparticles induce DNA damage towards human dermal fibroblasts in vitro. *Nanotoxicology* **3**, 161-171.
8. Bäckhed, F., Ding, H., Wang, T., Hooper, L.V., Koh, G.Y., Nagy, A., Semenkovich, C.F. and Gordon, J.I. (2004) The gut microbiota as an environmental factor that regulates fat storage. *Proceedings of the National Academy of Sciences of the United States of America* **101**, 15718-15723.
9. Beamish, L.A., Osornio-Vargas, A.R. and Wine, E. (2011) Air pollution: An environmental factor contributing to intestinal disease. *Journal of Crohn's and Colitis* **5**, 279-286.

10. Bian, S.-W., Mudunkotuwa, I.A., Rupasinghe, T. and Grassian, V.H. (2011) Aggregation and Dissolution of 4 nm ZnO Nanoparticles in Aqueous Environments: Influence of pH, Ionic Strength, Size, and Adsorption of Humic Acid. *Langmuir* **27**, 6059-6068.
11. Boffa, L.C., Lupton, J.R., Mariani, M.R., Ceppi, M., Newmark, H.L., Scalmati, A. and Lipkin, M. (1992) Modulation of Colonic Epithelial Cell Proliferation, Histone Acetylation, and Luminal Short Chain Fatty Acids by Variation of Dietary Fiber (Wheat Bran) in Rats. *Cancer Research* **52**, 5906-5912.
12. Bolster, C.H., Cook, K.L., Marcus, I.M., Haznedaroglu, B.Z. and Walker, S.L. (2010) Correlating Transport Behavior with Cell Properties for Eight Porcine *Escherichia coli* Isolates. *Environmental Science & Technology* **44**, 5008-5014.
13. Bolster, C.H., Haznedaroglu, B.Z. and Walker, S.L. (2009) Diversity in Cell Properties and Transport Behavior among 12 Different Environmental *Escherichia coli* Isolates. *J Environ Qual* **38**, 465-472.
14. Chen, Y.-S., Hung, Y.-C., Liao, I. and Huang, G.S. (2009) Assessment of the In Vivo Toxicity of Gold Nanoparticles. *Nanoscale Res Lett* **4**, 858-864.
15. Chowdhury, I., Hong, Y., Honda, R.J. and Walker, S.L. (2011) Mechanisms of TiO₂ nanoparticle transport in porous media: Role of solution chemistry, nanoparticle concentration, and flowrate. *Journal of Colloid and Interface Science* **360**, 548-555.
16. Chowdhury, I., Walker, S.L. and Mylon, S.E. (2013) Aggregate morphology of nano-TiO₂: role of primary particle size, solution chemistry, and organic matter. *Environmental Science: Processes & Impacts* **15**, 275-282.
17. Clemente, Jose C., Ursell, Luke K., Parfrey, Laura W. and Knight, R. (2012) The Impact of the Gut Microbiota on Human Health: An Integrative View. *Cell* **148**, 1258-1270.
18. Collins, M.D. and Gibson, G.R. (1999) Probiotics, prebiotics, and synbiotics: approaches for modulating the microbial ecology of the gut. *The American Journal of Clinical Nutrition* **69**, 1052s-1057s.
19. Cummings, J.H. (1984) Microbial Digestion of Complex Carbohydrates in Man. *Proceedings of the Nutrition Society* **43**, 35-44.

20. David, L.A., Maurice, C.F., Carmody, R.N., Gootenberg, D.B., Button, J.E., Wolfe, B.E., Ling, A.V., Devlin, A.S., Varma, Y., Fischbach, M.A., Biddinger, S.B., Dutton, R.J. and Turnbaugh, P.J. (2014) Diet rapidly and reproducibly alters the human gut microbiome. *Nature* **505**, 559-563.
21. Eboigbodin, K.E. and Biggs, C.A. (2008) Characterization of the extracellular polymeric substances produced by *Escherichia coli* using infrared spectroscopic, proteomic, and aggregation studies. *Biomacromolecules* **9**, 686-695.
22. Eckburg, P.B., Bik, E.M., Bernstein, C.N., Purdom, E., Dethlefsen, L., Sargent, M., Gill, S.R., Nelson, K.E. and Relman, D.A. (2005) Diversity of the Human Intestinal Microbial Flora. *Science* **308**, 1635-1638.
23. Elimelech, M., Jia, X., Gregory, J. and Williams, R. (1998) *Particle deposition & aggregation: measurement, modelling and simulation*: Butterworth-Heinemann, Woburn, MA, USA.
24. Frank, D.N., Robertson, C.E., Hamm, C.M., Kpadeh, Z., Zhang, T., Chen, H., Zhu, W., Sartor, R.B., Boedeker, E.C., Harpaz, N., Pace, N.R. and Li, E. (2011) Disease phenotype and genotype are associated with shifts in intestinal-associated microbiota in inflammatory bowel diseases. *Inflammatory Bowel Diseases* **17**, 179-184.
25. Frank, D.N., St. Amand, A.L., Feldman, R.A., Boedeker, E.C., Harpaz, N. and Pace, N.R. (2007) Molecular-phylogenetic characterization of microbial community imbalances in human inflammatory bowel diseases. *Proceedings of the National Academy of Sciences* **104**, 13780-13785.
26. Ge, Y., Priester, J.H., Van De Werfhorst, L.C., Schimel, J.P. and Holden, P.A. (2013) Potential Mechanisms and Environmental Controls of TiO₂ Nanoparticle Effects on Soil Bacterial Communities. *Environmental Science & Technology* **47**, 14411-14417.
27. Ge, Y., Schimel, J.P. and Holden, P.A. (2011) Evidence for Negative Effects of TiO₂ and ZnO Nanoparticles on Soil Bacterial Communities. *Environmental Science & Technology* **45**, 1659-1664.
28. Gottschalk, F., Sonderer, T., Scholz, R.W. and Nowack, B. (2009) Modeled Environmental Concentrations of Engineered Nanomaterials (TiO₂, ZnO, Ag, CNT, Fullerenes) for Different Regions. *Environmental Science & Technology* **43**, 9216-9222.

29. Griffin, B.A. and Jurinak, J.J. (1973) Estimation of activity coefficients from the electrical conductivity of natural aquatic systems and soil extracts. *Soil Science* **116**, 26-30.
30. Guarner, F. and Malagelada, J.-R. (2003) Gut flora in health and disease. *The Lancet* **361**, 512-519.
31. Gubéran, E., Usel, M., Raymond, L., Bolay, J., Fioretta, G. and Puissant, J. (1992) Increased risk for lung cancer and for cancer of the gastrointestinal tract among Geneva professional drivers. *British Journal of Industrial Medicine* **49**, 337-344.
32. Hahn, M.W. and Höfle, M.G. (1999) Flagellate Predation on a Bacterial Model Community: Interplay of Size-Selective Grazing, Specific Bacterial Cell Size, and Bacterial Community Composition. *Applied and Environmental Microbiology* **65**, 4863-4872.
33. Harris, P.J. and Ferguson, L.R. (1993) Dietary fibre: its composition and role in protection against colorectal cancer. *Mutation Research/Fundamental and Molecular Mechanisms of Mutagenesis* **290**, 97-110.
34. Hermansson, M. (1999) The DLVO theory in microbial adhesion. *Colloids and Surfaces B: Biointerfaces* **14**, 105-119.
35. Hooper, L.V., Midtvedt, T. and Gordon, J.I. (2002) How host-microbial interactions shape the nutrient environment of the mammalian intestine. *Annual Review of Nutrition* **22**, 283-307.
36. Hsiao, Elaine Y., McBride, Sara W., Hsien, S., Sharon, G., Hyde, Embriette R., McCue, T., Codelli, Julian A., Chow, J., Reisman, Sarah E., Petrosino, Joseph F., Patterson, Paul H. and Mazmanian, Sarkis K. (2013) Microbiota Modulate Behavioral and Physiological Abnormalities Associated with Neurodevelopmental Disorders. *Cell* **155**, 1451-1463.
37. Hueso, S., García, C. and Hernández, T. (2012) Severe drought conditions modify the microbial community structure, size and activity in amended and unamended soils. *Soil Biology and Biochemistry* **50**, 167-173.
38. Ivask, A., ElBadawy, A., Kaweeteerawat, C., Boren, D., Fischer, H., Ji, Z., Chang, C.H., Liu, R., Tolaymat, T., Telesca, D., Zink, J.I., Cohen, Y., Holden, P.A. and Godwin, H.A. (2013) Toxicity Mechanisms in *Escherichia coli* Vary for Silver Nanoparticles and Differ from Ionic Silver. *ACS Nano* **8**, 374-386.

39. Jiang, J., Oberdörster, G. and Biswas, P. (2009) Characterization of size, surface charge, and agglomeration state of nanoparticle dispersions for toxicological studies. *J Nanopart Res* **11**, 77-89.
40. Jiménez-Vera, R., Monroy, O., Corona-Cruz, A. and García-Garibay, M. (2008) Construction of a model of the human proximal colon. *World J Microbiol Biotechnol* **24**, 2767-2774.
41. Jürgens, K., Pernthaler, J., Schalla, S. and Amann, R. (1999) Morphological and Compositional Changes in a Planktonic Bacterial Community in Response to Enhanced Protozoan Grazing. *Applied and Environmental Microbiology* **65**, 1241-1250.
42. Kaida, T., Kobayashi, K., Adachi, M. and Suzuki, F. (2003) Optical characteristics of titanium oxide interference film and the film laminated with oxides and their applications for cosmetics. *Journal of cosmetic science* **55**, 219-220.
43. Kaida, T., Kobayashi, K., Adachi, M. and Suzuki, F. (2004) Optical characteristics of titanium oxide interference film and the film laminated with oxides and their applications for cosmetics. *Journal of cosmetic science* **55**, 219.
44. Kaplan, G.G., Dixon, E., Panaccione, R., Fong, A., Chen, L., Szyszkowicz, M., Wheeler, A., MacLean, A., Buie, W.D., Leung, T., Heitman, S.J. and Villeneuve, P.J. (2009) Effect of ambient air pollution on the incidence of appendicitis. *CMAJ : Canadian Medical Association Journal* **181**, 591-597.
45. Keller, A., McFerran, S., Lazareva, A. and Suh, S. (2013) Global life cycle releases of engineered nanomaterials. *Journal of Nanoparticle Research* **15**, 1-17.
46. Keller, A., Vosti, W., Wang, H. and Lazareva, A. (2014) Release of engineered nanomaterials from personal care products throughout their life cycle. *J Nanopart Res* **16**, 1-10.
47. Keller, A.A. and Lazareva, A. (2013a) Predicted Releases of Engineered Nanomaterials: From Global to Regional to Local. *Environmental Science & Technology Letters*.
48. Keller, A.A. and Lazareva, A. (2013b) Predicted Releases of Engineered Nanomaterials: From Global to Regional to Local. *Environmental Science & Technology Letters* **1**, 65-70.

49. Keller, A.A., Wang, H., Zhou, D., Lenihan, H.S., Cherr, G., Cardinale, B.J., Miller, R. and Ji, Z. (2010) Stability and Aggregation of Metal Oxide Nanoparticles in Natural Aqueous Matrices. *Environmental Science & Technology* **44**, 1962-1967.
50. Kelly, D., Campbell, J.I., King, T.P., Grant, G., Jansson, E.A., Coutts, A.G., Pettersson, S. and Conway, S. (2003) Commensal anaerobic gut bacteria attenuate inflammation by regulating nuclear-cytoplasmic shuttling of PPAR- γ and RelA. *Nature immunology* **5**, 104-112.
51. Khlebtsov, N. and Dykman, L. (2011) Biodistribution and toxicity of engineered gold nanoparticles: a review of in vitro and in vivo studies. *Chemical Society Reviews* **40**, 1647-1671.
52. Kim, I.S., Baek, M. and Choi, S.-J. (2010) Comparative cytotoxicity of Al₂O₃, CeO₂, TiO₂ and ZnO nanoparticles to human lung cells. *Journal of nanoscience and nanotechnology* **10**, 3453-3458.
53. Kiser, M.A., Westerhoff, P., Benn, T., Wang, Y., Pérez-Rivera, J. and Hristovski, K. (2009) Titanium Nanomaterial Removal and Release from Wastewater Treatment Plants. *Environmental Science & Technology* **43**, 6757-6763.
54. Kish, L., Hotte, N., Kaplan, G.G., Vincent, R., Tso, R., Gänzle, M., Rioux, K.P., Thiesen, A., Barkema, H.W. and Wine, E. (2013) Environmental particulate matter induces murine intestinal inflammatory responses and alters the gut microbiome. *PloS one* **8**, e62220.
55. Kjelleberg, S., Hermansson, M., Marden, P. and Jones, G.W. (1987) The Transient Phase Between Growth and Nongrowth of Heterotrophic Bacteria, with Emphasis on the Marine Environment. *Annual Review of Microbiology* **41**, 25-49.
56. Koeneman, B., Zhang, Y., Westerhoff, P., Chen, Y., Crittenden, J. and Capco, D. (2010) Toxicity and cellular responses of intestinal cells exposed to titanium dioxide. *Cell Biol Toxicol* **26**, 225-238.
57. Kong, J., Franklin, N.R., Zhou, C., Chapline, M.G., Peng, S., Cho, K. and Dai, H. (2000) Nanotube molecular wires as chemical sensors. *Science* **287**, 622-625.
58. Kulasekara, B.R., Kamischke, C., Kulasekara, H.D., Christen, M., Wiggins, P.A. and Miller, S.I. (2013) *c-di-GMP heterogeneity is generated by the chemotaxis machinery to regulate flagellar motility.*

59. Lepage, P., Häslér, R., Spehlmann, M.E., Rehman, A., Zvirbliene, A., Begun, A., Ott, S., Kupcinskis, L., Doré, J., Raedler, A. and Schreiber, S. (2011) Twin Study Indicates Loss of Interaction Between Microbiota and Mucosa of Patients With Ulcerative Colitis. *Gastroenterology* **141**, 227-236.
60. Levard, C., Hotze, E.M., Colman, B.P., Dale, A.L., Truong, L., Yang, X.Y., Bone, A.J., Brown, G.E., Tanguay, R.L., Di Giulio, R.T., Bernhardt, E.S., Meyer, J.N., Wiesner, M.R. and Lowry, G.V. (2013) Sulfidation of Silver Nanoparticles: Natural Antidote to Their Toxicity. *Environmental Science & Technology* **47**, 13440-13448.
61. Levard, C., Hotze, E.M., Lowry, G.V. and Brown, G.E. (2012) Environmental Transformations of Silver Nanoparticles: Impact on Stability and Toxicity. *Environmental Science & Technology* **46**, 6900-6914.
62. Ley, R.E., Bäckhed, F., Turnbaugh, P., Lozupone, C.A., Knight, R.D. and Gordon, J.I. (2005) Obesity alters gut microbial ecology. *Proceedings of the National Academy of Sciences of the United States of America* **102**, 11070-11075.
63. Ley, R.E., Turnbaugh, P.J., Klein, S. and Gordon, J.I. (2006) Microbial ecology: human gut microbes associated with obesity. *Nature* **444**, 1022-1023.
64. Limbach, L.K., Li, Y., Grass, R.N., Brunner, T.J., Hintermann, M.A., Müller, M., Gunther, D. and Stark, W.J. (2005) Oxide Nanoparticle Uptake in Human Lung Fibroblasts: Effects of Particle Size, Agglomeration, and Diffusion at Low Concentrations. *Environmental Science & Technology* **39**, 9370-9376.
65. Lombi, E., Donner, E., Taheri, S., Tavakkoli, E., Jämting, Å.K., McClure, S., Naidu, R., Miller, B.W., Scheckel, K.G. and Vasilev, K. (2013) Transformation of four silver/silver chloride nanoparticles during anaerobic treatment of wastewater and post-processing of sewage sludge. *Environmental Pollution* **176**, 193-197.
66. Lomer, M.C.E., Thompson, R.P.H., Commisso, J., Keen, C.L. and Powell, J.J. (2000) Determination of titanium dioxide in foods using inductively coupled plasma optical emission spectrometry. *Analyst* **125**, 2339-2343.
67. Long, R.Q. and Yang, R.T. (2001) Carbon nanotubes as superior sorbent for dioxin removal. *Journal of the American Chemical Society* **123**, 2058-2059.
68. López-Moreno, M.L., de la Rosa, G., Hernández-Viezas, J.A., Peralta-Videa, J.R. and Gardea-Torresdey, J.L. (2010) X-ray Absorption Spectroscopy (XAS) Corroboration of the Uptake and Storage of CeO₂ Nanoparticles and Assessment

of Their Differential Toxicity in Four Edible Plant Species. *Journal of Agricultural and Food Chemistry* **58**, 3689-3693.

69. Louis, P., Scott, K.P., Duncan, S.H. and Flint, H.J. (2007) Understanding the effects of diet on bacterial metabolism in the large intestine. *Journal of Applied Microbiology* **102**, 1197-1208.
70. Lovrić, J., Bazzi, H., Cuie, Y., Fortin, G.A., Winnik, F. and Maysinger, D. (2005) Differences in subcellular distribution and toxicity of green and red emitting CdTe quantum dots. *J Mol Med* **83**, 377-385.
71. Lowry, G.V., Espinasse, B.P., Badireddy, A.R., Richardson, C.J., Reinsch, B.C., Bryant, L.D., Bone, A.J., Deonaraine, A., Chae, S., Therezien, M., Colman, B.P., Hsu-Kim, H., Bernhardt, E.S., Matson, C.W. and Wiesner, M.R. (2012a) Long-Term Transformation and Fate of Manufactured Ag Nanoparticles in a Simulated Large Scale Freshwater Emergent Wetland. *Environmental Science & Technology* **46**, 7027-7036.
72. Lowry, G.V., Gregory, K.B., Apte, S.C. and Lead, J.R. (2012b) Transformations of Nanomaterials in the Environment. *Environmental Science & Technology* **46**, 6893-6899.
73. Maathuis, A.J.H., van den Heuvel, E.G., Schoterman, M.H.C. and Venema, K. (2012) Galacto-Oligosaccharides Have Prebiotic Activity in a Dynamic In Vitro Colon Model Using a ¹³C-Labeling Technique. *The Journal of Nutrition* **142**, 1205-1212.
74. Manichanh, C., Rigottier-Gois, L., Bonnaud, E., Gloux, K., Pelletier, E., Frangeul, L., Nalin, R., Jarrin, C., Chardon, P., Marteau, P., Roca, J. and Dore, J. (2006) Reduced diversity of faecal microbiota in Crohn's disease revealed by a metagenomic approach. *Gut* **55**, 205-211.
75. Marcotte, L., Kegelaer, G., Sandt, C., Barbeau, J. and Lafleur, M. (2007) An alternative infrared spectroscopy assay for the quantification of polysaccharides in bacterial samples. *Analytical Biochemistry* **361**, 7-14.
76. Marcus, I.M., Bolster, C.H., Cook, K.L., Opot, S.R. and Walker, S.L. (2012a) Impact of growth conditions on transport behavior of E. coli. *Journal of Environmental Monitoring* **14**, 984-991.

77. Marcus, I.M., Herzberg, M., Walker, S.L. and Freger, V. (2012b) *Pseudomonas aeruginosa* Attachment on QCM-D Sensors: The Role of Cell and Surface Hydrophobicities. *Langmuir* **28**, 6396-6402.
78. Marcus, I.M., Wilder, H.A., Quazi, S.J. and Walker, S.L. (2013) Linking Microbial Community Structure to Function in Representative Simulated Systems. *Applied and Environmental Microbiology* **79**, 2552-2559.
79. Martin, C.R. and Kohli, P. (2003) The emerging field of nanotube biotechnology. *Nature Reviews Drug Discovery* **2**, 29-37.
80. Matsuki, T., Watanabe, K., Fujimoto, J., Takada, T. and Tanaka, R. (2004) Use of 16S rRNA Gene-Targeted Group-Specific Primers for Real-Time PCR Analysis of Predominant Bacteria in Human Feces. *Applied and Environmental Microbiology* **70**, 7220-7228.
81. McCracken, C., Zane, A., Knight, D.A., Dutta, P.K. and Waldman, W.J. (2013) Minimal Intestinal Epithelial Cell Toxicity in Response to Short- and Long-Term Food-Relevant Inorganic Nanoparticle Exposure. *Chemical Research in Toxicology* **26**, 1514-1525.
82. McIntyre, A., Gibson, P.R. and Young, G.P. (1993) Butyrate production from dietary fibre and protection against large bowel cancer in a rat model. *Gut* **34**, 386-391.
83. McLauchlan, G., Fullarton, G.M., Crean, G.P. and McColl, K.E. (1989) Comparison of gastric body and antral pH: a 24 hour ambulatory study in healthy volunteers. *Gut* **30**, 573-578.
84. Miller, K. and Wood, J. (1996) Osmoadaptation by rhizosphere bacteria. *Annual Reviews Microbiology* **50**, 101-136.
85. Minekus, M., Smeets-Peeters, M., Bernalier, A., Marol-Bonnin, S., Havenaar, R., Marteau, P., Alric, M., Fonty, G. and Huis in't Veld, J.H.J. (1999) A computer-controlled system to simulate conditions of the large intestine with peristaltic mixing, water absorption and absorption of fermentation products. *Appl Microbiol Biotechnol* **53**, 108-114.
86. Mondot, S., Kang, S., Furet, J.P., Aguirre de Carcer, D., McSweeney, C., Morrison, M., Marteau, P., Doré, J. and Leclerc, M. (2011) Highlighting new phylogenetic specificities of Crohn's disease microbiota. *Inflammatory Bowel Diseases* **17**, 185-192.

87. Morita, R. (1986) *Autoecological studies and marine ecosystems*. New York: Wiley & Sons.
88. Nowack, B., Ranville, J.F., Diamond, S., Gallego-Urrea, J.A., Metcalfe, C., Rose, J., Horne, N., Koelmans, A.A. and Klaine, S.J. (2012) Potential scenarios for nanomaterial release and subsequent alteration in the environment. *Environmental Toxicology and Chemistry* **31**, 50-59.
89. Nugent, S.G., Kumar, D., Rampton, D.S. and Evans, D.F. (2001) Intestinal luminal pH in inflammatory bowel disease: possible determinants and implications for therapy with aminosaliculates and other drugs. *Gut* **48**, 571-577.
90. Orazzo, F., Nespoli, L., Ito, K., Tassinari, D., Giardina, D., Funis, M., Cecchi, A., Trapani, C., Forgeschi, G., Vignini, M., Nosetti, L., Pigna, S. and Zanobetti, A. (2009) Air Pollution, Aeroallergens, and Emergency Room Visits for Acute Respiratory Diseases and Gastroenteric Disorders among Young Children in Six Italian Cities. *Environmental Health Perspectives* **117**, 1780-1785.
91. Özel, R.E., Hayat, A., Wallace, K.N. and Andreescu, S. (2013) Effect of cerium oxide nanoparticles on intestinal serotonin in zebrafish. *RSC advances* **3**, 15298-15309.
92. Özel, R.E., Wallace, K.N. and Andreescu, S. (2014) Alterations of intestinal serotonin following nanoparticle exposure in embryonic zebrafish. *Environmental Science: Nano* **1**, 27-36.
93. Pelletier, D.A., Suresh, A.K., Holton, G.A., McKeown, C.K., Wang, W., Gu, B., Mortensen, N.P., Allison, D.P., Joy, D.C., Allison, M.R., Brown, S.D., Phelps, T.J. and Doktycz, M.J. (2010) Effects of Engineered Cerium Oxide Nanoparticles on Bacterial Growth and Viability. *Applied and Environmental Microbiology* **76**, 7981-7989.
94. Powell, J.J., Faria, N., Thomas-McKay, E. and Pele, L.C. (2010) Origin and fate of dietary nanoparticles and microparticles in the gastrointestinal tract. *Journal of Autoimmunity* **34**, J226-J233.
95. Rajilić-Stojanović, M., Maathuis, A., Heilig, H.G.H.J., Venema, K., de Vos, W.M. and Smidt, H. (2010) Evaluating the microbial diversity of an in vitro model of the human large intestine by phylogenetic microarray analysis. *Microbiology* **156**, 3270-3281.

96. Record Jr, M.T., Courtenay, E.S., Cayley, D.S. and Guttman, H.J. (1998) Responses of *E. coli* to osmotic stress: large changes in amounts of cytoplasmic solutes and water. *Trends in Biochemical Sciences* **23**, 143-148.
97. Reidy, B., Haase, A., Luch, A., Dawson, K. and Lynch, I. (2013) Mechanisms of Silver Nanoparticle Release, Transformation and Toxicity: A Critical Review of Current Knowledge and Recommendations for Future Studies and Applications. *Materials* **6**, 2295-2350.
98. Schäfer, A., Ustohal, P., Harms, H., Stauffer, F., Dracos, T. and Zehnder, A.J.B. (1998) Transport of bacteria in unsaturated porous media. *Journal of Contaminant Hydrology* **33**, 149-169.
99. Shvedova, A., Castranova, V., Kisin, E., Schwegler-Berry, D., Murray, A., Gandelsman, V., Maynard, A. and Baron, P. (2003) Exposure to Carbon Nanotube Material: Assessment of Nanotube Cytotoxicity using Human Keratinocyte Cells. *Journal of Toxicology and Environmental Health, Part A* **66**, 1909-1926.
100. Sunkara, L.T., Achanta, M., Schreiber, N.B., Bommineni, Y.R., Dai, G., Jiang, W., Lamont, S., Lillehoj, H.S., Beker, A. and Teeter, R.G. (2011) Butyrate enhances disease resistance of chickens by inducing antimicrobial host defense peptide gene expression. *PloS one* **6**, e27225.
101. Tazehkand, S.S., Torkzaban, S., Bradford, S.A. and Walker, S.L. (2008) Cell Preparation Methods Influence *Escherichia coli* D21g Surface Chemistry and Transport in Saturated Sand. *J Environ Qual* **37**, 2108-2115.
102. Thess, A., Lee, R., Nikolaev, P., Dai, H., Petit, P., Robert, J., Xu, C., Lee, Y.H., Kim, S.G. and Rinzler, A.G. (1996) Crystalline ropes of metallic carbon nanotubes. *Science-AAAS-Weekly Paper Edition* **273**, 483-487.
103. Thévenot, J., Etienne-Mesmin, L., Denis, S., Chalancon, S., Alric, M., Livrelli, V. and Blanquet-Diot, S. (2013) Enterohemorrhagic *Escherichia coli* O157:H7 Survival in an In Vitro Model of the Human Large Intestine and Interactions with Probiotic Yeasts and Resident Microbiota. *Applied and Environmental Microbiology* **79**, 1058-1064.
104. Thio, B.J.R., Zhou, D. and Keller, A.A. (2011) Influence of natural organic matter on the aggregation and deposition of titanium dioxide nanoparticles. *Journal of Hazardous Materials* **189**, 556-563.

105. Topping, D.L. and Clifton, P.M. (2001) *Short-Chain Fatty Acids and Human Colonic Function: Roles of Resistant Starch and Nonstarch Polysaccharides*.
106. Van den Abbeele, P., Grootaert, C., Marzorati, M., Possemiers, S., Verstraete, W., Gérard, P., Rabot, S., Bruneau, A., El Aidy, S., Derrien, M., Zoetendal, E., Kleerebezem, M., Smidt, H. and Van de Wiele, T. (2010) Microbial Community Development in a Dynamic Gut Model Is Reproducible, Colon Region Specific, and Selective for Bacteroidetes and Clostridium Cluster IX. *Applied and Environmental Microbiology* **76**, 5237-5246.
107. van der Werf, M.J. and Venema, K. (2000) Bifidobacteria: Genetic Modification and the Study of Their Role in the Colon. *Journal of Agricultural and Food Chemistry* **49**, 378-383.
108. van Herwaarden, A., Samsom, M. and Smout, A.J.P.M. (1999) 24-h Recording of Intra-gastric pH: Technical Aspects and Clinical Relevance. *Scandinavian Journal of Gastroenterology* **34**, 9-16.
109. van Herwaarden, M.S., A. J. P. M. Smout, M. (1999) 24-h Recording of Intra-gastric pH: Technical Aspects and Clinical Relevance. *Scandinavian Journal of Gastroenterology* **34**, 9-16.
110. Venema, K., van Nuenen, M.H.M.C., van den Heuvel, E.G., Pool, W. and van der Vossen, J.M.B.M. (2003) The Effect of Lactulose on the Composition of the Intestinal Microbiota and Short-chain Fatty Acid Production in Human Volunteers and a Computer-controlled Model of the Proximal Large Intestine. *Microbial Ecology in Health and Disease* **15**, 94-105.
111. Wallace, T.C., Guarner, F., Madsen, K., Cabana, M.D., Gibson, G., Hentges, E. and Sanders, M.E. (2011) Human gut microbiota and its relationship to health and disease. *Nutrition Reviews* **69**, 392-403.
112. Wang, P. and Keller, A.A. (2009) Natural and Engineered Nano and Colloidal Transport: Role of Zeta Potential in Prediction of Particle Deposition. *Langmuir* **25**, 6856-6862.
113. Weir, A., Westerhoff, P., Fabricius, L., Hristovski, K. and von Goetz, N. (2012) Titanium Dioxide Nanoparticles in Food and Personal Care Products. *Environmental Science & Technology* **46**, 2242-2250.

114. Wolf, R., Matz, H., Orion, E. and Lipozencić, J. (2003a) Sunscreens--the ultimate cosmetic. *Acta Dermatovenerol Croat* **11**, 158-162.
115. Wolf, R., Matz, H., Orion, E. and Lipozencić, J. (2003b) Sunscreens--the ultimate cosmetic. *Acta dermatovenerologica Croatica: ADC* **11**, 158.
116. Wong, J.M.W., de Souza, R., Kendall, C.W.C., Emam, A. and Jenkins, D.J.A. (2006) Colonic Health: Fermentation and Short Chain Fatty Acids. *Journal of Clinical Gastroenterology* **40**, 235-243.
117. Yamamoto, O. (2001) Influence of particle size on the antibacterial activity of zinc oxide. *International Journal of Inorganic Materials* **3**, 643-646.
118. Yang, Y. and Westerhoff, P. (2014) Presence in, and Release of, Nanomaterials from Consumer Products. In *Nanomaterial* eds. Capco, D.G. and Chen, Y. pp.1-17: Springer Netherlands.
119. Zeyons, O., Thill, A., Chauvat, F., Menguy, N., Cassier-Chauvat, C., Oréar, C., Daraspe, J., Auffan, M., Rose, J. and Spalla, O. (2009) Direct and indirect CeO₂ nanoparticles toxicity for Escherichia coli and Synechocystis. *Nanotoxicology* **3**, 284-295.

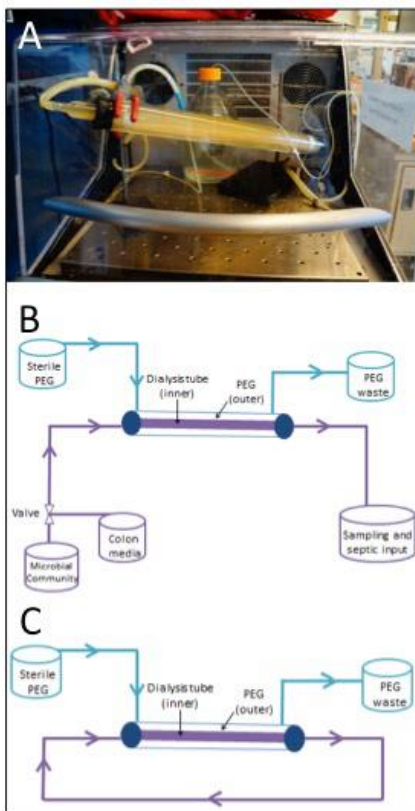
Supplemental Information for Chapter 2: Metal Oxide Nanoparticles Induce Phenotypic Changes in a Model Colon Gut Microbiota

Microbial community and model colon

A human colon was replicated by using a custom-built reactor¹¹⁵ which represented conditions inside of a proximal colon¹¹⁸ by maintaining the reactor at pH 5.5-7 and 37 °C inside an incubator (Barnstead MaxQ 4000; Thermo Scientific, Asheville, NC). The dialysis tube containing the microbial community and colon media inside of the reactor was encompassed by a polyethylene glycol (PEG) mixture, and the PEG was kept at a steady flow throughout the duration of the experiments as described previously⁹⁴. To mimic normal adult feedings, 100 mL of sterile colon media was pumped into the dialysis tubing three times per day, six hrs apart, with a rate of 5 mL/min⁹⁴. The colon media is not anaerobic or oxygen depleted⁹⁴.

FIG. S2.1.

Visual schematics of model colon system. (A) is a photograph of the model colon system inside of an incubator. Photo courtesy of A. Taylor. (B) is a diagram of the system during the Monday AM set-up and all feedings. The microbial community is added only on Monday AM. During all feedings the colon media is added. Colon media contains the nanoparticles during the appropriate exposure conditions. Both PEG waste and colon waste are located during the feedings. Not mentioned in the work, an additional study has used the colon waste as an input for a model septic system ^{115, 183}. (C) is the system during non-feeding times. The colon media circulates in a closed loop system.



Nanoparticle testing

To simulate conditions in the stomach and the potential of a low pH to alter the NPs physical-chemical properties before entering the intestines, additional controls monitored changes to the NPs as a function of pH. These control tests were conducted in tests outside of the colon reactor. Controls were conducted in sterile 1000 mL lidded flasks with 500 mL of sterile colon media. Controls consisted of the following combinations: colon media only or colon media with one of the NPs at the following concentrations: 0.01 μg ZnO NP/L, 0.01 μg CeO₂ NP/L, or 3 mg TiO₂ NP/L. Controls were also conducted with and without the microbial community. Controls with the microbial community were inoculated in the same manner and proportion as the colon reactor. Samples were collected from the batch tests at 0, 30, 60 min, and 24 hrs using a range of pH 2-8 at 0.5 increments¹⁸⁴⁻¹⁸⁶ and were measured in triplicate for the following tests: zeta potential, and hydrophobicity. These tests were performed in an identical manner to the washed bacteria cell samples from the colon effluent. Multiple control tests were conducted over a range of pH 2-8 at 0.5 increments.

Phenotypic characterization of microbial community

Cell concentration of the washed colon effluent cells was determined using a cell counting chamber¹⁸⁷, (BuerkerTürk chamber, Marienfeld Laboratory Glassware, Lauda-Königshofen, Germany) and a light microscope (Fisher Scientific Micromaster, Pittsburgh, PA). EPS (extracellular polymeric substance) was measured as total protein and total sugar by a multi-step process: fixation of cells in 0.22% formaldehyde solution,

separation via centrifugation, lyophilization, and finally colorimetric measurements following published methods ¹⁸⁸. The extraction process used here analyzes the EPS bound to the cell rather than the free EPS found in the colon effluent, which is removed via centrifugation. A zeta potential analyzer (ZetaPALS, Brookhaven Instruments Corp., Holtsville, NY) measured the EPM (electrophoretic mobility) of the washed cells ¹³⁹. A microbial adhesion to hydrocarbon (MATH) test quantified partitioning of cells into the hydrocarbon versus the KCl solution (electrolyte phase) and gave a measure of relative hydrophobicity ¹⁸⁹⁻¹⁹⁰. Cell size was established by capturing images taken of the washed bacteria in the KCl solution using a phase contrast microscope (Fisher Scientific Micromaster, Pittsburgh, PA), camera (Westover Scientific Digital MCD Model 2200), and imaging software (MicronUSB2 v. 1.09). Images containing $n > 50$ cells were then processed with Matlab (version 7.11.0.584 R2010b, The MathWorks, Inc., Natick, MA) in which cell radius, length, and width were confirmed ¹³³⁻¹³⁴. Many current studies in the literature have successfully used bacterial and enzymatic characterization tests in complex medias with the presence of NPs ¹⁹¹⁻¹⁹⁵. Due to the estimated low concentrations of NPs present in the bacterial cell solution prior to the washing and centrifugation steps (~0.0005 μg ZnO or CeO₂/45 mL washed bacterial solution, and 0.015 mg TiO₂/45 mL washed bacterial solution), it is therefore highly unlikely that NPs caused interference with tests.

Results

Data from Figure 1A, 1B, and 1C and from Figure 2A and 2B are displayed below per daily values.

FIG. S2.

Comparison of the production of butyric acid over the five-day long experiments in the model colon in the presence and absence of TiO₂, CeO₂, and ZnO NPs. SCFA samples were collected twice a day for a minimum of two weeks and analyzed in triplicate with GC-FID. Each data point is an average of data that was collected over the course of two experimental runs (two five-day long experiments) with samples in triplicate collected twice a day. Error bars indicate standard deviation.

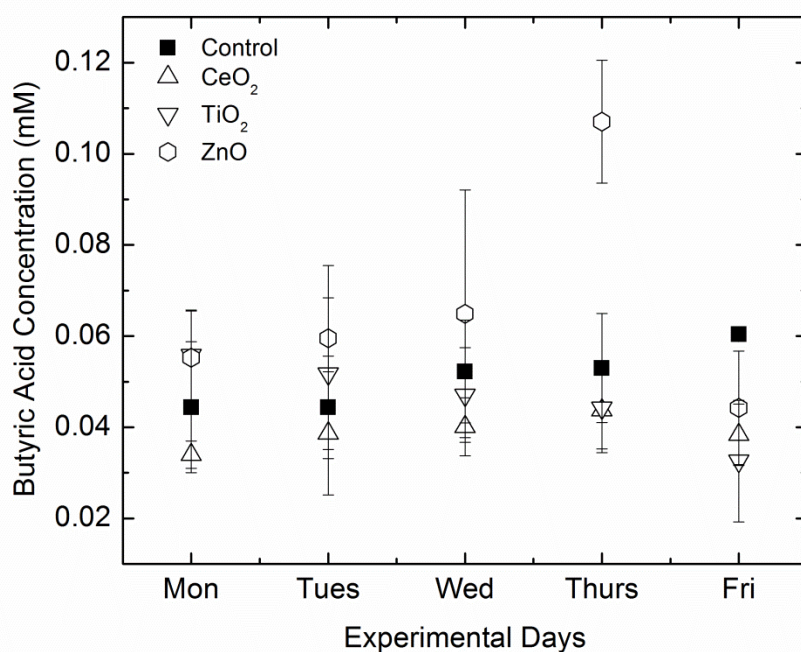


FIG. S3.

Comparison of the production of acetic acid over the five-day long experiments in the model colon in the presence and absence of TiO₂, CeO₂, and ZnO NPs. SCFA samples were collected twice a day for a minimum of two weeks and analyzed in triplicate with GC-FID. Each data point is an average data that was collected over the course of two experimental runs (two five-day long experiments) with samples in triplicate collected twice a day. Error bars indicate standard deviation.

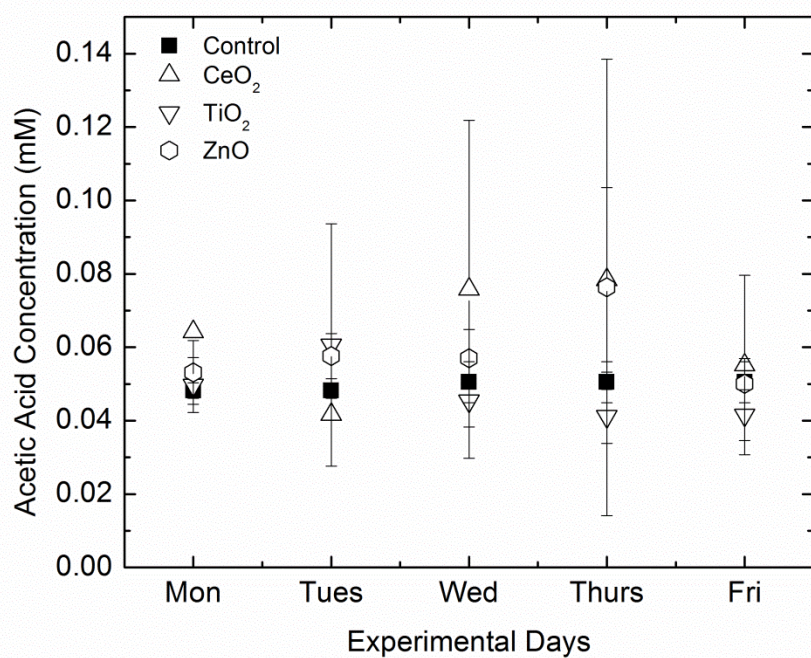


FIG. S4.

Hydrophobicity of the bacterial cells is displayed as a function of NP exposure in the model colon during the two runs of the five-day long experiments. Data is displayed per experimental day. Hydrophobicity was measured twice a day in triplicates. All measurements were made on washed cells from the colon effluent. Error bars indicate standard deviation.

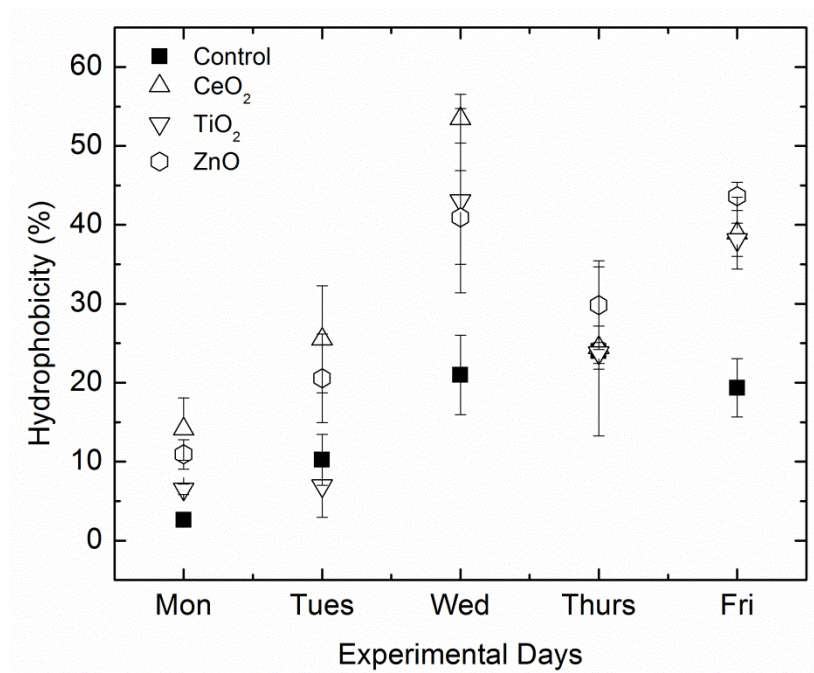


FIG. S5.

Electrophoretic mobility (EPM), an indicator of the relative surface charge, of the bacterial cells was measured in triplicate twice a day during the course of two runs of the five-day long experiments. All measurements were made on washed cells from the colon effluent. Error bars indicate standard deviation.

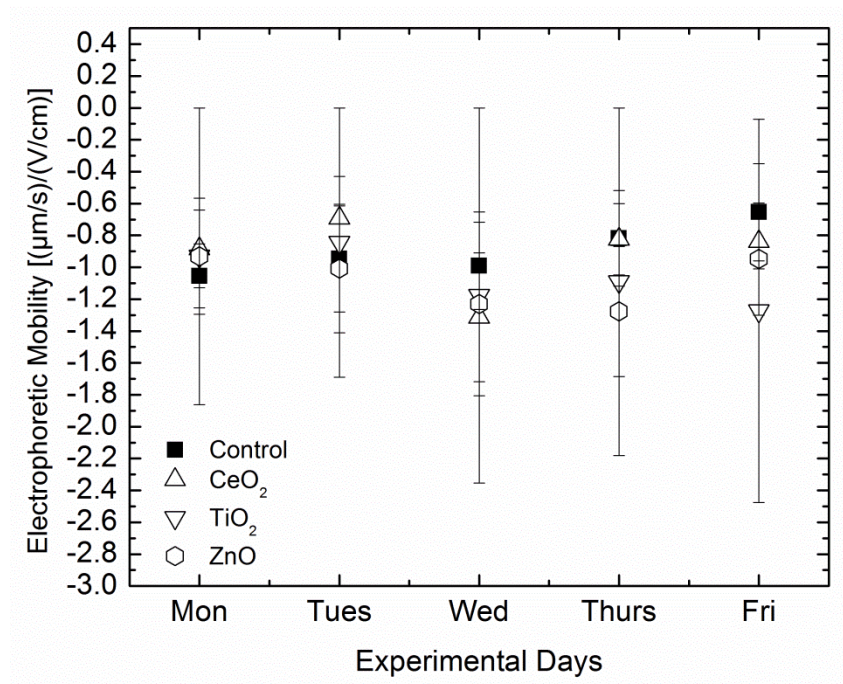


FIG. S6.

The average protein content of the extracellular polymeric substance (EPS) was measured in triplicate once a day during the course of the five-day long experiments for a minimum of two runs (two five-day long experiments). EPS samples were collected once a day from the colon effluent and analyzed for sugar and protein content in triplicate. Error bars indicate standard deviation.

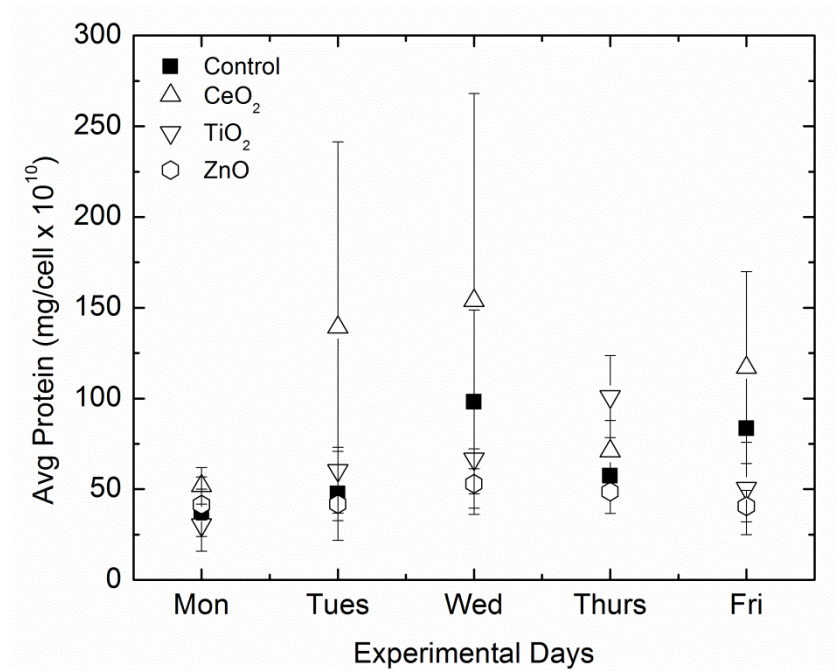
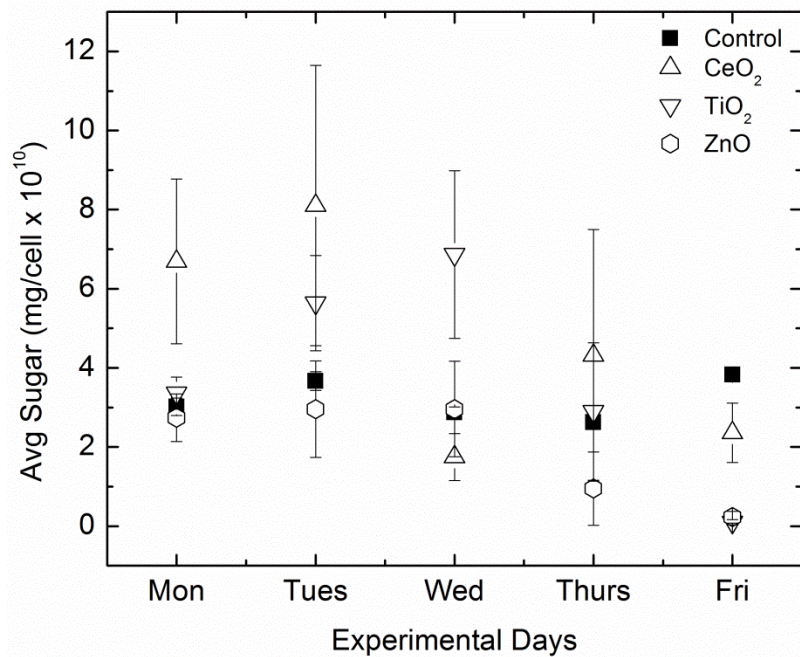


FIG. S7.

The average sugar content of the extracellular polymeric substance (EPS) was measured in triplicate once a day during the course of the five-day long experiments for a minimum of two runs (two five-day long experiments). EPS samples were collected once a day from the colon effluent and analyzed for sugar and protein content in triplicate. Error bars indicate standard deviation.



References

1. Adeleye, A. S., Conway, J. R., Perez, T., Rutten, P., and Keller, A. A. (2014). Influence of Extracellular Polymeric Substances on the Long-Term Fate, Dissolution, and Speciation of Copper-Based Nanoparticles. *Environmental Science & Technology* **48**(21), 12561-12568.
2. Fallingborg, J. (1999). Intraluminal pH of the human gastrointestinal tract. *Danish medical bulletin* **46**(3), 183-196.
3. Ge, Y., Priester, J. H., Van De Werfhorst, L. C., Walker, S. L., Nisbet, R. M., An, Y.-J., Schimel, J. P., Gardea-Torresdey, J. L., and Holden, P. A. (2014). Soybean Plants Modify Metal Oxide Nanoparticle Effects on Soil Bacterial Communities. *Environmental Science & Technology* **48**(22), 13489-13496.
4. Gong, A., Bolster, C., Benavides, M., and Walker, S. (2009). Extraction and Analysis of Extracellular Polymeric Substances: Comparison of Methods and Extracellular Polymeric Substance Levels in *Salmonella pullorum* SA 1685. *Environmental Engineering Science* **26**(10), 1523-1532.
5. Gong, A. S., Lanzl, C. A., Cwiertny, D. M., and Walker, S. L. (2011). Lack of Influence of Extracellular Polymeric Substances (EPS) Level on Hydroxyl Radical Mediated Disinfection of *Escherichia coli*. *Environmental Science & Technology* **46**(1), 241-249.
6. Hong, J., Rico, C. M., Zhao, L., Adeleye, A. S., Keller, A. A., Peralta-Videa, J. R., and Gardea-Torresdey, J. L. (2015). Toxic effects of copper-based nanoparticles or compounds to lettuce (*Lactuca sativa*) and alfalfa (*Medicago sativa*). *Environmental Science: Processes & Impacts* **17**(1), 177-185.
7. Jiménez-Vera, R., Monroy, O., Corona-Cruz, A., and García-Garibay, M. (2008). Construction of a model of the human proximal colon. *World Journal of Microbiology and Biotechnology* **24**(12), 2767-2774.
8. Kim, E. R., and Rhee, P.-L. (2012). How to interpret a functional or motility test-colon transit study. *Journal of neurogastroenterology and motility* **18**(1), 94-99.
9. Marcus, I. M., Bolster, C. H., Cook, K. L., Opot, S. R., and Walker, S. L. (2012a). Impact of growth conditions on transport behavior of *E. coli*. *Journal of Environmental Monitoring* **14**(3), 984-991.

10. Marcus, I. M., Herzberg, M., Walker, S. L., and Freger, V. (2012b). *Pseudomonas aeruginosa* Attachment on QCM-D Sensors: The Role of Cell and Surface Hydrophobicities. *Langmuir* **28**(15), 6396-6402.
11. Marcus, I. M., Wilder, H. A., Quazi, S. J., and Walker, S. L. (2013). Linking Microbial Community Structure to Function in Representative Simulated Systems. *Applied and Environmental Microbiology* **79**(8), 2552-2559.
12. Mojaverian, P. (1996). Evaluation of gastrointestinal pH and gastric residence time via the Heidelberg radiotelemetry capsule: Pharmaceutical application. *Drug Development Research* **38**(2), 73-85.
13. Nugent, S. G., Kumar, D., Rampton, D. S., and Evans, D. F. (2001). Intestinal luminal pH in inflammatory bowel disease: possible determinants and implications for therapy with aminosalicylates and other drugs. *Gut* **48**(4), 571-577.
14. Priester, J., Ge, Y., Chang, V., Stoimenov, P., Schimel, J., Stucky, G., and Holden, P. (2013). Assessing interactions of hydrophilic nanoscale TiO₂ with soil water. *Journal of Nanoparticle Research* **15**(9), 1-13.
15. Priester, J. H., Van De Werfhorst, L. C., Ge, Y., Adeleye, A. S., Tomar, S., Tom, L. M., Piceno, Y. M., Andersen, G. L., and Holden, P. A. (2014). Effects of TiO₂ and Ag Nanoparticles on Polyhydroxybutyrate Biosynthesis By Activated Sludge Bacteria. *Environmental Science & Technology* **48**(24), 14712-14720.
16. Taylor, A. A., and Walker, S. L. (2014). Effects of Copper Particles on a Model Septic System's Function and Microbial Community. *Environmental Science: Water Research & Technology*, in review.
17. Tazehkand, S. S., Torkzaban, S., Bradford, S. A., and Walker, S. L. (2008). Cell Preparation Methods Influence *Escherichia coli* D21g Surface Chemistry and Transport in Saturated Sand. *J. Environ. Qual.* **37**(6), 2108-2115.
18. Walker, S. L., Hill, J. E., Redman, J. A., and Elimelech, M. (2005). Influence of Growth Phase on Adhesion Kinetics of *Escherichia coli* D21g. *Applied and Environmental Microbiology* **71**(6), 3093-3099.
19. Walker, S. L., Redman, J. A., and Elimelech, M. (2005). Influence of Growth Phase on Bacterial Deposition: Interaction Mechanisms in Packed-Bed Column and Radial Stagnation Point Flow Systems. *Environmental Science & Technology* **39**(17), 6405-6411.

Chapter 3

Effects of Copper Particles on a Model Septic System's Function and Microbial Community

In Review at *Environmental Science: Water Research & Technology*

Taylor, A.A. and S.L. Walker

Chapter 3: Effects of Copper Particles on a Model Septic System's Function and Microbial Community

Abstract

There is concern surrounding the incorporation of nanoparticles into consumer products due to potential for toxicity and the increased risk of human and environmental exposures to these particles. Copper nanoparticles are found in many common consumer goods; therefore, the disposal and subsequent interactions between potentially toxic Cu-based nanoparticles and microbial communities may have detrimental impacts on wastewater treatment processes. This study investigates the effects of three copper particles (micron- and nano-scale Cu particles, and nano-scale $\text{Cu}(\text{OH})_2$ -based fungicide) on the function and operation of a model septic tank. Septic system analyses included water quality evaluation and microbial community characterization to detect changes in and relationships between the septic tank function and microbial community phenotype/genotype. As would be expected for optimal wastewater treatment, biological oxygen demand (BOD_5) was reduced by at least 63% during exposure to nano-scale Cu. A reduction in the pH occurred which was below the optimum anaerobic fermentation range during the micro Cu exposure, indicating that the organic waste may have undergone incomplete degradation. The copper fungicide, $\text{Cu}(\text{OH})_2$, caused an increase in total organic carbon (TOC) above the typical range for septic systems, which corresponded to increased BOD_5 during the majority of the $\text{Cu}(\text{OH})_2$ exposure. The changes in TOC and BOD_5 also demonstrate that the system was improperly treating waste. Overall, results imply individual exposures to the three Cu particles caused distinct

disruptions in septic tank function. However, it was observed that the system was able to recover to typical operating conditions after three weeks post-exposure. These results suggest that during periods of Cu introduction, there are likely pulses of improper waste treatment and incomplete organic breakdown.

Introduction

The release of engineered nanomaterials is an emerging ecological concern because initial studies indicate significant toxicity to multiple species including bacteria, mice, fish, and humans.¹⁹⁶⁻¹⁹⁹ . These nanomaterials may be released from consumer products into the environment at any point of a product's life, from manufacture to disposal.

Nanoparticles are becoming more prevalent in common consumer goods such as foods and cosmetics. These particles are likely to enter household drains from the disposal and use of consumer products, and ultimately, may be released from wastewater treatment plants (WWTPs) into the environment.^{31-32, 44} Therefore, understanding the interactions between nanomaterials and bacteria in engineered systems (e.g. laboratory-scale septic tank) can indicate the consequences of nanomaterials on wastewater treatment processes and the potential for environmental release. Here, the effect of nanoparticles on the function and operation of a septic tank will be investigated. Improperly functioning septic systems can result in groundwater contamination and disease outbreaks.^{62, 200-201}

A septic tank, which is an onsite, decentralized wastewater system,²⁰² was chosen for the nanoparticle exposure experiments because it is estimated that 20-30% of American households have this type of onsite treatment method, and a projected 25% of predicted planned developments will also use septic tanks for waste disposal.²⁰²⁻²⁰³ Additionally, 26% of households in Europe and 20% of Australian households also use septic systems.^{62, 204} It is critical that the function of these systems is maintained for sanitation and health. Essentially, the septic tank provides a waste separation process between the sludge, the floating material, and the wastewater in an anaerobic

environment in which digestion of the sludge and floating material occurs.⁵⁷ To date, no such studies have been performed to assess the effect of nanoparticles and septic system function.

Nanoparticles have been detected in municipal wastewater treatment systems,^{37, 46} and therefore, nanoparticles are also likely being introduced into onsite septic systems. At one sampling site, the raw sewage from a wastewater treatment plant (WWTP) contained 100-3000 µg/L of nano and larger-sized Titanium which was also absorbed in sludge biomass.³⁷ Additionally, many studies have looked at nanoparticle behavior in WWTPs: aggregation, removal efficiency, and fate, as well as the effects of NPs on wastewater biofilms, which in turn may affect the removal of nitrogen and phosphorus.⁴⁷⁻⁵⁶ Recently, published work has highlighted the predicted fate of nanomaterials in the environment. It is predicted that up to 22-200 metric tons/year of Cu and CuO_x are produced, with approximately 37 metric tons/year entering WWTPs.^{31, 38} Concentrations of 0.03 µg Cu/L may be present in WWTP effluent and up to 0.24 µg Cu/L is in biosolids.^{31, 38} In the San Francisco Bay region, it is predicted that 0.05 µg Cu/L is found in WWTP effluent and between 0.01 – 0.5 mg Cu/kg is in biosolids.³² Since many nanoparticle toxicity and transport studies are conducted in idealized lab settings,^{166, 205-206} little is known on how realistic conditions that are found in a septic tank may alter their physical-chemical characteristics. These changes will affect nanoparticle ion release or toxicity, with the potential end result of an improperly functioning septic tank.

Copper nanoparticles (Cu NPs) were chosen for introduction into the model septic tank in this work because Cu NPs are one of the most commonly used nanoparticle types.

Cu NPs are used in a wide range of applications including electronics, ceramics, inks, polymers, films, coatings, fungicides, cosmetics and personal care products, and other metal containing products.⁴¹⁻⁴³ Cu NPs are also used as a bacteriocide,⁴⁰ which can be incorporated into coatings, plastics, paints, and textiles. Recent work has shown Cu to be found in personal care products, and the predicted fate of these particles are WWTPs.⁴⁴⁻⁴⁵ Another source of copper into septic tanks, besides from personal care products, may be through the leaching of copper from household pipes.²⁰⁷⁻²⁰⁸ These common sources of nanoparticles and their potential impact to septic system operation are a concern since treated effluent from a decentralized treatment process is emitted directly into a soil leachfield and groundwater.^{60, 202-203, 209-210}

Under the Clean Water Act, the Environmental Protection Agency (EPA) regulates discharges into surface waters with the National Pollutant Discharge Elimination System (NPDES). This includes discharge from WWTPs, which is highly regulated.⁵⁸⁻⁶¹ However, septic systems are not regulated by the national government in the same manner as WWTPs. Septic tanks are typically regulated by local and state governments, which includes regulations covering septic tank design and installation permits,²¹⁰ and any associated inspections. Yet, the maintenance and operation of a septic tank for a single family home is most often left to the care and judgment of the homeowner.⁵⁷ As only 40% of all septic tanks are estimated to be properly functioning⁵⁷ it can be inferred that overall, septic tanks are indeed technically regulated, but the management and regular monitoring of septic tanks are not practically enforced.

Due to the lack of consistent monitoring of septic tanks, it is hypothesized that nanoparticles entering septic systems from the disposal of common consumer products via household drains may cause unknown, deleterious effects on the function and operation of the septic tank, resulting in either the release of untreated waste or nanoparticles into the groundwater. This work was developed to evaluate the impact of nanoparticle exposure on the septic tank, specifically, to (1) determine if exposure leads to deviation from baseline conditions and (2) to establish if Cu particles cause septic systems to insufficiently and unreliably treat wastewater. Tracking changes in septic tank influent and effluent using traditional wastewater quality tests, microbial community characterization, and microbial community sequencing allowed for the assessment of septic tank performance per Cu particle introduction. First, the baseline conditions of the septic system were defined, and subsequent impacts caused by the various Cu forms added in the system were measured. This work will have meaningful implications for improving wastewater treatment and for updating regulations for both WWTPs and decentralized septic systems.

Materials and Methods

Model Septic System

The septic system used for these experiments was developed and reported on previously.¹¹⁵ Details on the system and a digital image of the septic system are found in the supporting information (SI, Figure S1). Briefly, the influent added to the septic tank is

composed of three components: deionized water (DI H₂O), synthetic greywater, and colon waste.¹¹⁵ The composition of the colon waste and synthetic greywater is listed in the SI.

Nanoparticle Selection

Cu particles were chosen for this study as a potential perturbation in a septic tank system. The purpose of this work was to characterize the responses within the septic system, rather than to characterize the Cu materials. Specific characterization details such as size and purity are more thoroughly addressed in the SI and are from previous work.²¹¹ All Cu particles (nano Cu, micro Cu, and Cu(OH)₂) have been obtained through collaboration with the University of California Center for Environmental Implications of Nanotechnology (UC-CEIN) and were investigated because copper nanoparticles are thought to be an environmentally significant contaminant through pesticide application, personal products, and boat paints.⁴⁰⁻⁴³ The three Cu particles were manufactured by US Research Nanomaterials, Inc. (nano Cu), Sigma Aldrich (micro Cu), and TreeGeek (Cu(OH)₂). These three model particles were chosen to elicit effects between the nano-scale size (nano Cu), control bulk-size (micro Cu), and a nano-scale fungicide commercial product (Cu(OH)₂). Previous work conducted with these particles has measured the degree of dissolution, with nano Cu and Cu(OH)₂ being more soluble (>8 wt% dissolution) than micro Cu (<2 wt% dissolution).²¹¹

For the three individual septic tank experiments, 100 mg of the chosen Cu particle was added once per day during five consecutive weekdays, for three weeks, for a total of 1500 mg of the Cu particle per experiment. This equated to a final concentration of 10 ppm over the course of three weeks with the assumption of equal distribution in the primary and secondary chambers. 10 ppm was chosen based upon predicted concentrations of Cu found in WWTPs.^{31-32, 38} Three individual experiments (one experiment per Cu particle) were conducted in the system and consisted of: four weeks of baseline (no Cu), three weeks of Cu addition (total of 1500 mg denoted as Cu weeks 1-3), followed by three weeks where Cu was no longer added to the system (denoted as post-Cu weeks 1-3). The system was dismantled and cleaned between each experiment. More details on the Cu particle dosing procedure of the septic system are listed in the SI.

Water Quality Tests

For brevity, the water quality methodology and the water quality sampling schedule (Table S1) are presented in detail in the SI. Water quality tests include pH, total organic carbon, turbidity, and total suspended solids. These specific water quality tests were selected because they are traditionally associated with monitoring both WWTPs and septic tank systems.^{57, 212-213} Therefore, using literature values as a comparison, these tests were used to compare observable changes to the accepted reported literature values. This also allowed for ensuring the measured range in the system was within reason of the reported values. Additional water quality tests (alkalinity, conductivity, and hardness)

were also measured with the system but are reported in another study that determined the transformation of Cu particles and subsequent alterations on Cu toxicity.²¹¹

Bacteria Characterization

Microbial characterization techniques were selected based upon previous work with environmental microbial isolates and communities.^{115, 214} All microbial community testing for this study was conducted as reported in a prior study with the model septic system.¹¹⁵ Electrophoretic mobility (EPM, a surrogate for relative cell surface charge), hydrophobicity, cell concentration and cell size were measured from cells emitted in the effluent. The purpose of the bacteria characterization was to monitor changes in the microbial community as a function of the copper particle exposure. For consistency, all microbial characterization experiments were conducted once a week on the same day in triplicate. More details on the bacteria characterization tests, further methods and the sampling schedule (Table S1), are located in the SI.

Bacteria Community Metabolism and Sequencing

In this study, two main microbial community analyses were conducted. These tests were used as indirect analyses of microbial activity. The first test was a traditional method to detect biological activity and is a traditional water quality test, the five-day biological oxygen demand (BOD₅) test, and selected as a microbial metabolic activity indicator.

Effluent BOD₅ was determined by assessing the loss of dissolved oxygen (DO) by measuring initial DO (hour 0) and final DO (hour 120) using a DO probe (Thermo Electron corporation Model 033005D) with a standard protocol.²¹⁵ Regardless of whether the system is under aerobic or anaerobic conditions, this test is an excellent indicator of the amount of organic material present in the system.²¹⁶ For more detail on the BOD₅ protocol and the septic sampling schedule (Table S1), please refer to the SI.

The second microbial community analysis conducted was pyrosequencing to evaluate the microbial community “fingerprint”. Extraction, preparation, and pyrosequencing of all microbial samples collected from the septic system were followed exactly as in previous research with this model septic system.¹¹⁵ Additional details on the methods used for sequencing are located in the SI.

Copper Analysis

The amount of bioavailable or free Cu²⁺ ions emitted in the effluent from the septic system was determined using an Orion™ cupric solid state half-cell ion specific electrode (Cu ISE, Thermo Scientific), an Orion™ double junction Sure-Flow™ reference electrode (Thermo Scientific), and an Orion Star™ A214 pH/ISE meter (Thermo Scientific). This measurement did not include any Cu²⁺ ions bound to organic matter and inorganic species.²¹⁷⁻²¹⁸ Further information is provided in the SI on the calibrations, concentrations, and sample preparation.

Statistical Analyses

Statistical analyses were conducted individually for each parameter mentioned in the material and methods (e.g., all water quality tests, bacteria characterizations, and community sequencing) to identify significant trends as a function of Cu exposure and type. A Student t test was used and if P values were <0.05 , the data was considered significant. Data was analyzed on a per week basis. All experimental conditions (Cu weeks 1-3, post-Cu weeks 1-3) were individually compared to the baseline conditions. A student t test was also run on grouped data (e.g., all baseline weeks vs Cu weeks 1-3, and baseline weeks vs post-Cu weeks 1-3). All data values collected and used in statistical analyses are presented in Table S2. Statistical analyses were conducted with Excel 2011 (v.14.3.9, Microsoft, Redmond, WA) and with StatPlus®:mac LE.2009 (v.5.8.2.0, AnalystSoft Inc.).

Results

Four water quality tests (pH, total organic carbon, turbidity, and total suspended solids) commonly used to evaluate effluent quality from WWTPs and septic tanks were used in this study.^{62, 67-68, 219-220} These tests were selected because they are commonly used in WWTPs and decentralized waste treatment systems such as septic tanks.^{57, 65, 115, 212-213} Also, these tests are used for the regulation and monitoring purposes of these systems.^{203, 212} Therefore, the model septic tank's function can be verified using these traditional monitoring tools.

Tests were also selected to characterize the changes in the microbial community phenotype, metabolic activity, and community structure (cell hydrophobicity, electrophoretic mobility, cell size, cell concentration, BOD₅, and DNA sequencing) in the model septic system. The baseline data determined if there were any statistically significant deviation in operating parameters when compared to the Cu and post-Cu exposures. For all results, the baseline weeks (no Cu present in the system) were statistically the same ($P < 0.05$). Therefore, all baseline data was averaged for the sake of comparison to other experimental conditions with the Cu particles.

The purpose of the three weeks of analysis after the Cu addition (post-Cu weeks 1-3) was to determine if the effluent quality would return to values recorded during the baseline period. If the system returns to baseline values post-Cu exposure, this indicates that the system was able to re-establish its function. Because Cu and nano-scale Cu are known to have antibacterial effects, immediate changes, such as a loss of septic system function, are anticipated during the Cu exposure weeks (Cu weeks 1-3).²²¹⁻²²² The septic system was considered to undergo a loss of function if the Cu exposure (Cu weeks 1-3) or post-copper exposure conditions (post-Cu weeks 1-3) were not statistically identical to the baseline, and by comparisons to known septic system performance.^{62, 67-68, 212-213, 223} But, because of the three week residence time in septic systems,¹¹⁵ only the final copper exposure week, (post-Cu week 3) was analyzed with statistical tests and presented in the results (post-Cu weeks 1 and 2 values can be found in Table S2). This is because recovery of the microbial community was anticipated to be associated with the residence time of the system. Additionally, for ease of comparison and clarity, in each figure a

shaded box has been added to indicate the typical operating values for septic systems.²¹²⁻

²¹³ The results will be discussed below for each type of Cu particle added.

Baseline Conditions in the Septic System

The purpose of the baseline weeks and measurements was to establish the typical values during normal operating conditions without the presence of a disturbance, such as Cu. Water quality measurements, pH, TOC, and turbidity are found in Figure 1A-1C. For pH, the baseline effluent value was 7.0 ± 0.1 and the influent pH value was 7.6 ± 0.2 . The typical range for pH septic tank effluent is anticipated to be between 6.7-7.6.²¹²⁻²¹³ Due to consistency of the influent material, the influent pH remained constant at $\text{pH } 7.6 \pm 0.2$. For TOC, the baseline effluent average value was 54.8 ± 17.7 mg/L. The average influent TOC value was 89.1 ± 28.3 mg/L and was consistent for all experiments. Excepted effluent TOC values for a properly functioning septic tank are between 50-350 mg/L.²¹²⁻

²¹³ Turbidity is used here as an indirect measurement to determine mobilization of sludge, incomplete digestion of waste or higher loads of TSS in the effluent. Turbidity is determined by comparing the intensity of scattered light of the sample to standard reference materials.²¹⁵ Higher scattering indicates higher turbidity. Turbidity measurements are not a common test used for regulation purposes within a septic system. Here, a reference value for the system was designated for this work by using the National Primary Drinking Water Regulations for surface water treatment with nonconventional filtration.²²⁴ Based upon this regulation, typical effluent turbidity values for baseline

conditions in the septic tank were defined as <5 Nephelometric Turbidity Units (NTU). However, the average baseline effluent turbidity value was 11.3 ± 1.1 NTU. This value was expected to be higher than 5 NTU since drinking water and septic tank treatments have differing standards of regulation for amounts of total suspended solids. The turbidity influent value for all experiments was 78.5 ± 3.7 NTU (Figure 1C), and is in the range for expected influent values for household greywater which is 22-72 NTU.²²⁵ The TSS effluent baseline average value was 52.7 ± 7.6 mg/L (Figure S3). The TSS influent value was 57.0 ± 2.9 mg/L. TSS ranges from 40-140 mg/L in effluent,²¹³ with a removal efficiency of 60-80% expected.²²⁶⁻²²⁷ During baseline conditions, only an 8% reduction occurred from the influent to the effluent for TSS. BOD₅ (Figure 2B) baseline effluent was 82.0 ± 5.6 mg/L and the influent BOD₅ value was 127.0 ± 0.0 mg/L. BOD was reduced by ~35% in baseline conditions. A 30-50% reduction is anticipated for BOD₅ in real world septic tanks.²¹²⁻²¹³ The standard range for BOD₅ in a septic system has been reported between 35-200 mg/L.²¹²⁻²¹³

The microbial community structure was determined using pyrosequencing. The purpose of this was to determine the changes in the structure that the community experienced as a function of Cu particle exposure when compared to the baseline community structure. The baseline condition for the microbial community structure at the phyla level for all Cu experiments was as follows: Proteobacteria 83.9%, Firmicutes 4.2%, and Bacteroidetes 12.5% (Figure 2A). The Cu analysis using the Cu ion specific electrode will be discussed as a whole below in the Copper Analysis Results section.

Impact Nano Cu

The nano-scale Cu caused multiple effects on the effluent water quality and microbial community. The septic tank pH values during and following copper addition were between pH 6.8-7.2 and did not significantly change from the baseline pH ($\text{pH} = 7.0 \pm 0.1$, Figure 1A). These values during and after the Cu exposure are within the accepted range (6.7-7.6) of septic tank pH values.²¹²⁻²¹³ The final experimental week (post-Cu week 3) following exposure had a pH of 6.7 ± 0.0 .

The only significant TOC values during the nano Cu experiment (Figure 1B) were during nano Cu week 2 where a decrease in TOC ($16.7 \pm 0.2 \text{ mg/L}$) occurred and during the post-nano C week 3 condition with an increase in TOC occurred ($91.1 \pm 4.0 \text{ mg/L}$) when compared to the TOC average baseline condition ($54.8 \pm 17.7 \text{ mg/L}$, $P < 0.0001$). TOC was considered to maintain the baseline conditions for all other nano Cu experimental weeks. The 16.7 mg/L value was the lowest TOC value for all experimental conditions with all Cu particles. While the final week in the post-nano Cu exposure condition does have a significantly higher value than the baseline (91.1 mg/L vs. 54.8 mg/L), all TOC values for the nano Cu exposure were within anticipated levels for septic system function.²¹²⁻²¹³

The turbidity values (Figure 1C) for the nano Cu experiment show fluctuations during the nano Cu exposure weeks (nano Cu weeks 1-3, $2.5\text{-}4.6 \pm 0.4 \text{ NTU}$). Turbidity during the nano Cu exposure was significantly lower than the baseline and post-nano Cu exposure conditions ($P < 0.0005$). The baseline turbidity value for all experimental

conditions was 11.3 ± 1.1 NTU and the final post-nano Cu exposure value was 10.0 ± 0.1 NTU. There were not significant TSS data for any of the Cu particles, although the nano Cu exposure did show a decrease over time from the nano Cu exposure (TSS during nano Cu exposure weeks 1-3 was $38.1-41.6 \pm 10.4$ mg/L) to the final post-nano Cu exposure week (TSS 29.0 ± 10.6 mg/L). TSS values were well below the anticipated range (40-140 mg/L) for TSS in septic tank effluent²¹³ and a 28-49% reduction occurred from the influent to the effluent for the three nano Cu exposure weeks and for the final post exposure week.

The lowest BOD₅ value recorded for the nano Cu experiment was during week 1 of the nano Cu exposures (34.0 ± 6.4 mg/L, Figure 2B). For all conditions (baseline, nano Cu exposure, and post-nano Cu exposure), the BOD₅ experienced a significant reduction ranging from 35-73%.

Microbial community phenotype can be affected by perturbances in aquatic systems.¹¹⁵ Therefore, because septic system function is linked directly to metabolic activity of the microbial community, changes occurring to the community phenotype were used as non-traditional indicators of the system's function. Results for the bacteria characterization tests (hydrophobicity, electrophoretic mobility, cell size, and cell concentration) are presented in the SI and in Figure S2. While the bacteria characterization did not overall have meaningful trends or any correlation with changes in the water quality tests, significant changes did occur. For example, cell hydrophobicity increased during the nano Cu exposure ($64.4 \pm 0.3\%$) when compared to the baseline

(24.3-45.8 ± 0.6-5.0%) and had the highest hydrophobicity values for any Cu exposure (SI).

Here, pyrosequencing was used to investigate how Cu particles alter the microbial community structure, which has important implications in wastewater processing.²²⁸ This study is not the first to observe changes in the microbial community structure at the phyla level. In fact, many studies have reported changes at the phyla level and suggested analysis at this taxonomic group as a monitoring tool for various types of wastewater treatment.²²⁸⁻²³¹ For the sequencing data in this study, the following phyla, Acidobacteria, Actinobacteria, Chloroflexi, Synergistetes, and Cyanobacteria were not statistically analyzed in the community structure because when combined, these three phyla made up less than 1% of the community structure for all experimental conditions and weeks. The baseline condition for the microbial community structure for all Cu experiments was as follows: Proteobacteria 83.9%, Firmicutes 4.2%, and Bacteroidetes 12.5%. Only one phylum, Firmicutes, had a significant change during the course of the nano Cu experiment (Figure 2A). The amount of Firmicutes (4.2%) present in baseline conditions significantly increased during nano Cu exposures (nano Cu weeks 1-3, 11.1-19.8%, P=0.003) and Proteobacteria decreased from 83% in the baseline to between 67.3-76.7% in during the majority of the nano Cu exposures and during the final week of the post exposure condition (nano Cu weeks 2 and 3, and post-nano Cu week 3). However, all other changes in the community other than the percent changes in the Firmicutes were not significant.

Impact of Micro Cu

The micron-scale Cu caused numerous deviations in the measured effluent water quality (pH, BOD₅, and turbidity) from the baseline septic tank values (Figure 1). Over the three weeks of micro Cu addition, pH was significantly lower than the baseline average (pH 7.0 ± 0.1 , Figure 1A). For example, after the initial week of copper introduction, the pH (6.3 ± 0.1) was significantly lower than the average baseline value (pH 7.0 ± 0.1 , $P < 0.001$). In the second and third weeks (pH 6.6 ± 0.1 and 6.7 ± 0.1 , respectively) the pH was also below typical pH range for septic tanks ($6.7-7.6$),²¹³ albeit these values were not significantly different from the baseline ($P > 0.05$). However, when evaluated together and analyzed, the average pH of the three weeks of micron-scale Cu injection (pH 6.5 ± 0.1) was also significantly lower than the baseline average (pH 7.0 ± 0.1 , $P < 0.05$). After three weeks without further copper addition, the effluent pH had a pH value of 6.8 ± 0.2 .

TOC values for the micro Cu exposure (weeks 1-3) were between 47.0-49.8 mg/L (Figure 1B) and the final post-micro Cu exposure value for TOC was 47.0 ± 20.8 mg/L. All of these weeks were considered the same as baseline average conditions (54.8 ± 17.7 mg/L, $P = 0.3$). The typical range of TOC in septic tank effluent during the micro Cu experiment was well within the anticipated values based upon real world septic systems.²¹²⁻²¹³

Effluent turbidity decreased during the micro Cu experiment when compared to the baseline (Figure 1). When grouped and analyzed, the overall micro Cu exposure (2.5 ± 0.3 NTU) was significantly lower than the baseline turbidity (11.3 ± 1.1 NTU). The

final post-micro Cu exposure week had a value of 1.5 ± 0.6 NTU. While not displayed in Figure 1, the post-micro Cu week 1 exposure has the highest turbidity value for all experiments with a value 24.0 ± 0.2 NTU (SI, Table S2, $P < 0.001$). The Micro Cu exposure and post-micro Cu exposure did not cause significant changes in TSS (SI, Figure S3). There were not significant TSS data for any of the Cu particles, although the micro Cu particles did show a decrease in TSS over time. There was a 78% reduction of TSS from the influent to the effluent during the micro Cu exposure weeks. The final post-Cu exposure week had an 87% reduction in TSS. These are in the expected range of TSS reduction in a functioning septic system.²²⁶⁻²²⁷

The micro Cu addition BOD₅ values had two significant increases in BOD₅, during the first (241.7 ± 7.6 mg/L) and third weeks (223.3 ± 1.1 mg/L). The final week in the post-micro Cu exposure had a BOD₅ of 26.8 ± 8.3 mg/L, which was the lowest BOD₅ value recorded for all of the experiments. The baseline effluent value for BOD₅ was 82.0 ± 5.6 mg/L (Figure 2B) and the influent BOD₅ value was 127.0 ± 0.0 mg/L for all Cu experimental tests. During the micro Cu experiment, a 30-78% reduction in BOD₅ from the influent to the effluent was experienced only for the baseline, micro Cu exposure week 2, and the final post-micro Cu exposure week. All other weeks did not experience the anticipated percent reduction associated with a functioning septic system.

Results for the bacteria characterization tests (hydrophobicity, electrophoretic mobility, cell size, and cell concentration) are presented in the SI and in Figure S2. While the bacteria characterization did not overall have meaningful trends or any correlation with changes in the water quality tests, significant changes did occur. Here, cells

experienced a change in electrophoretic mobility (EPM, a surrogate for surface charge) and became more negative during the micro Cu exposure (-1.5 ± 0.3 to -1.6 ± 0.3 [$\mu\text{m/s}/(\text{V/cm})$]) when compared to the baseline (-1.0 ± 0.2 to -1.4 ± 0.3 [$\mu\text{m/s}/(\text{V/cm})$]).

For the pyrosequencing data, the baseline condition for the microbial community structure for all Cu experiments was as follows: Proteobacteria 83.9%, Firmicutes 4.2%, and Bacteroidetes 12.5%. While no significant changes to the microbial community structure occurred during the micro Cu experiment (Figure 2A), some trends are worth noting. The micro Cu exposure condition showed Firmicutes maintained a constant level in the community between 1.7-3.4%. Proteobacteria was the dominant community for the duration of micro Cu addition (64.4-74.6% of population) and Bacteroidetes ranged between 23.6-32.2%. All post-micro Cu microbial community structure data was within the same range as the baseline and micro Cu exposure.

Impact of $\text{Cu}(\text{OH})_2$

$\text{Cu}(\text{OH})_2$ impacted numerous water quality parameters. For pH, the final week in the $\text{Cu}(\text{OH})_2$ exposure had the highest pH (7.5 ± 0.1) for all experimental conditions (Figure 1A) and while this value is significantly higher than the baseline average (baseline pH = 7.0 ± 0.1 , $P < 0.001$), it is still within the typical pH range for a septic system.²¹²⁻²¹³ The post- $\text{Cu}(\text{OH})_2$ week 3 value is pH 7.1 ± 0.1 . All other experimental pH values were within the anticipated pH range for septic systems.²¹²⁻²¹³

The TOC values for the Cu(OH)₂ addition ranged from 82.5-208.2 mg/L, and were significantly higher from the average baseline condition (54.8 ± 17.7 mg/L) and when compared to the post-Cu(OH)₂ value (75.8 ± 2.8 mg/L), (P=0.0009 and P=0.02 respectively, Figure 1). However, the post-Cu(OH)₂ exposure was not significantly different from the baseline. The Cu(OH)₂ exposure resulted in the two highest TOC values, 208.2 ± 136.4 and 94.2 ± 5.9 mg/L, for all experimental conditions with all Cu particles. Yet the TOC values measured under all Cu(OH)₂ conditions were within the expected range for TOC in septic tank effluent (50-350 mg/L²¹²⁻²¹³), which indicates the system is still operating within typical conditions.

Turbidity increased during the Cu(OH)₂ experiment. The second highest turbidity value for all experiments was during the third week of the Cu(OH)₂ exposure (22.2 ± 1.4 NTU, Figure 1C). Overall, when grouped and analyzed, the Cu(OH)₂ exposure (10.1-22.2 ± 0.7 NTU) was significantly higher in turbidity when compared to the baseline (11.3 ± 1.1 NTU, P<0.006). Cu(OH)₂ experiments had higher turbidity overall when compared to the micro Cu and nano Cu experiments. The final week of the post-Cu(OH)₂ condition was 6.4 ± 0.2 NTU. All turbidity values for the Cu(OH)₂ exposure were above both the baseline average and the defined baseline value of <5 NTU. However, these effluent values are well below the range for expected influent values for household greywater.²²⁵ TSS data was not significantly impacted by any of the Cu particles. It is worthwhile to note that Cu(OH)₂ TSS values increased during weeks 2-3 of the Cu(OH)₂ exposure (SI, Figure S3) when compared to the baseline (baseline = 52.7 ± 7.6 mg/L, week 2 exposure = 60.3 ± 8.2 mg/L, and week 3 exposure = 54.8 ± 5.6 mg/L). For Cu(OH)₂ exposure

week 1 and for the post-Cu(OH)₂ final exposure week, a 19% and 26% reduction occurred in TSS from the influent to the effluent. The increase in TSS during Cu(OH)₂ exposure weeks 2 and 3 correlates with an increase seen in TOC.

The baseline effluent value for BOD₅ was 82.0 ± 5.6 mg/L (Figure 2B) and the influent BOD₅ value was 127.0 ± 0.0 mg/L for all Cu experiments. Half of the Cu(OH)₂ exposure had significantly higher BOD₅ values (267.0 ± 4.8 and 208.5 ± 12.0 mg/L, respectively, P<0.05). The 267.0 mg/L value was the highest BOD₅ value recorded for all Cu experiments conducted. These two weeks were above the expected BOD₅ values for septic tank systems (35-200 mg/L).²¹²⁻²¹³ Two weeks (Cu(OH)₂ week 1 and post-Cu(OH)₂ week 3) were significantly lower than the baseline effluent BOD₅ (30.3 ± 29.2 mg/L and 31.2 ± 3.6 mg/L, respectively). BOD₅ experienced a 76% reduction for these two weeks.

Results for the bacteria characterization tests (hydrophobicity, electrophoretic mobility, cell size, and cell concentration) are presented in the SI and in Figure S2. While the bacteria characterization did not overall have meaningful trends or any correlation with changes in the water quality tests, significant changes did occur. During the Cu(OH)₂ exposure, the most negative EPM value was recorded for the bacterial cells (-2.4 ± 0.4 [(μm/s)/(V/cm)], SI, Figure S2).

The Cu(OH)₂ particle caused significant changes in the microbial community structure. Phyla results in Figure 2A show that Proteobacteria significantly decreased during the Cu(OH)₂ addition (60.0-68.6%) and for post-Cu(OH)₂ exposure (60.8%) when compared to the baseline Proteobacteria percentage (83.9%). Proteobacteria remained the dominant phyla during all Cu experiments. Firmicutes was significantly higher for the

Cu(OH)₂ exposure (8.5-10.7%) when compared to the Firmicutes baseline (4.2%). The post-Cu(OH)₂ Firmicutes percentage was also significantly higher (25.3%) than the baseline.

Copper Analysis

The purpose of the copper ion specific electrode (Cu ISE) was to determine the amount of free Cu²⁺ ions emitted in the effluent (Figure 1D). The baseline average for Cu²⁺ ions was 0.0 ± 0.0 ppm. The highest recorded Cu²⁺ ion concentration in the effluent was during Cu(OH)₂ week 3 at 4.9 ± 0.8 ppm. Micro Cu was measured as having 1.0 ± 0.3 ppm during micro Cu week 3 and 1.8 ± 2.5 ppm during post-micro Cu week 3. Post-nano Cu week 3 had a value of 1.5 ± 1.1 ppm. All other values were below 0.2 ppm. Both the micro Cu and nano Cu showed an increase in Cu²⁺ ion concentration over the course of the experiments. Data is not available for micro Cu week 1. These values are in agreement from previous published work determining the total amount of Cu emitted from a septic system.²¹¹

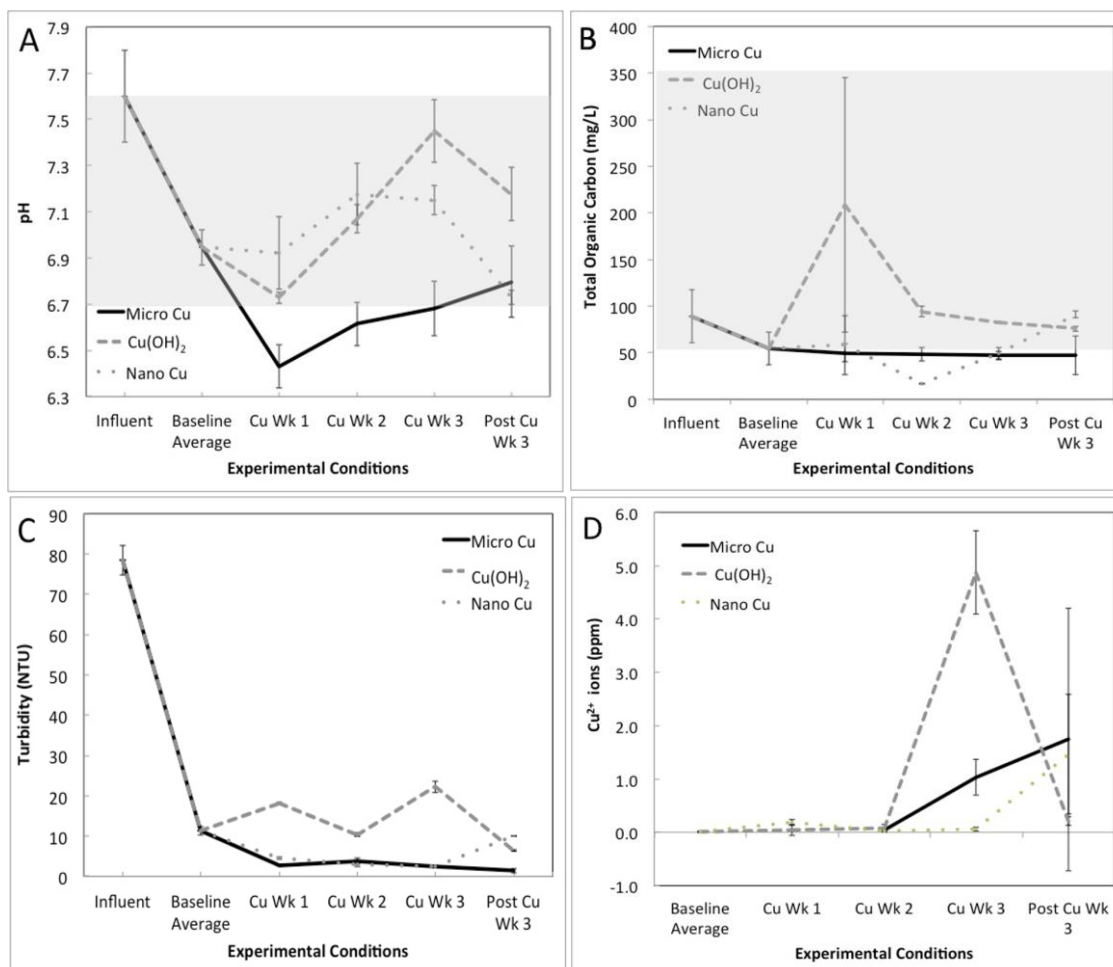


Figure 3.1. Changes in water quality parameters pH (A), TOC (B), and turbidity (C), and Cu²⁺ free ion concentration (D) were measured over the course of three independent ten-week experiments for micro Cu (solid line), Cu(OH)₂ (dashed line), and nano Cu (dotted line). The influent measurement is an average of three total readings taken during baseline week 4, Cu week 3, and Post Cu week 3. The baseline average is four week of pre-Cu measurements averaged together, Cu weeks 1-3 are three weeks in which Cu particles are added once a day, and post-Cu week 3 is the final week of three weeks in which Cu particles are no longer added and in which conditions in the septic tank were anticipated to return to baseline conditions. A shaded box indicates the typical septic system range²¹²⁻²¹³ for each test to give better clarification on when the septic system is in or out of range. Influent pH was maintained at 7.6 for during all experimental conditions due to consistency of influent material (colon waste, DI H₂O, and greywater).

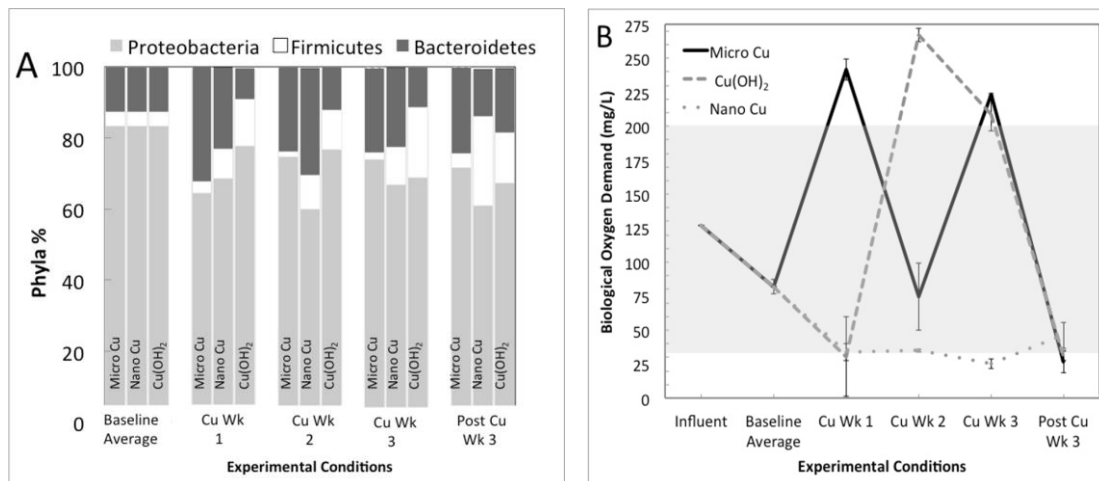


Figure 3.2. Changes in microbial community phyla (A) and biological oxygen demand (B) over the course of three independent ten-week experiments for micro Cu (solid line), Cu(OH)₂ (dashed line), and nano Cu (dotted line). The influent measurement is an average of three readings; influent liquid components remained constant over the course of the experiments. The baseline average is four week of pre-Cu measurements averaged together, Cu weeks 1-3 are three weeks in which Cu particles are added once a day, and post-Cu week 3 is the final week of three weeks in which Cu particles are no longer added and in which conditions in the septic tank were anticipated to return to baseline conditions. A shaded box indicates the typical septic system range²¹²⁻²¹³ for each test to give better clarification on when the septic system in out of range.

Discussion

Septic System Water Quality Parameters

The septic tank was affected minimally for the pH parameter except for the micro Cu exposure weeks. Since pH is used as an indicator for septic system function, this data indicate that septic system performance was minimally impacted with the exception of the micro Cu exposure. The baseline septic tank effluent pH ranged between 6.7 and 7.1 (average 6.9 ± 0.1). The overall average effluent pH for all experimental conditions (with and without the three Cu particles) was 6.9 ± 0.2 . Typical values associated with real

world septic tanks shows the average effluent pH to be between 6.7-7.6 for optimal treatment of waste; this is in agreement with the previously established work with this model septic system and septic tank effluent characterization publications.^{115, 212, 232} Previous work with this system¹¹⁵ had an overall effluent pH average of 6.8, which again falls within the documented range for septic system effluent.

Changes in pH are an important indicator of the microbial processes occurring within the septic system. The addition of micro Cu resulted in the greatest pH disturbance from baseline conditions (6.4-6.6 vs. 6.7-7.6), which was a decrease from the ideal range. When compared to baseline conditions, micro Cu caused the most significant decrease in pH and was not in the ideal range for methanogenesis²³² for two weeks during the micro Cu exposure. Here, the data demonstrates that consumer products with different types of Cu materials can have a range of effects on an anaerobic treatment system. However, recent work has shown that regardless of the type of Cu material, organic waste within the septic system mitigates toxicity effects due to transformation, speciation, and sedimentation of the Cu particles.²¹¹ In anaerobic treatment, decreases in pH can be an indirect measurement of an accumulation of volatile fatty acids (VFAs) within the system,^{49,55} which are produced by bacteria through anaerobic degradation of waste,^{49,55} which can lower the pH in the system. Methanogenesis, the last process in septic system fermentation and an important step in the degradation of waste,^{56,57} occurs ideally between pH 6.7-7.4. Hence, it is often the most sensitive phase and the rate-limiting step in the fermentation process,²³²⁻²³⁴ and will be affected by acid production.⁵⁸ If the Cu particles negatively affect the bacteria necessary for specific steps in fermentation,²³³⁻²³⁴

the system may no longer be able to buffer the acid production, causing a decrease in pH which can lead to untreated effluent emitted into the leachfield. Because methanogenic and acidogenic microorganisms have an optimal pH range within septic systems,²³² failure to maintain this optimal range can lead to septic system failure, e.g., improper treatment of the wastewater. Therefore, pH is important indicator of distress in the system, and incompletely treated waste will also lead to higher turbidity in the effluent. While methane production and methanogen population of the microbial community structure were not directly measured, previous research has indicated that the inhibitory threshold of Cu is 0.5 ppm in anaerobic systems.⁶³ The metabolic activity of key microbial populations in wastewater treatment plants, specifically denitrifiers, are inhibited by 50% with a dose of 0.95 ppm Cu.²³⁵

Water clarity, or turbidity, is an important test for verifying the effectiveness water treatment processes since it indicates indirectly the mobilization of sludge, incomplete digestion of waste, or higher loads of TSS in the effluent. For context, turbidity of treated drinking water is regulated to fall within 0-1 NTU.²²⁴ However, a septic tank's turbidity is not federally regulated and is anticipated to have higher values due to the presence of total suspended solids when compared with treated drinking water turbidity standards. Additionally, a disruption in the function of the septic system can also lead to greater turbidity values. Here, a reference value for the system was determined using the National Primary Drinking Water Regulations for surface water treatment with nonconventional filtration.²²⁴ Based upon this regulation, typical turbidity values for baseline conditions in the septic system were considered ideal if the effluent

was measured as <5 Nephelometric Turbidity Units (NTU). Domestic wastewater influent for a WWTP can have a turbidity ranging from 186-328 NTU²³⁶ and a reduction of turbidity in the secondary effluent is typically between 80-98%.²³⁷ In the septic tank with the absence of Cu particles, the system reduced influent turbidity by ~90%. In fact, for the nano Cu experiments, the system was capable of achieving a >90% reduction of turbidity, while the micro and Cu(OH)₂ showed turbidity reduced to between 70-90%. Because Cu is well documented to settle into sediment and sludge layers,²¹¹ it was anticipated that Cu was not bioavailable or disrupting the microbes within the liquid layer in the primary chamber. Here, turbidity was reduced to within the accepted ranges, indicating that the system was well conditioned to handle the perturbances experienced.

In engineered wastewater settings, TOC values are typically related to the amount of natural organic matter (NOM), such as humic and fulvic acids. These acids are present in the water and impact turbidity readings. However, in this study effluent TOC is based upon the acid and sugar content of the degraded organic constituents from the model colon which may be less complex in structure. The TOC effluent value was anticipated to be between 50-350 mg/L.²¹²⁻²¹³ All conditions (baseline and all Cu experiments) maintained a TOC value below 350 mg/L, indicating that the system stayed within the typical range for septic systems. Increases in the TOC during the Cu(OH)₂ exposure also correspond to increases in BOD₅ for the Cu(OH)₂ exposure. The TOC measurements indicate the lack of any system failure. Here, failure was defined as the system's inability to treat waste; one attribute indicating failure is increased loads of organic material present in the effluent. TOC is composed of dissolved organic carbon (DOC) and soluble

organic carbon (SOC). SOC is composed predominately of volatile acids. These acids can lower the pH within the septic system. Therefore, the presence of increased amounts of TOC can result in lower pH. This is noted for week 1 of the Cu(OH)₂ exposure. During week 2 of the nano Cu exposure, a decrease in TOC may be related to the increase in pH, yet these values are still within the documented typical ranges for TOC and pH for septic tanks. There is no clear relationship between TOC and pH trends with the micro Cu exposure. The fact that each Cu particle causes distinct behavior with the TOC data demonstrates that effects are likely related to the particle properties such as size or chemical composition.

Alkalinity, which was measured in the system in an additional study and is worth noting, increased over time in the system.²¹¹ High alkalinity is often thought to act as a buffer in aqueous systems to perturbances such as metals.²³⁸ However, the literature reports that alkalinity may or may not have an effect on Cu toxicity to aquatic organisms.²³⁸ Rather, the interplay of pH, alkalinity, organic matter, and total suspended solids play a more important role in determining Cu toxicity and the speciation of Cu in aquatic environments.^{211, 238}

Septic System Microbial Community Characterization

Changes to the microbial community's phenotype were monitored throughout the course of the experiments to determine phenotypic changes associated with the presence of Cu particles. These additional techniques were selected based upon previous work that used

these methods to characterize bacteria in aqueous environments,^{115, 214} specifically assessments associated with environmental microbial community analyses such as hydrophobicity, surface charge (electrophoretic mobility, EPM, a surrogate of surface charge), and cell size.^{137, 139} While significant changes did occur in the characterization tests, there were no meaningful trends that correlated with water quality data. These results are found entirely in the SI (Figure S2). These tests can give insight into changes occurring to the microbial community that are often associated with stress conditions, and these fluctuations could be used as additional indicators that the septic system is not operating optimally. For example, changes in cell hydrophobicity have been associated with biofilm formation.^{115, 143} Previous work with the septic system showed a baseline hydrophobicity cell value of $40.1 \pm 2.8\%$ and an increase in hydrophobicity was noted with a pathogen perturbation ($51.8 \pm 8.4\%$).¹¹⁵ Here, the average baseline hydrophobicity fluctuated between 24-45% with experimental Cu particle conditions causing hydrophobicity to range between 20-64%. No distinct pattern was observed when comparing the hydrophobicity responses to the three Cu particles. Additionally, it is worthy to note that the likelihood of biofilm growth varied dramatically based not only on the presence of Cu particles, but also on the stage and timing of the experiments.

Another characterization test, surface charge, is an indicator of the stability and attachment potential for the microbial community, with higher absolute values indicating greater stability.¹⁴⁵ EPM values for bacteria in aqueous environments are typically negative.²³⁹ A positive EPM value recorded with nano Cu suggests aggregate formation of the bacteria with nano Cu, with nano Cu likely coating the bacteria, thus changing its

surface charge.²⁴⁰ Surface charge values for the microbial community from previous work with the septic system show a baseline EPM of -1.1 ± 0.37 ($\mu\text{m/s}/(\text{V/cm})$) and -1.24 ± 0.18 with a pathogen perturbation.¹¹⁵ Here, the EPM baseline was -1.23 ± 0.25 ($\mu\text{m/s}/(\text{V/cm})$) and overall the septic system had greater fluctuations in EPM ranging from -2.38 to 0.90 ($\mu\text{m/s}/(\text{V/cm})$) in the presence of Cu particles when compared to effects caused by a pathogen. $\text{Cu}(\text{OH})_2$ had the greatest change in surface charge since positive values were measured. Nano Cu had the greatest variation in bacterial surface charge. Therefore, EPM may be a useful tool to determine changes within septic systems and to predict the fate or aggregation of nanomaterials and bacteria in the effluent.^{137, 241}

Finally, changes in cell size, particularly a decrease in cell size, can be attributed to stress on the cell.^{151, 242} The greatest decrease in cell size compared to the baseline was during post- $\text{Cu}(\text{OH})_2$ exposure. Of the three Cu, the micro Cu resulted in the least amount of fluctuation in bacterial size over the course of the experiments. Cell size is often monitored in microbial communities to determine cell viability and environmental stress.²⁴³⁻²⁴⁵

Septic System Microbial Community and Metabolism

Biological oxygen demand (BOD_5) is another common test for determining microbial activity and water quality in wastewater treatment, and this test determines the amount of oxygen required by the microbes present in wastewater to degrade organic matter and oxidize inorganic material and nitrogen.²¹⁵ Essentially, this test is a measurement of

organic material present in the system. Typical values from the literature demonstrate that the secondary effluent BOD₅ from a septic tank should be between 35-200 mg/L.²¹² In agreement with what is expected for function septic tanks, BOD₅ showed a 30-50% reduction between the influent and the baseline conditions.^{212, 226-227, 246-247} Micro Cu and Cu(OH)₂ caused the largest increase in BOD₅ and did not result in a subsequent reduction in BOD₅ for four weeks. High BOD₅ values indicate that there is an increased oxygen demand for the oxidation and degradation of organic waste in the effluent and verifies the presence of organic waste in the effluent. In contrast, low BOD₅ values mean the presence of less organic material or indirectly, less microbial activity. One limitation of the BOD₅ test is the inability to differentiate between amount of organic material and microbial activity, since the test is effectively measuring oxygen consumed over a five day period. The amount of oxygen consumed is often a proxy for the amount of organic material present in the system. A reason for the final low BOD₅ values could be that the Cu particles, the type of organic waste, or the amount of oxygen affected the bacteria that actively play a role in the breakdown of the waste, leading to a major shift in the community structure.²⁴⁸⁻²⁴⁹ In this work, changes in the community structure occurred during the same experimental weeks as high pulses in BOD₅ for Cu(OH)₂ weeks 1-3 (Proteobacteria decreased and Firmicutes increased). This parameter is often used as a tool for indirectly determining the amount of organic pollution present.²⁵⁰ At the end of the post-Cu week exposures, all BOD₅ values were relatively low (between 26-46 mg/L) and showed a 64-80% reduction in BOD₅. This indicates that the septic system was able

to return to baseline conditions in terms of the amount of organic waste present in the secondary effluent.

The microbial community was analyzed using pyrosequencing and metabolic tests to determine the changes that the community experienced as a function of Cu particles when compared to the baseline community characteristics. Many studies use changes to the microbial community structure at the phyla level as a monitoring tool for various types of wastewater treatment.²²⁸⁻²³¹ The microbial community from the effluent was pyrosequenced to determine the structure of the community for the baseline conditions, all Cu conditions, and all post-Cu conditions. At the phyla level, Proteobacteria made up the majority of the community in all conditions, even though Cu(OH)₂ did cause a significant decrease in this phylum (15-23% decrease from baseline condition). Other studies have confirmed the dominance of Proteobacteria in wastewater conditions.^{115, 229, 251} Proteobacteria encompass organisms that are known to oxidize ammonia in wastewater systems.²³¹ Firmicutes are also regularly found in wastewater and have been reported to have low resistance to the shear forces present in WWTPs, therefore occupying a select niche in wastewater microbial communities.²⁵²⁻²⁵³ The phyla Firmicutes includes bacteria that are able to ferment.²⁵⁴ Bacteroidetes are also commonly found in wastewater habitats and are believed to have an important role in anaerobic decomposition of complex organic matter.²⁵⁵ Both nano Cu and Cu(OH)₂ caused significant increases in the Firmicutes phylum. In multiple studies it has been shown that community stability is not often associated with the functional stability of the system, possibly due to functional redundancy, and that microbial community structure in

multiple types of WWTPs is highly and continuously variable despite stable function.²⁵⁶⁻

²⁶¹ In fact, one study suggests that the less stable a community's structure, the more stable the waste degradation performance.²⁶² In the current work, the microbial community at the phyla level was significantly altered for the nano Cu exposure (Firmicutes increased) and during the Cu(OH)₂ exposure (Proteobacteria decreased and Firmicutes increased). These fluctuations indicate that the community structure is not stable. While not evaluated in this study, one other phenomenon to consider is the possibility of increased bacterial resistance to Cu, which is often mediated by plasmids.²⁶³

Copper Analysis

The Cu²⁺ ion concentration emitted in the effluent was measured to determine the amount of Cu²⁺ ions released in the effluent. Cu²⁺ ions have demonstrated toxicity to organisms such as bacteria,²⁶⁴ and therefore, effects seen in the system may be due to free ions released from the Cu particles rather than the Cu particles. It is important to note that Cu toxicity resistance may be possible in bacteria through plasmids and other mechanisms.²⁶⁵ Work has also shown that a decreasing pH will increase the solubility of copper and lead to greater dissolution and an increase in the presence of Cu²⁺ ions.¹⁹¹ Here, the Cu²⁺ ion concentration during the micro Cu experiment may have increased due to the drop in pH during this experimental condition. It should be noted that results may have some inaccuracy due to interfering constituents such as Fe²⁺ (Fe²⁺ ions are a minimal component of the medium¹), divalent ions, the complexity of the sewage matrix such as

high concentrations of organics.²⁶⁶ These Cu²⁺ ion concentrations released in the effluent are in agreement from previous published work determining the total amount of Cu emitted from a septic system and are in the 1-5 ppm range.²¹¹

Conclusion and environmental implications

Septic system failure is defined as the release of nutrients and pathogens in effluent discharge.²⁶⁷ Therefore, it is important to understand the effects of any contaminants that may enter and alter septic system function, such as various Cu particles present in common consumer items. Here, multiple testing strategies were used to thoroughly characterize a septic system with and without Cu NPs. The septic system experienced various transformations with the Cu exposure such as fluctuations in the water quality (pH, BOD₅, and turbidity), microbial community phenotypic changes (hydrophobicity surface charge, and size), and variation in the microbial community composition. Overall, the septic system function was robust and managed the various Cu perturbances. Even with weekly fluctuations in the experiments, the data suggests that 100% of the time, the water quality parameters and microbial composition and activity were recovering towards baseline conditions by final week in the experiment (post-Cu week three) and most likely would be able to return to, or maintain the baseline conditions after such a perturbation, regardless of the particle type. The release of untreated wastewater or Cu particles into the leachfield may occur on a week-by-week basis and this may vary depending on specific conditions within the system (microbial community composition, pH, BOD₅, TOC), and it likely to differ between septic systems. However, the subsequent entry of

the effluent into the leachfield and groundwater may have negligible amounts of copper. It is important to note that nanoparticles have unknown and negative effects on WWTPs and will also undergo transformations in anaerobic environments that can alter toxicity effects. Therefore, similar effects and impacts are likely to occur within septic systems.^{51, 54, 268-269} For example sulfidation of metals in wastewater occurs and influences metal toxicity^{266, 269} and readily occurs in anaerobic environments with organic matter present, such as a septic system. The release of engineered nanomaterials into the groundwater does have known^{201, 270} and further unknown negative impacts on the environment and on human health.

References

1. Kang, S.; Pinault, M.; Pfefferle, L. D.; Elimelech, M., Single-Walled Carbon Nanotubes Exhibit Strong Antimicrobial Activity. *Langmuir* **2007**, *23* (17), 8670-8673.
2. Nel, A.; Xia, T.; Mädler, L.; Li, N., Toxic Potential of Materials at the Nanolevel. *Science* **2006**, *311* (5761), 622-627.
3. Wiesner, M. R.; Lowry, G. V.; Alvarez, P.; Dionysiou, D.; Biswas, P., Assessing the risks of manufactured nanomaterials. *Environmental Science & Technology* **2006**, *40* (14), 4336-4345.
4. Xia, T.; Kovochich, M.; Liong, M.; Mädler, L.; Gilbert, B.; Shi, H.; Yeh, J. I.; Zink, J. I.; Nel, A. E., Comparison of the Mechanism of Toxicity of Zinc Oxide and Cerium Oxide Nanoparticles Based on Dissolution and Oxidative Stress Properties. *ACS Nano* **2008**, *2* (10), 2121-2134.
5. Keller, A.; McFerran, S.; Lazareva, A.; Suh, S., Global life cycle releases of engineered nanomaterials. *J Nanopart Res* **2013**, *15* (6), 1-17.
6. Keller, A.; Vosti, W.; Wang, H.; Lazareva, A., Release of engineered nanomaterials from personal care products throughout their life cycle. *J Nanopart Res* **2014**, *16* (7), 1-10.
7. Keller, A. A.; Lazareva, A., Predicted Releases of Engineered Nanomaterials: From Global to Regional to Local. *Environmental Science & Technology Letters* **2013**, *1* (1), 65-70.
8. Beal, C. D.; Gardner, E. A.; Menzies, N. W., Process, performance, and pollution potential: A review of septic tank–soil absorption systems. *Soil Research* **2005**, *43* (7), 781-802.
9. Borchardt, M. A.; Bradbury, K. R.; Alexander, E. C.; Kolberg, R. J.; Alexander, S. C.; Archer, J. R.; Braatz, L. A.; Forest, B. M.; Green, J. A.; Spencer, S. K., Norovirus Outbreak Caused by a New Septic System in a Dolomite Aquifer. *Ground Water* **2011**, *49* (1), 85-97.
10. Yates, M. V., Septic Tank Density and Ground-Water Contamination. *Ground Water* **1985**, *23* (5), 586-591.

11. EPA. Decentralized wastewater treatment systems: memorandum of understanding. EPA, Ed. Washington DC, 2011.
12. EPA, Decentralized Systems Technology Fact Sheet Septic Tank - Soil Absorption Systems. Systems, Ed. Washington DC, 1999.
13. Williams, R.; Keller, V.; Voß, A.; Bärlund, I.; Malve, O.; Riihimäki, J.; Tattari, S.; Alcamo, J., Assessment of current water pollution loads in Europe: estimation of gridded loads for use in global water quality models. *Hydrological Processes* **2012**, *26* (16), 2395-2410.
14. Canter, L. W.; Knox, R. C., *Septic tank system effects on ground water quality*. Lewis Publishers, Inc: 1985.
15. Kiser, M. A.; Westerhoff, P.; Benn, T.; Wang, Y.; Pérez-Rivera, J.; Hristovski, K., Titanium Nanomaterial Removal and Release from Wastewater Treatment Plants. *Environmental Science & Technology* **2009**, *43* (17), 6757-6763.
16. Westerhoff, P.; Song, G.; Hristovski, K.; Kiser, M. A., Occurrence and removal of titanium at full scale wastewater treatment plants: implications for TiO₂ nanomaterials. *Journal of Environmental Monitoring* **2011**, *13* (5), 1195-1203.
17. Chowdhury, I.; Hong, Y.; Honda, R. J.; Walker, S. L., Mechanisms of TiO₂ nanoparticle transport in porous media: Role of solution chemistry, nanoparticle concentration, and flowrate. *Journal of Colloid and Interface Science* **2011**, *360* (2), 548-555.
18. Maurer-Jones, M. A.; Lin, Y.-S.; Haynes, C. L., Functional Assessment of Metal Oxide Nanoparticle Toxicity in Immune Cells. *ACS Nano* **2010**, *4* (6), 3363-3373.
19. Samberg, M. E.; Oldenburg, S. J.; Monteiro-Riviere, N. A., Evaluation of silver nanoparticle toxicity in skin in vivo and keratinocytes in vitro. *Environmental health perspectives (Online)* **2010**, *118* (3), 407.
20. Benn, T. M.; Westerhoff, P., Nanoparticle Silver Released into Water from Commercially Available Sock Fabrics. *Environmental Science & Technology* **2008**, *42* (11), 4133-4139.
21. Choi, O.; Deng, K. K.; Kim, N.-J.; Ross Jr, L.; Surampalli, R. Y.; Hu, Z., The inhibitory effects of silver nanoparticles, silver ions, and silver chloride colloids on microbial growth. *Water Research* **2008**, *42* (12), 3066-3074.

22. García, A.; Delgado, L.; Torà, J. A.; Casals, E.; González, E.; Puentes, V.; Font, X.; Carrera, J.; Sánchez, A., Effect of cerium dioxide, titanium dioxide, silver, and gold nanoparticles on the activity of microbial communities intended in wastewater treatment. *Journal of Hazardous Materials* **2012**, 199–200 (0), 64-72.
23. Jarvie, H. P.; Al-Obaidi, H.; King, S. M.; Bowes, M. J.; Lawrence, M. J.; Drake, A. F.; Green, M. A.; Dobson, P. J., Fate of Silica Nanoparticles in Simulated Primary Wastewater Treatment. *Environmental Science & Technology* **2009**, 43 (22), 8622-8628.
24. Kaegi, R.; Voegelin, A.; Sinnet, B.; Zuleeg, S.; Hagendorfer, H.; Burkhardt, M.; Siegrist, H., Behavior of Metallic Silver Nanoparticles in a Pilot Wastewater Treatment Plant. *Environmental Science & Technology* **2011**, 45 (9), 3902-3908.
25. Kiser, M. A.; Ryu, H.; Jang, H.; Hristovski, K.; Westerhoff, P., Biosorption of nanoparticles to heterotrophic wastewater biomass. *Water Research* **2010**, 44 (14), 4105-4114.
26. Limbach, L. K.; Bereiter, R.; Müller, E.; Krebs, R.; Gälli, R.; Stark, W. J., Removal of Oxide Nanoparticles in a Model Wastewater Treatment Plant: Influence of Agglomeration and Surfactants on Clearing Efficiency. *Environmental Science & Technology* **2008**, 42 (15), 5828-5833.
27. Mu, H.; Chen, Y.; Xiao, N., Effects of metal oxide nanoparticles (TiO₂, Al₂O₃, SiO₂ and ZnO) on waste activated sludge anaerobic digestion. *Bioresour. Technol.* **2011**, 102 (22), 10305-10311.
28. Sheng, Z.; Liu, Y., Effects of silver nanoparticles on wastewater biofilms. *Water Research* **2011**, 45 (18), 6039-6050.
29. Zheng, X.; Wu, R.; Chen, Y., Effects of ZnO Nanoparticles on Wastewater Biological Nitrogen and Phosphorus Removal. *Environmental Science & Technology* **2011**, 45 (7), 2826-2832.
30. Lazareva, A.; Keller, A. A., Estimating Potential Life Cycle Releases of Engineered Nanomaterials from Wastewater Treatment Plants. *ACS Sustainable Chemistry & Engineering* **2014**, 2 (7), 1656-1665.
31. Maynard, A.; Michelson, E., The nanotechnology consumer products inventory. *Woodrow Wilson International Center for Scholars, Washington, DC, accessed March* **2006**, 23.

32. Nasibulin, A.; Ahonen, P. P.; Richard, O.; Kauppinen, E.; Altman, I., Copper and Copper Oxide Nanoparticle Formation by Chemical Vapor Nucleation From Copper (II) Acetylacetonate. *J Nanopart Res* **2001**, *3* (5-6), 383-398.
33. Yang, J.-g.; Okamoto, T.; Ichino, R.; Bessho, T.; Satake, S.; Okido, M., A Simple Way for Preparing Antioxidation Nano-copper Powders. *Chemistry Letters* **2006**, *35* (6), 648-649.
34. Grosell, M.; Blanchard, J.; Brix, K.; Gerdes, R., Physiology is pivotal for interactions between salinity and acute copper toxicity to fish and invertebrates. *Aquatic toxicology* **2007**, *84* (2), 162-172.
35. Kessler, R., Engineered Nanoparticles in Consumer Products: Understanding a New Ingredient. *Environmental Health Perspectives* **2011**, *119* (3), A120-A125.
36. Hong, P. K. A.; Macauley, Y. Y., Corrosion and Leaching of Copper Tubing Exposed to Chlorinated Drinking Water. *Water, Air, & Soil Pollution* **1998**, *108* (3-4), 457-471.
37. Subramanian, K. S.; Connor, J. W.; Meranger, J. C., Leaching of antimony, cadmium, copper, lead, silver, tin and zinc from copper piping with non-lead-based soldered joints. *Journal of Environmental Science and Health . Part A: Environmental Science and Engineering and Toxicology* **1991**, *26* (6), 911-929.
38. EPA, Centralized Waste Treatment Effluent Limitations Guidelines and Pretreatment Standards (40 CFR 437). Office. of Water, Ed. Washington, D.C., 2001.
39. EPA, Alternative Waste Management Techniques for Best Practicable Waste Treatment. Washington, D.C, February 11, 1976; Vol. 43, pp 6190-6191.
40. EPA, The report to Congress: Waste Disposal Practices and their Effects on Ground Water EPA 570/9-77-001. Washington, D.C, June 1977.
41. Federal Water Pollution Control Act Amendments of 1972. In Public Law 92-500, Ed. 1972.
42. EPA, NPDES Permit Writers' Manual. EPA-833-B-96-003. Water, O. o., Ed. Washington, D.C., 1996.

43. EPA, Protecting the Nation's Waters Through Effective NPDES Permits A Strategic Plan FY 2001 and Beyond. Office of Water, Ed. Washington, D.C., 2001.
44. Marcus, I. M.; Wilder, H. A.; Quazi, S. J.; Walker, S. L., Linking Microbial Community Structure to Function in Representative Simulated Systems. *Applied and Environmental Microbiology* **2013**, 79 (8), 2552-2559.
45. Lin, S.; Taylor, A. A.; Ji, Z.; Chang, C. H.; Kinsinger, N. M.; Ueng, W.; Walker, S. L.; Nel, A. E., Understanding the Transformation, Speciation, and Hazard Potential of Copper Particles in a Model Septic Tank System using Zebrafish to Monitor the Effluent. *ACS Nano* **2015**.
46. Brandes, M., Characteristics of Effluents from Gray and Black Water Septic Tanks. *Journal (Water Pollution Control Federation)* **1978**, 50 (11), 2547-2559.
47. Crites, R.; Technobanoglous, G., *Small and decentralized wastewater management systems*. McGraw-Hill: 1998.
48. Taylor, A. A.; Marcus, I. M.; Guysi, R. L.; Walker, S. L., Metal oxide nanoparticles induce phenotypic changes in a model colon gut microbiota. *Environmental Engineering Science* **2015**.
49. American Public Health Association, *Standard methods for the examination of water and wastewater*. 17 ed.; American Public Health Association: 1989.
50. Burleson, G. R.; Murray, T. M.; Pollard, M., Inactivation of Viruses and Bacteria by Ozone, With and Without Sonication. *Applied Microbiology* **1975**, 29 (3), 340-344.
51. Sanders, J. R., The effect of pH upon the copper and cupric ion concentrations in soil solutions. *Journal of Soil Science* **1982**, 33 (4), 679-689.
52. Temminghoff, E. J. M.; Van der Zee, S. E. A. T. M.; de Haan, F. A. M., Copper Mobility in a Copper-Contaminated Sandy Soil as Affected by pH and Solid and Dissolved Organic Matter. *Environmental Science & Technology* **1997**, 31 (4), 1109-1115.
53. Wisconsin State Department of Health, Rule Development Committee Issue Research Report: Septic Tank Effluent Values. 2004.

54. Hickey, J. L. S.; Duncan, D. L., Performance of Single Family Septic Tank Systems in Alaska. *Journal (Water Pollution Control Federation)* **1966**, *38* (8), 1298-1309.
55. Wisconsin Department of Natural Resources, Introduction to Anaerobic Digestion Study Guide. Resources, D. o. N., Ed. Madison, 1992.
56. Zaveri, R. M.; Flora, J. R. V., Laboratory septic tank performance response to electrolytic stimulation. *Water Research* **2002**, *36* (18), 4513-4524.
57. Septic Tank Effluent Values. Wisconsin State Department of Health, Ed. 2004.
58. Grass, G.; Rensing, C.; Solioz, M., Metallic Copper as an Antimicrobial Surface. *Applied and Environmental Microbiology* **2011**, *77* (5), 1541-1547.
59. Ruparelia, J. P.; Chatterjee, A. K.; Duttagupta, S. P.; Mukherji, S., Strain specificity in antimicrobial activity of silver and copper nanoparticles. *Acta Biomaterialia* **2008**, *4* (3), 707-716.
60. Siedlecka, E.; Kumirska, J.; Ossowski, T.; Glamowski, P.; Gołębiowski, M.; Gajdus, J.; Kaczyński, Z.; Stepnowski, P., Determination of volatile fatty acids in environmental aqueous samples. *Pol. J. Environ. Stud* **2008**, *17* (3), 351-356.
61. EPA, National Interim Primary Drinking Water Regulations. Office of Water Supply, Ed. Washington, D.C., 1976.
62. Casanova, L. M.; Gerba, C. P.; Karpiscak, M., Chemical and microbial characterization of household greywater. *Journal of Environmental Science and Health, Part A* **2001**, *36* (4), 395-401.
63. Bounds, T., Design and performance of septic tanks. ASTM Speical technical Publication **1997**, *1324*, 217-234.
64. Rock, C. A.; Boyer, J. A., Influence of design on septic tank effluent quality. *Proceedings of 8th northwest on-site wastewater treatment short course and equipment exhibition* **1995**.
65. Yang, Y.; Quensen, J.; Mathieu, J.; Wang, Q.; Wang, J.; Li, M.; Tiedje, J. M.; Alvarez, P. J. J., Pyrosequencing reveals higher impact of silver nanoparticles than Ag⁺ on the microbial community structure of activated sludge. *Water Research* **2014**, *48* (0), 317-325.

66. Hu, M.; Wang, X.; Wen, X.; Xia, Y., Microbial community structures in different wastewater treatment plants as revealed by 454-pyrosequencing analysis. *Bioresource Technology* **2012**, *117* (0), 72-79.
67. Nielsen, P. H.; Saunders, A. M.; Hansen, A. A.; Larsen, P.; Nielsen, J. L., Microbial communities involved in enhanced biological phosphorus removal from wastewater - a model system in environmental biotechnology. *Current Opinion in Biotechnology* **2012**, *23* (3), 452-459.
68. Wagner, M.; Loy, A.; Nogueira, R.; Purkhold, U.; Lee, N.; Daims, H., Microbial community composition and function in wastewater treatment plants. *Antonie Van Leeuwenhoek* **2002**, *81* (1-4), 665-680.
69. Bitton, G., *Wastewater Microbiology*. 3 ed.; John Wiley & Sons: Hoboken, New Jersey, 2005.
70. Chen, Y.; Cheng, J. J.; Creamer, K. S., Inhibition of anaerobic digestion process: A review. *Bioresource Technology* **2008**, *99* (10), 4044-4064.
71. Murto, M.; Björnsson, L.; Mattiasson, B., Impact of food industrial waste on anaerobic co-digestion of sewage sludge and pig manure. *Journal of Environmental Management* **2004**, *70* (2), 101-107.
72. D'Amato, V. A.; Bahe, A.; Bounds, T.; Comstock, B.; Konsler, T.; Liehr, S. K.; Long, S. C.; Ratanaphruks, K.; Rock, C. A.; Sherman, K., Factor Affecting the Performance of Primary Treatment in Decentralized Wastewater Systems, In *Decentralized Systems: Final Report*, Ed. IWA Publishing: London, 2008.
73. Ochoa-Herrera, V.; León, G.; Banihani, Q.; Field, J. A.; Sierra-Alvarez, R., Toxicity of copper(II) ions to microorganisms in biological wastewater treatment systems. *Science of The Total Environment* **2011**, *412-413* (0), 380-385.
74. Chu, L.; Li, S., Filtration capability and operational characteristics of dynamic membrane bioreactor for municipal wastewater treatment. *Separation and Purification Technology* **2006**, *51* (2), 173-179.
75. Delgado, S.; Diaz, F.; Garcia, D.; Otero, N., Behaviour of Inorganic Coagulants in Secondary Effluents from a Conventional Wastewater Treatment Plant. *Filtration & Separation* **2003**, *40* (7), 42-46.

76. Eastman, J. A.; Ferguson, J. F., Solubilization of Particulate Organic Carbon during the Acid Phase of Anaerobic Digestion. *Journal (Water Pollution Control Federation)* **1981**, *53* (3), 352-366.
77. Erickson, R. J.; Benoit, D. A.; Mattson, V. R.; Leonard, E. N.; Nelson, H. P., The effects of water chemistry on the toxicity of copper to fathead minnows. *Environmental Toxicology and Chemistry* **1996**, *15* (2), 181-193.
78. Bolster, C. H.; Cook, K. L.; Marcus, I. M.; Haznedaroglu, B. Z.; Walker, S. L., Correlating Transport Behavior with Cell Properties for Eight Porcine Escherichia coli Isolates. *Environmental Science & Technology* **2010**, *44* (13), 5008-5014.
79. Tazehkand, S. S.; Torkzaban, S.; Bradford, S. A.; Walker, S. L., Cell Preparation Methods Influence Escherichia coli D21g Surface Chemistry and Transport in Saturated Sand. *J. Environ. Qual.* **2008**, *37* (6), 2108-2115.
80. Schäfer, A.; Ustohal, P.; Harms, H.; Stauffer, F.; Dracos, T.; Zehnder, A. J. B., Transport of bacteria in unsaturated porous media. *Journal of Contaminant Hydrology* **1998**, *33* (1-2), 149-169.
81. Elimelech, M.; Jia, X.; Gregory, J.; Williams, R., *Particle deposition & aggregation: measurement, modelling and simulation*. Butterworth-Heinemann: 1998.
82. Wilson, W. W.; Wade, M. M.; Holman, S. C.; Champlin, F. R., Status of methods for assessing bacterial cell surface charge properties based on zeta potential measurements. *Journal of Microbiological Methods* **2001**, *43* (3), 153-164.
83. Jiang, W.; Mashayekhi, H.; Xing, B., Bacterial toxicity comparison between nano- and micro-scaled oxide particles. *Environmental Pollution* **2009**, *157* (5), 1619-1625.
84. Haznedaroglu, B. Z.; Kim, H. N.; Bradford, S. A.; Walker, S. L., Relative Transport Behavior of Escherichia coli O157:H7 and Salmonella enterica Serovar Pullorum in Packed Bed Column Systems: Influence of Solution Chemistry and Cell Concentration. *Environmental Science & Technology* **2009**, *43* (6), 1838-1844.
85. Kjelleberg, S.; Hermansson, M.; Marden, P.; Jones, G. W., The Transient Phase Between Growth and Nongrowth of Heterotrophic Bacteria, with Emphasis on the Marine Environment. *Annual Review of Microbiology* **1987**, *41* (1), 25-49.

86. Tate, R. L., *Microbial autecology: a method for environmental studies*. Wiley: 1986.
87. Bakken, L.; Olsen, R., The relationship between cell size and viability of soil bacteria. *Microb Ecol* **1987**, *13* (2), 103-114.
88. Palumbo, A. V.; Ferguson, R. L.; Rublee, P. A., Size of Suspended Bacterial Cells and Association of Heterotrophic Activity with Size Fractions of Particles in Estuarine and Coastal Waters. *Applied and Environmental Microbiology* **1984**, *48* (1), 157-164.
89. Torrella, F.; Morita, R. Y., Microcultural Study of Bacterial Size Changes and Microcolony and Ultramicrocolony Formation by Heterotrophic Bacteria in Seawater. *Applied and Environmental Microbiology* **1981**, *41* (2), 518-527.
90. Siegrist, R. L.; Anderson, D. L.; Converse, J. C., *Onsite treatment and disposal of restaurant wastewater*. University of Wisconsin--Extension, Division of Economic and Environmental Development: 1984.
91. EPA, Onsite Wastewater Treatment Systems Manual EPA625/R-00-008. Cincinnati, Ohio, 2002; pp 4-38.
92. Lüdemann, H.; Arth, I.; Liesack, W., Spatial Changes in the Bacterial Community Structure along a Vertical Oxygen Gradient in Flooded Paddy Soil Cores. *Applied and Environmental Microbiology* **2000**, *66* (2), 754-762.
93. Oved, T.; Shaviv, A.; Goldrath, T.; Mandelbaum, R. T.; Minz, D., Influence of Effluent Irrigation on Community Composition and Function of Ammonia-Oxidizing Bacteria in Soil. *Applied and Environmental Microbiology* **2001**, *67* (8), 3426-3433.
94. Henze, M., *Wastewater treatment: biological and chemical processes*. Springer Science & Business Media: 2002.
95. Tomaras, J.; Sahl, J. W.; Siegrist, R. L.; Spear, J. R., Microbial Diversity of Septic Tank Effluent and a Soil Biomat. *Applied and Environmental Microbiology* **2009**, *75* (10), 3348-3351.
96. Larsen, P.; Nielsen, J. L.; Svendsen, T. C.; Nielsen, P. H., Adhesion characteristics of nitrifying bacteria in activated sludge. *Water Research* **2008**, *42* (10-11), 2814-2826.

97. Wilén, B.-M.; Onuki, M.; Hermansson, M.; Lumley, D.; Mino, T., Microbial community structure in activated sludge floc analysed by fluorescence in situ hybridization and its relation to floc stability. *Water Research* **2008**, *42* (8–9), 2300-2308.
98. Kragelund, C.; Levantesi, C.; Borger, A.; Thelen, K.; Eikelboom, D.; Tandoi, V.; Kong, Y.; Krooneman, J.; Larsen, P.; Thomsen, T. R.; Nielsen, P. H., Identity, abundance and ecophysiology of filamentous bacteria belonging to the Bacteroidetes present in activated sludge plants. *Microbiology* **2008**, *154* (3), 886-894.
99. Diaz, E. E.; Stams, A. J. M.; Amils, R.; Sanz, J. L., Phenotypic properties and microbial diversity of methanogenic granules from a full-scale UASB reactor treating brewery wastewater. *Applied and Environmental Microbiology* **2006**, *72* (7), 4942-4949.
100. Otawa, K.; Asano, R.; Ohba, Y.; Sasaki, T.; Kawamura, E.; Koyama, F.; Nakamura, S.; Nakai, Y., Molecular analysis of ammonia-oxidizing bacteria community in intermittent aeration sequencing batch reactors used for animal wastewater treatment. *Environmental Microbiology* **2006**, *8* (11), 1985-1996.
101. Cytryn, E.; Minz, D.; Gelfand, I.; Neori, A.; Gieseke, A.; de Beer, D.; van Rijn, J., Sulfide-Oxidizing Activity and Bacterial Community Structure in a Fluidized Bed Reactor from a Zero-Discharge Mariculture System. *Environmental Science & Technology* **2005**, *39* (6), 1802-1810.
102. Fernández, A.; Huang, S.; Seston, S.; Xing, J.; Hickey, R.; Criddle, C.; Tiedje, J., How Stable Is Stable? Function versus Community Composition. *Applied and Environmental Microbiology* **1999**, *65* (8), 3697-3704.
103. Gentile, M.; Yan, T.; Tiquia, S. M.; Fields, M. W.; Nyman, J.; Zhou, J.; Criddle, C. S., Stability in a Denitrifying Fluidized Bed Reactor. *Microb Ecol* **2006**, *52* (2), 311-321.
104. Miura, Y.; Hiraiwa, M. N.; Ito, T.; Itonaga, T.; Watanabe, Y.; Okabe, S., Bacterial community structures in MBRs treating municipal wastewater: Relationship between community stability and reactor performance. *Water Research* **2007**, *41* (3), 627-637.
105. Wittebolle, L.; Van Vooren, N.; Verstraete, W.; Boon, N., High reproducibility of ammonia-oxidizing bacterial communities in parallel sequential batch reactors. *Journal of Applied Microbiology* **2009**, *107* (2), 385-394.

106. Zumstein, E.; Moletta, R.; Godon, J.-J., Examination of two years of community dynamics in an anaerobic bioreactor using fluorescence polymerase chain reaction (PCR) single-strand conformation polymorphism analysis. *Environmental Microbiology* **2000**, *2* (1), 69-78.
107. Fernandez, A. S.; Hashsham, S. A.; Dollhopf, S. L.; Raskin, L.; Glagoleva, O.; Dazzo, F. B.; Hickey, R. F.; Criddle, C. S.; Tiedje, J. M., Flexible Community Structure Correlates with Stable Community Function in Methanogenic Bioreactor Communities Perturbed by Glucose. *Applied and Environmental Microbiology* **2000**, *66* (9), 4058-4067.
108. Cervantes, C.; Gutierrez-Corona, F., Copper resistance mechanisms in bacteria and fungi. *FEMS microbiology reviews* **1994**, *14* (2), 121-137.
109. Flemming, C. A.; Trevors, J. T., Copper toxicity and chemistry in the environment: a review. *Water, Air, & Soil Pollution* **1989**, *44* (1-2), 143-158.
110. Adeleye, A. S.; Conway, J. R.; Perez, T.; Rutten, P.; Keller, A. A., Influence of Extracellular Polymeric Substances on the Long-Term Fate, Dissolution, and Speciation of Copper-Based Nanoparticles. *Environmental Science & Technology* **2014**, *48* (21), 12561-12568.
111. Sterritt, R. M.; Lester, J. N., Significance and behaviour of heavy metals in waste water treatment processes III. Speciation in waste waters and related complex matrices. *Science of The Total Environment* **1984**, *34* (1-2), 117-141.
112. Ahmed, W.; Neller, R.; Katouli, M., Evidence of septic system failure determined by a bacterial biochemical fingerprinting method. *Journal of Applied Microbiology* **2005**, *98* (4), 910-920.
113. Brar, S. K.; Verma, M.; Tyagi, R. D.; Surampalli, R. Y., Engineered nanoparticles in wastewater and wastewater sludge – Evidence and impacts. *Waste Management* **2010**, *30* (3), 504-520.
114. Kim, B.; Park, C.-S.; Murayama, M.; Hochella, M. F., Discovery and Characterization of Silver Sulfide Nanoparticles in Final Sewage Sludge Products. *Environmental Science & Technology* **2010**, *44* (19), 7509-7514.
115. Hagedorn, C.; Mc Coy, E. L.; Rahe, T. M., The Potential for Ground Water Contamination from Septic Effluents¹. *J. Environ. Qual.* **1981**, *10* (1), 1-8.

Supplemental Information for Chapter 3: Effects of Copper Particles on a Model Septic System's Function and Microbial Community

Background

The total waste treatment process of the septic tank entails two components: (1) a buried two compartment tank which collects household waste and where initial degradation of the waste occurs, (2) and the associated soil absorption system, where clarified effluent percolates through the soil for filtration before entering the ground water.⁵⁷

Materials and Methods

Model Septic System

The septic tank is a scaled-down version of a two compartment style septic tank, with a volume of 2:1 in the primary and secondary chambers (144 and 72 L); the septic tank was made from an acrylic fish tank.²⁴⁷ Three times a day 100 mL of colon effluent from the model colon bioreactor^{115, 214} was added to the septic tank and diluted at a ratio of 16.5:1 (deionized water (DI) : colon effluent) for simulating toilet flushing, followed by a ratio of 1:2 of diluted colon to synthetic greywater to simulate the addition two-thirds of household waste from other sources than the toilet.^{212, 271}

The colon media used within the model colon is composed of the following materials on a per liter basis: 4.5 g NaCl, 2.5 g K₂HPO₄, 0.45 g CaCl₂·2H₂O, 0.5 g MgSO₄·7H₂O, 0.005 g FeSO₄·7H₂O, 0.05 g ox bile, 0.01 g hemin, 0.4 g cysteine, 0.6 g pectin, 0.6 g xylan, 0.6 g arabinogalactan, 0.6 g amylopectin, 5.0 g starch, 2.0 mL Tween

80, 3.0 g bactopectone, and 3.0 g casein. After autoclaving, a vitamin mix was filter sterilized and added to the media. 1.0 mL vitamin mix is added per liter and contains: 1.0 mg menadione, 2.0 mg D-biotin, 0.5 mg vitamin B₁₂, 10.0 mg pantothenate, 5.0 mg nicotinamide, 5.0 mg para-amino-benzoic acid, and 4.0 mg thiamine.^{115, 214} “Digested” colon media from the microbial community within the model colon reactor is added to the septic system as part of the influent. A digital picture and diagram schematic of the model colon system can be found in previous publications.^{115, 214} The synthetic greywater is composed of the following materials on a per liter basis: 20 mg humic acid, 50 mg kaolin, 50 mg cellulose, 0.5 mM CaCl₂, 10 mM NaCl, and 1 mM NaHCO₃ at pH 8.^{115, 214} The model septic tank was designed to have a typical residence time of three weeks in the primary compartment.^{115, 247}

The model septic tank required three weeks to fill before beginning experiments. This was followed by four weeks of operation without Cu particles with the purpose of monitoring and assessing typical baseline operating conditions (defined as baseline average). Next Cu particles were added once a day for three weeks (defined as Cu weeks 1-3), which was followed by three weeks where no additional Cu particles were added (defined as post-Cu weeks 1-3). The purpose of the post-Cu weeks was to determine if the septic tank could return to its baseline conditions following the perturbation. While Cu particles were no longer added during post-Cu exposure, the assumption was made that Cu added during the prior three weeks (Cu weeks 1-3) was likely still present in the system or effluent. The colon effluent was added from a reactor built in the lab to simulate a model colon.^{115, 214} The colon contained a microbial community developed

from human feces,^{115, 214} and is a reproducible laboratory representation of an *in situ* microbial community as would be found in a septic tank from household waste.

Nanoparticle Selection

A previous study conducted characterizations of the three Cu particles used in this work.²¹¹ The characterization work has shown the following size in deionized water (DI H₂O): nano Cu as 1164 ± 202 nm and Cu(OH)₂ as 889 ± 156 nm using HT-DLS (high throughput dynamic light scattering instrument, Dynapro Plate Reader, Wyatt Technology).²¹¹ Micro Cu size was not collected due to fast particle sedimentation.²¹¹ The primary size of the particles are as follows: 10 nm Cu(OH)₂, >1000 nm micro Cu, and 200-1000 nm nano Cu²¹¹. The zeta potential of the particles were measured in DI H₂O and are were as follows: nano Cu -46.3 ± 1.6 mV, micro Cu -32.5 ± 2.9 mV, and Cu(OH)₂ -45.1 ± 0.8 mV.²¹¹ The micro and nano Cu manufacturers claim over 99.5% purity. The primary particle sizes are 200-1000 nm (nano Cu), >10 μm (micro Cu), and 10 nm (Cu(OH)₂). ICP-OES (inductively coupled plasma optical emission spectrometry, ICPE-9000, Shimadzu) determined that the purity of the materials was as follows: nano Cu 84.8 ± 2.7 wt%, micro Cu 94.9 ± 1.4 wt%, and Cu(OH)₂ 47.1 ± 2.6 wt%.²¹¹ Cu particles were selected based upon dissolution categories. Cu(OH)₂ and nano Cu were considered highly dissolvable (>8 wt % dissolution) and micro Cu was considered to have low dissolution (<2 wt % dissolution)²¹¹. For context, the maximum contaminant level of copper allowed in drinking water is 1.3 ppm.²²⁴

The dosing regimen is as follows: Cu particles were added five-days a week into the septic system for three weeks for a total of 500 mg per week and 1500 mg total per experiment. Cu particles were added daily to the septic system at 3 pm along with deionized water, colon waste, and synthetic greywater. More details on the experimental regimen is listed below in Table S1.

Water Quality Characterization

Four standard water quality tests: pH, total organic carbon (TOC), turbidity, and total suspended solids (TSS) were selected for monitoring effluent from the model septic system. These water quality tests were specifically chosen based upon their common usage in WWTPs and septic systems,^{62, 67-68, 219-220} and are necessary for comparison of operating conditions between baseline, or normal operating condition, and conditions when copper is present in the model septic system. Changes in pH were monitored twice a week (Table S1) in triplicate on the effluent using a pH probe (Thermo Scientific Orion Star double junction electrode). Turbidity of the effluent was measured once a week and an initial reading of the influent was taken using a Hach 2100N Turbidimeter (Hach Company, Loveland, CO) with <0.1, 1, 10, 20, and 200 NTUs StablCal® Formazin Turbidity Standards (Hach Company, Loveland, CO). All samples were collected and quantified during the week at consistent time points (Table S1) to eliminate any sampling biases.

Total organic carbon (TOC) is the amount of carbon bound in organic compounds and is a standard measurement in water and wastewater analysis.²¹⁵ Here, total TOC was measured rather than soluble TOC. TOC was determined using a TOC analyzer (OI Analytical, Aurora 1030 Combustion Model) following previously published methods.¹¹⁵ Measurements were taken twice a week (Table S1) from the septic tank effluent and every three weeks from the influent with each sampling event involving collection and analysis of three replicates. The TOC analyzer evaluated the non-purgable organic carbon (NPOC); this is done by first removing the inorganic carbon (in the form of carbon dioxide), and then subtracting this value from the reading of total carbon to give the total organic carbon fraction.²¹⁵ NPOC includes dissolved organic carbon (DOC) and suspended organic carbon (SOC).²⁷² Samples were stored at 4 °C for up to one month prior to analysis as longer storage may result in carbon loss and sample bias.²⁷³

Total suspended solids (TSS) were measured from the septic tank effluent once a week in triplicate using a vacuum filtration apparatus and oven.²¹⁵ The sampling dates and times are consistent on a weekly basis and are listed in Table S1. For this text a control was used, which consisted of filtering deionized water. Samples were assessed every hour for five hours or until weight loss was < 4% from the previous weight.²¹⁵ A Whatman 934-AH glass microfiber filter with a pore size of 1.5 µm was chosen based on the volume of sample, time required to yield an appropriate sample size, and for meeting typical requirements for wastewater sampling (method 2540D).²¹⁵

Additional methods and data regarding septic tank parameters that are not reported in this paper (alkalinity, hardness, and conductivity) and can be found in a separate publication.²¹¹

Bacteria Characterization

Before testing, effluent samples underwent three washing steps with centrifugation (3,700 x g). The pellet, containing bacterial cells, was resuspended in 10 mM KCl¹¹⁵ such that suspended cells could be evaluated by the following characterization methods. Electrophoretic mobility (EPM, a surrogate for surface charge) was analyzed using a zeta potential analyzer (ZetaPALS, Brookhaven Instruments, NY).^{48, 115, 241, 274} Cell hydrophobicity was analyzed by the microbial adhesion to hydrocarbon (MATH) test in which cell partitioning is quantified by using a hydrocarbon and electrolyte phase.^{115, 275} The mean size of the bacteria was determined by capturing (Westover Scientific, Westover Digital Camera MCD Model 2200 Version 2.0.0) three images of the bacteria (n>20) and determining the spherical radius using a light contrast microscope (Fisher Scientific, Micromaster) and imaging software (MatLab, MathWorks, Natwick, MA, Version 7.11.0).¹¹⁵

Bacteria Community Metabolism and Sequencing

BOD₅ (biological oxygen demand, amount of oxygen consumed over a five-day period) was calculated from the difference between the initial and final dissolved oxygen (DO) levels. An effluent sample was collected once a week at a consistent time point for measuring BOD₅. A total of three replicates of a 2% effluent dilution, which were prepared from the collected effluent sample, and three replicates of deionized water blanks were tested each week (Table S1).²¹⁵

Septic effluent samples were collected and DNA extracted once a week for baseline weeks, all Cu injection weeks, and for the three final post-copper injection weeks. DNA was sent to Research Laboratory and Testing (Lubbock, TX) for bacterial tag-encoded FLX amplicon sequencing (bTEFAP) using the primers Gray28F (5=GAGTTTGATCNTGGCTCAG) and Gray519r (5=GTNTTACNGCGGCKGCTG).^{115, 276} Data was then analyzed with previously published methods²⁷⁶⁻²⁷⁹ that include denoising, assigning operational taxonomic units (OTUs) using USEARCH²⁸⁰ (with 77-80% identity score for phyla level), and finally using BLASTN+ to determine taxonomic identities.²⁷⁶⁻²⁷⁹ All pyrosequencing data were between 1,700 and 11,000 reads. By removing rare operational units (OTUs) and singletons and adding sequences from other technical replicate sequencing runs, the comparability of the amplicon sequencing data was enhanced.¹¹⁵ The purpose of the pyrosequencing was to determine a “fingerprint” of the microbial population under each experimental and baseline condition.

Copper Analysis

A five-point calibration curve was first conducted before each measurement using a cupric standard 0.1 M Cu^{2+} (Thermo Scientific) in DI H_2O with concentrations of 10^{-2} M, 10^{-3} M, 10^{-4} M, 10^{-5} M, and a blank which is equivalent to 635.5 ppm, 63.55 ppm, 6.355 ppm, 0.6355 ppm, and 0 ppm, respectively. An additional calibration curve was also conducted using baseline effluent from the septic system with the cupric standard. The samples were prepared based upon previous work, including ionic strength adjustments to minimize interferences and sample biases.²⁸¹⁻²⁸² pH was not adjusted, and only the free concentration of Cu^{2+} ions was determined rather than the Cu bound to organic matter and inorganic species.²¹⁷⁻²¹⁸ All reagents used in this study were analytical grade. Measurements were made in 10 mL samples from the effluent twice a week in triplicate. The inner and outer filling solutions of the electrodes were filled as recommended by the manufacturer's manual.

Sampling Schedule for Septic System

The system underwent consistent sampling time points each week. The times all experiments began and sample collection are listed in Table S1.

Table S1.

Experimental sampling schedule. The model colon was fed a media simulating digested food three times a day at 9 am, 3 pm, and 9 pm. BOD₅ and TSS were performed once a week with three replicates. Alkalinity, hardness, pH, conductivity, TOC, DLS, and zeta potential were performed twice a week in three replicates. All bacteria characterization experiments were performed every Wednesday. All of these analyses were conducted on collected effluent under this sampling regime for the baseline experiments (first four weeks with no copper addition) as well as during the three weeks of copper introduction (Cu weeks 1-3, three individual experiments for nano Cu, micro Cu, or Cu(OH)₂), and for the three post-Cu weeks, in which copper was no longer added, but still expected to be in the system.

	Sunday	Monday	Tuesday	Wednesday	Thursday	Friday
Time						
9:00 AM	Seed	Set up colon/ feed colon/ Collect colon waste	Feed colon/collect colon waste	Feed colon/collect colon waste	Feed colon/collect colon waste	Feed colon/collect colon waste
	colon microbes	All liquid components into septic	All liquid components into septic	All liquid components into septic Begin TSS (5 hrs in oven)	All liquid components into septic	All liquid components into septic
9:30 AM				All bacteria experiments		
10:00 AM		DLS/ZP		(cell conc., ZP, sizing, EPS, Part 1	DLS/ZP	
10:30 AM		pH/conductivity		hydrophobicity, DNA extraction)	pH/conductivity	
11:00 AM			TOC sample collected		TOC sample collected	
2:00 PM		Alkalinity Hardness		Finish up TSS	Alkalinity Hardness	
3:00 PM		Feed colon/collect colon waste Dose w/ Cu All liquid components into septic	Feed colon/collect colon waste Dose w/ Cu All liquid components into septic	Feed colon/collect colon waste Dose w/ Cu All liquid components into septic EPS Part 2	Feed colon/collect colon waste Dose w/ Cu All liquid components into septic	Feed colon/collect colon waste Dose w/ Cu All liquid components into septic Take apart colon Prepare colon for following week
4:00 PM		BOD ₅ part 2 (hour 120)		BOD ₅ part 1 (hour 0)		
9:00 PM		Feed colon/collect colon waste All liquid components into septic	Feed colon/collect colon waste All liquid components into septic	Feed colon/collect colon waste All liquid components into septic	Feed colon/collect colon waste All liquid components into septic	

Table footnotes:

DLS = dynamic light scattering to determine particle size

ZP = zeta potential to determine surface charge (EPM)

BOD₅ = biological oxygen demand, oxygen consumed over five-day period

TOC = total organic carbon

TSS = total suspended solids

EPS = extracellular polymeric substances

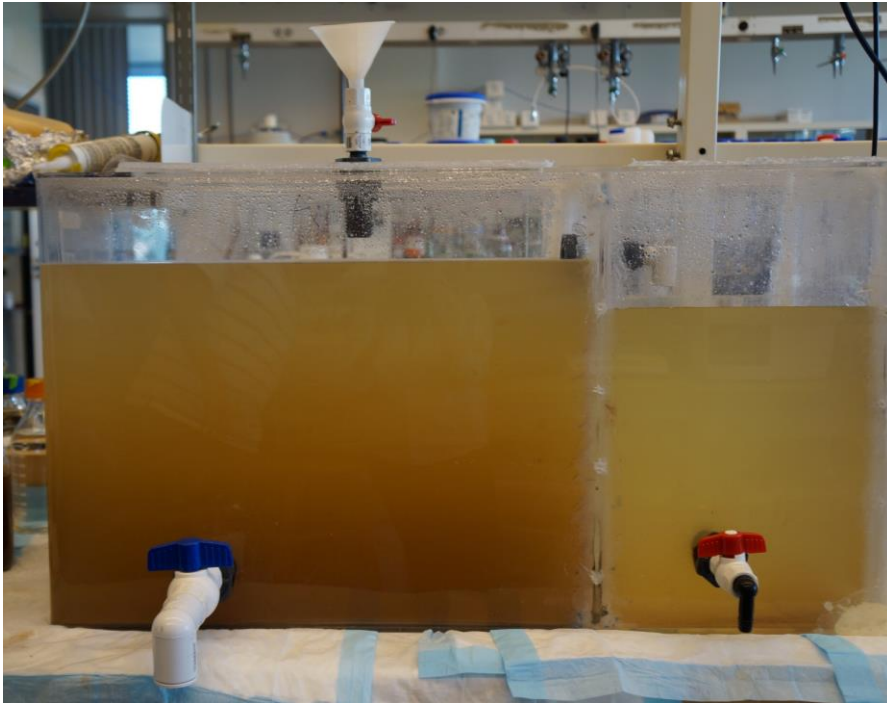
Cell conc. = cell concentration

Effluent was collected every week for all experimental conditions. TOC samples were collected twice a week and stored in 4 °C and were run within one month of collection.²⁷³ EPS samples were stored at -80 °C following the EPS Part 2 procedure on Wednesday at 3 PM. EPS samples were analyzed once a month in bulk. The colon was set-up every Monday AM using an in vitro model colon bioreactor and a microbial community donated and developed by a healthy 26-year-old female who had not had antibiotics in over eight months.^{115,247}

Alkalinity, hardness, and conductivity data are found in another publication.²¹¹

Figure S1

Digital image of model laboratory-scale septic tank. Photo courtesy of A. Taylor.



Results

Raw data collected in the experiments are reported here.

Table S2

All raw values (average and SD, where SD is the standard deviation) for all experiments conducted. The table is divided based upon test and Cu particle used. Raw values here are recorded with four significant figures. Water quality data throughout the main article are reported with three significant figures.

		Influent	Baseline wk 1	Baseline wk 2	Baseline wk 3	Baseline wk 4	Cu wk 1	Cu wk 2	Cu wk 3	Post Cu wk 1	Post Cu wk 2	Post Cu wk 3
pH												
Micro Cu	Avg	7.60	7.15	7.12	6.78	6.73	6.43	6.62	6.68	7.08	6.62	6.80
	SD	0.20	0.06	0.09	0.12	0.03	0.09	0.09	0.12	0.07	0.09	0.15
Cu(OH) ₂	Avg	7.60	7.15	7.12	6.78	6.73	6.73	7.07	7.45	7.39	7.04	7.18
	SD	0.20	0.06	0.09	0.12	0.03	0.02	0.06	0.14	0.15	0.28	0.12
Nano Cu	Avg	7.60	7.15	7.12	6.78	6.73	6.92	7.18	7.15	7.12	6.78	6.73
	SD	0.20	0.06	0.09	0.12	0.03	0.16	0.13	0.06	0.09	0.12	0.03
TOC (mg/L)												
Micro Cu	Avg	89.08	46.32	41.66	90.82	51.91	49.81	48.15	46.97	36.79	50.12	46.97
	SD	28.26	8.56	1.08	0.78	3.61	9.43	6.93	4.52	0.53	4.00	20.78
Cu(OH) ₂	Avg	89.08	46.32	41.66	90.82	51.91	208.20	94.18	82.51	91.79	62.22	75.81
	SD	28.26	8.56	1.08	0.78	3.61	136.47	5.89	1.47	5.77	33.87	2.78
Nano Cu	Avg	89.08	46.32	41.66	90.82	51.91	58.34	16.79	49.44	55.59	57.72	91.16
	SD	28.26	8.56	1.08	0.78	3.61	31.82	0.42	6.20	1.85	18.94	3.96

Turbidity (NTU)												
Micro Cu	Avg	78.50	12.50	11.20	10.30	N/A	2.63	3.73	2.38	23.97	3.86	1.47
	SD	3.73	0.30	0.42	0.36	N/A	0.07	0.72	0.07	0.15	0.14	0.58
Cu(OH) ₂	Avg	78.50	12.50	11.20	10.30	N/A	18.17	10.41	22.20	15.10	15.87	6.39
	SD	0.00	0.30	0.42	0.36	N/A	0.15	0.51	1.39	0.30	0.55	0.15
Nano Cu	Avg	78.50	12.50	11.20	10.30	N/A	4.55	3.06	2.48	5.16	5.74	10.03
	SD	0.00	0.30	0.42	0.36	N/A	0.37	0.60	0.29	0.30	0.47	0.06
BOD₅ (mg/L)												
Micro Cu	Avg	127.00	60.50	86.60	75.00	91.20	241.67	74.50	223.33	316.50	248.17	26.75
	SD	0.10	N/A	N/A	N/A	N/A	7.64	24.50	1.06	47.22	20.74	8.13
Cu(OH) ₂	Avg	127.00	66.50	93.00	89.20	91.20	30.33	267.00	208.50	25.25	26.83	31.17
	SD	0.10	N/A	N/A	N/A	N/A	29.20	4.77	12.02	10.75	15.43	3.55
Nano Cu	Avg	127.00	63.50	94.00	82.10	91.20	34.00	35.00	25.33	7.25	46.33	46.33
	SD	0.10	N/A	N/A	N/A	N/A	6.38	1.00	3.62	2.75	9.65	9.65
Hydrophobicity (%)												
Micro Cu	Avg	N/A	45.81	35.77	24.30	38.47	32.48	37.09	33.33	26.53	22.59	24.62
	SD	N/A	4.62	2.50	0.57	5.03	3.41	1.29	1.04	0.88	1.92	2.80
Cu(OH) ₂	Avg	N/A	45.81	35.77	24.30	38.47	20.13	29.02	35.41	27.15	38.27	41.52
	SD	N/A	4.62	2.50	0.57	5.03	4.60	1.87	5.19	4.84	1.84	3.72
Nano Cu	Avg	N/A	45.81	35.77	24.30	38.47	64.39	51.89	21.44	42.37	38.43	32.87
	SD	N/A	4.62	2.50	0.57	5.03	0.30	2.54	2.90	1.36	1.26	5.66
EPM [(μm/s)/(V/cm)]												
Micro	Avg	N/A	-1.16	-1.02	-1.34	-1.39	-1.55	-1.58	-1.46	-1.46	-1.09	-1.14

Cu		SD	N/A	0.19	0.24	0.31	0.27	0.24	0.34	0.28	0.16	0.18	0.25
Cu(OH) ₂	Avg	N/A	-1.16	-1.02	-1.34	-1.39	-1.34	-1.95	-1.92	-1.09	-2.39	-1.54	
	SD	N/A	0.00	0.00	0.00	0.00	0.49	0.37	0.26	0.55	0.35	0.43	
Nano Cu	Avg	N/A	-1.16	-1.02	-1.34	-1.39	-0.71	-0.65	0.90	-2.00	-2.30	-1.99	
	SD	N/A	0.00	0.00	0.00	0.00	0.63	0.27	0.26	0.43	0.26	0.32	

Cell radius (µm)												
Micro Cu	Avg	0.60	0.55	0.55	0.56	0.52	0.53	0.51	0.54	0.57	0.61	0.57
	SD	0.03	0.01	0.00	0.01	0.02	0.02	0.02	0.04	0.01	0.01	0.02
Cu(OH) ₂	Avg	0.60	0.55	0.55	0.56	0.52	0.55	0.50	0.64	0.57	0.25	0.43
	SD	0.03	0.01	0.00	0.01	0.02	0.00	0.02	0.03	0.03	0.01	0.02
Nano Cu	Avg	0.60	0.55	0.55	0.56	0.52	0.59	0.50	0.44	0.52	0.53	0.52
	SD	0.03	0.01	0.00	0.01	0.02	0.07	0.02	0.02	0.04	0.06	0.04

TSS (mg/L)												
Micro Cu	Avg	57.03	54.79	57.72	45.72	52.65	33.40	35.58	40.76	44.01	57.60	25.17
	SD	2.90	5.61	6.84	6.84	11.01	14.19	10.69	5.55	9.66	3.22	13.07
Cu(OH) ₂	Avg	57.03	54.79	57.72	45.72	52.65	46.15	60.31	54.79	33.80	44.01	42.28
	SD	2.90	5.61	6.84	6.84	11.01	16.94	8.18	5.61	13.73	7.68	13.36
Nano Cu	Avg	57.03	54.79	57.72	45.72	52.65	41.60	38.75	38.10	34.09	31.67	29.01
	SD	2.90	5.61	6.84	6.84	11.01	6.85	6.22	18.21	2.81	5.89	10.58

Cell concentration (10¹⁰ cell/mL)												
Micro Cu	Avg	N/A	0.58	0.73	0.75	0.55	0.55	0.35	0.38	0.38	1.05	0.63

	SD	N/A	N/A	N/A	N/A	N/A	N/A	N/A	N/A	N/A	N/A	N/A
Cu(OH) ₂	Avg	N/A	0.58	0.73	0.75	0.55	1.50	0.25	0.48	1.50	N/A	N/A
	SD	N/A	N/A	N/A	N/A	N/A	N/A	N/A	N/A	N/A	N/A	N/A
Nano Cu	Avg	N/A	0.58	0.7					0.18	0.10	0.40	N/A
	SD	N/A	N/A	N/A	N/A	N/A	N/A	N/A	N/A	N/A	N/A	N/A

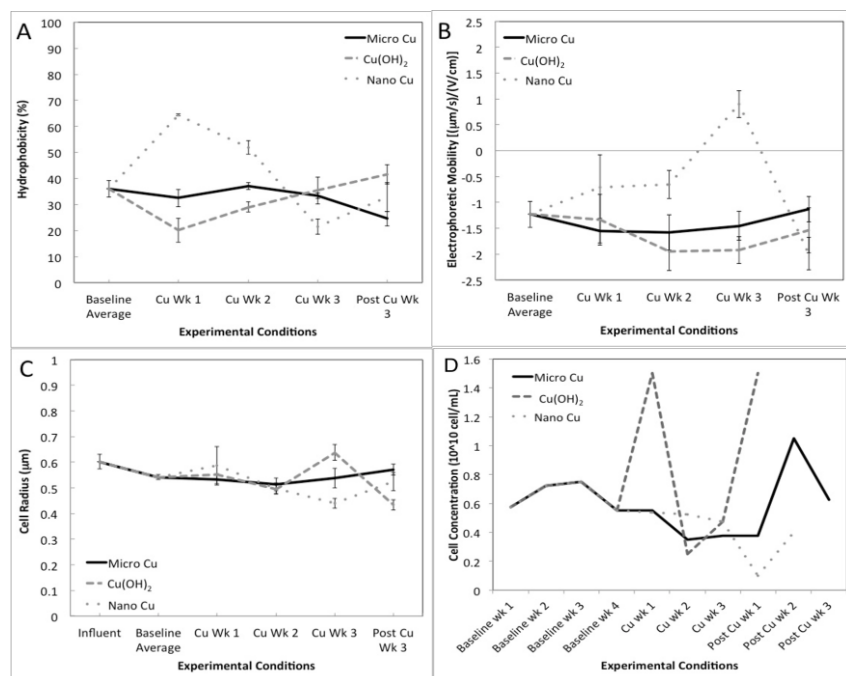
Cu²⁺ ions (ppm)												
Micro Cu	Avg	N/A	N/A	N/A	N/A	N/A	N/A	0.04	1.04	N/A	1.30	1.75
	SD	N/A	N/A	N/A	N/A	N/A	N/A	0.01	0.34	N/A	0.40	2.47
Cu(OH) ₂	Avg	N/A	0.02	0.01	0.01	0.01	0.05	0.07	4.87	0.02	0.00	0.21
	SD	N/A	0.03	0.01	0.00	0.00	0.11	0.07	0.78	0.02	0.00	0.08
Nano Cu	Avg	N/A	0.02	0.01	0.01	0.01	0.18	0.03	0.06	0.88	1.30	1.47
	SD	N/A	0.03	0.01	0.00	0.00	0.05	0.03	0.04	1.39	2.72	1.12

Results and Discussion

Bacteria Characterization

Figure S2

Changes in effluent bacteria characterization parameters (A-D) where hydrophobicity (A), electrophoretic mobility (B), cell size (C), and cell concentration (D) were measured over the course of three independent ten-week experiments for micro Cu (solid line), Cu(OH)₂ (dashed line), and nano Cu (dotted line). The influent measurement is an average of three readings; influent liquid components remained constant over the course of the experiments. The baseline average is four weeks of pre-Cu measurements averaged together, Cu weeks 1-3 are three weeks in which Cu particles are added once a day, and post-Cu week 3 is the final week of three weeks in which Cu particles are no longer added (post-Cu weeks 1-3) and in which conditions in the septic tank were anticipated to return to baseline conditions.



Impact of Nano Cu

Cell phenotype characterizations (hydrophobicity, electrophoretic mobility, cell concentration, and cell size) were performed to determine if deviations in septic system function could be assessed using other methods besides water quality tests. Bacteria hydrophobicity for a majority of the nano Cu exposure (nano Cu weeks 1-2, $58.3 \pm 7.0\%$) was significantly higher than the baseline weeks ($36.10 \pm 3.81\%$, $P < 0.001$, Figure S2 A). The post-Cu exposure hydrophobicity was considered the same as the baseline weeks ($32.9 \pm 5.7\%$, $P > 0.05$). Bacterial cells exposed to nano Cu had the highest hydrophobicity values for all of the experiments during the nano Cu addition (weeks 1 and 2, $64.4 \pm 0.3\%$ and $51.9 \pm 2.5\%$, respectively). For nano Cu, the EPM for all grouped conditions (baseline vs. nano Cu weeks 1-3 vs. post-nano Cu weeks 1-3) were significantly different from one another ($P \leq 0.01$, Figure S2 B), with baseline values of -1.2 ± 0.3 ($\mu\text{m/s})/(\text{V/cm})$, nano Cu exposure as -0.2 ± 0.9 ($\mu\text{m/s})/(\text{V/cm})$, and -1.9 ± 0.3 ($\mu\text{m/s})/(\text{V/cm})$ for post-nano Cu exposure. Nano Cu is the only condition that caused positive surface charge values (0.9 ± 0.3 ($\mu\text{m/s})/(\text{V/cm})$) during the final week of the nano Cu addition, yet the final week of the post-nano Cu exposure had the most negative EPM value for all experiments (-1.99 ± 0.32 ($\mu\text{m/s})/(\text{V/cm})$). The cell size for nano Cu conditions significantly decreased during the nano Cu addition (nano Cu weeks 2 and 3, 0.49 ± 0.2 μm and

0.44 ± 0.03 μm, respectively, P<0.001) when compared to baseline cell size (0.54 ± 0.01 μm). All other weeks were considered identical to the baseline for cell size (P>0.05). There were neither clear trends nor significant changes in the cell concentration data for any of the Cu exposures (Figure S2 D). Cell concentration data is missing for the last two weeks of the Cu(OH)₂ exposure (Cu(OH)₂ post weeks 2 and 3) and for the final week of the nano Cu experiment; therefore, cell concentration data is discussed only in the SI.

Impact of Micro Cu

The baseline average cell hydrophobicity for all Cu experiments was 36.10 ± 3.18% (Figure S2 A). The micro Cu exposure was not different from the baseline hydrophobicity (34.30 ± 2.50%). The final week of the post-micro Cu exposure (24.6 ± 2.80%) was significantly lower from both the baseline and the micro Cu hydrophobicities (P=0.005 and P<0.001, respectively). The surface charge (EPM, Figure S2 B) baseline average for all Cu experiments was -1.23 ± 0.25 (μm/s)/(V/cm). The micro Cu exposure (-1.59 ± 0.07 (μm/s)/(V/cm)) was significantly more negative (P<0.001) when compared to both the baseline condition (-1.23 ± 0.25 (μm/s)/(V/cm)) and the post-micro Cu exposure (-1.14 ± 0.25 (μm/s)/(V/cm), P<0.001). Post-micro Cu conditions and the baseline were not significantly different

for EPM data. For bacteria cell size, the micro Cu exposure size ($0.53 \pm 0.01 \mu\text{m}$) was smaller ($P=0.04$) when compared to the baseline cell size ($0.54 \pm 0.01 \mu\text{m}$) and to post-micro Cu cell size ($0.57 \pm 0.02 \mu\text{m}$).

Impact of $\text{Cu}(\text{OH})_2$

For cell hydrophobicity (Figure S2 A), the hydrophobicity during the $\text{Cu}(\text{OH})_2$ addition ($28.20 \pm 3.88\%$) was significantly lower than both the baseline ($36.10 \pm 3.81\%$) and the post- $\text{Cu}(\text{OH})_2$ exposure hydrophobicities ($41.52 \pm 3.72\%$, $P=0.002$ and $P=0.048$, respectively). The baseline and post- $\text{Cu}(\text{OH})_2$ hydrophobicities were significantly different ($P<0.001$). $\text{Cu}(\text{OH})_2$ had the lowest hydrophobicity value for all experiments during week 1 of the $\text{Cu}(\text{OH})_2$ addition ($20.13 \pm 4.60\%$).

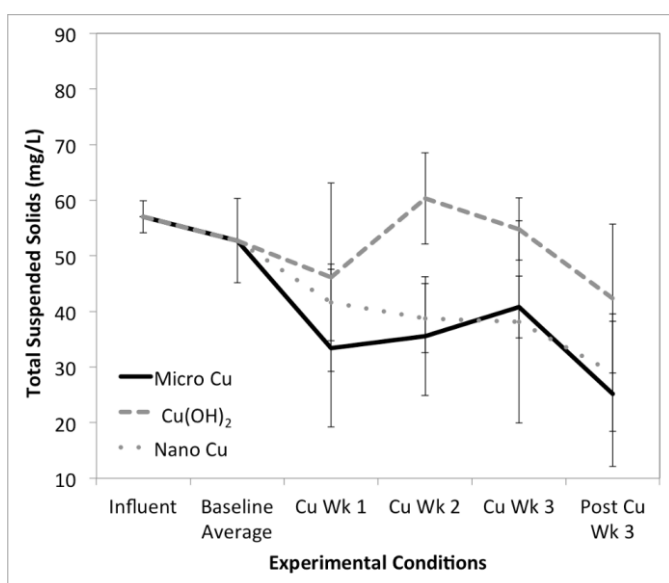
Two of the three weeks during the $\text{Cu}(\text{OH})_2$ exposure had the most negative values collected for surface charge (EPM) for all Cu experiments, -1.95 ± 0.37 and $-1.92 \pm 0.26 (\mu\text{m/s})/(\text{V/cm})$, following the value collected during the final week of the post-nano Cu exposure ($-1.99 \pm 0.32 (\mu\text{m/s})/(\text{V/cm})$). The baseline value ($-1.23 \pm 0.25 (\mu\text{m/s})/(\text{V/cm})$) was significantly less negative ($P<0.05$) than the $\text{Cu}(\text{OH})_2$ addition and the post- $\text{Cu}(\text{OH})_2$ exposure ($-1.54 \pm 0.43 (\mu\text{m/s})/(\text{V/cm})$). Variations in cell size were also recorded. Overall, the $\text{Cu}(\text{OH})_2$ exposure cell size ($0.56 \pm 0.07 \mu\text{m}$, three week average) was not significantly different from the baseline cell size (0.54 ± 0.01

μm), except for the individual $\text{Cu}(\text{OH})_2$ week 3 which had a larger cell size ($0.64 \pm 0.02 \mu\text{m}$, $P=0.01$) than the baseline. The post- $\text{Cu}(\text{OH})_2$ cell size was significantly smaller in size ($0.41 \pm 0.20 \mu\text{m}$) than the baseline ($P=0.01$).

Total Suspended Solids (TSS)

Figure S3

Changes in the water quality parameter total suspended solids (TSS) over the course of three independent ten-week experiments for micro Cu (solid line), $\text{Cu}(\text{OH})_2$ (dashed line), and nano Cu (dotted line). The influent measurement is an average of three total readings taken during baseline week 4, Cu week 3, and post-Cu week 3. The baseline average is four week of pre-Cu measurements averaged together, Cu weeks 1-3 are three weeks in which Cu particles are added once a day, and post-Cu week 3 is the final week of three weeks in which Cu particles (post-Cu weeks 1-3) are no longer added and in which conditions in the septic tank were anticipated to return to baseline conditions. Typical TSS values for septic tanks range between 40-140 mg/L of TSS.²¹³



Typical TSS values for septic tanks range between 40-140 mg/L of TSS.²¹³ There were neither clear trends nor significant changes in the TSS data (Figure S3). The final post-exposure week (micro Cu post week 3) had the lowest TSS value of 25 mg/L. During the micro exposures (micro Cu post week 2) the second highest TSS value of 57 mg/L was recorded. The post-nano Cu exposure condition did not return to baseline conditions (52.7 mg/L); the post-nano Cu exposure weeks were overall significantly lower (31.6 mg/L) than the baseline weeks ($P < 0.01$). The final post-nano Cu exposure weeks (nano Cu post week 3) had the lowest recorded TSS value of 29 mg/L and the highest TSS value (nano Cu post week 2, 60 mg/L). $\text{Cu}(\text{OH})_2$ did not cause significant changes in TSS and during the $\text{Cu}(\text{OH})_2$ exposure, the highest TSS value (60 mg/L, Figure 1B) was recorded for this form of Cu.

TSS are the portion of the effluent sample making up the solid residue that remains on the filter after filtering, evaporation, and drying of the sample.²¹⁵ TSS can be correlated with turbidity measurements, the difference being TSS gives actual weights of the material collected from the sample.²¹⁵ Typical TSS values for septic tanks range between 40-140 mg/L of TSS²¹³ and TSS values should show a 60-80% removal efficiency of TSS from the influent to the effluent.^{226-227, 246-247} While the TSS results shown in Figure S1 demonstrate that all experimental conditions are within the expected range for TSS, the removal efficiency percentage did not reach 60-80%. This indicates that the system may not have been functioning optimally.

However, all other water quality tests during baseline conditions indicate that the system was functioning like a real-world septic system. No other clear patterns were noted among the various Cu NP treatments.

References

1. Canter, L. W.; Knox, R. C., *Septic tank system effects on ground water quality*. Lewis Publishers, Inc: 1985.
2. EPA, Onsite Wastewater Treatment Systems Manual EPA625/R-00-008. Cincinnati, Ohio, 2002; pp 4-38.
3. Marcus, I. M.; Wilder, H. A.; Quazi, S. J.; Walker, S. L., Linking Microbial Community Structure to Function in Representative Simulated Systems. *Applied and Environmental Microbiology* **2013**, *79* (8), 2552-2559.
4. Taylor, A. A.; Marcus, I. M.; Guysi, R. L.; Walker, S. L., Metal oxide nanoparticles induce phenotypic changes in a model colon gut microbiota. *Environmental Engineering Science* **2015**.
5. Brandes, M., Characteristics of Effluents from Gray and Black Water Septic Tanks. *Journal (Water Pollution Control Federation)* **1978**, *50* (11), 2547-2559.
6. Nghiem, L. D.; Oschmann, N.; Schäfer, A. I., Fouling in greywater recycling by direct ultrafiltration. *Desalination* **2006**, *187* (1-3), 283-290.
7. Lin, S.; Taylor, A. A.; Ji, Z.; Chang, C. H.; Kinsinger, N. M.; Ueng, W.; Walker, S. L.; Nel, A. E., Understanding the Transformation, Speciation, and Hazard Potential of Copper Particles in a Model Septic Tank System using Zebrafish to Monitor the Effluent. *ACS Nano* **2015**.
8. EPA, National Interim Primary Drinking Water Regulations. Supply, O. o. W., Ed. Washington, D.C., 1976.
9. Beal, C. D.; Gardner, E. A.; Menzies, N. W., Process, performance, and pollution potential: A review of septic tank–soil absorption systems. *Soil Research* **2005**, *43* (7), 781-802.
10. Health, W. S. D. o., Rule Development Committee Issue Research Report: Septic Tank Effluent Values. 2004.
11. Hickey, J. L. S.; Duncan, D. L., Performance of Single Family Septic Tank Systems in Alaska. *Journal (Water Pollution Control Federation)* **1966**, *38* (8), 1298-1309.
12. Resources, W. D. o. N., Introduction to Anaerobic Digestion Study Guide. Resources, D. o. N., Ed. Madison, 1992.
13. Zaveri, R. M.; Flora, J. R. V., Laboratory septic tank performance response to electrolytic stimulation. *Water Research* **2002**, *36* (18), 4513-4524.

14. Association, A. P. H.; Association, A. W. W.; Federation, W. P. C.; Federation, W. E., *Standard methods for the examination of water and wastewater*. 17 ed.; American Public Health Association.: 1989.
15. Analytical, O., *Aurora 1030 Combustion TOC Analyzer Operator's Manual*. 2.1 ed.; College Station, Texas, 2012.
16. Schumacher, B. A., Methods for the determination of total organic carbon (TOC) in soils and sediments. *Ecological Risk Assessment Support Center* **2002**, 1-23.
17. Choi, O.; Deng, K. K.; Kim, N.-J.; Ross Jr, L.; Surampalli, R. Y.; Hu, Z., The inhibitory effects of silver nanoparticles, silver ions, and silver chloride colloids on microbial growth. *Water Research* **2008**, *42* (12), 3066-3074.
18. Gutman, J.; Walker, S. L.; Freger, V.; Herzberg, M., Bacterial Attachment and Viscoelasticity: Physicochemical and Motility Effects Analyzed Using Quartz Crystal Microbalance with Dissipation (QCM-D). *Environmental Science & Technology* **2012**, *47* (1), 398-404.
19. Haznedaroglu, B. Z.; Kim, H. N.; Bradford, S. A.; Walker, S. L., Relative Transport Behavior of Escherichia coli O157:H7 and Salmonella enterica Serovar Pullorum in Packed Bed Column Systems: Influence of Solution Chemistry and Cell Concentration. *Environmental Science & Technology* **2009**, *43* (6), 1838-1844.
20. Walker, S. L.; Redman, J. A.; Elimelech, M., Influence of growth phase on bacterial deposition: Interaction mechanisms in packed-bed column and radial stagnation point flow systems. *Environmental Science & Technology* **2005**, *39* (17), 6405-6411.
21. Dowd, S. E.; Sun, Y.; Wolcott, R. D.; Domingo, A.; Carroll, J. A., Bacterial tag-encoded FLX amplicon pyrosequencing (bTEFAP) for microbiome studies: bacterial diversity in the ileum of newly weaned Salmonella-infected pigs. *Foodborne pathogens and disease* **2008**, *5* (4), 459-472.
22. Andreotti, R.; Perez de Leon, A.; Dowd, S.; Guerrero, F.; Bendele, K.; Scoles, G., Assessment of bacterial diversity in the cattle tick Rhipicephalus (Boophilus) microplus through tag-encoded pyrosequencing. *BMC Microbiology* **2011**, *11* (1), 6.
23. Handl, S.; Dowd, S. E.; Garcia-Mazcorro, J. F.; Steiner, J. M.; Suchodolski, J. S., *Massive parallel 16S rRNA gene pyrosequencing reveals highly diverse fecal bacterial and fungal communities in healthy dogs and cats*. 2011; Vol. 76, p 301-310.
24. Pitta, D.; Pinchak, W.; Dowd, S.; Osterstock, J.; Gontcharova, V.; Youn, E.; Dorton, K.; Yoon, I.; Min, B.; Fulford, J. D.; Wickersham, T.; Malinowski, D., Rumen Bacterial Diversity

Dynamics Associated with Changing from Bermudagrass Hay to Grazed Winter Wheat Diets. *Microb Ecol* **2010**, 59 (3), 511-522.

25. Edgar, R. C., Search and clustering orders of magnitude faster than BLAST. *Bioinformatics* **2010**, 26 (19), 2460-2461.
26. Buckley, J. A., The bioavailability of copper in wastewater to *Lemna minor* with biological and electrochemical measures of complexation. *Water Research* **1994**, 28 (12), 2457-2467.
27. Sauvé, S.; McBride, M. B.; Hendershot, W. H., Ion-selective electrode measurements of copper(II) activity in contaminated soils. *Arch. Environ. Contam. Toxicol.* **1995**, 29 (3), 373-379.
28. Sanders, J. R., The effect of pH upon the copper and cupric ion concentrations in soil solutions. *Journal of Soil Science* **1982**, 33 (4), 679-689.
29. Temminghoff, E. J. M.; Van der Zee, S. E. A. T. M.; de Haan, F. A. M., Copper Mobility in a Copper-Contaminated Sandy Soil as Affected by pH and Solid and Dissolved Organic Matter. *Environmental Science & Technology* **1997**, 31 (4), 1109-1115.
30. Crites, R.; Technobanoglous, G., *Small and decentralized wastewater management systems*. McGraw-Hill: 1998.
31. Bounds, T., Design and performance of septic tanks. *ASTM SPECIAL TECHNICAL PUBLICATION* **1997**, 1324, 217-234.
32. Rock, C. A.; Boyer, J. A., Influence of design on septic tank effluent quality. *Proceedings of 8th northwest on-site wastewater treatment short course and equipment exhibition* **1995**.
33. Siegrist, R. L.; Anderson, D. L.; Converse, J. C., *Onsite treatment and disposal of restaurant wastewater*. University of Wisconsin--Extension, Division of Economic and Environmental Development: 1984.

Chapter 4

Understanding the Transformation, Speciation, and Hazard Potential of Copper Particles in a Model Septic Tank System Using Zebrafish to Monitor the Effluent

Reproduced with Permission from *ACS Nano*, Copyright 2015, ACS.

Lin, S., A.A. Taylor, Z. Ji, C.H. Chang, N.M. Kinsinger, W. Ueng, S.L. Walker, and A.E. Nel (Just accepted 01-27-2015)
DOI: 10.1021/nn507216f.

Chapter 4: Understanding the Transformation, Speciation, and Hazard Potential of Copper Particles in a Model Septic Tank System Using Zebrafish to Monitor the Effluent

Abstract

Although copper-containing nanoparticles are used in commercial products such as fungicides and bactericides, we presently do not understand the environmental impact on other organisms that may be inadvertently exposed. In this study, we used the zebrafish embryo as a screening tool to study the potential impact of two nano Cu-based materials, CuPRO and Kocide, in comparison to nano-sized and micron-sized Cu and CuO particles in their pristine form (0 - 10 ppm) as well as following their transformation in an experimental wastewater treatment system. This was accomplished by construction of a modeled domestic septic tank system from which effluents could be retrieved at different stages following particle introduction (10 ppm). The Cu speciation in the effluent was identified as non-dissolvable inorganic $\text{Cu}(\text{H}_2\text{PO}_2)_2$ and non-diffusible organic Cu by X-ray diffraction, inductively coupled plasma mass spectrometry (ICP-MS), diffusive gradients in thin-films (DGT), and Visual MINTEQ software. While the nanoscale materials, including the commercial particles, were clearly more potent (showing 50% hatching interference above 0.5 ppm) than the micron-scale particulates, the Cu released from the particles in the septic tank underwent transformation into non-bioavailable species that failed to interfere with the function of the zebrafish embryo hatching enzyme. Moreover, we

demonstrate that the addition of humic acid, as an organic carbon component, could lead to a dose-dependent decrease in Cu toxicity in our high content zebrafish embryo screening assay. Thus, the use of zebrafish embryo screening, in combination with the effluents obtained from a modeled exposure environment, enables a novel bioassay approach to follow the change in the speciation, and hazard potential of Cu particles instead of difficult-to-perform direct particle tracking.

Introduction

Nano-enabled Cu products are increasingly being used for commercial applications, including as antibacterial and antifungal agents that can be applied for spraying of vegetation or as a marine anti-fouling paint on the hulls of boats and ships.²⁸³⁻²⁸⁹ For example, CuPRO and Kocide are Cu(OH)₂-based nano-products used as antifungal agents to spray agricultural crops and lawns. While clearly beneficial for eradicating bacterial and fungal growth, inadvertent exposure of other environmental species, such as fish or fish embryos, has not received sufficient attention because it is difficult to model complicated exposure environments. In addition to identifying relevant environmental species to serve as organisms for predictive toxicological assessment,²⁹⁰⁻²⁹¹ it is important to consider the fate, transport, and transformation of Cu particles in the exposure environment.²⁹² Not only it is challenging to track the presence and behavior of commercially applied nanoparticles in complex exposure environments, but we also need to consider the impact of pH, ionic strength, light exposure, and the presence of natural organic matters on the fate, transformation and possible hazardous impact of these materials.²⁹²⁻²⁹³

Because of the complexity of tracking the environmental fate and transformation of commercial nanomaterials, it is helpful to use simulated exposure scenarios to obtain information that can be used to support environmental risk assessment.²⁹⁴⁻²⁹⁵ One approach is the use of life cycle analysis (LCA) to delineate

potential hotspots of exposure that can be used to obtain predictive environmental concentrations (PEC) for risk assessment.²⁹⁶ In a recent study of Cu-based nanomaterials, Keller *et al.* have provided assessments of environmental exposure routes, based on which the proportional distribution of commercial products to air, landfill, soil, and the aquatic disposal sites could be estimated.²⁹⁷ This work has identified Cu entry into wastewater treatment systems (industrial, community or private houses) as an important life cycle stage during which aquatic exposure can occur. Since 20-30% of American households use a septic tank system for sewage treatment,²⁰²⁻²⁰³ we have established a laboratory-scale septic tank system to model the fate, transport and speciation of nanoparticles. In contrast to intensive monitoring of industrial wastewater treatment plants (WWTPs),²⁹⁸⁻³⁰⁸ household septic tanks are not scrutinized or regulated to the same degree.^{57-61, 209-210, 224, 309} Moreover, up to 40% of domestic septic tank systems do not function properly,⁵⁷ and the impact of commercial nanomaterials have not been considered on the function and efficiency of these wastewater treatment (WWT) systems.

Given this background, we designed a study wherein we combined the use of a model septic system with our zebrafish high content screening (HCS) platform for assessing the toxicological potential of nano- and micron-sized Cu and CuO, including the commercial nano Cu(OH)₂-based particulates, CuPRO and Kocide. The septic tank system allows modeling of the fate, transport, and transformation of these

materials in a decentralized WWT utility. The zebrafish embryo is a sensitive screening platform to access nanoparticle release and speciation of the Cu at a molecular level, namely the active center of the zebrafish hatching enzyme 1 (ZHE1).³¹⁰ Moreover, this metalloprotease enzyme serves as a delicate abiotic marker that can predict the ionic metal and metal oxide species that can disrupt embryo hatching.³¹¹ We demonstrate that even though nano-sized Cu particles are more toxic than micron-scale particulates, particle transformation and Cu speciation at different stages of the WWT process led to a significant change in hazard potential, regardless of the particle composition or size. The hazard reduction was accompanied by the formation of insoluble inorganic as well as non-diffusible organic Cu species, which are not bioavailable to the hatching apparatus. Our results demonstrate a novel approach to assessing the environmental transformation of nano Cu without the necessity of direct particle tracking.

Materials and Methods

Cu Particle Acquisition and Physicochemical Characterization

Six Cu particles, including nano-sized Cu and CuO, micron-sized Cu and CuO, and two nano Cu(OH)₂-based fungicides (CuPRO and Kocide) were used in this study. They were purchased in powder form from commercially available vendors. Nano Cu

was from US Research Nanomaterials, Inc., and nano CuO, micro Cu, and micro CuO were from Sigma Aldrich. CuPRO 2005 was from SePRO, and Kocide 3000 was from DuPont. All materials were used, as received, without further purification or modification. Physicochemical characterization, including primary particle size, shape, crystal structure, purity, and endotoxin levels were assessed on all materials. Transmission electron microscopy (TEM) and scanning electron microscopy (SEM) were used to measure the primary particle size and shape. X-ray diffraction (XRD) was used to determine the crystal structure of each particle. Purity was measured by inductively coupled plasma optical emission spectroscopy (ICP-OES) and presented as weight percentage of each main component per unit mass of Cu particles (i.e. Cu(OH)₂ in Kocide and CuPRO; Cu in nano Cu and micro Cu; CuO in nano CuO and micro CuO, respectively). The hydrodynamic sizes and surface charge of the particles dispersed in deionized water (DI H₂O) and Holtfreter's medium were determined by a high throughput dynamic light scattering instrument (HT-DLS, Dynapro Plate Reader, Wyatt Technology) and a ZetaPALS instrument (Brookhaven Instruments, Holtsville, NY), respectively. The dissolution characteristics of Cu particles were analyzed by ICP-OES through ultracentrifugation, as described by Lin *et al.* Briefly Cu particle suspensions (in DI H₂O and Holtfreter's medium) were kept at 28.5 °C for 48 h and centrifuged for 1 h at 20,000g. The supernatants were collected for quantification of elemental Cu content, using ICP-OES.

Septic Tank Design and Effluent Sample Collection

A septic tank system, comprised of primary and secondary chambers,³¹² was used to simulate the fate, transport and transformation of the Cu particles in a decentralized wastewater treatment process. Details of the septic tank construction and function appear in the SI. Briefly, before dosing of the primary chamber with Cu particles, the tank system underwent four weeks of conditioning. The effluent collected from the secondary chamber during this period was considered as “background”. Subsequently, nano Cu, CuPRO or micro Cu were introduced into the primary chamber (three individual experiments) daily for three weeks, by mixing with synthetic grey water and colon waste from a model colon reactor to mimic household wastewater. The total quantities of Cu particles added to the septic system amounted to 500, 1000, and 1500 mg, at the culmination of weeks 1 - 3, respectively. This was equivalent to Cu concentrations of 3.33, 6.67, and 10 ppm, respectively. This period was followed by a three week interval during which no new particles were added to the septic tank but during which effluents were collected on a weekly basis. These were labeled week 1 - 6 effluents for each of the particle types being assessed. The final concentration of 10 ppm was selected based upon predicted concentrations of Cu found in WWTPs^{31-32, 38}. Moreover, since the system has a three week residence time of liquids, it was anticipated that an effect would not be observed with dosing the system once due to

the amount of liquid that enters the primary chamber on a weekly basis (~75 L per week). With general use of a septic system, it was estimated that waste from the household would contain a steady stream of a low concentration of nanomaterials from consumer products. Therefore, we selected to dose the system over a three week period with a dose of ~3.3 ppm per week (or a final total concentration of 10 ppm).

Toxicity Assessment Using Zebrafish Embryo High Content Screening (HCS)

Our robotic and automated system for zebrafish embryo hatching was used to assess the impact of as-received Cu particles, “background” effluent, week 1 - 6 effluents, as well as “background” effluent spiked with known concentrations (0.125 - 1 ppm) of Cu²⁺ and nano Cu. Details of our embryo HCS screening protocol appear in the SI and reference 38.

Copper Partitioning, Transformation and Speciation

To quantify the Cu content of the septic system, inductively coupled plasma mass spectrometry (ICP-MS) was used to measure the elemental Cu concentrations in the primary chamber sludge as well as the various effluents. The method for sample digestion and ICP analysis appear in the SI. Cu particle transformation and inorganic speciation was assessed by X-ray diffraction (XRD) analysis. Ten mL of each effluent was dried on the sample stub prior to XRD spectral acquisition, using a Panalytical

X'Pert Pro diffractometer (Cu K α radiation). Inorganic Cu species were identified by comparing the diffraction peaks in the effluents with a standard spectral library. However, since this technique cannot be used for organic Cu, organic Cu speciation was modeled by the Windows software program, Visual MINTEQ (version 3.1, 2014, KTH Royal Institute of Technology, Stockholm, Sweden).³¹³ A “sweep” function was used to determine the organic Cu speciation in the presence of humic acid (HA) as a source of dissolved organic matters (DOM, as appears in the effluent). The percentage distribution of organic-Cu vs. Cu²⁺ was calculated and plotted against increasing HA concentrations (0 - 100 ppm). These results were supplemented by using the diffusive gradients in thin-films method (DGT Research Ltd) to measure the diffusible effluent content of Cu²⁺. Each DGT unit is comprised of a nitrocellulose membrane filter, diffusion and resin gel layers to isolate the diffusible Cu²⁺ from the non-diffusible organic-Cu complexes in the effluent. After incubation of the DGT unit in the effluent for 3 days at 28 °C, the resin gel was retrieved and digested in nitric acid, before performance of ICP-OES.

Statistical Methods

Results were statistically analyzed using two-side Student's t-test. The difference is regarded as statistically significant with $p < 0.05$. Data are reported as the mean \pm standard deviation from at least three separate experiments.

Results

Acquisition and Physicochemical Characterization of a Cu Particle Library

To conduct our study, we assembled a library of particles that included nano-sized Cu and CuO, micron-sized Cu and CuO, and two Cu(OH)₂-based commercial fungicides, Kocide and CuPRO. Comprehensive physicochemical characterization of the particles was undertaken, and the results are shown in Table 4.1. Transmission electron microscopy (TEM) showed a nano CuO size range of 20 - 100 nm, with nano Cu exhibiting a broader size distribution of 200 - 1000 nm. Representative images are shown in Figure S4.1. By comparison, micron-sized Cu and CuO particles were ≥ 2 μm in size. Although the commercial fungicides, Kocide and CuPRO, claim to include nano Cu(OH)₂ as an active ingredient, only CuPRO showed discernable particles of ~ 20 nm while the Kocide TEM images showed amorphous materials with no definable particles. Most particles observed in our library had irregular shapes,

except micro Cu which had a dendritic appearance (Figure S4.1). X-ray diffraction (XRD) analysis confirmed the presence of orthorhombic $\text{Cu}(\text{OH})_2$ as the main chemical ingredient of CuPRO and Kocide. Highly crystalline, monoclinic CuO was the only phase identified in nano- and micron-sized CuO samples. Although no oxides were detected in the micron-sized Cu sample, a significant amount of Cu_2O was present in nano Cu, likely as a result of surface oxidation.

When introduced into deionized water and Holtfreter's medium, the hydrodynamic diameters of the Cu particles ranged from 400 nm to 2 μm . All particles had a narrow range of zeta-potentials (-16 to -22 mV) in Holtfreter's medium, likely as a result of surface coating by alginate, which was included as a dispersal agent that is present in natural aquatic environment (Table 4.1). Particle purity was assessed by ICP-OES and the presence of each ingredient was expressed as weight percentage (wt%) relative to the weight of the powdered formulation. The $\text{Cu}(\text{OH})_2$ content of Kocide and CuPRO were 40 wt% and 47 wt%, respectively, which is similar to the manufacturers' data. The Cu purity content was used to convert the nominal particle concentrations into elemental Cu concentrations for the planning of zebrafish exposure experiments.

Particle dissolution plays a critical role in hazard generation by metal and metal oxide nanoparticles.^{310-311, 314-315} We have previously demonstrated that dissolution of CuO nanoparticles in Holtfreter's medium can affect hatching

interference in zebrafish embryos as a result of the inhibitory effect of Cu^{2+} on the active center of the metalloprotease hatching enzyme, ZHE1.³¹¹ Use of ICP-OES to determine Cu particle dissolution in Holtfreter's medium revealed three dissolution categories based on the wt% dissolution (Figure 4.1A). That is, while the two fungicides as well as nano Cu were highly dissolvable (> 8 wt% dissolution), nano CuO occupied an intermediate range (2-8 wt% dissolution), with micro Cu and CuO showing < 2 wt% solubility.

Table 4.1 Physicochemical Characterization of Cu Particles.

Physicochemical characterizations	Technique	Unit	Particles					
			Kocide	CuPRO	micro Cu	micro CuO	nano Cu	nano CuO
Primary Size	TEM	nm	N/A ^a	~10	>10000	200-2000	200-1000	20-100
Phase & Structure	XRD		Orthorhombic Cu(OH) ₂ , Impurities	Orthorhombic Cu(OH) ₂ , Impurities	Cubic Cu	Monoclinic CuO	Cubic Cu, Cubic Cu ₂ O	Monoclinic CuO
Shape/Morphology	TEM		Irregular	Irregular	Dendritic	Irregular	Irregular	Irregular
Size in DI H ₂ O	HT-DLS	nm	1397±143	889±156	n/a ^c	1316±176	1164±202	420±15
Zeta Potential in DI H ₂ O	ZetaPALS	mV	-53.8±0.7	-45.1±0.8	-32.5±2.9	-28.5±0.9	-46.3±1.6	-16.5±0.8
Size in H buffer (w/alginate)	HT-DLS	nm	1172±104	953±88	n/a ^c	1349±62	2714±719	459±4
Zeta Potential in H buffer (w/alginate)	ZetaPALS	mV	-19.9±0.8	-22.9±0.6	-19.9±0.8	-16.2±1.5	-15.9±1.4	-18.8±0.9
Purity ^b	ICP-OES	wt.%	39.9±1.4	47.1±2.6	94.9±1.4	92.8±1.1	84.8±2.7	88.3±1.3

^a Primary size cannot be obtained because particles are of undefined morphology.

^b Purity refers to weight percentage of each main component (i.e., Cu(OH)₂ in Kocide and CuPRO; Cu in micro Cu and nano Cu; CuO in micro CuO and nano CuO, respectively)

^c Hydrodynamic size cannot be obtained because of fast particle sedimentation.

Use of As-received Cu Particles to Study Their Impact on Zebrafish Embryo Hatching

We used our robotic arm for picking and plating fertilized zebrafish embryos into 96-well plates, followed by automated imaging to identify embryo hatching in the presence of the particles in our library. Healthy embryos were exposed to particles at concentrations of 0 - 10 ppm at 4 hours post fertilization (hpf) before determining hatching outcome at 72 hpf, using our automated imaging equipment and phenotyping software.^{310-311, 316} Please note that we converted the nominal particle concentrations into elemental Cu concentrations to allow comparison of materials with different levels of impurity. Expression of the % embryo hatching vs. log[Cu] concentration (ppb) demonstrated dose-dependent hatching interference by the fungicides as well as nano Cu and CuO, with the micron-sized materials showing comparatively little effect (Figure 4.1B). The same data was expressed as linear dose response curve of Cu particle concentrations (0 – 2.5 ppm) vs. % hatching in Figure S4.2, with error bars indicating standard deviation. Using CuCl₂ as positive control allowed us to express the hierarchical hatching interference as: CuCl₂ > nano Cu > CuPRO = Kocide > nano CuO > micro Cu = micro CuO. Statistically significant hatching interference was observed at 0.1 ppm CuCl₂, 0.25 ppm nano Cu, 0.3 ppm CuPRO and Kocide, and 0.5 ppm nano CuO, respectively. The particle ranking is in good agreement with the dissolution profiles, showing a Pearson's correlation coefficient of 0.873 for the IC₅₀

values (concentration yielding 50% hatching interference) *vs.* wt% particle dissolution. Overall, higher dissolution rates were strongly correlated to lower IC₅₀ values. Toxicological outcomes, including morphological abnormalities and mortality, were also monitored throughout the development of embryos upon Cu particles exposure. No significant effects on embryo morphology or mortality were observed within the concentration range of all Cu particles.

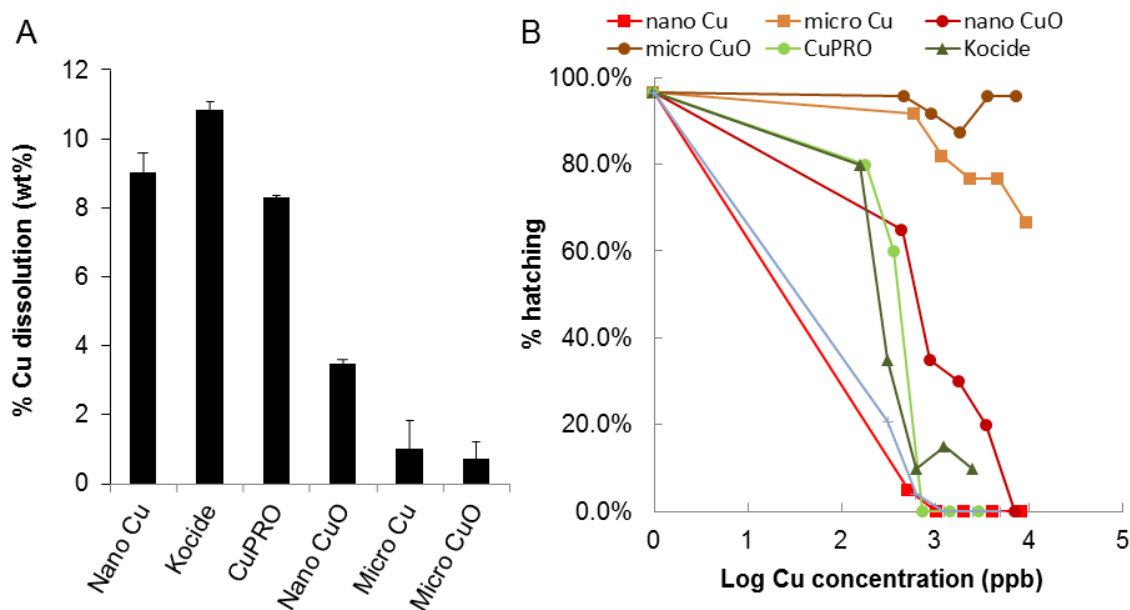


Figure 4.1.

Cu dissolution and hatching interference of as-received Cu particles. (A) Calculation of the weight percent dissolution of nano Cu, Kocide and CuPRO (highly soluble); nano CuO (intermediate solubility); and micro Cu and CuO (minimally soluble). (B) Percent hatching of zebrafish embryos exposed to as-received Cu particles (0 - 10 ppm) for 72 hours, commencing at 4 hours post-fertilization. The dose dependent curve is expressed as % hatching *vs.* Log [Cu] (ppb).

Use of Septic Tank Effluents to Study the Effect of Cu Particle Transformation on Zebrafish Embryo Hatching

While Cu is efficacious as a bactericide or a fungicide, the environmental impact of Cu on other environmental species that may be inadvertently exposed, needs to be considered. Since it has been shown by LCA modeling that nano Cu gains access to WWTPs,²⁹⁷ we developed a model septic tank system to simulate an exposure environment in which particles could be introduced to study their transformation and speciation on another aquatic species. The zebrafish was chosen because of their well-studied utility for nanosafety studies, including the demonstration of a high level of sensitivity of the zebrafish embryo to nano Cu.³¹⁰⁻³¹¹ We reasoned that the toxicity profiling of the effluent would be informative for studying Cu speciation as a means of following the particle transformation rather than tracking the particles directly. Figure 2A shows the design of the model septic tank system to generate effluents for assessment of zebrafish toxicity. Based on their hazard ranking and dissolution characteristics, nano Cu, CuPRO, and micro Cu, were selected from the library materials for introduction to the septic tank. Prior to adding the particles, the septic tank underwent four weeks of conditioning by introducing simulated wastewater into the primary chamber, followed by weekly collection of effluents from the secondary chamber. These effluents were pooled and regarded as “background” effluent, which

served as a control to rule out possible interference of non-Cu materials in the effluent on embryo hatching. Each type of particle was added in individual experiments, daily for 3 weeks, to reach a cumulative dose of 10 ppm by the end of week 3. The effluents were collected from the secondary chamber, weekly for 3 weeks (week 1 - 3), as well as for an additional 3 weeks (week 4 - 6) during which no particles were introduced. The “background” as well as the week 1 - 6 effluents were used to assess the impact on zebrafish embryo hatching. As a positive control, we used 0.5 ppm nano Cu in Holtfreter’s medium; this dose leads to 50% hatching interference (Figure 4.2B). Interestingly, all effluents, irrespective of whether they were from “background” origin or collected after the addition of Cu to the tank, did not interfere with embryo hatching (Figure 4.2B). The effluent did not affect the embryo morphology or the survival rate (Figure S4.2B). The lack of an effect by the effluents signified that there was either no significant Cu carryover or that the Cu in the effluent was not bioavailable for hatching interference.

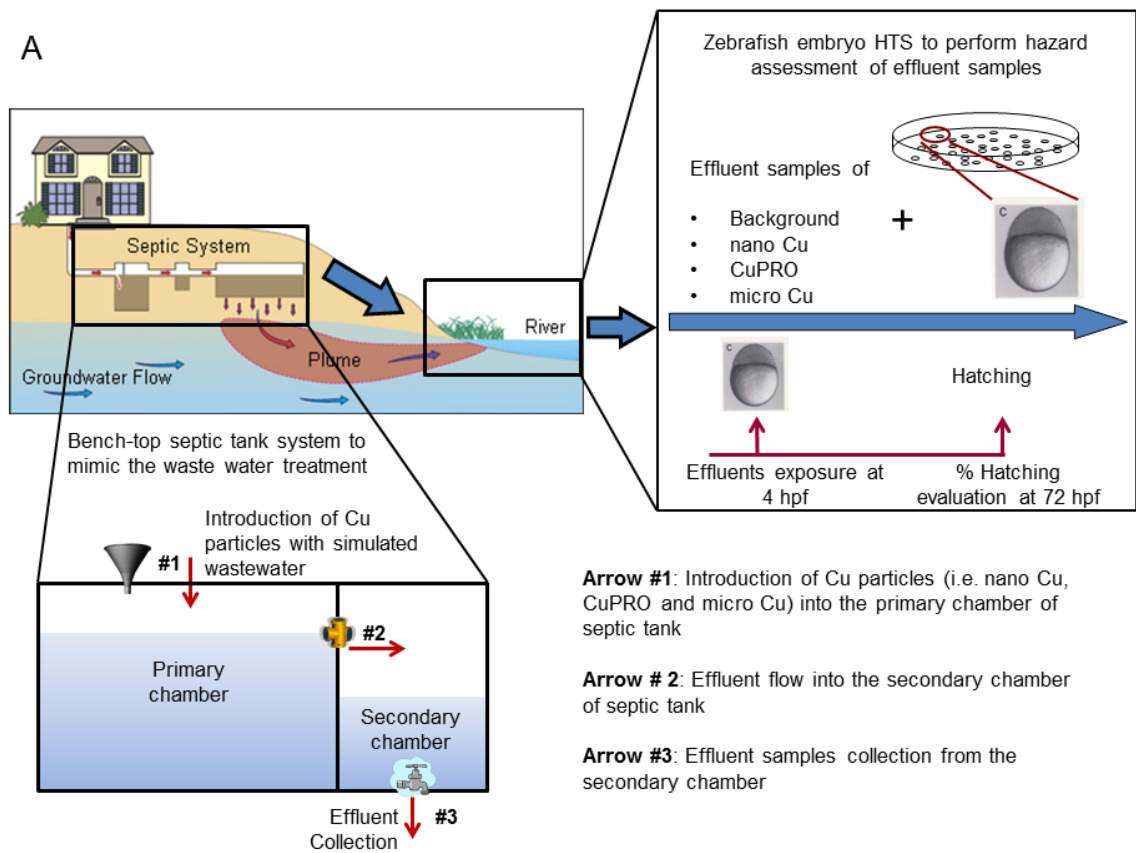


Figure 4.2A.

Combined use of a model septic tank and zebrafish embryo high content screening to study the effects of Cu-containing effluents on embryo hatching. (A) Schematic diagram of the model septic system to generate effluents for testing in zebrafish embryos.

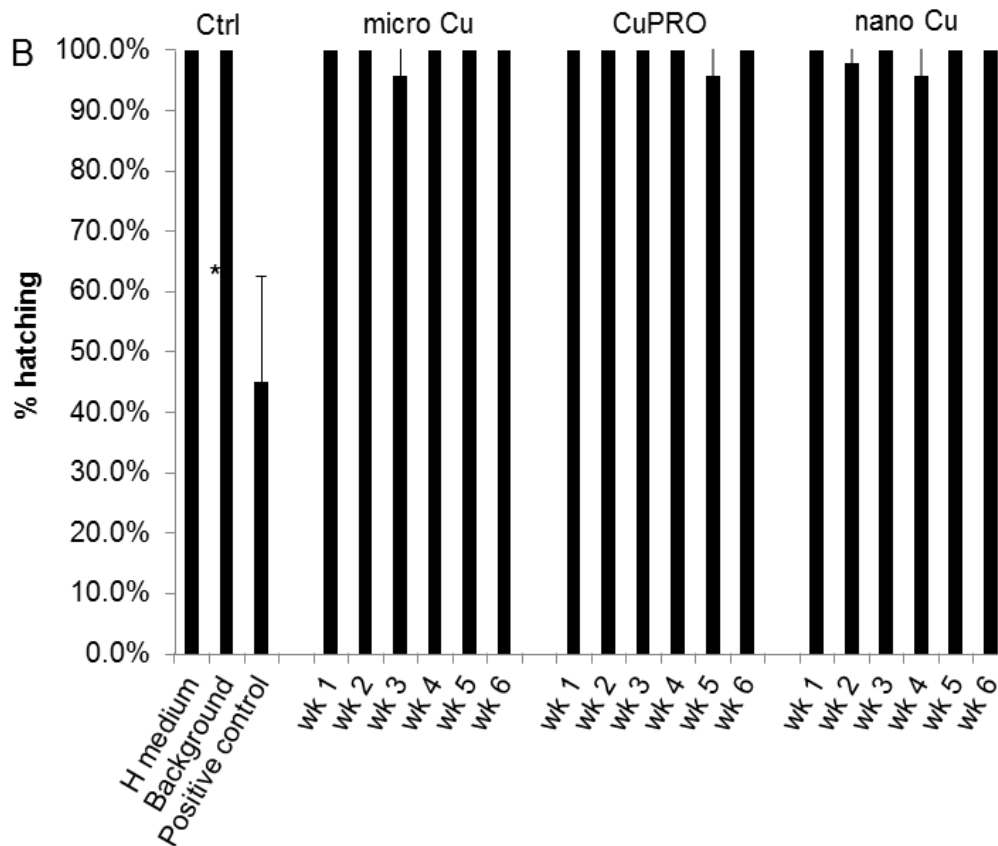


Figure 4.2B.

Combined use of a model septic tank and zebrafish embryo high content screening to study the effects of Cu-containing effluents on embryo hatching. (B) Percent hatching of zebrafish embryos exposed to the effluents collected weekly from the nano Cu, CuPRO, and micro Cu groups for 6 weeks. The introduction of 0.5 ppm nano Cu in Holtfreter's medium was used as a positive control. Symbol * denotes statistical significance at $p < 0.05$.

Cu Speciation Explains the Lack of Toxicity in the Zebrafish Assay

In order to assess Cu in the effluent, ICP-MS was used to measure the elemental Cu content in the weekly effluent collections, as shown in Figure 4.3A. This

demonstrated a progressive increase in the elemental Cu content over the course of the first 3 weeks, beyond which there was a gradual reduction in Cu content during weeks 4 - 6. The nano Cu and CuPRO effluents showed consistently higher Cu concentrations compared to micro Cu. Interestingly, the Cu content of the effluents collected during weeks 2 - 4 following the introduction of nano Cu and CuPRO was higher than the threshold levels (indicated by the dashed lines in Figure 4.3A), at which, the as-received nano Cu and CuPRO would have caused significant hatching interference. This finding suggests that Cu in the effluent may not be bioavailable as a result of Cu speciation after particle introduction.

In order to assess the Cu particle transformation, XRD analysis was performed on week 3 effluents collected after addition of nano Cu, CuPRO, and micro Cu. These results were compared to the XRD peaks of the as-received materials. As shown in Figure 4.3B, the characteristic XRD profiles of the as-received Cu particles could no longer be seen in the effluents. Instead, the effluents showed new peaks at ~ 12.39 and ~ 24.76 degrees (2θ CuK α), which represent water-insoluble inorganic $\text{Cu}(\text{H}_2\text{PO}_2)_2$, as well as CuSO_4 , respectively. These Cu species appear in the effluent as early as 1 week after the introduction of the particles (Figure S4.3). The presence of a NaCl crystalline peaks reflect a “background” ingredient in the effluent (Figure 4.3B). To identify other potential Cu species, we also performed X-ray photoelectron spectroscopy (XPS) analysis on both the Cu particles and the Cu-containing effluent.

However in most cases, the Cu content was too low to be detected, therefore no additional information on the Cu speciation was obtained (data not shown). All considered, these results show that Cu particles undergo transformation in the septic tank, resulting in the formation of new Cu species.

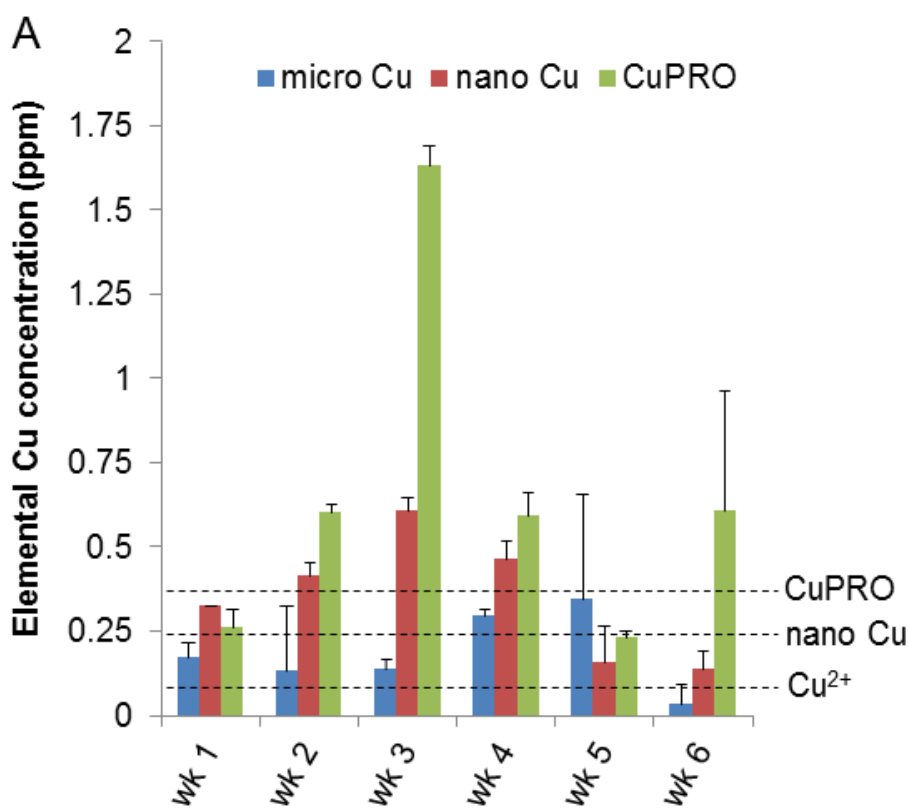


Figure 4.3A.

Characterization of the septic effluents. (A) ICP-MS measurements were undertaken to quantify elemental Cu in the effluents collected on a weekly basis following the introduction of the different particle types. The dashed lines represent the as-received Cu^{2+} , nano Cu and CuPRO concentrations providing ~50% hatching interference in Holtfreter's medium.

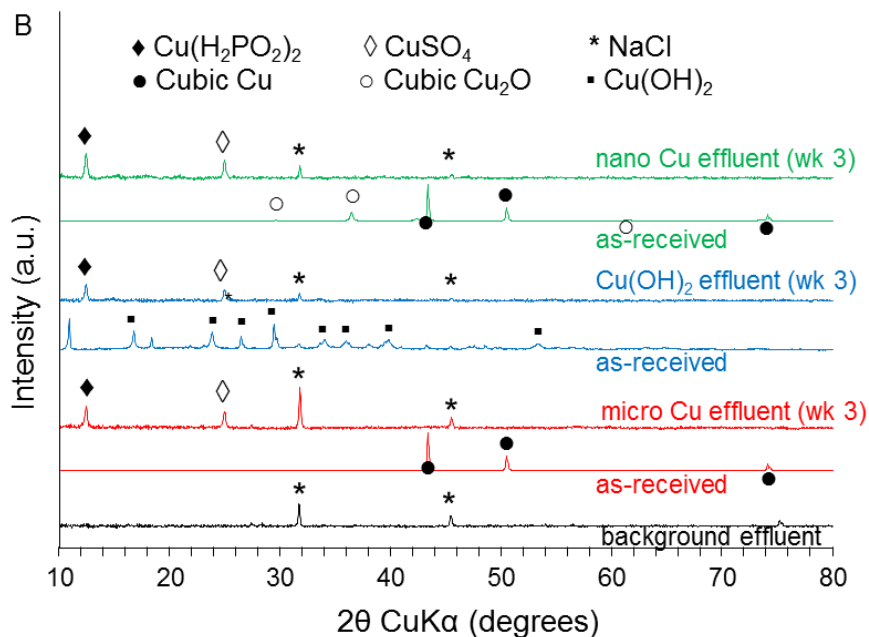


Figure 4.3B.

Characterization of the septic effluents. (B) XRD analysis on the as-received particulates as well as the corresponding effluents at week 3.

In addition to the detection of inorganic Cu species, it is possible that there could also be the formation of organic Cu, which cannot be detected by XRD. In order to address this possibility, we used Visual MINTEQ software to model the chemical speciation of Cu in the presence of organic material. Our first modeling attempt introduced humic acid (HA) as a source of dissolved organic matter (DOM) to the effluent. The predominant species of Cu in Holtfreter's medium, which is devoid of HA, is Cu²⁺, which comprises ~ 75% of the total Cu content (Figure 4.3C). However, upon the introduction of 100 ppm HA to the aqueous environment, the

amount of Cu^{2+} rapidly decreases to $\sim 2\%$ of the total Cu, while the organic-bound Cu increased to $\sim 90\%$ (Figure 4.3C).

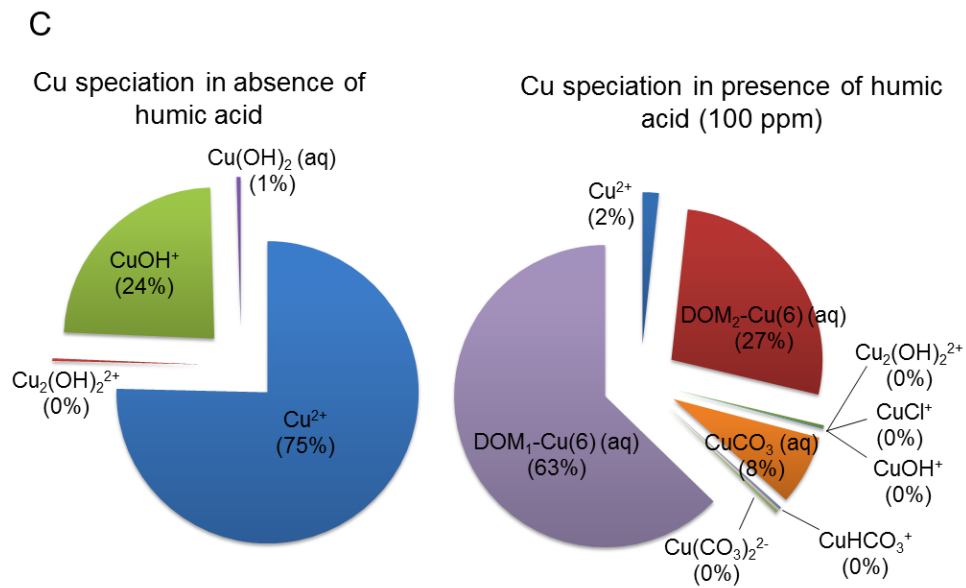


Figure 4.3C.

Characterization of the septic effluents. (C) Visual MINTEQ modeling to show Cu speciation in the presence and absence of Dissolved Organic Matter (DOM). Humic acid (HA) was used as a form of DOM in the Visual MINTEQ modeling. Without the presence of DOM, Cu^{2+} is the dominant species, accounting for 75% of the total Cu. The presence of 100 ppm DOM decreases the Cu^{2+} content precipitously (to 2%) as a result of metal complexation. DOM-bound Cu ($\text{DOM}_1\text{-Cu}(6)$: 63%, and $\text{DOM}_2\text{-Cu}(6)$: 27%) accounts for 90% of the total Cu. DOM_1 and DOM_2 are used by the Visual MINTEQ software to distinguish different humic components.

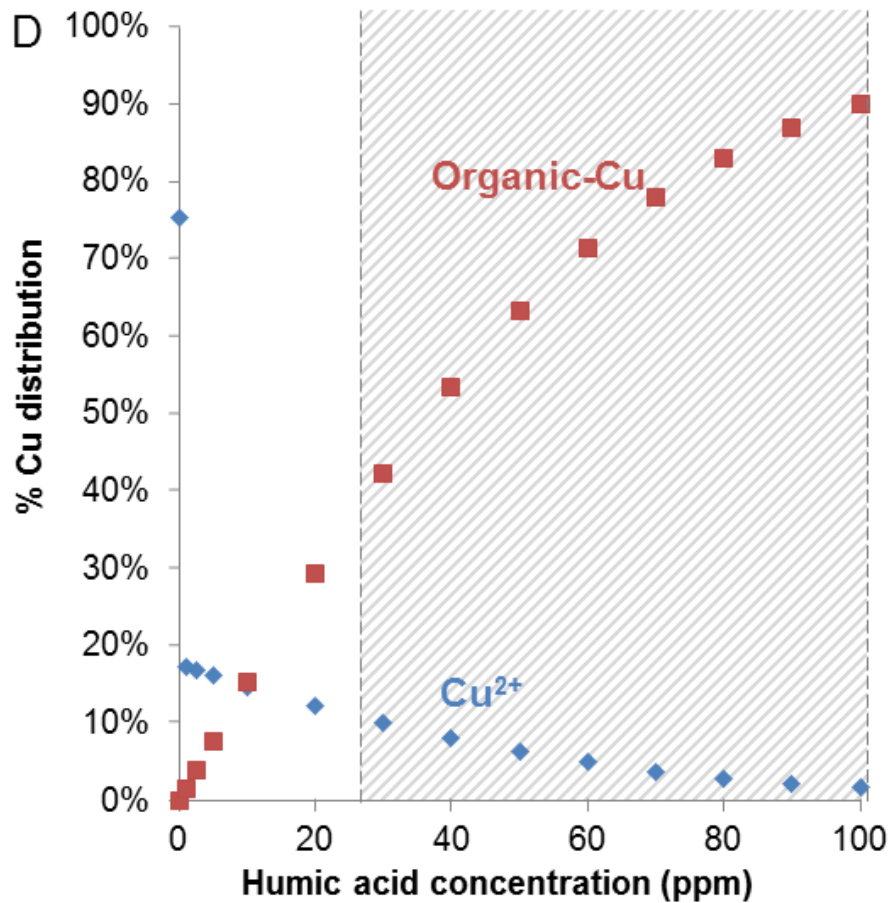


Figure 4.3D.

Characterization of the septic effluents.(D) Visual MINTEQ modeling to show the Cu distribution into ionic (Cu^{2+}) and organic Cu following the introduction of incremental amounts of humic acid. The grey area indicates the humic acid concentration range (30 – 100 ppm) that is expected in the septic tank effluent.

This trend is progressive for incremental amounts of HA in the model, as shown in Figure 4.3D. As indicated by the shaded area, which represents the HA concentration range (30 – 100 ppm) in the effluent, the organic-bound Cu comprised > 65% of total Cu while the Cu^{2+} content accounted < 10%.

To provide experimental support for the Visual MINTEQ modeling, we also used methodology for diffusive gradients in thin-films (DGT) to quantify the diffusible Cu^{2+} content of the effluent as a % of the total Cu.³¹⁷⁻³¹⁸ Soaking of the DGT unit, comprised of a nitrocellulose membrane filter, diffusion gel and resin gel layers (Figure 4.4, insert), in the effluent showed that the % Cu^{2+} (determined by ICP-OES) is < 18% of the total Cu in week 3 effluents for all particle types introduced into the septic tank (Figure 4.4). This is in reasonable agreement with the Visual MINTEQ calculation. All considered, the above data suggest that particle transformation in the septic tank results in Cu speciation, with organic non-bioavailable Cu being the dominant species, which lacks the ability to interfere in embryo hatching.

Experimental Addition of Natural Organic Matters Decreases Cu Particle Toxicity

To provide direct experimental evidence that HA impacts Cu toxicity, Holtfreter's medium was spiked with 0.5 or 1 ppm Cu^{2+} following which HA was added in the amounts of 0 - 500 ppm. These mixtures were tested for their effects on embryo hatching. As shown in Figure 4.5A, an HA concentration as low as 7.8 ppm could significantly reverse the Cu^{2+} interference in embryo hatching, with 100% protection at HA concentrations > 15 ppm. Similar protective effects were seen using a Suwannee River NOM solution (125 ppm) as well as "background" effluent (Figure 4.5B). Furthermore, the comparison between "background" effluent and Holtfreter's medium spiked with Cu^{2+} or nano Cu at 0.125 – 1 ppm revealed that HA present in

the “background” effluent, could significantly reverse hatching interference by both ionic and nano Cu (Figure 4.5C and D).

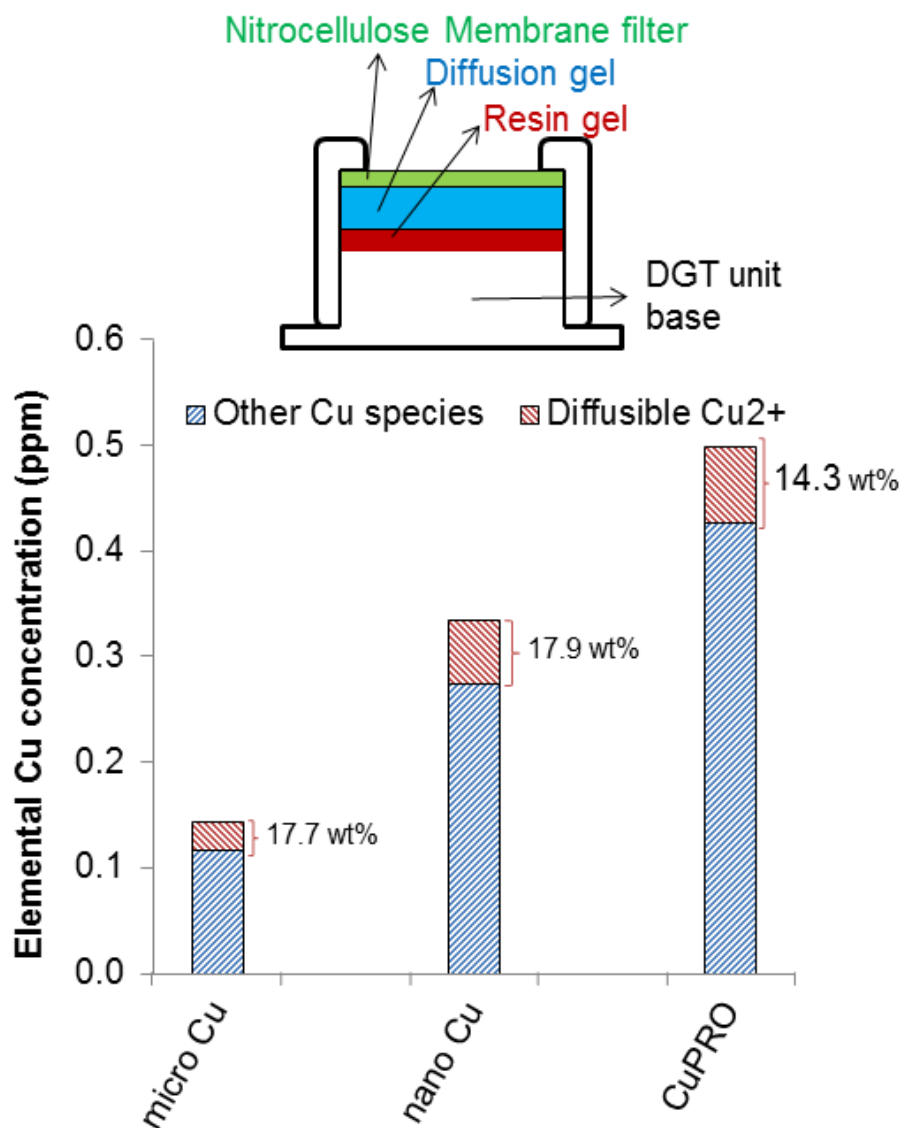


Figure 4.4.

Use of the methodology for diffusive gradients in thin-films (DGT) to quantify diffusible Cu²⁺ in the effluents. Schematic diagram of a DGT unit comprised of a nitrocellulose membrane filter, a gel for diffusion, and a resin gel layer (insert). Separation of the diffusible Cu²⁺ and organic Cu in the effluent collected during week 3 (post introduction of micro Cu, nano Cu and CuPRO) was undertaken by incubation the DGT unit in the effluents for 3 days at 28 °C. The resin gel was retrieved and digested in nitric acid, before performance of ICP-OES.

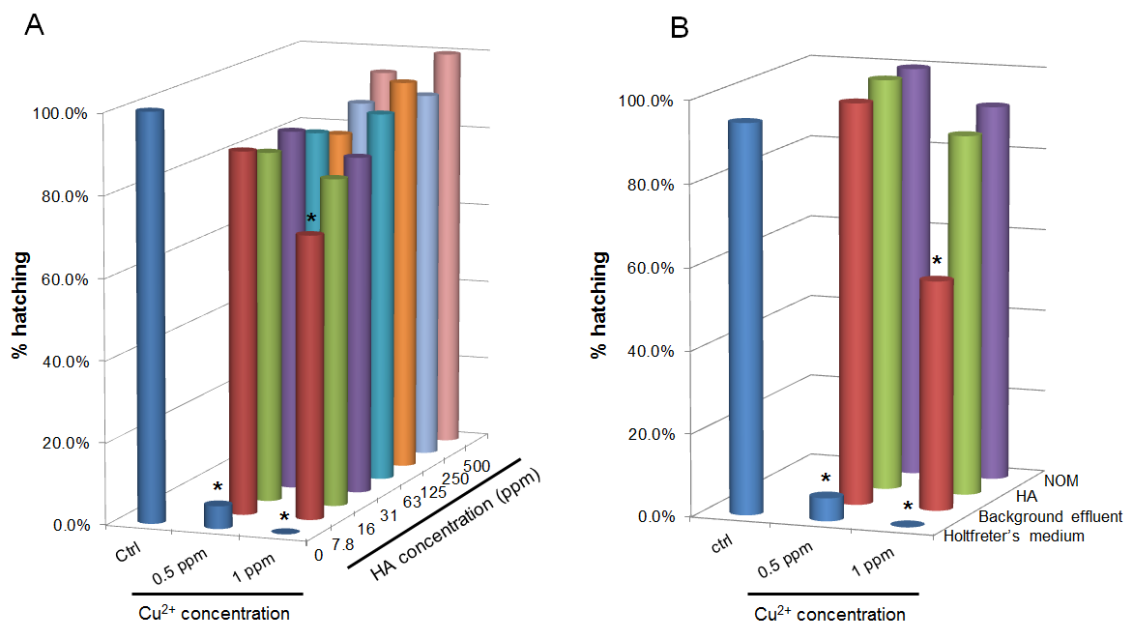


Figure 4.5A/B.

The addition of humic acid (HA) decreased Cu toxicity. (A) The effect of humic acid (0 - 500 ppm) on hatching interference by 0.5 and 1 ppm Cu²⁺ in Holtfreter's medium. (B) Comparison of the effect of Suwannee River NOM (100 ppm) with humic acid (100 ppm) and "background" effluent for their effects on embryo hatching in the presence of 0.5 and 1 ppm Cu²⁺ in Holtfreter's medium. The data in the 3D bar chart represent average of 3 individual experiments in which the standard deviation varied less than 6%.

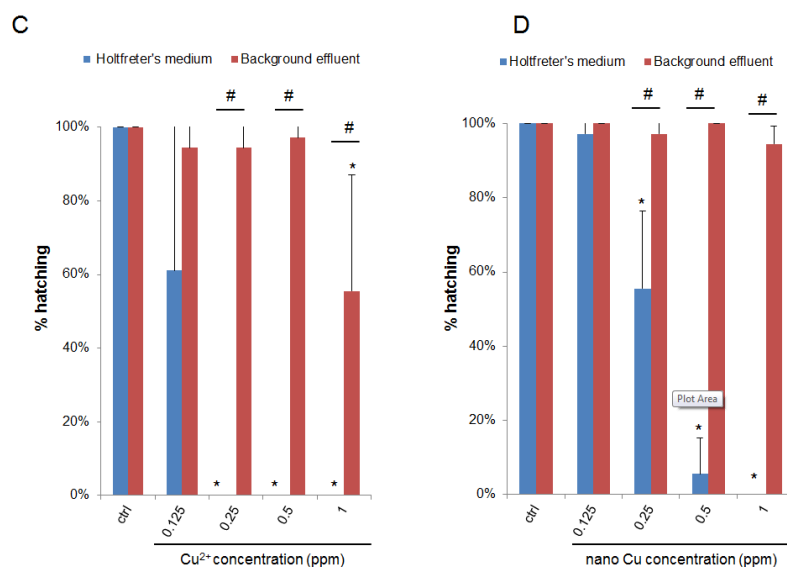


Figure 4.5C/D.

The addition of humic acid (HA) decreased Cu toxicity. (C) Comparison of the effect of known concentrations (0.125, 0.25, 0.5 and 1 ppm) of Cu²⁺ directly spiked into Holtfreter's medium or into "background" effluent. (D) Comparison of the effect of zebrafish embryos exposed to known concentrations (0.125, 0.25, 0.5 and 1 ppm) of nano Cu directly spiked into Holtfreter's medium or into "background" effluent. The * and # symbols denote statistical significance at $p < 0.05$.

However, in the absence of HA in Holtfreter's medium, Cu²⁺ and nano Cu showed significant hatching interference at 0.125 and 0.25 ppm, respectively. Spiking of Holtfreter's with "background" effluent increased the concentrations of hatching interference by Cu²⁺ and nano Cu to >1 ppm.

Discussion

In this study, we used a model septic tank system and zebrafish hatching interference to investigate the impact of particulate Cu transformation and speciation to obtain

information on the inadvertent hazard potential of commercial Cu nanoparticles outside of their immediate scope of use. We demonstrated that while the Cu dissolution played a key role in determining the hazard potential of the as-received particles, the transformation of these materials in a septic tank system rendered the Cu non-bioavailable to the zebrafish hatching bioassay system, thereby preventing an effect on hatching interference. The decrease in Cu toxicity was due to Cu speciation to insoluble inorganic and non-diffusive organic Cu species, which does not interfere with the hatching enzyme. We also demonstrated that the addition of humic acid (HA) led to a dose-dependent decrease of Cu toxicity as a result of the organic complexation of Cu. These data demonstrate that it is possible to address the environmental hazard of particulate Cu (including nano Cu) through the use of simulation studies that can be used for modeling the complexity of the environmental fate and transformation of these materials.

The increased commercialization of nanotechnology is introducing a wave of nano-enabled products to the marketplace. While a great deal of consideration has been given to the safety of workers and consumers, much less is known regarding the environmental implications of nanotechnology. In this study, using the effluent from a model septic tank system, we investigated the hazard potential of Cu particles (including nanoparticles used as fungicides) at different stages of the septic tank operation to project what might happen to a fish embryo at the aquatic disposal sites

for the effluent. Our results show a significant decrease in Cu toxicity in the effluent compared to the as-received materials, suggesting that the ingredients in the septic tank is effective for mitigating the hazardous impact of Cu particles in a fish embryo model that is frequently used for nanotoxicology studies.²⁹⁰⁻²⁹¹ The decrease in embryo toxicity was observed at all stages of the wastewater treatment process (Figure 4.2B), irrespective of the amount of Cu introduced (Figure 4.3A). The presence of organic matter in the septic tank effluent acts as an effective buffer of the hatching interference effect exerted by the ionic and particulate Cu (Figure 4.5).

Cu is considered as an environmental toxicant of concern to aquatic invertebrates and vertebrates. Although the total Cu content (of all Cu species) is commonly used to establish national and regional guidelines for water quality, Cu toxicity is generally known to reside in Cu^{2+} being released rather than the total Cu content.^{286, 319-322} In our study, all Cu particles, irrespective of composition and size, underwent particle transformation in the septic tank, resulting in Cu speciation to Cu^{2+} , insoluble $\text{Cu}_2(\text{PO}_2)_2$, as well as organic Cu species (Figure 4.3B, 4.3C, and Figure S4.3). Thus, although the total Cu content in the effluent was clearly higher than the concentrations at which Cu^{2+} , nano Cu, or CuPRO interfere in embryo hatching, the chemical complexation in the effluents, results in < 18 wt% of total Cu being available as Cu^{2+} (Figure 4.4). These quantities are insufficient for hatching interference. We suggest, therefore, that a more appropriate standard for Cu toxicity

should include chemical speciation and a test for bioavailability rather than just relying on total Cu content. Natural organic matter such as HA provides effective organic complexation of Cu^{2+} to act as a buffer of Cu toxicity (Figure 4.5). These results corroborate our previous demonstration that interference in embryo hatching and inhibition of ZHE1 activity by Cu^{2+} , Zn^{2+} , Ni^{2+} , or Cr^{3+} can be reversed by the metal chelator, diethylene triamine pentaacetic acid (DTPA).³¹⁰⁻³¹¹ It is also worthwhile mentioning that the presence of humic acid in the septic tank system might influence the dissolution characteristics of the Cu particles introduced. According to Keller et al., the presence of organic matter (i.e. extracellular polymeric substance, EPS) resulted in a higher dissolution of Cu particles. However, since the amount of humic acid in the septic tank system (30 - 100 ppm) was orders of magnitude higher than the total Cu (Figure 4.3A), most of the dissolved Cu^{2+} ions from the particles would remain organically chelated.

The combined use of a septic tank model and a zebrafish assay to assess Cu toxicity introduces a practical approach to assess the hazard of nanoparticles and nano-enabled products in complex environmental settings. We took advantage of a small-scale domestic septic tank model that provides easy access to effluent that could be sampled and tested at various intervals and stages of the WWT process. We demonstrate that the effluent could be used for hazard assessment and Cu speciation even though it is difficult to monitor the physical presence and physicochemical

characteristics of the particles under these exposure conditions. The use of the zebrafish embryo as a bioassay screening tool to exam embryo toxic effect could be expanded and refined to include other environmentally relevant organisms that could be in harm's way if nanoparticles are introduced into the environment. While for proof-of-principle testing, a fixed amount of particles (10 ppm) were used, which could be orders of magnitude higher than actual environmental exposures, our approach can be easily adapted for a range of metal and metal oxide nanoparticles at different concentrations. These adaptations can be based on LCA, which identifies the hot spots of exposure that can be subsequently modeled to provide information about the amount of exposure and speciation that can be addressed by environmental modeling software being developed by the UC Center for the Environmental Implications of Nanotechnology (UC CEIN).

Conclusion

In summary, we have successfully combined the use of a model septic tank system and zebrafish HCS to study the hazard potential of Cu-based particles and fungicides before and after introduction into a WWT system. We demonstrate that the Cu containing effluent has significantly reduced impact on zebrafish embryo hatching. This toxicity decrease is due to particle transformation and Cu speciation to less

bioavailable species, among which humic acid was used to show how organic speciation can reduce Cu toxicity to zebrafish.

References

1. Adeleye, A. S.; Conway, J. R.; Perez, T.; Rutten, P.; Keller, A. A. Influence of Extracellular Polymeric Substances on the Long-term Fate, Dissolution, and Speciation of Copper-based Nanoparticles. *Environ. Sci. Technol.* **2014**, *48*, 12561-12568.
2. Thomas, K.; Raymond, K.; Chadwick, J.; Waldock, M. The Effects of Short-term Changes in Environmental Parameters on the Release of Biocides from Antifouling Coating: Cuprous Oxide and Tributyltin. *Appl. Organometallic Chem.* **1999**, *13*, 453-460.
3. Ribolzi, O.; Valles, V.; Gomez, L.; Voltz, M. Speciation and Origin of Particulate Copper in Runoff Water from a Mediterranean Vineyard Catchment. *Environ. Pollut.* **2002**, *117*, 261-271.
4. Giesy, J. P.; Newell, A.; Laversee, G. J. Copper Speciation in Soft, Acid, Humic Waters: Effects on Copper Bioaccumulation by and Toxicity to *Simocephalus Serrulatus*. *Sci. Total Environ.* **1983**, *28*, 23-36.
5. Arias, M.; Lopez, E.; Fernandez, D.; Soto, B. Copper Distribution and Dynamics in Acid Vineyard Soils Treated with Copper-Based Fungicides. *Soil Science* **2004**, *169*, 796-805.
6. Ren, G.; Hu, D.; Cheng, E. W.; Vargas-Reus, M. A.; Reip, P.; Allaker, R. P. Characterisation of Copper Oxide Nanoparticles for Antimicrobial Applications. *Int. J. Antimicrob. Agents* **2009**, *33*, 587-590.
7. Cioffi, N.; Torsi, L.; Ditaranto, N.; Tantillo, G.; Ghibelli, L.; Sabbatini, L.; Bleve-Zacheo, T.; Alessio, M. D.; Zambonin, P. G.; Traversa, E. Copper Nanoparticle/Polymer Composites with Antifungal and Bacteriostatic Properties. *Chem. Mater.* **2005**, *17*, 5255-5262.
8. Lin, S.; Zhao, Y.; Nel, A. E.; Lin, S. Zebrafish: an *in vivo* Model for Nano EHS Studies. *Small* **2013**, *9*, 1608-1618.

9. Fako, V. E.; Furgeson, D. Y. Zebrafish as a correlative and predictive model for assessing biomaterial nanotoxicity. *Adv. Drug. Deliv. Rev.* **2009**, *61*, 478-86.
10. Lowry, G. V.; Gregory, K. B.; Apte, S. C.; Lead, J. R. Transformations of Nanomaterials in the Environment. *Environ. Sci. Technol.* **2012**, *46*, 6893-6899.
11. Klaine, S. J.; Alvarez, P. J. J.; Batley, G. E.; Fernandes, T. F.; Handy, R. D.; Lyon, D. Y.; Mahendra, S.; Mclaughlin, M. J.; Lead, J. R. Nanomaterials in the Environment: Behavior, Fate, Bioavailability, and Effects. *Environ. Toxicol. Chem.* **2008**, *27*, 1825-1851.
12. Mueller, N. C.; Nowack, B. Exposure Modeling of Engineered Nanoparticles in the Environment. *Environ. Sci. Technol.* **2008**, *42*, 4447-4453.
13. Nowack, B. Is Anything out There? *Nano Today* **2009**, *4*, 11-12.
14. Beaudrie, C. E.; Kandlikar, M.; Satterfield, T. From Cradle-to-Grave at the Nanoscale: Gaps in U.S. Regulatory Oversight along the Nanomaterial Life Cycle. *Environ. Sci. Technol.* **2013**, *47*, 5524-5534.
15. Keller, A. A.; Lazareva, A. Predicted Releases of Engineered Nanomaterials: From Global to Regional to Local. *Environ. Sci. Technol. Lett.* **2014**, *1*, 65-70.
16. EPA, Decentralized Systems Technology Fact Sheet Septic Tank - Soil Absorption Systems. Washington DC, 1999.
17. EPA, Decentralized wastewater treatment systems: memorandum of understanding. Washington DC, 2011.
18. Benn, T. M.; Westerhoff, P. Nanoparticle Silver Released into Water from Commercially Available Sock Fabrics. *Environ. Sci. Technol.* **2008**, *42*, 4133-4139.
19. Choi, O.; Deng, K. K.; Kim, N.-J.; Ross Jr, L.; Surampalli, R. Y.; Hu, Z. The Inhibitory Effects of Silver Nanoparticles, Silver Ions, and Silver Chloride Colloids on Microbial Growth. *Water Res.* **2008**, *42*, 3066-3074.

20. García, A.; Delgado, L.; Torà, J. A.; Casals, E.; González, E.; Punes, V.; Font, X.; Carrera, J.; Sánchez, A. Effect of Cerium Dioxide, Titanium Dioxide, Silver, and Gold Nanoparticles on the Activity of Microbial Communities Intended in Wastewater Treatment. *J. Hazard. Mater.* **2012**, *199–200*, 64-72.
21. Jarvie, H. P.; Al-Obaidi, H.; King, S. M.; Bowes, M. J.; Lawrence, M. J.; Drake, A. F.; Green, M. A.; Dobson, P. J. Fate of Silica Nanoparticles in Simulated Primary Wastewater Treatment. *Environ. Sci. Technol.* **2009**, *43*, 8622-8628.
22. Kaegi, R.; Voegelin, A.; Sinnet, B.; Zuleeg, S.; Hagendorfer, H.; Burkhardt, M.; Siegrist, H. Behavior of Metallic Silver Nanoparticles in a Pilot Wastewater Treatment Plant. *Environ. Sci. Technol.* **2011**, *45*, 3902-3908.
23. Kiser, M. A.; Ryu, H.; Jang, H.; Hristovski, K.; Westerhoff, P. Biosorption of Nanoparticles to Heterotrophic Wastewater Biomass. *Water Res.* **2010**, *44*, 4105-4114.
24. Kiser, M. A.; Westerhoff, P.; Benn, T.; Wang, Y.; Pérez-Rivera, J.; Hristovski, K. Titanium Nanomaterial Removal and Release from Wastewater Treatment Plants. *Environ. Sci. Technol.* **2009**, *43*, 6757-6763.
25. Limbach, L. K.; Bereiter, R.; Müller, E.; Krebs, R.; Gälli, R.; Stark, W. J. Removal of Oxide Nanoparticles in a Model Wastewater Treatment Plant: Influence of Agglomeration and Surfactants on Clearing Efficiency. *Environ. Sci. Technol.* **2008**, *42*, 5828-5833.
26. Mu, H.; Chen, Y.; Xiao, N. Effects of Metal Oxide Nanoparticles (TiO₂, Al₂O₃, SiO₂ and ZnO) on Waste Activated Sludge Anaerobic Digestion. *Bioresource Technol.* **2011**, *102*, 10305-10311.
27. Sheng, Z.; Liu, Y. Effects of Silver Nanoparticles on Wastewater Biofilms. *Water Res.* **2011**, *45*, 6039-6050.

28. Zheng, X.; Wu, R.; Chen, Y. Effects of ZnO Nanoparticles on Wastewater Biological Nitrogen and Phosphorus Removal. *Environ. Sci. Technol.* **2011**, *45*, 2826-2832.
29. Federal Water Pollution Control Act Amendments of 1972. In Public Law 92-500, Ed. 1972.
30. EPA, Manual for Evaluating Public Drinking Water Supplies. Washington, D.C., 1971.
31. EPA, National Interim Primary Drinking Water Regulations. Washington, D.C., 1976.
32. EPA, NPDES Permit Writers' Manual. EPA-833-B-96-003. Washington, D.C., 1996.
33. EPA, Centralized Waste Treatment Effluent Limitations Guidelines and Pretreatment Standards (40 CFR 437). Washington, D.C., 2001.
34. EPA, Protecting the Nation's Waters Through Effective NPDES Permits A Strategic Plan FY 2001 and Beyond. Washington, D.C., 2001.
35. EPA, Alternative Waste Management Techniques for Best Practicable Waste Treatment. Washington, D.C, **1976**, *43*, 6190-6191.
36. EPA, The report to Congress: Waste Disposal Practices and their Effects on Ground Water EPA 570/9-77-001. Washington, D.C, June 1977.
37. Canter, L. W.; Knox, R. C., *Septic Tank System Effects on Ground Water Quality*. Lewis Publishers, Inc: 1985.
38. Lin, S.; Zhao, Y.; Xia, T.; Meng, H.; Ji, Z.; Liu, R.; George, S.; Xiong, S.; Wang, X.; Zhang, H., et al. High Content Screening in Zebrafish Speeds up Hazard Ranking of Transition Metal Oxide Nanoparticles. *ACS Nano* **2011**, *5*, 7284-7295.

39. Lin, S.; Zhao, Y.; Ji, Z.; Ear, J.; Chang, C. H.; Zhang, H.; Low-Kam, C.; Yamada, K.; Meng, H.; Wang, X., et al. Zebrafish High-Throughput Screening to Study the Impact of Dissolvable Metal Oxide Nanoparticles on the Hatching Enzyme, ZHE1. *Small* **2013**, *9*, 1776-1785.
40. Xia, T.; Zhao, Y.; Sager, T.; George, S.; Pokhrel, S.; Li, N.; Schoenfeld, D.; Meng, H.; Lin, S.; Wang, X., et al. Decreased Dissolution of ZnO by Iron Doping Yields Nanoparticles with Reduced Toxicity in the Rodent Lung and Zebrafish Embryos. *ACS Nano* **2011**, *5*, 1223-1235.
41. Wang, X.; Ji, Z.; Chang, C. H.; Zhang, H.; Wang, M.; Liao, Y. P.; Lin, S.; Meng, H.; Li, R.; Sun, B., et al. Use of coated silver nanoparticles to understand the relationship of particle dissolution and bioavailability to cell and lung toxicological potential. *Small* **2014**, *10*, 385-98.
42. Liu, R.; Lin, S.; Rallo, R.; Zhao, Y.; Damoiseaux, R.; Xia, T.; Lin, S.; Nel, A.; Cohen, Y. Automated phenotype recognition for zebrafish embryo based in vivo high throughput toxicity screening of engineered nano-materials. *PLoS One* **2012**, *7*, e35014.
43. Amato, E. D.; Simpson, S. L.; Jarolimek, C. V.; Jolley, D. F. Diffusive Gradients in Thin Films Technique Provide Robust Prediction of Metal Bioavailability and Toxicity in Estuarine Sediments. *Environ. Sci. Technol.* **2014**, *48*, 4485-4494.
44. Luider, C. D.; Crusius, J.; Playle, R. C.; Curtis, P. J. Influence of natural organic matter source on copper speciation as demonstrated by Cu binding to fish gills, by ion selective electrode, and by DGT gel sampler. *Environ. Sci. Technol.* **2004**, *38*, 2865-2872.
45. Cuppett, J. D.; Duncan, S. E.; Dietrich, A. M. Evaluation of copper speciation and water quality factors that affect aqueous copper tasting response. *Chem. Senses* **2006**, *31*, 689-97.

46. Pagenkopf, G. K.; Russo, R. C.; Thurston, R. V. Effect of Complexation on Toxicity of Copper to Fishes. *J. Fish. Res. Board Can.* **1974**, *31*, 462-465.
47. Stauber, J. L.; Florence, T. M. Mechanism of Toxicity of Ionic Copper and Copper Complexes to Algae. *Mar. Biol.* **1987**, *94*, 511-519.
48. Flemming, C. A.; Trevors, J. T. Copper Toxicity and Chemistry in the Environment: A Review. *Water Air Soil Pollut.* **1989**, *44*, 143-158.
49. Marcus, I. M.; Wilder, H. A.; Quazi, S. J.; Walker, S. L. Linking Microbial Community Structure to Function in Representative Simulated Systems. *Appl. Environ. Microbiol.* **2013**, *79*, 2552-2559.
50. Gustafsson, J. P. Visual MINTEQ ver. 3.0. Available at <http://www2.lwr.kth.se/English/OurSoftware/vminteq>**2010**.

Supplemental Information for Chapter 4: Understanding the Transformation, Speciation, and Hazard Potential of Copper Particles in a Model Septic Tank System Using Zebrafish to Monitor the Effluent

Additional Information on Materials and Methods

Septic Tank Setup

The septic system is a scaled-down version of a two-chamber septic tank, with a volume of 2:1 for the primary and secondary chambers.¹¹⁵ The simulated household waste includes colon waste, DI water, and synthetic greywater.¹¹⁵ The effluent samples used in this study were collected from the secondary chamber on a weekly basis (Figure 4.2A).

Zebrafish Embryo HCS

Healthy embryos at 2 hour post fertilization (2 hpf) were collected after adult spawning and washed three times in Holtfreter's medium. The embryos were robotically picked and plated into 96-well plates, placing one embryo in each well. One hundred microliters of each as-received Cu particle suspension at nominal particle concentrations of 0.625, 1.25, 2.5, 5, and 10 ppm were added to the wells at 4 hpf. The exposure dose was designed to cover a broad range of concentrations of

which nanoparticles might be found in the wastewater effluent. To achieve robust statistical calculation, six replicate trials were carried out, using 12 embryos each. The observations on hatching interference, morphological abnormalities and mortality were carried out every 24 h for five consecutive days through the use of bright-field high content microscopic imaging (ImageXpress Micro, Molecular Devices). The HCS results were also confirmed by examining the embryos under conventional dissecting microscope. Due to the differences in purities among Cu particles, the nominal particle concentration was further converted to total Cu concentration, based on ICP-OES measurements. The hatching percentage of each replicate was calculated in relation to the Cu concentration for each particle. Using the same protocol, one hundred microliter aliquots of the effluent from the septic tank were used for directly exposure of the embryos, starting at 4 hpf. In order to compare CuCl₂ and Cu particles directly spiked into the “background” effluent, known concentrations (0.5 and 1 ppm) of CuCl₂, nano Cu, CuPRO and micro Cu were spiked into this effluent and mixed by vortexing, prior to the embryo exposure.

Sludge and Effluent Sample Digestion for ICP-MS Measurements

Both the primary chamber sludge samples and the effluent samples were digested before ICP-MS measurements. The digestion of sludge samples (collected at week 6)

were undertaken on lyophilized material. All samples were digested in triplicate using a protocol adopted from the EPA method, 3050B.³²³ Samples were placed in glass digestion vessels with 10 mL 1:1 HNO₃:H₂O solution and heated to 95°C for 10 minutes. Subsequently, 5 mL aliquots of concentrated HNO₃ were added, heated for 30 minutes, and repeated until no fumes were coming off. The samples were allowed to cool and 2 mL of water and 3 mL of 30% hydrogen peroxide (H₂O₂) were added to each sample. Samples were heated to 95°C (without boiling) and successive 1 mL aliquots of H₂O₂ were added until effervescence ceased. Samples were cooled and diluted to 100 mL using DI H₂O. The solutions were analyzed using an Agilent 7700 series ICP-MS (Santa Clara, CA, USA). A mass balance was also performed based on the ICP-MS measurements on both sludge and effluent, with the aim to determine the distribution of Cu content within the septic tank system. Based on the ICP-MS measurements, the Cu masses per dry sludge weight (mg Cu/g sludge) were as follows: 77.1 ± 28.8 mg nano Cu/g sludge, 51.4 ± 5.9 mg micro Cu/g sludge, and 7.7 ± 1.4 mg CuPRO/g sludge. The total Cu in the effluent accounted for less than 1% of the total Cu added to the septic tank system per each experiment.

Water Quality Characterization

Water quality was assessed during (1) baseline conditioning, (2) the addition of Cu particles over a 3 week period, and (3) a 3-week period without further particle addition. Changes in conductivity were monitored, using a conductivity probe (YSI 3200 Conductivity Instrument Model # 3200 115V). Alkalinity was measured twice a week from the effluent using a titration method.²¹⁵ The effluent from the septic tank typically has alkalinity values equivalent to 260-300 mg/L CaCO₃.²¹² Hardness was measured twice a week from the effluent using test strips (Hach Company SofCheck water quality test strips for total hardness). All analyses were performed in triplicate twice a week.

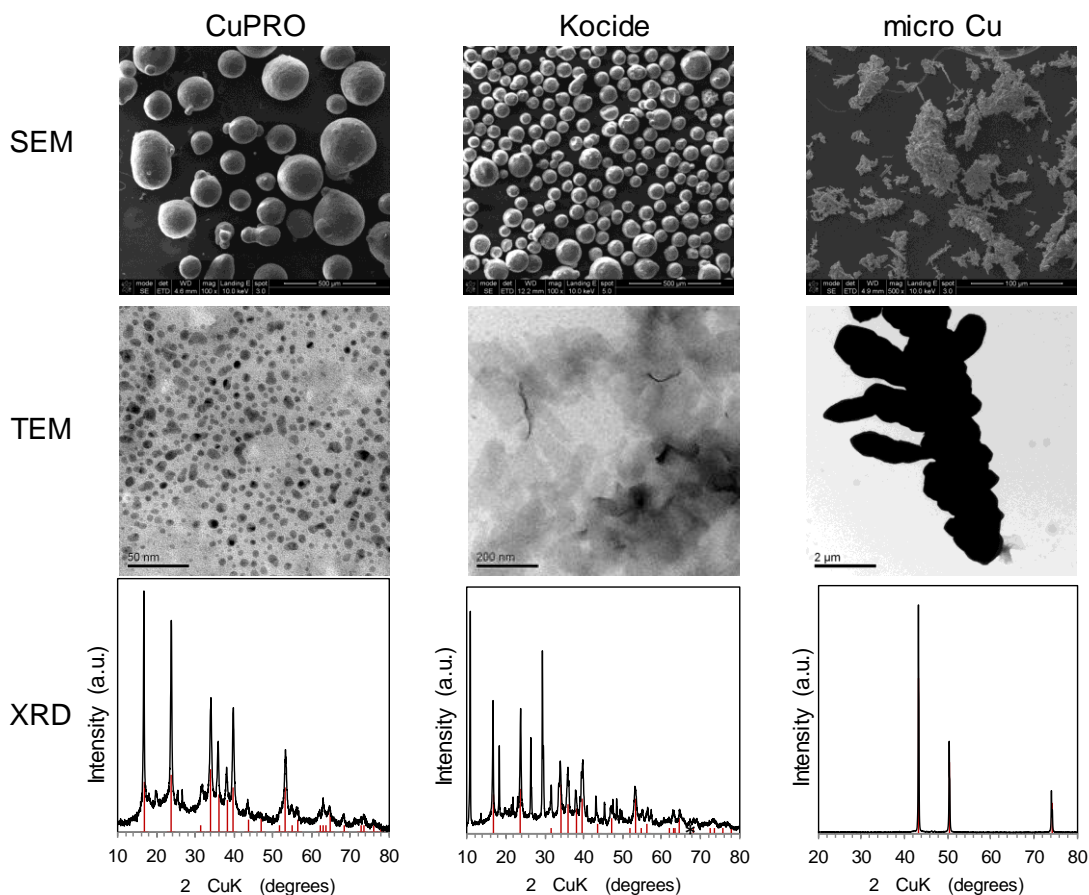


Figure S4.1A.

Physicochemical analysis of Cu particles. Representative scanning electron microscopy (SEM), transmission electron microscopy (TEM), and X-ray diffraction (XRD) spectra of copper particles, including CuPRO, Kocide and micro Cu. For SEM and XRD, samples were prepared by placing the particle powder directly on the SEM and XRD sample holders prior to data acquisition. For TEM, particles were dispersed in DI H₂O at 50 µg/mL and dried on a TEM grid prior to imaging. The primary particle size, shape, and crystal structure of all copper particles are summarized in Table 1 of the manuscript.

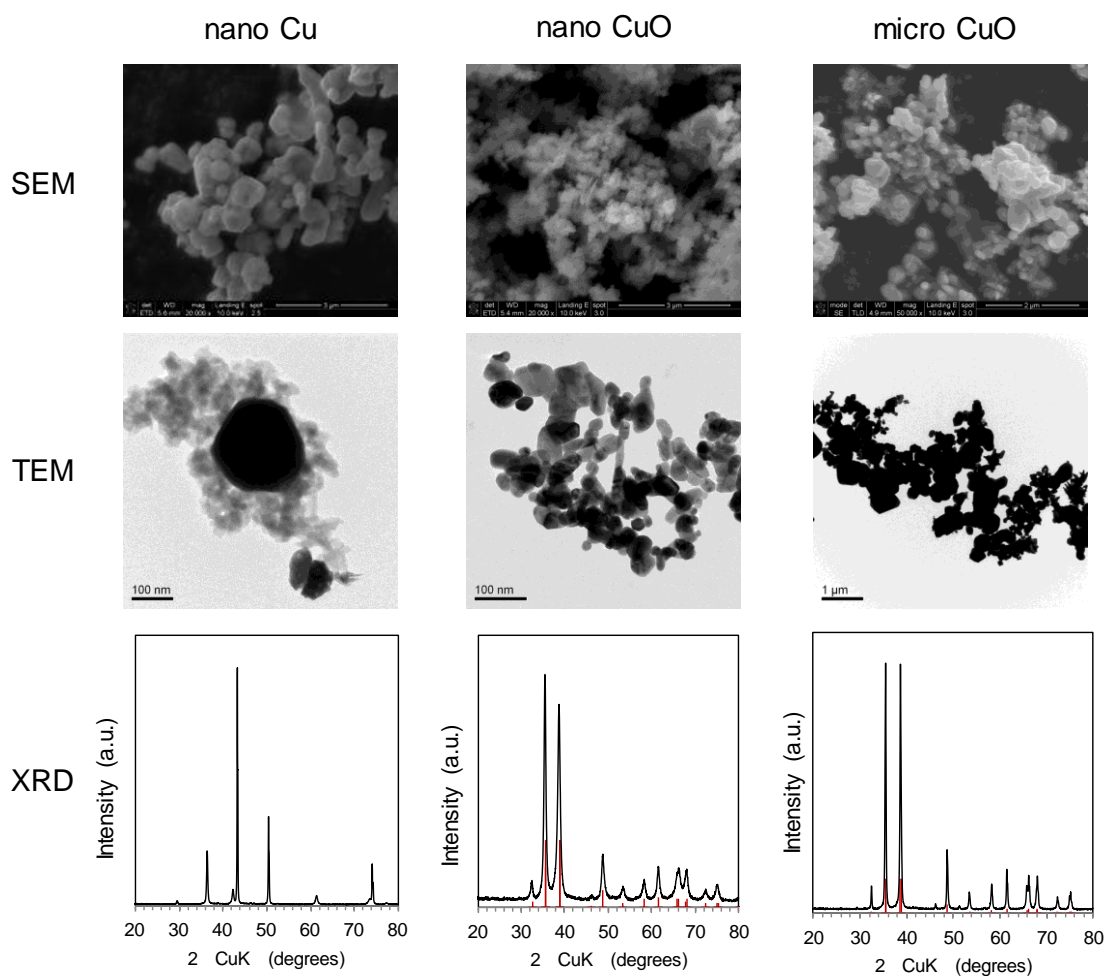


Figure S4.1B.

Physicochemical analysis of Cu particles. Representative scanning electron microscopy (SEM), transmission electron microscopy (TEM), and X-ray diffraction (XRD) spectra of copper particles, including nano Cu, nano CuO and micro CuO. Similar procedures, as described in Figure S4.1A, were used to characterize these Cu particles

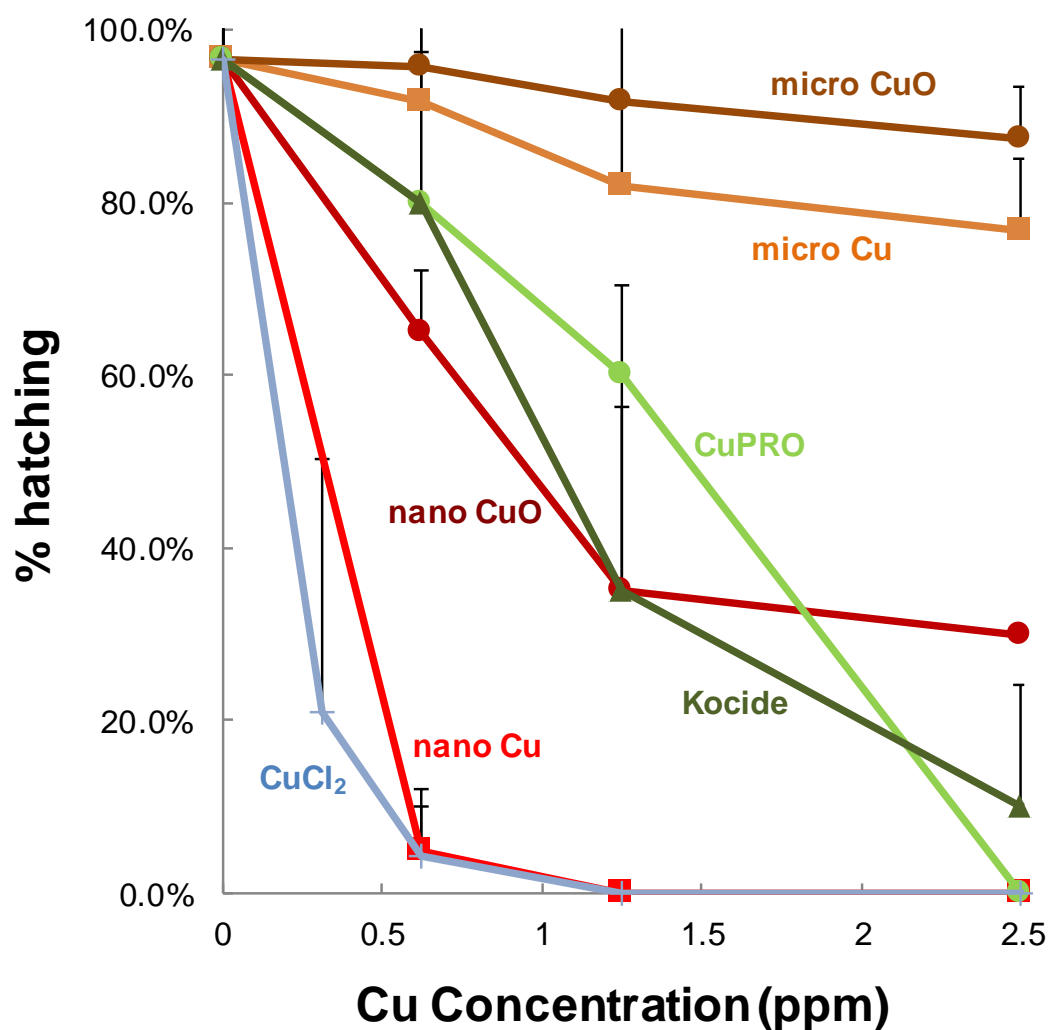


Figure S4.2A.

Percent hatching of zebrafish embryos exposed to as-received Cu particles and CuCl₂ at 0 – 2.5 ppm in Holtfreter's medium for 72 hours. Exposure commenced at 4 hours post-fertilization. These are data for the same experiment as in Figure 4.1B but expressed as % hatching vs. Cu concentration (ppm) instead of Log [Cu] (ppb). The error bars indicate standard deviation of three separate experiments.

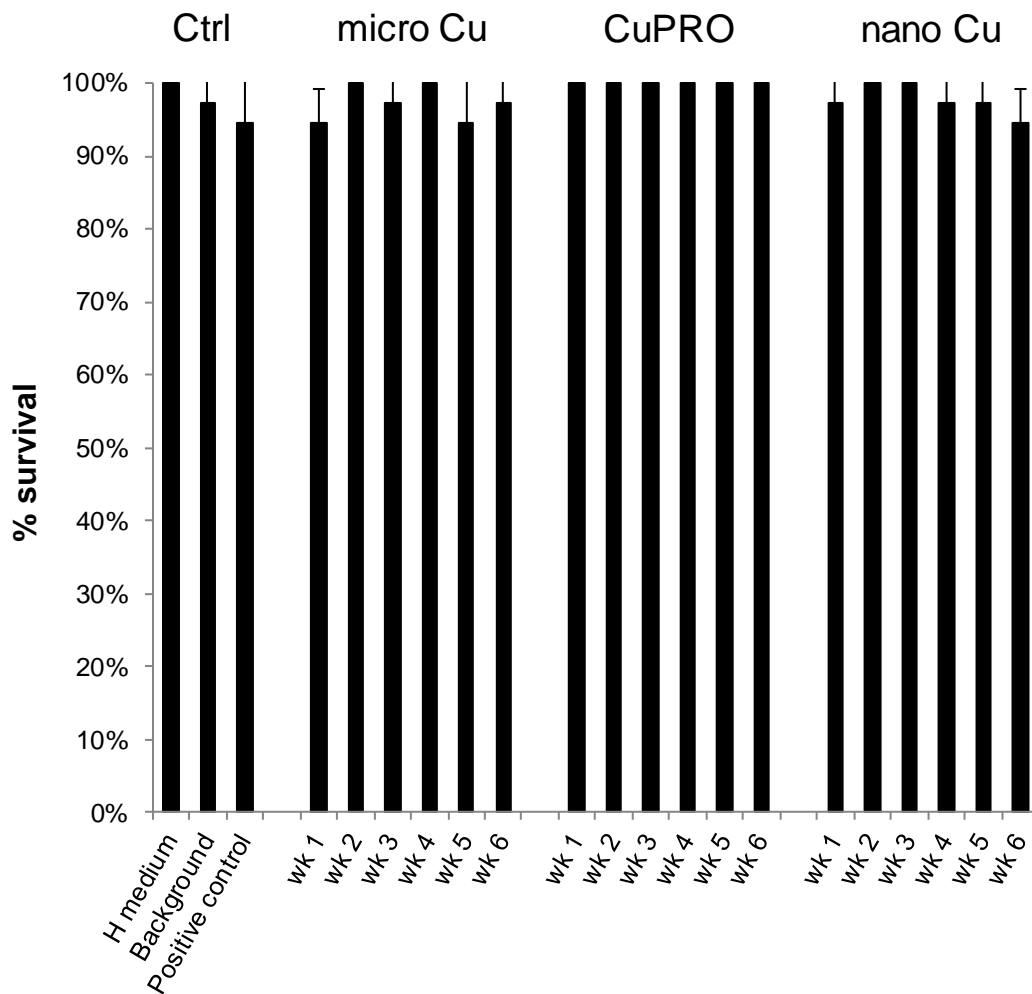


Figure S4.2B.

Percent survival of zebrafish embryos exposed to the effluents collected weekly from the nano Cu, CuPRO, and micro Cu groups for 6 weeks. The introduction of 0.5 ppm nano Cu in Holtfreter's medium significantly reduced the percent hatching of zebrafish embryos (Figure 4.2B) but did not affect the percent survival of zebrafish embryos at 3 days post fertilization.

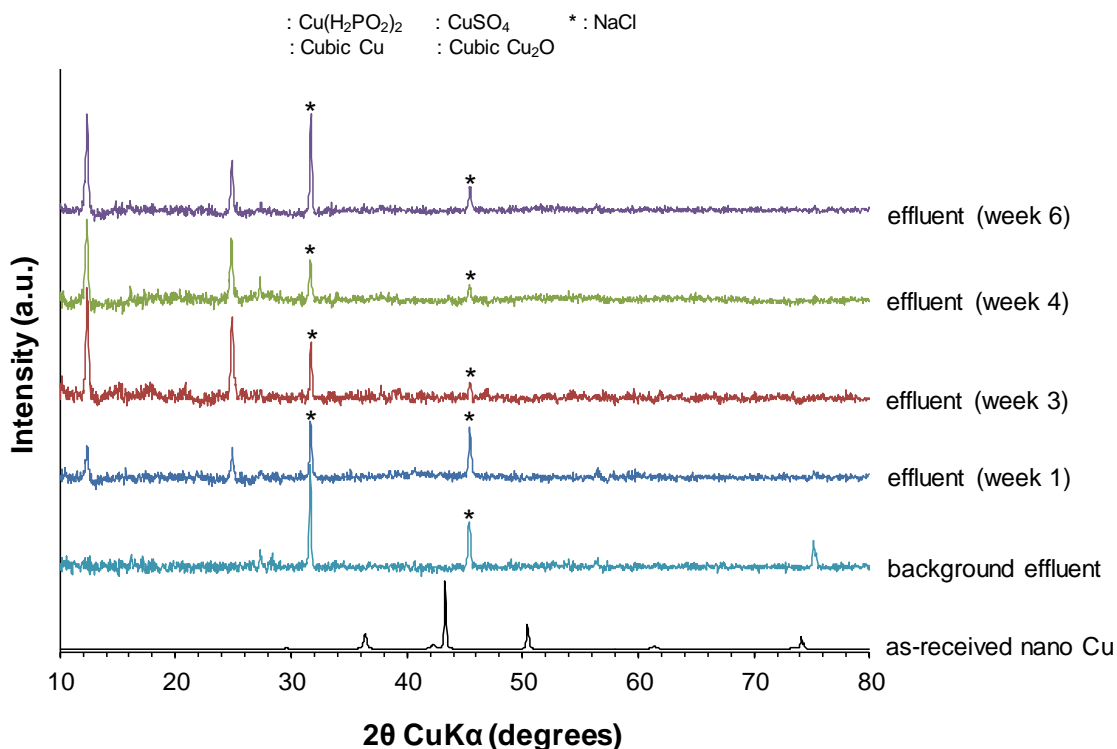


Figure S4.3.

XRD spectra of the as-received nano Cu, “background” effluent, and effluents collected from the septic system after weeks 1, 3, 4 and 6 following the addition of nano Cu particles. XRD spectrum of as-received nano Cu (black) displayed signature peaks for cubic Cu_2O and cubic Cu crystal structures. The “background” effluent (cyan), prior to nano Cu exposure showed the signature peaks for NaCl, a major ingredient of the septic tank effluent. No signature peaks for nano Cu crystal structures were present in the XRD analysis of the effluent samples. Besides NaCl crystals, an insoluble copper compound, $\text{Cu(H}_2\text{PO}_2)_2$ was identified in the nano Cu treated effluent samples based on the peak at 12.39° . This represents an inorganic speciation of nano Cu in the septic tank.

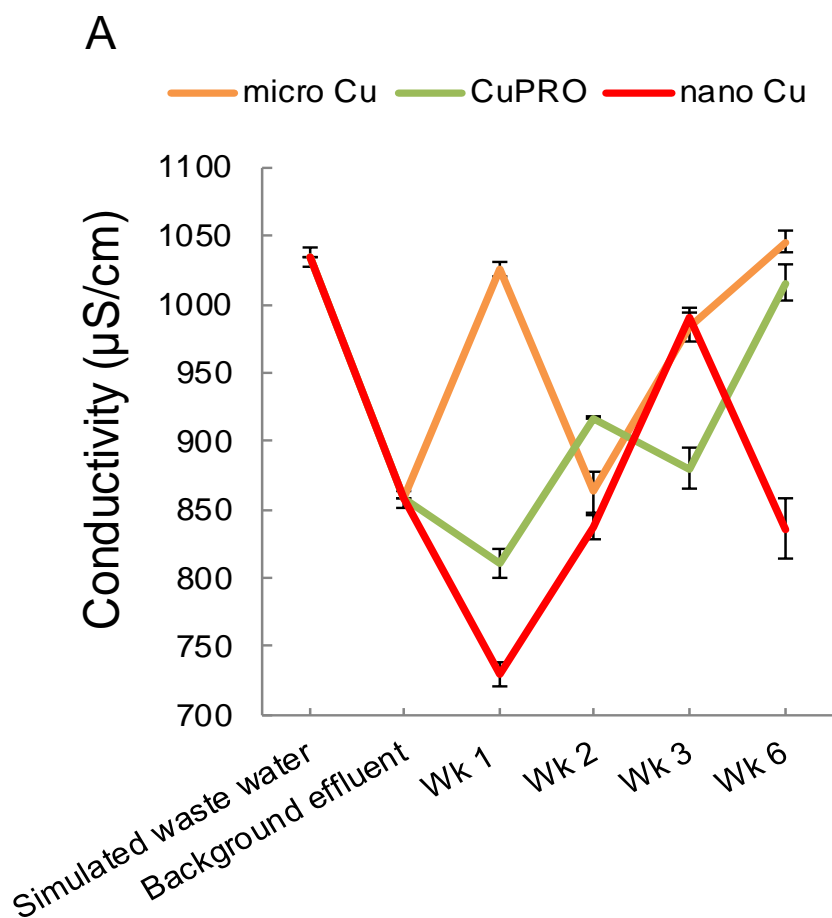


Figure S4.4A.

Water quality characteristics in the septic tank system, including conductivity, alkalinity and hardness. These characteristics were monitored during baseline conditioning, the 3-week period during which Cu particles were added, as well as the 3-week period beyond. Micro Cu, CuPRO and nano Cu are labeled in yellow, green, and red, respectively. (A) The conductivity data shows fluctuations without an overall trend. The conductivity for micro Cu effluents (between 863.12 ± 15.17 to 1045.78 ± 8.08 $\mu\text{S}/\text{cm}$) is either equal to or greater than the “background” effluent value (858.03 ± 6.13 $\mu\text{S}/\text{cm}$), while the conductivity of CuPRO effluents range from 810.53 ± 11.02 to 1015.60 ± 13.67 $\mu\text{S}/\text{cm}$. The nano Cu conductivity values ranged between 729.45 ± 8.07 to 990.62 ± 7.44 $\mu\text{S}/\text{cm}$.

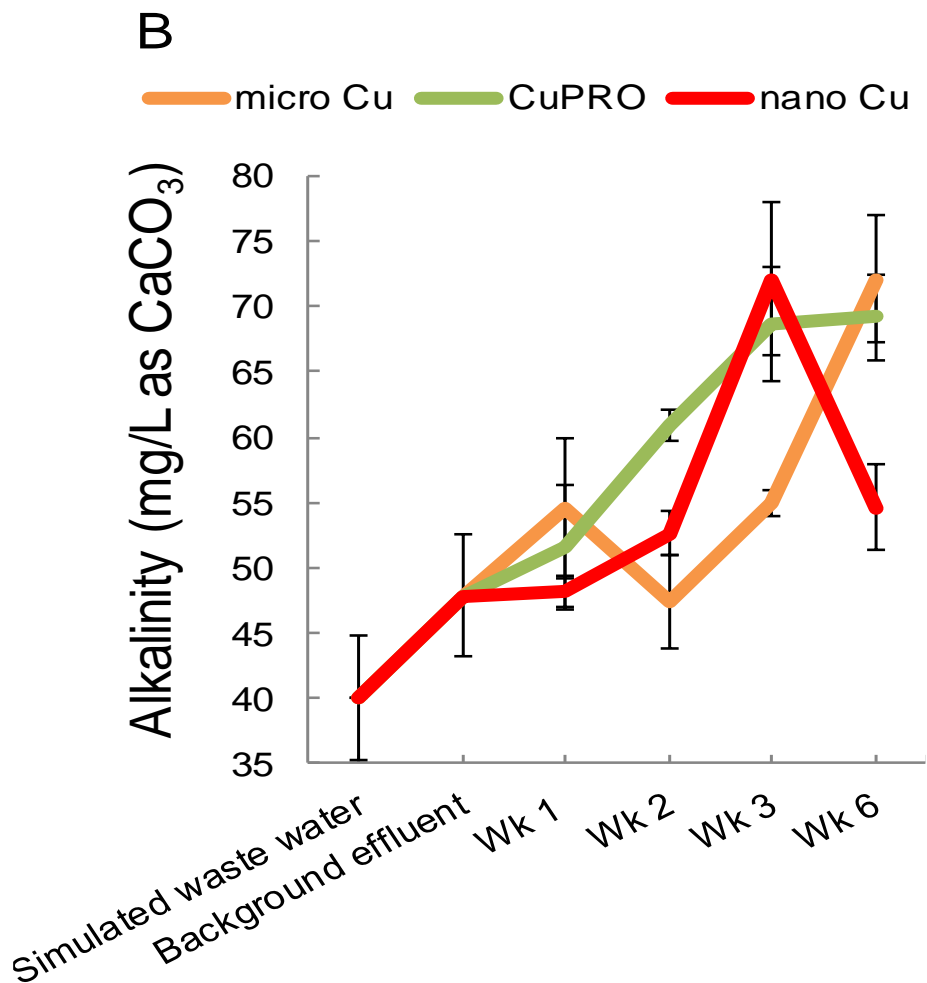


Figure S4.4B.

(B) The alkalinity data show a trend towards increased values for all Cu particle effluents. The average hardness for “background” effluent was equivalent to 47.86 ± 4.68 mg/L CaCO₃. The average alkalinity values for micro Cu effluents ranged from 47.44 ± 3.59 to 72.08 ± 4.83 mg/L, while related values for CuPRO were 51.61 ± 4.79 to 69.21 ± 3.30 mg/L. The average alkalinity values for nano Cu were equivalent to 48.24 ± 1.18 to 72.05 ± 5.84 mg/L CaCO₃. Since alkalinity is a good indication of metal speciation and metal bioavailability in the aqueous environments,³²⁴⁻³²⁵ the increase in alkalinity supports the formation of Cu complexes in the septic tank system.²⁸⁹

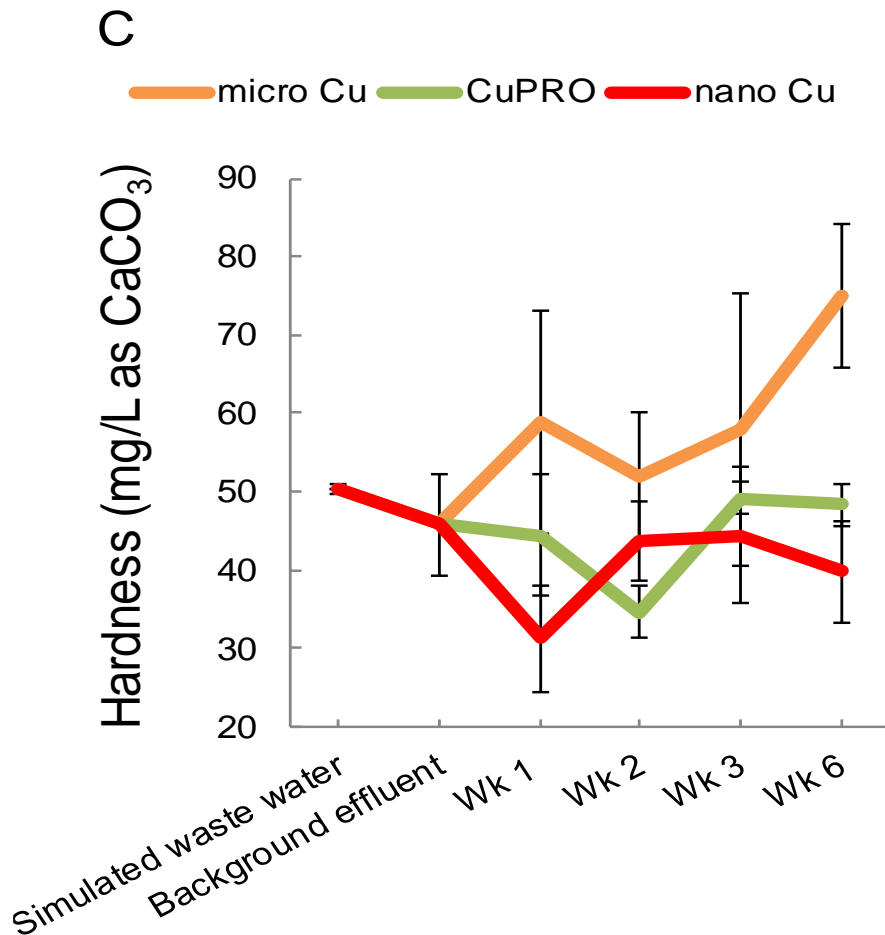


Figure S4.4C.

(C) The hardness data shows a slight increase for the micro Cu effluents, with CuPRO and nano Cu effluents remaining stable over time. The average hardness for “background” effluent was 45.85 ± 6.53 mg/L CaCO₃. The hardness for the micro Cu effluents ranges from 52.00 ± 8.30 to 75.00 ± 9.25 mg/L as CaCO₃. The hardness for CuPRO was 34.72 ± 3.40 to 49.17 ± 2.04 mg/L and for nano Cu the value was 31.28 ± 6.87 to 44.44 ± 8.62 mg/L as CaCO₃. It is important to note that while there were some deviations in the conductivity, alkalinity, and hardness of the Cu particle effluents compared to the “background” effluent, these changes did not impact the overall function and operation of the septic tank system.

References

1. Marcus, I. M.; Wilder, H. A.; Quazi, S. J.; Walker, S. L. Linking Microbial Community Structure to Function in Representative Simulated Systems. *Appl. Environ. Microbiol.* **2013**, *79*, 2552-2559.
2. EPA, Acid digestion of sediments, sludges, and soils. Revision 2 ed., **1996**, 1-12.
3. American Public Health Association, American Water Works Association, Water Pollution Control Federation and Water Environment Federation. Standard Methods for the Examination of Water and Wastewater. 17 ed., American Public Health Association, **1989**.
4. Brandes, M. Characteristics of Effluents from Gray and Black Water Septic Tanks. *J Water Pollut. Con. F.* **1978**, *50*, 2547-2559.
5. Allen, H. E.; Hansen, D. J. The Importance of Trace Metal Speciation to Water Quality Criteria. *Water Env. Res.* **1996**, *68*, 42-54.
6. Spry, D. J.; Wiener, J. G. Metal Bioavailability and Toxicity to Fish in Low-Alkalinity Lakes: A Critical Review. *Environ. Pollut.* **1991**, *71*, 243-304.
7. Pagenkopf, G. K.; Russo, R. C.; Thurston, R. V. Effect of Complexation on Toxicity of Copper to Fishes. *J. Fish Res. Board Can.* **1974**, *31*, 462-465.

Chapter 5

Summary and General Conclusions

Chapter 5: Summary and General Conclusions

The overall goal of this doctoral work was to determine the effects of various nanomaterials on microbial communities in engineered systems. A reproducible microbial community was used within the model colon bioreactor and within the model septic system. Both systems were dosed with relevant concentrations of nanomaterials that could either (1) be ingested through food and water, or (2) could enter a septic system through the disposal of consumer products that contain nanomaterials. Both systems were characterized with and without the nanomaterials present. Additionally, the microbial community of the septic system was also characterized to determine population changes caused by the nanomaterials. The general properties that were measured included cell concentration, sugar and protein content of the extracellular polymeric substance (EPS), electrophoretic mobility (EPM, surface charge), hydrophobicity, cell size, short chain fatty acid (SCFA) production, pH, and conductivity (Chapter 2). These tests plus additional analyses (alkalinity, hardness, biological oxygen demand, total suspended solids, total organic carbon, and microbial community structure) were performed in Chapter 3.

Chapter 2 highlighted the effects of three metal oxide nanomaterials at relevant concentrations ($0.01 \mu\text{gL}^{-1}$ ZnO, $0.01 \mu\text{gL}^{-1}$ CeO₂, and 3mgL^{-1} TiO₂) on the gut microbial community in a model colon bioreactor. Results indicate nanomaterials cause the microbial community's phenotype to partition into three distinct phases:

initial conditions, a transition period, and a homeostatic phase, with the NP-exposed community displaying significant differences ($P < 0.05$) from the unexposed community in multiple phenotypic traits. Notably, phenotypes including short chain fatty acid (SCFA) production, hydrophobicity, sugar content of the extracellular polymeric substance, and electrophoretic mobility, which indicates changes in the community's stability, were affected by the nanomaterials. The TiO_2 nanomaterial led to extended phenotypic transformations for hydrophobicity when compared to the other nanomaterials, likely due to its lack of dissociation and greater stability. This work demonstrated that these commonly used nanomaterials do cause significant changes to the microbial community's phenotype within a model human gut, suggesting that more realistic systems such as our model are needed for future toxicity screenings as they better simulate the actual exposure scenario. Diverse analyses, including techniques traditionally used for environmental microbial analysis, are also needed to further characterize changes in the microbial community phenotype, and can provide a depth of information that could complement microbial community sequencing data and medical-based enzyme assays. The techniques used in this dissertation may offer unique insights not associated with current colonic health indicators.

In Chapter 3, effects of three copper particles (micron- and nano-scale Cu particles, and nano-scale $\text{Cu}(\text{OH})_2$ -based fungicide) on the function and operation of a

model septic tank were investigated. Copper nanoparticles are found in many common consumer goods; therefore, the disposal and subsequent interactions between Cu-based nanoparticles and microbial communities may have detrimental impacts on wastewater treatment processes. Septic system analyses included water quality evaluation and microbial community characterization to detect changes in and relationships between the septic tank function and microbial community phenotype/genotype. During exposure to nano-scale Cu, biological oxygen demand (BOD) was reduced by at least 63%. Micron-scale Cu caused a reduction in the pH outside the optimum anaerobic fermentation range, indicating that the organic waste may have undergone incomplete degradation. The copper fungicide, $\text{Cu}(\text{OH})_2$, caused an increase in total organic carbon, which corresponded to increased BOD during the majority of the $\text{Cu}(\text{OH})_2$ exposure. Overall, results imply exposure to Cu particles caused disruption in septic tank function. However, it was observed that the system was able to recover to typical operating conditions after three weeks post-exposure. These results suggest that during periods of Cu introduction, there are likely pulses of improper waste treatment and incomplete organic breakdown. Here, a variety of bacteria characterization and standard wastewater quality tests were used together with a system simulating a realistic wastewater environment determined were used to determine the effects of nanomaterials on a microbial community.

The study described in Chapter 4 was motivated by the work found in Chapter 3. Here, a high through-put screening method was used to study the effects of the septic tank effluent on zebrafish embryo development. This work demonstrates the potential for environmental hazard of commercial copper-based particles used for fungicidal or bactericidal applications. In order to study the exposure potential of six Cu-based particles, namely nano-sized Cu and CuO, micron-sized Cu and CuO, and nano Cu(OH)₂-based CuPRO and Kocide, a zebrafish high throughput platform was used to compare the effects of the as-purchased materials as well as the “processed” materials through a model septic system. While the nanoscale materials were clearly more potent than the micron-scale particulates in interfering embryo hatching, the “processed” nano Cu, CuPRO and micro Cu by the model septic system demonstrated a steep decline in embryo toxicity, regardless of particle composition and size. The decreased toxicity was accompanied by Cu transformation into inorganic [e.g., Cu(H₂PO₂)₂] and organic Cu species that did not interfere with embryo hatching. Moreover, we demonstrated that the addition of natural organic matters could lead to a dose-dependent decrease in Cu toxicity in the embryos. Thus, the use of zebrafish screening, in combination with materials obtained from a real-life exposure scenario, provides a novel way to study the change in the hazard potential of commercial Cu-based particulates during partitioning, transformation, and speciation. This novel investigation demonstrated the need to combine toxicity tests such as high through-

put screening with characterization methods to monitor changes with engineered systems and microbial communities. Here, characterization methods such as wastewater quality tests (alkalinity, hardness, biological oxygen demand, total suspended solids, pH, conductivity, and total organic carbon) plus phenotypic characterization of the microbial community (cell concentration, sugar and protein content of the extracellular polymeric substance, electrophoretic mobility, hydrophobicity, cell size, short chain fatty acid production) were found to provide a useful approximation of toxicity potential for future studies. Particularly, combining these analyses with tools such as pyrosequencing, ICP-MS, and high throughput screening was found to produce great depth of information useful for assessing toxicity in complex matrices, such as a septic system.

The findings from this dissertation provide critical insights into the importance of studying microbial communities more holistically in realistic environments. These studies have demonstrated the need to update toxicity tests such that they more accurately reflect real exposure scenarios simulating environmental conditions. Results have the potential to inform scientists and influence new regulations not only for nanomaterials present in food and personal care products, but also how septic tanks are monitored and managed.

Recent regulations, such as the European Union's REACH which was implemented on June 1, 2007 (regulation on registration, evaluation, authorization, and restriction of chemicals:

http://ec.europa.eu/enterprise/sectors/chemicals/reach/index_en.htm), have begun to address the need for alternative toxicity tests rather than relying on animal models. New regulations will require the design of alternative testing methods, but also that these new approaches are thoroughly validated. This is especially important as numerous types of tests will be needed for assessing many different categories of compounds of interest: pesticides, pharmaceuticals, nanomaterials, by-products of manufacturing processes, heavy metals, and other contaminants of emerging concern. Various tests may also be needed to reflect the different sources of exposure and hazard potentials for all these diverse types of compounds. Future directions for toxicological studies will need new combinations of useful tools that could provide additional information for studies using complex matrices and microbial communities. This could include using techniques from the growing field of epigenetics and proteomics; these types of tests could give information on genetic expression and cellular activity of representative microbial communities. Improving and designing testing strategies for microbial communities that include diverse methods can be enhanced from the data presented in this dissertation. Future research will benefit from expanding upon the combinations of testing methods used in these projects.

Appendix A

Deposition and Disinfection of *Escherichia coli* O157:H7 on Naturally Occurring Photoactive Materials in a Parallel Plate Chamber

Reproduced with Permission from Environmental Science: Processes & Impacts, Copyright 2014, The Royal Society of Chemistry.

Taylor, A.A., I. Chowdhury, A.S. Gong, D.M. Cwiertny, and S.L. Walker. Environmental Science: Processes & Impacts, volume 16(2), pages 194-202, 2014.

Appendix A: Deposition and Disinfection of *Escherichia coli* O157:H7 on Naturally Occurring Photoactive Materials in a Parallel Plate Chamber

Abstract

Dissolved organic matter in combination with iron oxides has been shown to facilitate photochemical disinfection through the production of reactive oxygen species (ROS) under UV and visible light. However, due to the extremely short lifetime of these radicals, the disinfection efficiency is limited by the successful transport of ROS to bacterial surfaces. This study was designed to quantitatively investigate the role of collector surfaces [bare quartz, hematite (α -Fe₂O₃) coated quartz, and Suwannee River humic acid (SRHA)], extracellular polymeric substance (EPS) level (full and partially coated), and solution chemistry (ionic strength, IS) on bacterial interaction with ROS-producing substrates. With few exceptions, bacterial deposition studies in a parallel plate (PP) flow chamber studies revealed increasing cell adhesion with IS. Furthermore, interaction between collector surfaces and cells can be explained by electrostatic forces, with negatively charged SRHA reducing and positively charged α -Fe₂O₃ enhancing bacterial deposition significantly. Increased deposition was also observed with full EPS content, indicating the ability of EPS to facilitate interaction between cells and particles in the aquatic environment. In complementary disinfection studies conducted with simulated light, viability loss was observed for cells fully coated with EPS when attached to α -Fe₂O₃ under all IS conditions. Based

upon our prior study in which EPS was found to not inhibit hydroxyl radical activity toward bacteria, we proposed that in heterogeneous systems EPS might promote disinfection by facilitating cell interactions with higher concentrations of ROS expected closer to reactive substrates (e.g., SRHA and α -Fe₂O₃). Our findings on the mechanism and controlling factors of cell interactions with photoactive substrates provide insight as to the role of ionic strength in photochemical disinfection processes.

Introduction

Escherichia coli O157:H7 is a notorious strain that has been involved in numerous outbreak events causing foodborne and waterborne diseases, resulting in hemolytic-uremic syndrome.³²⁶ In the United States alone, O157:H7 causes an average of 75,000 infections and 61 deaths each year.³²⁷ *E. coli* O157:H7 can be associated with various farm animals as sources for contamination of water and food,³²⁸⁻³²⁹ as well as causing impairment to surface water associated with agricultural run-off.

Energy from the sun can be exploited to drive photochemical disinfection, a natural attenuation process critical to pathogen persistence in surface waters. Previous work has looked at indirect photochemical disinfection processes (i.e., those involving reactive oxygen species, or ROS, generated from sensitizers like dissolved organic matter) and quantified disinfection rates as a function of various bacterial and solution parameters (cell type, cell polymer presence, sensitizer type, solution chemistry, etc.). For example, our prior work revealed the insensitivity of disinfection rate to cellular extracellular polymeric substances (EPS) levels in a homogeneous (i.e., constituents fully dissolved) aquatic system with nitrate photolysis as a source of hydroxyl radical.³³⁰

In heterogeneous systems, however, such as those with insoluble natural organic matter present, studies have suggested the existence of microenvironments near the sensitizer interface where ROS concentrations can be more than two orders

of magnitude greater than the bulk, resulting in much faster disinfection³³¹ and inactivation³³² rates. Due to the short life span of the ROS, successful disinfection requires prompt transport of ROS from point of production to cell surfaces.³³³⁻³³⁴ It has been shown that bacterial EPS have the ability to initiate adhesion processes to form aggregates or biofilms.³³⁵⁻³³⁶ Accordingly, EPS should contribute to cell interaction with photoactive surfaces and possibly influence ROS access to the cell surface. There is a need, therefore, for a study to explore the contribution of cell adhesion to photoactive surfaces to the ultimate disinfection of the cells, and the contribution of EPS levels to this process.

The interactions between cells and surfaces depend on many factors. Common controlling factors influencing cell-surface interactions or biofilm formation in water include classical Derjaguin–Landau–Verwey–Overbeek (DLVO) type forces (van der Waals and electrostatic interaction),³³⁷⁻³³⁸ gravity,³³⁹⁻³⁴⁰ steric repulsion,³⁴¹ electrosteric force,³⁴²⁻³⁴³ hydrophobic properties,³⁴⁴ and hydration conditions of cells and solid surfaces³⁴⁵. The interactions between cells and surfaces in water also depend on solution chemistry including pH, ionic strength (IS), and valence.³⁴⁶⁻³⁴⁷ Other than these physicochemical factors, the interactions also depend on biological factors like quorum sensing,³⁴⁸ and the presence of bacterial surface macromolecules including flagella, pili, fimbriae, proteins, lipopolysaccharides (LPS), and EPS.^{326, 349} Previous studies on *E. coli* O157:H7 transport and adhesion in porous media revealed

deviation from DLVO predictions due to electrosteric repulsion,³⁵⁰ pH associated electrosteric stabilization,³⁵¹ and the presence of EPS.³⁵⁰⁻³⁵² However, the mechanisms involved in interactions between O157:H7 cells and photoactive substrates responsible for ROS production (such as $\bullet\text{OH}$, $^1\text{O}_2$, and H_2O_2) have not been clearly determined.

Many studies have focused on the role of surface macromolecules in regards to cell interaction and adhesion behavior in systems such as batch adhesion tests,³⁵³ packed-bed columns,^{275, 354-357} radial stagnation point flow (RSPF) systems,^{275, 342-343, 358} parallel plate (PP) flow chamber,³⁵⁹ and direct observation through atomic force microscopy (AFM)³⁶⁰⁻³⁶². A number of these studies demonstrated surface macromolecules play a significant role in well controlled adhesion experimental systems. However, results deviate on the contribution of macromolecules where some suggest an increase in adhesion,^{353, 355, 358} and others observed hindrance.^{342-343, 353-354} Due to the discrepancy in the literature, a straightforward experimental system with well-defined conditions focusing on a specific macromolecule is needed to investigate the disinfection scenario where cells interact with photoactive surfaces.

This study was designed to investigate the role of the adhesion between cells and naturally occurring photoactive materials on the disinfection of bacteria. Specifically, we examined the adhesion behavior of *E. coli* O157:H7 on representative photoactive substrates in a PP flow chamber while also conducting

complementary disinfection experiments with these photoactive materials using a solar simulator.^{39-41, 5} The PP flow chamber system simulates the condition where the flow stream is parallel to collector surfaces in porous media, and the fundamental mechanisms influencing bacteria adhesion to solid surfaces can be revealed in a well-defined hydrodynamic flow field. This technique can provide fundamental insight through direct observation of the bacterial interactions with model sensitizing agents SRHA and iron oxide (hematite, α -Fe₂O₃) under a microscope with cells of varying EPS levels. The working hypothesis for this study was that greater levels of interaction between the cell and solid collector surfaces (made of the desired ROS-generating material) will lead to a higher potential for successful disinfection under UV and visible light.

Methods and Methods

Cell Selection, Preparation, and Characterization

A pathogenic strain *E. coli* O157:H7/pGFP strain 72 with ampicillin resistance was chosen as a model organism in this study.³⁶³⁻³⁶⁴ This strain was selected because it is a rod-shaped, Gram-negative bacteria with very good fluorescence expression.³⁶⁴ Details on cell preparation and culture are mentioned in Supporting Information. The concentrations of bacteria were determined by direct visualization under a light

microscope (Fisher Scientific Micromaster) with a cell counting chamber (Buerker–Türk chamber, Marienfeld Laboratory Glassware, Lauda-Königshofen, Germany). The cell concentrations used in the deposition and disinfection portions of this study were 10^8 cells/mL and 5×10^8 cells/mL, respectively. The final cell suspensions were made in the background solution of the subsequent disinfection or deposition experiment (1, 10, or 100 mM KCl). All solutions used were made from reagent grade chemicals (Fisher Scientific) and deionized (DI) water (Millipore, Billerica, MA). A wide range of characterization was conducted to determine the surface properties of bacterial cells mentioned in detail in the Supporting Information. In brief, zeta potentials of *E. coli* were determined through electrokinetic properties, while cell size was measured from microscopic image analysis. Hydrophobicity of bacteria was determined by a partitioning test referred to as Microbial Adhesion to Hydrocarbons (MATH). Potentiometric titration was utilized to determine the acidity and surface charge densities of *E. coli*. Fourier transform infrared spectroscopy (FT-IR) was used to determine functional groups on full and partial EPS coated bacteria.

Surface Preparation and Characterization

Quartz slides (9 mm x 20 mm) (Electron Microscopy Sciences, Ft. Washington, PA) were used for the deposition and disinfection studies. Prior to coating or direct use in

experiments they were cleaned following the protocol described in the Supporting Information and elsewhere.³⁶⁵ For select experiments with organic matter, the quartz surfaces were cleaned with the procedure mentioned above, and subsequently were coated with Suwannee River humic acid (SRHA) according to a previously established flow through method.⁵

For iron oxide (α -Fe₂O₃) disinfection experiments, the clean glass slides (9 mm x 20 mm) (Fisherbrand®) were hand coated with 25 μ L of the α -Fe₂O₃ solution for an even distribution. The slides were allowed to dry and were kept in the dark until experiments. Subsequent analysis via XRD confirmed the deposited phase as hematite (data not shown). The detailed coating procedure is mentioned in the Supporting Information.

Parallel Plate Experiments

Deposition behavior of *E. coli* O157:H7 was observed in real time with a custom-made PP flow cell system, inserted on the stage of an upright fluorescence microscope BX-51 (Olympus, Tokyo, Japan).³⁶⁶ Images were taken by a 40 \times objective lens passing through a fluorescent filter set (Chroma Technology Corp., Brattleboro, VT). The flow cell is rectangular shaped with an inner chamber 6 cm \times 1 cm \times 0.0762 cm in size, formed by attaching the deck, rubber gasket, and a microscope glass slide with

a thin layer of vacuum grease. The flow deck was made with a pocket in the center, 9 mm in width, 20 mm in length (parallel to flow direction), and 1.5 mm in depth. This pocket allows for different collector surface samples (PP coupons) of this size to be inserted into the pocket and be fixed with vacuum grease. The inlet of the flow cell was attached to a 60 mL syringe pump where the flow rate of the bacterial solution was kept at 0.1 mL/min for all conditions. The concentration of bacterial solution was optimized to be 10^8 cells/mL in the flow cell for all conditions tested. Images of bacterial deposition on desired surfaces were taken by QImaging Retiga EXi digital camera (QImaging, Surrey, BC, Canada) every 30 sec over the course of 30 min and then analyzed with the supplied software (SimplePCI, Precision Instruments, Inc., Minneapolis, MN). The number of cells attached to the surface for five or more consecutive images were counted and the particle flux was determined from the linear slope of the number of cells deposited versus time and normalized by the microscope viewing area ($230 \mu\text{m} \times 170 \mu\text{m}$). Resulting bacterial transfer rate coefficients k (m/sec) were calculated from the deposition flux J (cells/sec \times m²), and injection concentration C_0 (cells/m³).

$$k = \frac{J}{c_0} \quad (1)$$

Bacterial Disinfection Experiments

Cell preparation and characterization for the disinfection study followed protocols mentioned in sections 2.1 and 2.2. Disinfection experiments were conducted with a solar simulator, following protocols utilized in previous work⁵. Briefly, a collimated beam of light from a 450 W O₃-free Xe arc lamp (Newport Corporation, Irvine, CA) was passed through a 320 nm filter to generate light in the UV and visible range. A 50 mL (37 mm ID) jacketed beaker kept at 25°C via a circulating water bath (Thermo Scientific, Waltham, MA) was employed for all experiments. Experiments used quartz and α -Fe₂O₃-coated quartz in the presence and absence of light (i.e., dark) across a range of IS. Experiments were conducted with the jacketed beaker containing three quartz or α -Fe₂O₃-coated slides in the jacketed beaker. Experiments at 1 and 10 mM KCl were conducted over 80 minutes and sampled in 20 minute intervals (i.e., 0, 20, 60, and 80 min) while experiments at 100 mM KCl were conducted up to 140 min with 20 min sampling intervals because more time was needed to observe an effect. Dark control experiments were conducted under the same parameters; however, the beakers were covered in foil to eliminate light exposure and allowed to sit in a dark room for 20 min intervals at 25°C.

To quantify the percentage of viable *E. coli* that adhered to the slides, the Live/Dead BacLight kit (L-13152; Molecular Probes, Eugene, OR) and a fluorescent

microscope (BX 51, Olympus, Japan) with a red/green fluorescence filter set (Chroma Technology Corp., Brattleboro, VT) was utilized. Additionally, a planktonic sample was removed from the jacketed beaker and viewed with the Live/Dead kit to quantify effects of the light and/or α -Fe₂O₃ on the free floating cells.

Results and Discussion

Characterization of E. coli O157:H7 and Collector Surfaces

Both *E. coli* O157:H7 and coated surfaces were characterized over a wide range of solution chemistry and the results are reported in Table A.1. The streaming potential of all three types of collector surfaces (bare quartz, SRHA-coated, and α -Fe₂O₃-coated) became less negative (or transitioned to positive) with greater IS. The zeta potentials of bare quartz appeared to be the most negative at 1 mM KCl and increased with IS towards neutral. For SRHA coated surfaces, the coating seemed to result in slightly more negative zeta potential (-23.4 ± 1.0 mV) in 10 mM KCl than bare quartz (-19.8 mV). However, in 100 mM KCl, the charge of SRHA coated surface was reversed to a positive value (19.7 ± 24.4 mV) due to charge screening at high IS. The α -Fe₂O₃ coating on the glass surface resulted in positive zeta potentials in both 10 and 100 mM KCl (pH 5.6) and a more positive value was observed in 100 mM (44.8 ± 25.4 mV) than in 10 mM (0.1 ± 1.89 mV) KCl.

Bacterial surfaces appear to be near neutral according to electrokinetic characterization; whereas, most nonpathogenic *E. coli* are more negatively charged at similar pH and IS conditions.^{5, 48} The zeta potential of O157:H7 also showed less sensitivity to the changing IS³⁵⁰⁻³⁵² as compared to other nonpathogenic *E. coli* strains.³⁶⁷⁻³⁶⁸ Similar values of O157:H7 zeta potentials were found with full and partial EPS coated cells in 1 and 10 mM KCl where no significant difference was detected between full EPS bacteria and their partial EPS counterpart ($p > 0.1$). In 100 mM KCl, zeta potential of full

EPS cells was observed to be significantly higher than in the partial EPS counterpart ($p < 0.1$). Additional characterization of bacterial cell surfaces was conducted to determine the difference in surface characteristics between full and partial EPS-coated O157:H7. Potentiometric titration results are summarized in Table A.1 and Figure A.1. Figure A.1 shows that acidity as well as surface charge density of partial EPS-coated O157:H7 were notably lower than full EPS-coated O157:H7. This indicates that sonication successfully removed the surface polymers of bacteria. However, the shape of potentiometric titration curve remained identical for both partial and full EPS-coated O157:H7, indicating that the sonication protocol used in this study did not create an artifact biasing collection of only certain surface polymers of the bacteria. FT-IR was conducted to determine the functional groups removed during sonication. FT-IR results (Figure A.5, located in SI at end of Appendix A)

indicate that the major functional group removed due to sonication was C=O stretching from proteins (1650 cm^{-1}).

Table A.1

IS (mM)	Collector surface zeta potential (mV) ^a		O157:H7 zeta potential (mV)		Cell size (µm) ^f	Hydrophobicity ^g	Acidity ^h (meq/10 ⁸ cells) × 10 ⁻⁶	Charge density ^h (µC/cm ²)
	quartz ^b	SRHA-coated	α-Fe ₂ O ₃ -coated	partial EPS ^e				
1	-24.7	ND ^c	ND	full EPS ^{sd} -2.7±0.3	0.55	38%	Full: 13.0 ± 1.4	Full: 329.9 ± 35.9
10	-19.8	-23.4±1.0	0.1±1.5	-0.2±2.1	0.58	76%	Partial: 8.5 ± 0.7	Partial: 215.7 ± 17.9
100	-3.4	19.6±24.4	44.8±25.7	2.3±1.9	0.53	58%		

^a Collector surface zeta potential measured using a streaming potential analyzer (EKA).

^b Quartz surface zeta potentials from reference.⁴¹

^c ND: not determined.

^d "O157:H7 with full EPS" zeta potentials measured with freshly harvested cells diluted in test electrolytes.

^e "O157:H7 partial EPS" zeta potentials measured with cells after applying probe sonication for EPS extraction.

^f Cell size was determined from microscopic image analysis.

^g Hydrophobicity of bacterial cells was determined by Microbial Adhesion to Hydrocarbons (MATH) test.

^h Acidity and surface charge densities were calculated from potentiometric titration results in 1.0 mM NaCl.

Adhesion Behavior of O157:H7 in the Parallel Plate Flow Chamber

Experimental results from O157:H7 transport experiments with the three test collector surfaces as a function of ionic strength and with full or partial EPS bacteria are reported in Figure A.2.

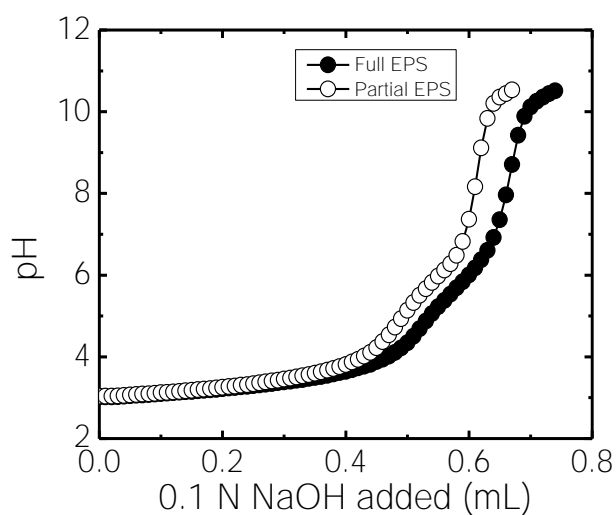


Figure A.1.

Potentiometric titration of *E. coli* 0157:H7 with full and partial EPS. Solution chemistry used was 10 mM KCl. Titration was conducted from pH 3 to 11 using 0.1 M NaOH as a titrant. Procedure of EPS removal was mentioned in the Supporting Information.

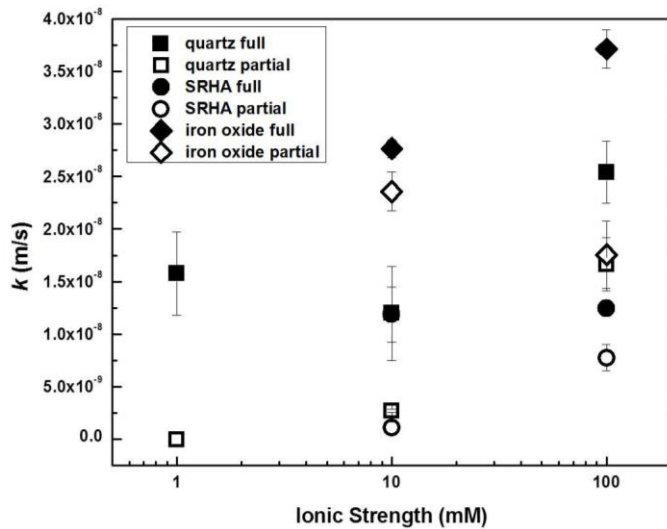


Figure A.2.

O157:H7 bacterial mass transfer rate coefficient (k) as a function of IS observed in the PP flow chamber with quartz, SRHA, and α -Fe₂O₃ as solid collectors. Full or partial refers to EPS levels. Error bars indicate one standard deviation.

Effect of Collector Surface on Adhesion Behavior of O157:H7

Surface coating was found to impact deposition trends across the range of IS conditions tested. For example, the bacterial transfer rate coefficient (k) on the bare quartz in 10 mM KCl was $1.32 \times 10^{-8} \pm 4.93 \times 10^{-9}$ m/s and $2.98 \times 10^{-9} \pm 1.42 \times 10^{-10}$ m/s for full and partial EPS, respectively. Full EPS-coated cells attached to both bare and SRHA-coated quartz similarly at 10 mM ($1.32 \times 10^{-8} \pm 4.93 \times 10^{-9}$ m/s and $1.31 \times 10^{-8} \pm 2.87 \times 10^{-9}$ m/s respectively). This indicates that the SRHA-coated surface did not provide additional steric hindrance towards the full EPS-coated bacteria. Partially-

coated EPS bacteria, on the other hand, attached less on SRHA ($k=1.19\times 10^{-9}\pm 6.46\times 10^{-10}$ m/s) than on quartz, whereas k on quartz was 2.5 times greater than that on the SRHA-coating. Hence, removal of EPS from the bacterial cell surface influenced the cellular interactions with SRHA-coated surfaces.

Solid surfaces with α -Fe₂O₃ coating appeared to be more favorable for bacterial deposition than bare quartz surfaces in 10mM KCl for both full and partial EPS-coated bacteria. Specifically, deposition on α -Fe₂O₃ resulted in 2.3 and 8.7 times greater mass transfer ($k=3.04\times 10^{-8}\pm 9.36\times 10^{-10}$ m/s for full EPS; $k=2.60\times 10^{-8}\pm 2.05\times 10^{-9}$ m/s for partial EPS) than on quartz, respectively.

The bacterial transfer rate coefficients (k) on the bare quartz in 100 mM KCl were $2.79\times 10^{-8}\pm 3.25\times 10^{-9}$ m/s and $1.83\times 10^{-8}\pm 2.77\times 10^{-9}$ m/s for full and partial EPS, respectively. The SRHA coating made the surface less favorable than bare quartz in 100 mM KCl for both full and partially EPS-coated bacteria ($k=1.36\times 10^{-8}\pm 5.42\times 10^{-10}$ m/s for full EPS and $k=8.53\times 10^{-9}\pm 1.36\times 10^{-9}$ m/s for partial EPS). Comparing the bacterial transfer rate coefficients for full and partial EPS in 100 mM KCl, the transfer rate coefficients in quartz were about 2 times greater than on SRHA. Similar to what was observed in 10 mM KCl, the α -Fe₂O₃ coating caused an increased transfer rate to the surface (1.5 times for full EPS and 1.1 times for partial EPS) as compared to the bare quartz.

Addition of a surface coating, either natural organic matter or α -Fe₂O₃, generally resulted in significant differences in transfer rate coefficients, as determined with a Student's *t* test. Insignificant differences were only found between 1) quartz and SRHA-coated quartz in 10 mM KCl with full EPS; 2) quartz and α -Fe₂O₃-coated glass in 100 mM KCl with partial EPS. The reason the surface coatings impacted the extent of attachment is due to a combination of mechanisms. Notably, electrostatic interactions were crucial. For example, the addition of SRHA coating on the quartz increased the negativity of quartz surface, thus reducing the attractive forces between bacterial surfaces and the solid. The greater deposition on α -Fe₂O₃-coated surfaces than on bare quartz is likely due to the positively charged coating (as confirmed by zeta potential measurements) leading to greater electrostatic attraction with the negatively charged bacteria (as compared to cellular interaction with the negatively charged bare quartz). A number of previously reported studies corroborate these trends. For example, negatively charged latex colloids were found to deposit less in porous media when both the silica 0.2-mm spherical soda-lime glass beads and colloids were coated with humic acid.³⁶⁹ Similarly, transport studies in porous media which reported substantial bacterial attachment on α -Fe₂O₃, which was subsequently reduced by the addition of both SRHA and soil humic acid at a concentration of 2.5 mg/L dissolved organic content.³⁷⁰⁻³⁷¹ Another study found increased bacterial

deposition rates occurred with Fe-coated sand and enhanced bacterial surface coverage of sediment surfaces.³⁷²

EPS Effect on Adhesion Behavior of E. coli O157:H7

Generally, lower bacterial transfer rate coefficients (k) were observed for cells with partial EPS than with full EPS across all conditions tested. For example at 100 mM KCl, the k values were $2.54 \times 10^{-8} \pm 2.95 \times 10^{-9}$ m/s and $1.66 \times 10^{-8} \pm 2.52 \times 10^{-9}$ m/s for full and partial EPS on quartz surfaces, respectively, where the rate coefficient k for cells with full EPS is 1.5 times greater than for cells with partial EPS in the same condition. At 10 mM KCl, significantly lower deposition was observed with partial EPS than full EPS, with $k = 2.71 \times 10^{-9} \pm 1.29 \times 10^{-10}$ m/s (partial EPS) and $1.20 \times 10^{-8} \pm 4.48 \times 10^{-9}$ m/s (full EPS), where the rate coefficient k for cells with full EPS is 4.3 times that for cells with partial EPS in the same solution. With SRHA coated surfaces, k values for cells with full EPS in 10 and 100 mM accounts for 11 and 1.6 times greater than partial EPS. With the α -Fe₂O₃ coating, k values for cells with the full EPS in 10 and 100 mM resulted in 1.2 and 2.1 times more than with partial EPS. This indicates that EPS association with cell surfaces may facilitate the interaction between cells and collector surfaces. Previous studies reported adhesion of bacteria increase with more EPS produced and present around the cells,^{335, 373-374} which is in agreement with these

reported trends (Figure A.2). Overall, the data suggest that EPS facilitates the association between bacteria and solid surfaces through a combination of mechanisms. These include polymer bridging³⁷⁵⁻³⁷⁷ in lower IS and an increase of heterogeneity³⁷⁸⁻³⁷⁹ on bacterial surfaces.

Adhesion Behavior of E. coli O157:H7 as a Function of Ionic Strength

Increasing IS generally was found to enhance the amount of deposition. This was the case for cells with partial EPS on quartz and SRHA, as well as cells with full EPS on α -Fe₂O₃. Specifically, the k values for cells with partial EPS onto quartz and SRHA increased by ~6 and ~7 times when the IS was increased from 10 to 100 mM. The value of k for cells with the full EPS onto the α -Fe₂O₃ increased just above 30% over that same change in solution chemistry.

The difference between bacterial cells deposited on quartz surfaces with full EPS at 1 and 10 mM KCl was insignificant ($p > 0.1$). Bacterial cells with full EPS attached similarly on SRHA coated quartz in 10 and 100 mM KCl with no significant difference ($p > 0.1$). The only deviation from this trend of increasing IS leading to greater deposition was for cells with partial EPS depositing on α -Fe₂O₃ surfaces. Bacterial cells with partial EPS attached less on α -Fe₂O₃ in 100 mM KCl ($k=1.75 \times 10^{-8} \pm 3.18 \times 10^{-9}$ m/s) than in 10 mM KCl ($k=2.36 \times 10^{-8} \pm 1.86 \times 10^{-9}$ m/s). Possible

mechanisms include the stabilization of the surface polymers by the increased IS,^{365,}
³⁸⁰ or the extraction of EPS from cells may have altered the local charge
heterogeneity,^{189, 378, 381} such that the electrostatic attractive force of the surface may
be reduced in 100 mM KCl.

Bacterial Disinfection

To relate deposition to disinfection, a viability analysis was performed in an attempt
to relate cell death with sensitizer exposure under varying IS (Figure A.3). As might
be expected, generally irradiated samples (open symbols) tended to show more
viability loss than dark controls (solid symbols), consistent with photodisinfection.
Interestingly, data also suggest that association with a surface can also promote
viability loss. This behavior is most obvious at the highest ionic strength condition
considered (100 mM), where cells adhered to quartz and hematite exhibited (i) greater
viability loss compared to planktonic cells under identical conditions (compare Figure
A.3E and A.3F), and (ii) the largest loss of viability observed under any IS condition.
At lower IS (i.e., 1 and 10 mM), little if any difference in viability loss was observed
between attached and planktonic cells. This is consistent with greater attachment
achieved at higher IS assisting in light-facilitated disinfection mechanisms. Finally,
trends in disinfection with respect to light versus dark and attached versus planktonic

cells were essentially identical between quartz and hematite systems, suggesting that the nature of the surface may be of limited importance – as compared to the degree of attachment and proximity to the sensitizer - when considering such heterogeneous photochemical disinfection processes.

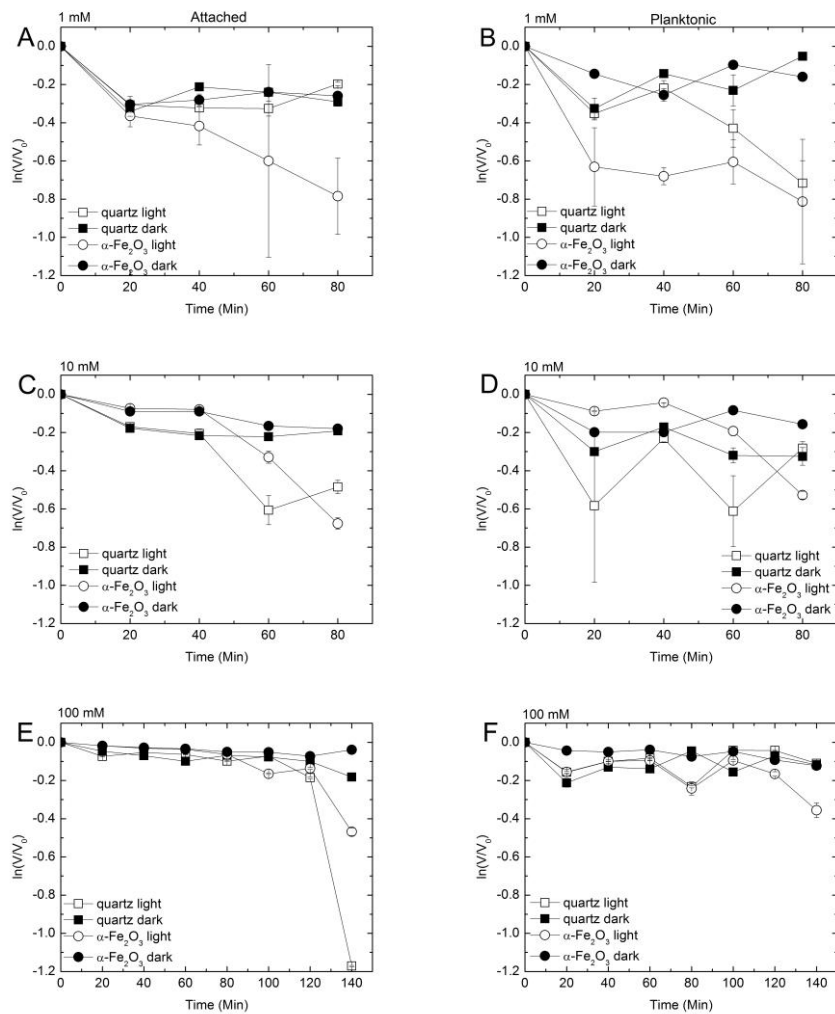


Figure A.3.

Survival of *E. coli* 0157:H7 with coated and uncoated α -Fe₂O₃ quartz slides as a function for attached and planktonic bacteria at 1 (A and B), 10 (C and D), and 100 (E and F) mM KCl. Experiments were conducted under both light (open symbols) and dark (solid symbols) conditions where A, C, and E report data for attached bacteria and B, D, and F show results for the planktonic cells. Error bars indicated one standard deviation.

Mechanistic Interpretations

*Predicted Interactions Between *E. coli* O157:H7 Cells and Collector Surfaces*

To understand the interactions between *E. coli* O157:H7 and the collector surfaces, zeta potential measurements were performed at the same solution chemistries used in transport experiments. These values were used to predict the interaction forces between cells and surfaces according to DLVO theory³³⁷⁻³³⁸ (Table A.3, located in SI at end of Appendix A). The DLVO calculations based on resulting zeta potential values (Table A.3) indicated there were no energy barriers to cell interactions with all three surfaces, for cells with either full and partial EPS at 10 and 100 mM KCl. The energy barrier in 1 mM KCl for both full and partial EPS coated cells was very low, below 10 kT in value, which may be overcome by other attractive forces like Brownian motion³⁸² and diffusion³⁶⁹. These predictions suggest chemically favorable conditions for O157:H7 interaction with the surfaces under all conditions tested in the PP system. This indicates that the differences observed in cellular attachment are mainly due to changes in surface macromolecules in bacterial cells (full EPS vs partial EPS) and deposition surfaces (bare quartz vs SRHA-coated).

Disinfection of Attached and Planktonic Cells

Previous results⁴⁶ suggest that planktonic lag phases in photochemical disinfection may take up to two hours under 10 mM KCl conditions; for 100 mM in this study, a delayed lag phase of 130 min was established for both attached and planktonic experiments. The greater lag time is correlated with an increase in IS (Figure A.3E and A.3F), which seems to suggest the bacteria have a greater tolerance to the light and α -Fe₂O₃ presumably due to enhanced bacterial aggregation at high IS.

At high IS, cells can also attach to appropriate surfaces to a greater extent. While our data certainly appears to indicate that surface attachment promotes viability loss upon irradiation, the mechanism of disinfection remains unclear and merits further investigation. It is tempting to attribute the viability loss observed in hematite systems to reactive oxygen species (ROS) that can be generated in the near surface region from Fe(II) generated via the photoreduction of structural Fe(III) in the hematite lattice. However, hematite photoreduction to yield Fe(II) is usually quite slow at neutral pH and is likely not sufficient to produce appreciable concentrations of ROS necessary to drive disinfection, although we cannot rule out the possibility that EPS could promote Fe(II) formation if able to form a complex with lattice Fe(III) that is a chromophore.

Evidence against an ROS-mediated disinfection route is also obtained from results with irradiated quartz slides, which tended to produce comparable, and occasionally greater, extents of viability loss than in hematite-containing systems. As ROS will not be generated in non-photoactive SiO₂ systems, other mechanisms responsible for viability should be considered, including the role that surfaces may play in concentrating or reflecting light and heat, both of which would be expected to promote cell die off.

Implications for Photodisinfection

The decrease of the bacterial EPS level lowered the deposition of cells as expected. This indicates the bacterial macromolecules enhance interactions with other surfaces in aquatic systems. The SRHA surface coating lowered the rate of deposition in both 10 and 100 mM KCl as compared to bare quartz. In contrast, the α -Fe₂O₃ surface coating resulted in greater attachment on the surface than on quartz. These observations clearly demonstrate that electrostatic forces play a significant role on O157:H7 deposition as demonstrated in the PP system.

Deposition of bacteria with full and partial EPS increased with greater IS. The general trend of increased attachment with IS agreed with DLVO calculations. The few exceptions suggest that some behaviors are not captured by classic DLVO theory,

specifically caused by the presence of EPS³⁸³, which causes surface heterogeneity³⁸⁴⁻
³⁸⁵ and facilitates steric interactions^{353, 360}.

While more work is warranted, we conclude that increased association between bacteria and surfaces promote photochemical disinfection by generating a microenvironment less hospitable for cell survival. For photoactive substrates, the near surface region could be rich in ROS, thereby increasing the likelihood of reaction with cell surfaces. In addition, surfaces may also concentrate light and via absorption produce localized regions of higher temperature that may facilitate greater rates of photodisinfection. Through enhancing the production of EPS, the effect of EPS may be exploited to maximize interactions with surrounding agents. Approaches to alter EPS production, and hence cell-sensitizer interactions, include modifying carbon sources, the carbon to nitrate ratio, phosphate, and nutrient levels.³⁸⁶⁻³⁸⁷ The formation of bacterial surface macromolecules and their composition can also be optimized for greater photochemical disinfection by means of modifying related solution chemistry conditions, e.g., IS³⁶⁰, pH³⁸⁸, and temperature³⁸⁹⁻³⁹⁰. Additionally, the more favorable interactions between bacteria and α -Fe₂O₃ surfaces suggest the presence of colloidal iron may also facilitate photochemical disinfection in natural waters.

References

1. Law, D., Virulence factors of *Escherichia coli* O157 and other Shiga toxin-producing E-coli. *Journal of Applied Microbiology* **2000**, *88*, (5), 729-745.
2. Mead, P. S.; Slutsker, L.; Dietz, V.; McCaig, L. F.; Bresee, J. S.; Shapiro, C.; Griffin, P. M.; Tauxe, R. V., Food-related illness and death in the United States. *Emerging Infectious Diseases* **1999**, *5*, (5), 607-625.
3. Armstrong, G. L.; Hollingsworth, J.; Morris, J. G., Emerging foodborne pathogens: *Escherichia coli* O157:H7 as a model of entry of a new pathogen into the food supply of the developed world. *Epidemiologic Reviews* **1996**, *18*, (1), 29-51.
4. Olsen, S. J.; Miller, G.; Breuer, T.; Kennedy, M.; Higgins, C.; Walford, J.; McKee, G.; Fox, K.; Bibb, W.; Mead, P., A waterborne outbreak of *Escherichia coli* O157 : H7 infections and hemolytic uremic syndrome: Implications for rural water systems. *Emerging Infectious Diseases* **2002**, *8*, (4), 370-375.
5. Gong, A. S.; Lanzl, C. A.; Cwiertny, D. M.; Walker, S. L., Influence of Varying Levels of Extracellular Polymeric Substances (EPS) on Hydroxyl Radical Mediated Disinfection of *Escherichia coli*. In University of California, Riverside: Submitted to Environmental Science & Technology, 2011.
6. Latch, D. E.; McNeill, K., Microheterogeneity of singlet oxygen distributions in irradiated humic acid solutions. *Science* **2006**, *311*, (5768), 1743-1747.
7. Kohn, T.; Grandbois, M.; McNeill, K.; Nelson, K. L., Association with natural organic matter enhances the sunlight-mediated inactivation of MS2 coliphage by singlet oxygen. *Environmental Science & Technology* **2007**, *41*, (13), 4626-4632.
8. Gogniat, G.; Thyssen, M.; Denis, M.; Pulgarin, C.; Dukan, S., The bactericidal effect of TiO₂ photocatalysis involves adsorption onto catalyst and the loss of membrane integrity. *Fems Microbiology Letters* **2006**, *258*, (1), 18-24.
9. Cho, M.; Chung, H. M.; Choi, W. Y.; Yoon, J. Y., Different inactivation Behaviors of MS-2 phage and *Escherichia coli* in TiO₂ photocatalytic disinfection. *Applied and Environmental Microbiology* **2005**, *71*, (1), 270-275.
10. Frank, B. P.; Belfort, G., Polysaccharides and sticky membrane surfaces: critical ionic effects. *Journal of Membrane Science* **2003**, *212*, (1-2), 205-212.

11. Costerton, J. W.; Geesey, G. G.; Cheng, K. J., How bacteria stick. *Scientific American* **1978**, 238, (1), 86-95.
12. Derjaguin, B., A theory of interaction of particles in presence of electric double layers and the stability of lyophobic colloids and disperse systems. *Acta Physicochimica Urss* **1939**, 10, (3), 333-346.
13. Verwey, E. J. W., Theory of the stability of lyophobic colloids. *Journal of Physical and Colloid Chemistry* **1947**, 51, (3), 631-636.
14. Yiantsios, S. G.; Karabelas, A. J., The effect of gravity on the deposition of micron-sized particles on smooth surfaces. *International Journal of Multiphase Flow* **1998**, 24, (2), 283-293.
15. Chen, G. X.; Hong, Y. S.; Walker, S. L., Colloidal and Bacterial Deposition: Role of Gravity. *Langmuir* **2010**, 26, (1), 314-319.
16. Yoshioka, K.; Sakai, E.; Daimon, M.; Kitahara, A., Role of steric hindrance in the performance of superplasticizers for concrete. *Journal of the American Ceramic Society* **1997**, 80, (10), 2667-2671.
17. Kuznar, Z. A.; Elimelech, M., Cryptosporidium oocyst surface macromolecules significantly hinder oocyst attachment. *Environmental Science & Technology* **2006**, 40, (6), 1837-1842.
18. Kuznar, Z. A.; Elimelech, M., Role of surface proteins in the deposition kinetics of *Cryptosporidium parvum* oocysts. *Langmuir* **2005**, 21, (2), 710-716.
19. Ong, Y. L.; Razatos, A.; Georgiou, G.; Sharma, M. M., Adhesion forces between E-coli bacteria and biomaterial surfaces. *Langmuir* **1999**, 15, (8), 2719-2725.
20. Pringle, J. H.; Fletcher, M., Influence of substratum hydration and adsorbed macromolecules on bacterial attachment to surfaces. *Applied and Environmental Microbiology* **1986**, 51, (6), 1321-1325.
21. Li, Q.; Logan, B. E., Enhancing bacterial transport for bioaugmentation of aquifers using low ionic strength solutions and surfactants. *Water Research* **1999**, 33, (4), 1090-1100.

22. Kuznar, Z. A.; Elimelech, M., Adhesion kinetics of viable *Cryptosporidium parvum* oocysts to quartz surfaces. *Environmental Science & Technology* **2004**, *38*, (24), 6839-6845.
23. Parsek, M. R.; Greenberg, E. P., Acyl-homoserine lactone quorum sensing in Gram-negative bacteria: A signaling mechanism involved in associations with higher organisms. *Proceedings of the National Academy of Sciences of the United States of America* **2000**, *97*, (16), 8789-8793.
24. Ryu, J. H.; Beuchat, L. R., Biofilm formation by *Escherichia coli* O157 : H7 on stainless steel: Effect of exopolysaccharide and curli production on its resistance to chlorine. *Applied and Environmental Microbiology* **2005**, *71*, (1), 247-254.
25. Kim, H. N.; Hong, Y.; Lee, I.; Bradford, S. A.; Walker, S. L., Surface Characteristics and Adhesion Behavior of *Escherichia coli* O157:H7: Role of Extracellular Macromolecules. *Biomacromolecules* **2009**, *10*, (9), 2556-2564.
26. Kim, H. N.; Bradford, S. A.; Walker, S. L., *Escherichia coli* O157:H7 Transport in Saturated Porous Media: Role of Solution Chemistry and Surface Macromolecules. *Environmental Science & Technology* **2009**, *43*, (12), 4340-4347.
27. Kim, H. N.; Walker, S. L.; Bradford, S. A., Macromolecule mediated transport and retention of *Escherichia coli* O157:H7 in saturated porous media. *Water Research* **2010**, *44*, (4), 1082-1093.
28. Rijnaarts, H. H. M.; Norde, W.; Lyklema, J.; Zehnder, A. J. B., DLVO and steric contributions to bacterial deposition in media of different ionic strengths. *Colloids and Surfaces B-Biointerfaces* **1999**, *14*, (1-4), 179-195.
29. Williams, V.; Fletcher, M., *Pseudomonas fluorescens* adhesion and transport through porous media are affected by lipopolysaccharide composition. *Applied and Environmental Microbiology* **1996**, *62*, (1), 100-104.
30. Gargiulo, G.; Bradford, S.; Simunek, J.; Ustohal, P.; Vereecken, H.; Klumpp, E., Bacteria transport and deposition under unsaturated conditions: The role of the matrix grain size and the bacteria surface protein. *Journal of Contaminant Hydrology* **2007**, *92*, (3-4), 255-273.
31. Rajagopalan, R.; Tien, C., Trajectory analysis of deep-bed filtration with sphere-in-cell porous-media model. *Aiche Journal* **1976**, *22*, (3), 523-533.

32. Walker, S. L.; Redman, J. A.; Elimelech, M., Influence of growth phase on bacterial deposition: Interaction mechanisms in packed-bed column and radial stagnation point flow systems. *Environmental Science & Technology* **2005**, *39*, (17), 6405-6411.
33. Ginn, T. R.; Wood, B. D.; Nelson, K. E.; Scheibe, T. D.; Murphy, E. M.; Clement, T. P., Processes in microbial transport in the natural subsurface. *Advances in Water Resources* **2002**, *25*, (8-12), 1017-1042.
34. Walker, S. L.; Redman, J. A.; Elimelech, M., Role of cell surface lipopolysaccharides in Escherichia coli K12 adhesion and transport. *Langmuir* **2004**, *20*, (18), 7736-7746.
35. Gomez-Suarez, C.; Pasma, J.; van der Borden, A. J.; Wingender, J.; Flemming, H. C.; Busscher, H. J.; van der Mei, H. C., Influence of extracellular polymeric substances on deposition and redeposition of Pseudomonas aeruginosa to surfaces. *Microbiology-Sgm* **2002**, *148*, 1161-1169.
36. Abu-Lail, N. I.; Camesano, T. A., Role of ionic strength on the relationship of biopolymer conformation, DLVO contributions, and steric interactions to bioadhesion of Pseudomonas putida KT2442. *Biomacromolecules* **2003**, *4*, (4), 1000-1012.
37. Fang, H. H. P.; Chan, K. Y.; Xu, L. C., Quantification of bacterial adhesion forces using atomic force microscopy (AFM). *Journal of Microbiological Methods* **2000**, *40*, (1), 89-97.
38. Goddard, D. T.; Steele, A.; Beech, I. B., Towards in situ atomic force microscopy imaging of biofilm growth on stainless steel. *Scanning Microscopy* **1996**, *10*, (4), 983-988.
39. Bradford, S. A.; Simunek, J.; Walker, S. L., Transport and straining of E-coli O157 : H7 in saturated porous media. *Water Resources Research* **2006**, *42*, (12).
40. Fratamico, P. M.; Deng, M. Y.; Strobaugh, T. P.; Palumbo, S. A., Construction and characterization of Escherichia coli O157:H7 strains expressing firefly luciferase and green fluorescent protein and their use in survival studies. *Journal of Food Protection* **1997**, *60*, (10), 1167-1173.

41. Chen, G. X.; Walker, S. L., Role of solution chemistry and ion valence on the adhesion kinetics of groundwater and marine bacteria. *Langmuir* **2007**, *23*, (13), 7162-7169.
42. Chen, G.; Beving, D. E.; Bedi, R. S.; Yan, Y. S.; Walker, S. L., Initial Bacterial Deposition on Bare and Zeolite-Coated Aluminum Alloy and Stainless Steel. *Langmuir* **2009**, *25*, (3), 1620-1626.
43. Bolster, C. H.; Haznedaroglu, B. Z.; Walker, S. L., Diversity in Cell Properties and Transport Behavior among 12 Different Environmental Escherichia coli Isolates. *Journal of Environmental Quality* **2009**, *38*, (2), 465-472.
44. Kim, H. N.; Walker, S. L., Escherichia coli transport in porous media: Influence of cell strain, solution chemistry, and temperature. *Colloids and Surfaces B-Biointerfaces* **2009**, *71*, (1), 160-167.
45. Franchi, A.; O'Melia, C. R., Effects of natural organic matter and solution chemistry on the deposition and reentrainment of colloids in porous media. *Environmental Science & Technology* **2003**, *37*, (6), 1122-1129.
46. Johnson, W. P.; Logan, B. E., Enhanced transport of bacteria in porous media by sediment-phase and aqueous-phase natural organic matter. *Water Research* **1996**, *30*, (4), 923-931.
47. Johnson, W. P.; Martin, M. J.; Gross, M. J.; Logan, B. E., Facilitation of bacterial transport through porous media by changes in solution and surface properties. *Colloids and Surfaces a-Physicochemical and Engineering Aspects* **1996**, *107*, 263-271.
48. Bolster, C. H.; Mills, A. L.; Hornberger, G. M.; Herman, J. S., Effect of surface coatings, grain size, and ionic strength on the maximum attainable coverage of bacteria on sand surfaces. *Journal of Contaminant Hydrology* **2001**, *50*, (3-4), 287-305.
49. Li, B. K.; Logan, B. E., Bacterial adhesion to glass and metal-oxide surfaces. *Colloids and Surfaces B-Biointerfaces* **2004**, *36*, (2), 81-90.
50. Olofsson, A. C.; Hermansson, M.; Elwing, H., N-acetyl-L-cysteine affects growth, extracellular polysaccharide production, and bacterial biofilm formation on solid surfaces. *Applied and Environmental Microbiology* **2003**, *69*, (8), 4814-4822.

51. Frank, B. P.; Belfort, G., Intermolecular forces between extracellular polysaccharides measured using the atomic force microscope. *Langmuir* **1997**, *13*, (23), 6234-6240.
52. Skillman, L. C.; Sutherland, I. W.; Jones, M. V., The role of exopolysaccharides in dual species biofilm development. *Journal of Applied Microbiology* **1999**, *85*, 13S-18S.
53. Fletcher, M.; Floodgat, Gd, An electron-microscopic demonstration of an acidic polysaccharide involved in the adhesion of a marine bacterium to solid surfaces. *Journal of General Microbiology* **1973**, *74*, (FEB), 325-334.
54. Omoike, A.; Chorover, J., Spectroscopic study of extracellular polymeric substances from *Bacillus subtilis*: Aqueous chemistry and adsorption effects. *Biomacromolecules* **2004**, *5*, (4), 1219-1230.
55. Tsuneda, S.; Aikawa, H.; Hayashi, H.; Yuasa, A.; Hirata, A., Extracellular polymeric substances responsible for bacterial adhesion onto solid surface. *Fems Microbiology Letters* **2003**, *223*, (2), 287-292.
56. Vadillo-Rodriguez, V.; Busscher, H. J.; van der Mei, H. C.; de Vries, J.; Norde, W., Role of lactobacillus cell surface hydrophobicity as probed by AFM in adhesion to surfaces at low and high ionic strength. *Colloids and Surfaces B-Biointerfaces* **2005**, *41*, (1), 33-41.
57. Wuertz, S.; Spaeth, R.; Hinderberger, A.; Griebe, T.; Flemming, H. C.; Wilderer, P. A., A new method for extraction of extracellular polymeric substances from biofilms and activated sludge suitable for direct quantification of sorbed metals. *Water Science and Technology* **2001**, *43*, (6), 25-31.
58. Walker, S. L.; Hill, J. E.; Redman, J. A.; Elimelech, M., Influence of growth phase on adhesion kinetics of *Escherichia coli* D21g. *Applied and Environmental Microbiology* **2005**, *71*, (6), 3093-3099.
59. Hahn, M. W.; O'Melia, C. R., Deposition and reentrainment of Brownian particles in porous media under unfavorable chemical conditions: Some concepts and applications. *Environmental Science & Technology* **2004**, *38*, (1), 210-220.

60. Jucker, B. A.; Zehnder, A. J. B.; Harms, H., Quantification of polymer interactions in bacterial adhesion. *Environmental Science & Technology* **1998**, *32*, (19), 2909-2915.
61. Stewart, P. S.; Murga, R.; Srinivasan, R.; Debeer, D., Biofilm structural heterogeneity visualized by 3 microscopic methods. *Water Research* **1995**, *29*, (8), 2006-2009.
62. Wimpenny, J.; Manz, W.; Szewzyk, U., Heterogeneity in biofilms. *Fems Microbiology Reviews* **2000**, *24*, (5), 661-671.
63. Bonet, R.; Simonpujol, M. D.; Congregado, F., Effects of nutrients on exopolysaccharide production and surface-properties of *Aeromonas-salmonicida*. *Applied and Environmental Microbiology* **1993**, *59*, (8), 2437-2441.
64. Kornmann, H.; Duboc, P.; Marison, I.; von Stockar, U., Influence of nutritional factors on the nature, yield, and composition of exopolysaccharides produced by *Gluconacetobacter xylinus* I-2281. *Applied and Environmental Microbiology* **2003**, *69*, (10), 6091-6098.
65. P. V. Bhaskar, a. N. B. B., Microbial extracellular polymeric substances in marine biogeochemical processes. *CURRENT SCIENCE* **2005**, *88*, (1), 45-53.
66. Nichols, C. M.; Bowman, J. P.; Guezennec, J., Effects of incubation temperature on growth and production of exopolysaccharides by an Antarctic sea ice bacterium grown in batch culture. *Applied and Environmental Microbiology* **2005**, *71*, (7), 3519-3523.
67. Veiga, M. C.; Jain, M. K.; Wu, W. M.; Hollingsworth, R. I.; Zeikus, J. G., Composition and role of extracellular polymers in methanogenic granules. *Applied and Environmental Microbiology* **1997**, *63*, (2), 403-407.

Supporting Information for Appendix A: Deposition and Disinfection of *Escherichia coli* O157:H7 on Naturally Occurring Photoactive Materials in a Parallel Plate Chamber

Introduction

In this Supporting Information section, additional materials and methods are described including cell selection, preparation, characterization, extraction of EPS, cell surface characterization, and surface preparation for deposition and disinfection experiments.

Additional Materials and Methods

Cell Selection, Preparation, and Characterization

A pathogenic strain *E. coli* O157:H7/pGFP strain 72 with ampicillin resistance was chosen as a model organism in this study.³⁶³⁻³⁶⁴ This strain was selected because it is a rod-shaped, Gram-negative bacteria with very good fluorescence expression.^{364, 391}

Bacterial cells were pre-cultured by inoculating bacterial colonies streaked from a Luria-Bertani (LB) agar plate into 5 mL LB media (Fisher Scientific, Fair Lawn, NJ).

Cells were grown in the presence of 0.1 g/L ampicillin the day before the experiment and incubated at 37°C in an incubator overnight (16 hours). The pre-culture step was followed by a culturing process in which 2 mL of the pre-culture was added to 200 mL of LB media (1:100 v/v) and incubated at 37°C for 3.5 hours to reach mid-

exponential growth phase. After reaching this growth stage, the culture was harvested by centrifugation (5804R; Eppendorf, Hamburg, Germany) with a fixed-angle rotor (F-34-6-38; Eppendorf) at 4°C 3700 g for 15 min to separate the cells from the growth media. The centrifugation step was at 4°C 3700 g for 15 min, followed by decanting the supernatant, and resuspending in 10 mL of electrolyte (10 mM KCl, Fisher Scientific). This was repeated twice to remove all traces of growth media. Next, a stock suspension was prepared by resuspending the pellet in 5 mL of electrolyte, at the same ionic strength required for subsequent transport or cell characterization steps.

The concentrations of bacteria were determined by direct visualization under a light microscope (Fisher Scientific Micromaster) with a cell counting chamber (Buerker–Türk chamber, Marienfeld Laboratory Glassware, Lauda-Königshofen, Germany). The resulting cell concentrations in this particular study were in between 4×10^{10} and 6×10^{10} bacteria/mL. All solutions used were made from reagent grade chemicals (Fisher Scientific) and deionized (DI) water (Millipore, Billerica, MA).

Extraction of EPS by Sonication Technique.

Bacterial EPS was extracted through a previously established protocol applying probe sonication (Omni-Ruptor 250, Omni International, Kennesaw, GA) and centrifugation

(Eppendorf).³⁹² Bacteria in stock solution were re-suspended in 10 mL of 1, 10 or 100 mM KCl. A 5/32" Micro-Tip sonicating probe (Omni International) was immersed 10 cm into the solution in a 15 mL centrifuge tube. The temperature was maintained below 4°C by immersing the tube in an ice bath throughout the sonication process. Sonication was repeatedly applied to the bacterial cells by way of five sec duration pulses with five sec rest periods in between at a fixed intensity (30% of the 150 Watt = 45 Watt) for a total of 300 sec. After sonication, the bacterial solution was centrifuged at 4°C and 4000g for 20 min (Eppendorf), and the supernatant was collected and passed through a 0.22 µm filter (Millipore, Fisher Scientific) for further EPS composition analysis. Finally, the pellet was resuspended in electrolyte for subsequent characterization and transport experiments.

The sugar and protein content of the EPS were evaluated through the Phenol-Sulfuric Acid (PSA) method³⁹³ and the Lowry method³⁹⁴ with Xanthan gum (Sigma-Aldrich corporation, St. Louis, MO) and bovine serum albumin (BSA, 1mg/mL) (Fisher BioReagents, Fisher Scientific) as the standards, respectively. Both are colorimetric methods where the chemical reaction induced color change can be measured by spectroscopy (BioSpec-mini, Shimadzu Corp. Kyoto, Japan) and compared with a standard curve for sugar or protein concentration. The sugar level was determined by adding 50 µL of 80% (v/v) phenol and then 5 mL of highly concentrate sulfuric acid (95.5% Fisher Scientific) into 2 mL of an extracted EPS

sample. The mixing of these chemicals produces heat and a color change. Therefore, the solution required 10 min at room temperature to cool down, followed by immersion in a water bath (Lab-Line Instruments, Inc., Melrose Park, IL) at 25-30°C for 20 min, and finally, room temperature incubation for 4 hr to stabilize the color before measuring the absorbance at 480 nm (Biospec-mini, Shimadzu Corp.). The protein level was evaluated by adding 1.5 mL of alkaline copper reagent (made by mixing 1 mL of 2% $\text{Na}_2\text{C}_4\text{H}_4\text{O}_6$, 1 mL of 1% CuSO_4 , and 98 mL of 2% NaCO_3 in 0.1 M NaOH) to 0.3 mL of EPS sample. After adding the alkaline copper reagent, the sample required incubation at room temperature for 10 min. Next, 75 μL of Folin reagent (Folin and Ciocalteu's Phenol Reagent, MP Biomedicals, LLC, Germany) was added into the mixture, the solution was vortexed (AutoTouch Mixer Model 231, Fisher Scientific), and incubated at room temperature for 30 min before measuring absorbance at 500 nm (Biospec-mini, Shimadzu Corp.). All chemicals used were ACS grade (Fisher Scientific).

Cell Surface Characterization.

Bacterial cell sizes, surface charge densities, hydrophobicity, and zeta potentials were determined according to previous established protocols.³⁶⁷ The size and shape of bacteria were evaluated by taking images of 10^{10} bacteria/mL with a light microscope

(Fisher Scientific Micromaster). Images with more than 50 cells were processed through MATLAB software (Matlab, the MathWorks, Inc., Natick, MA), and individual bacteria widths and lengths were determined to calculate the effective diameters.

Surface charge densities were evaluated by potentiometric titrations in an auto titrator (798 MPT Titrino, Metrohm, Switzerland). Briefly the amounts of base added into bacterial solution for the pH value to increase from 4 to 10 were measured. The bacterial concentration in the titrator was 1×10^8 bacteria/mL, and the base used to titrate the bacterial solution was 0.1 N NaOH.

The hydrophobicity of the bacterial cells was measured by the microbial adhesion to hydrocarbon test (MATH test).³⁹⁵ The relative hydrophobicity was determined by the percentage of 4 mL bacterial cells partitioned into 1 mL of n-dodecane (laboratory grade, Fisher Scientific) after vortexing for 2 min (AutoTouch Mixer Model 231, Fisher Scientific) and a 15-min room temperature incubation. The optical density of the water phase was determined by spectroscopy (Shimadzu Corp.), and the percentage of bacteria which passed to the oil phase was calculated.

The bacterial electrophoretic mobility (EPM) was measured by a ZetaPALS analyzer (Brookhaven Instruments Corporation, Holtsville, NY) in 1, 10, and 100 mM KCl with unadjusted pH (5.6-5.8). Bacterial solution was diluted to an optical density of $OD_{600} = 0.2$ to 0.225 before running through ZetaPALS. The zeta potential of the

cells was then calculated by electrophoretic mobility values using the Smoluchowski equation.³⁹⁶

Surface Preparation and Characterization

Glass and quartz slides (9mm x 20mm) were used for the deposition and disinfection studies, respectively. Prior to coating or direct use in experiments they were cleaned by the subsequent method: slides were placed in a 2% (v/v) extran solution and sonicated for 15 min. The slides were then rinsed with deionized water and immediately placed in a 2% (v/v) RBS35 solution and sonicated for 15 min at 50°C. Slides were again rinsed with deionized water and sat in Nochromix overnight. Slides were rinsed six times with deionized water and then stored in sterile Petri plates until usage.

For select experiments with organic matter, the quartz surfaces were cleaned with the procedure mentioned above, and subsequently were coated with Suwannee River humic acids (SRHA) according to a previously established flow through method.³⁹⁷ In between flowing DI water and KCl solutions, 2 mL of poly-L-lysine (PLL)-free solution, 2 mL PLL, 2 mL PLL-free, and 2 mL SRHA solution were flowed through the system. PLL-free solution was comprised of 10 mM N-(2-Hydroxyethyl) piperazine-N²-(2-ethanesulfonic acid) (HEPES) (Sigma-Aldrich, St.

Louis, MO) and 100 mM KCl. PLL solution was made by adding 0.1 g/L PLL into PLL free solution. SRHA solution was made by adding 28.3 mg of dry SRHA powder (International Humic Substance Society) into 52 mL DI water and shaken for 2 hrs. All solutions made were passed through 0.22 μm cellulose acetate membrane filters. When flowing through the PP flow cell, the PLL binds to the quartz. Subsequently, the SRHA solution was passed through the flow cell and bound to the PLL layer. Hence a layer of SRHA was formed on the quartz surface.

For iron oxide ($\alpha\text{-Fe}_2\text{O}_3$) disinfection experiments, the clean glass slides were hand coated with 25 μL of the $\alpha\text{-Fe}_2\text{O}_3$ solution for an even distribution. The slides were allowed to dry and were kept in the dark until experiments. In order to coat the surfaces with $\alpha\text{-Fe}_2\text{O}_3$ for the PP experiments, an additional pretreatment of the glass was required. Following the cleaning procedure described above, the glass slides were treated with Piranha solution (the mixture of 30% H_2O_2 and 95.6% H_2SO_4 in 1:3 v/v ratio) to hydroxylate the glass surface, making the glass surface hydrophilic. The hydrophilic glass then was coated with $\alpha\text{-Fe}_2\text{O}_3$ nanoparticles with a spin coating method at room temperature and 1500 rpm for 25 sec using a Laurell spin coater (WS-400A-6NPP/LITE) (Laurell Technologies Corp.; Johnstown, PA). The $\alpha\text{-Fe}_2\text{O}_3$ solution used in the spin coating was made by the following method. $\alpha\text{-Fe}_2\text{O}_3$ nanoparticles were made by adding 24 mL of 1 M ferric nitrate solution into 200 mL of boiling DI water at a steady speed of about 1 mL every 30 sec (finish adding 24 mL

in 12 min).³⁹⁸ The solution turned from light brown to dark brown to very dark brown, and then the reaction took place to turn the solution to dark red under boiling conditions. The solution was boiled on a hot plate to reduce the volume from 200 mL to 100 mL in about 30 min. After forming 100 mL of a dense solution, followed by a cooling step, dark red precipitate formed with very small particle sizes (5-10 nm). Next, a 10-min 9000 rpm centrifugation was applied to the solution. After centrifugation the supernatant was decanted and 100 mL DI water added and vortexed to re-dissolve the α -Fe₂O₃ in DI water at a dilution of 1:10 v/v. Afterward, the coated glass samples were dried at room temperature.

Before each PP experiment, the α -Fe₂O₃-coated glass slide was first cleaned with DI and ethanol, and then installed in the flow cell. The cleaning process with DI water and ethanol did not substantially remove the α -Fe₂O₃ coating. To ensure the glass substrate was successfully coated with α -Fe₂O₃, the glass before and after the coating process was analyzed via a Cary® 50UV-Vis spectrophotometer (Agilent Technologies, Santa Clara, CA) where the difference in absorbance was attributed to the presence of the α -Fe₂O₃ nanoparticle coating (Figure A.4).

Table A.2. O157:H7 Bacterial Transfer Rate Coefficients (k) for O157:H7 with Full or Partial EPS on Quartz, SRHA-, and α -Fe₂O₃-coated Surfaces.

Collector Surface	Ionic Strength (mM KCl)	EPS	k (m/s)
Quartz	100	Full	$2.54 \times 10^{-8} \pm 2.95 \times 10^{-9}$
Quartz	100	Partial	$1.66 \times 10^{-8} \pm 2.52 \times 10^{-9}$
Quartz	10	Full	$1.20 \times 10^{-8} \pm 4.48 \times 10^{-9}$
Quartz	10	Partial	$2.71 \times 10^{-9} \pm 1.29 \times 10^{-10}$
Quartz	1	Full	$1.58 \times 10^{-8} \pm 3.95 \times 10^{-9}$
Quartz	1	Partial	ND ¹
Quartz SRHA	100	Full	$1.24 \times 10^{-8} \pm 4.93 \times 10^{-10}$
Quartz SRHA	100	Partial	$7.75 \times 10^{-9} \pm 1.24 \times 10^{-9}$
Quartz SRHA	10	Full	$1.19 \times 10^{-8} \pm 2.61 \times 10^{-9}$
Quartz SRHA	10	Partial	$1.08 \times 10^{-9} \pm 5.87 \times 10^{-10}$
Glass iron oxide	100	Full	$3.71 \times 10^{-8} \pm 1.85 \times 10^{-9}$
Glass iron oxide	100	Partial	$1.75 \times 10^{-8} \pm 3.18 \times 10^{-9}$
Glass iron oxide	10	Full	$2.76 \times 10^{-8} \pm 8.51 \times 10^{-10}$
Glass iron oxide	10	Partial	$2.36 \times 10^{-8} \pm 1.86 \times 10^{-9}$

¹ND: No deposition detected.

Table A.3. DLVO interaction energies between *E. coli* O157:H7 and collector surfaces

Energy Barrier Height¹ (<i>kT</i>)						
IS (mM)	O157:H7 with full EPS			O157:H7 with partial EPS		
	quartz	SRHA	α -Fe ₂ O ₃	quartz	SRHA	α -Fe ₂ O ₃
1	5.6	ND	ND	9.77	ND	ND
10	NB ²	NB	NB	NB	NB	NB
100	NB	NB	NB	NB	NB	NB

¹ Energy barrier heights calculated using DLVO theory.³³⁷⁻³³⁸ Hamaker constant used was 6.5×10^{-21} J.³⁹⁹

² NB: no energy barrier.

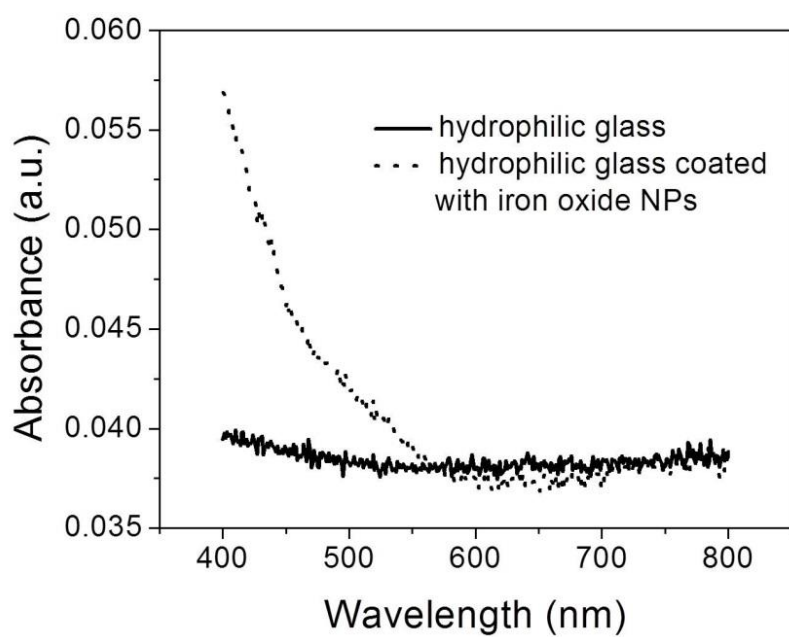


Figure A.4.

Absorbance values of substrates from UV-visible spectroscopy with and without α - Fe_2O_3 coating on glass surface. The trend of increasing absorbance at lower wavelengths is indicative of the α - Fe_2O_3 nanoparticles coating the glass substrate.

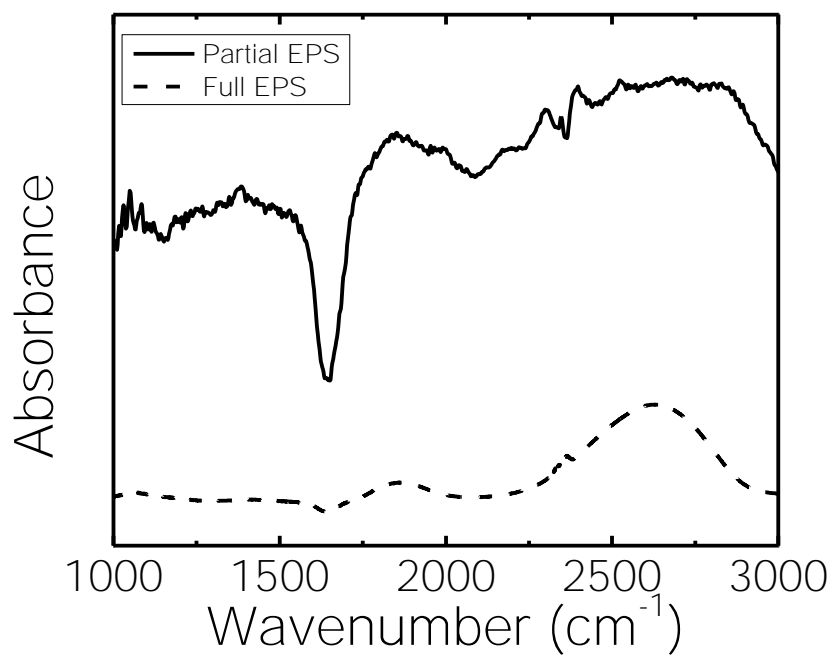


Figure A.5.

Fourier transform infrared spectroscopy (FT-IR) of supernatant from partial and full EPS in *E. coli* 0157: H7. Major functional group removed due to sonication was C=O stretching from proteins (1650 cm⁻¹).

References.

1. (a) Bradford, S. A.; Simunek, J.; Walker, S. L., Transport and straining of E-coli O157 : H7 in saturated porous media. *Water Resources Research* **2006**, *42* (12);
(b) Fratamico, P. M.; Deng, M. Y.; Strobaugh, T. P.; Palumbo, S. A., Construction and characterization of Escherichia coli O157:H7 strains expressing firefly luciferase and green fluorescent protein and their use in survival studies. *Journal of Food Protection* **1997**, *60* (10), 1167-1173.
2. Fratamico, P. M.; Deng, M. Y.; Strobaugh, T. P.; Palumbo, S. A., Construction and characterization of Escherichia coli O157: H7 strains expressing firefly luciferase and green fluorescent protein and their use in survival studies. *Journal of Food Protection*® **1997**, *60* (10), 1167-1173.
3. Gong, A. S.; Bolster, C. H.; Benavides, M.; Walker, S. L., Extraction and analysis of extracellular polymeric substances: Comparison of methods and extracellular polymeric substance levels in Salmonella pullorum SA 1685. *Environmental Engineering Science* **2009**, *26* (10), 1523-1532.
4. Dubois, M.; Gilles, K. A.; Hamilton, J. K.; Rebers, P. A.; Smith, F., Colorimetric method for determination of sugars and related substances. *Analytical Chemistry* **1956**, *28* (3), 350-356.
5. Lowry, O. H.; Rosebrough, N. J.; Farr, A. L.; Randall, R. J., Protein measurement with the Folin phenol reagent. *Journal of Biological Chemistry* **1951**, *193* (1), 265-275.
6. Bolster, C. H.; Haznedaroglu, B. Z.; Walker, S. L., Diversity in Cell Properties and Transport Behavior among 12 Different Environmental Escherichia coli Isolates. *Journal of Environmental Quality* **2009**, *38* (2), 465-472.
7. Pembrey, R. S.; Marshall, K. C.; Schneider, R. P., Cell surface analysis techniques: What do cell preparation protocols do to cell surface properties? *Applied and Environmental Microbiology* **1999**, *65* (7), 2877-2894.
8. Elimelech, M.; Gregory, J.; Jia, X.; Williams, R. A., Particle Deposition and Aggregation: Measurement, Modeling and Simulation. Butterworth-Heinemann: 1995; p 441.

9. Chen, K. L.; Elimelech, M., Interaction of Fullerene (C-60) Nanoparticles with Humic Acid and Alginate Coated Silica Surfaces: Measurements, Mechanisms, and Environmental Implications. *Environmental Science & Technology* **2008**, *42* (20), 7607-7614.
10. Mulvaney, P.; Cooper, R.; Grieser, F.; Meisel, D., Charge trapping in the reductive dissolution of colloidal suspensions of iron (III) oxides. *Langmuir* **1988**, *4* (5), 1206-1211.
11. (a) Derjaguin, B., A theory of interaction of particles in presence of electric double layers and the stability of lyophobic colloids and disperse systems. *Acta Physicochimica Urss* **1939**, *10* (3), 333-346; (b) Verwey, E. J. W., Theory of the stability of lyophobic colloids. *Journal of Physical and Colloid Chemistry* **1947**, *51* (3), 631-636.
12. Redman, J. A.; Walker, S. L.; Elimelech, M., Bacterial adhesion and transport in porous media: Role of the secondary energy minimum. *Environmental Science & Technology* **2004**, *38* (6), 1777-1785.

Appendix B

D-Amino Acids Inhibit Initial Bacterial Adhesion: Thermodynamic Evidence

Reproduced with Permission from Biotechnology & Bioengineering Copyright 2015, John Wiley & Sons, Inc.

Xing, S.F., X.F. Sun, A.A. Taylor, S.L. Walker, Y.F. Wang, and S.G. Wang. Biotechnology & Bioengineering, 2014 (published online ahead of print) DOI: 10.1002/bit.25479

Appendix B: D-Amino Acids Inhibit Initial Bacterial Adhesion: Thermodynamic Evidence

Abstract

Bacterial biofilms are structured communities of cells enclosed in a self-produced hydrated polymeric matrix that can adhere to inert or living surfaces. D-amino acids were previously identified as self-produced compounds that mediate biofilm disassembly by causing the release of the protein component of the polymeric matrix. However, whether exogenous D-amino acids could inhibit initial bacterial adhesion is still unknown. Here, the effect of the exogenous amino acid D-tyrosine on initial bacterial adhesion was determined by combined use of chemical analysis, force spectroscopic measurement, and theoretical predictions. The surface thermodynamic theory demonstrated that the total interaction energy increased with more D-tyrosine, and the contribution of Lewis acid-base interactions relative to the change in the total interaction energy was much greater than the overall nonspecific interactions. Finally, atomic force microscopy (AFM) analysis implied that the hydrogen bond numbers and adhesion forces decreased with the increase in D-tyrosine concentrations. D-tyrosine contributed to the repulsive nature of the cell and ultimately led to the inhibition of bacterial adhesion. This study provides a new way to regulate biofilm formation by manipulating the contents of D-amino acids in natural or engineered systems.

Introduction

Bacterial adhesion to solid surfaces is an important issue in a number of disciplines, ranging from biomedical engineering to wastewater treatment technologies.⁴⁰⁰⁻⁴⁰²

Many microbes naturally grow as biofilms and may have beneficial traits for cleanup of wastewater, off-gas, soils, etc.^{400, 403} They are also known for their ability to convert agriculturally derived materials to products of commercial value such as alcohols and organic acids.⁴⁰⁴ Although certain biofilms can be beneficial, other biofilms pose severe problems, such as the corrosion and obstruction of water pipes or fouling of membranes in filtration systems.⁴⁰⁵⁻⁴⁰⁶ Thus, understanding the mechanism of biofilm formation and effectively regulating its formation and disassembly for human purposes is important for many biotechnology fields.

Biofilms are aggregates of microbes embedded in a matrix of extracellular polymeric substances (EPS), which consist of different types of biopolymers including polysaccharides, proteins, lipids, and extracellular DNA.⁴⁰⁷⁻⁴⁰⁸ Found on almost all types of submerged surfaces, biofilms are a majority of the biomass in natural and engineered systems.⁴⁰⁹⁻⁴¹⁰ During biofilm formation, bacterial adhesion onto abiotic and biotic surfaces is the key determinant in initial cell attachment.⁴¹¹ The physicochemical factors of bacterial cells and the surfaces govern this critical initial step in biofilm formation processes.⁴¹²⁻⁴¹⁴

Biofilm formation requires several physiological and physicochemical steps.⁴¹⁵ Bacterial adhesion has been shown to be a function of the physicochemical and thermodynamic properties of both bacterial surfaces and substrates based on analysis of surface charge and hydrophilicity measurements (i.e., the cell surface free energy); both parameters are significantly influenced by EPS content on bacterial surfaces.⁴¹⁶⁻⁴²⁰ Recently, it has been reported that some molecular signals govern quorum-sensing, which serves as a switching mechanism between successive phases of biofilm development.⁴²¹⁻⁴²² As one of the quorum sensing molecules, self-produced D-amino acids (D-AAAs), can promote biofilm disassembly and reduce microbial attachment.^{400, 406, 423} In natural environments and engineered systems, various species of bacteria interact with each other, with the majority of excreted amino acids in the L-isomer form, with only some bacteria excreting D-AAAs. These excreted D-AAAs may affect other bacterial species in the microbial community and cause biofilm disruption. The precise role of exogenous D-AAAs in the initial bacterial adhesion to substratum surface is not clear yet, and how D-AAAs trigger variations in surface interactions of bacteria still needs to be revealed.

Initial bacterial adhesion is generally determined by the Derjaguin-Landau-Verwey-Overbeek (DLVO) theory, which is expressed as the sum of Lifshitz-van der Waals interactions and electrostatic interactions.⁴²⁴ The classical DLVO theory was projected to describe the stability of colloidal suspensions. It involves the estimation

of the energy from the electrostatic double-layer force and an attractive Lifshitz-van der Waals force (in the case of two identical surfaces). The Lewis acid-base interaction has been added to the DLVO theory (extended DLVO theory, XDLVO) to reconcile the discrepancy between the theoretical prediction and experimental results.⁴²⁵⁻⁴²⁶ In addition to theoretical predictions, experimental studies regarding interactions between bacteria and substrates have been conducted. For instance, atomic force microscopy (AFM) has been utilized for surface adhesion force measurement for bacteria attached to solid substrates.⁴²⁷⁻⁴²⁸ However, the information on bacteria interfacial interactions and the assessment of adhesion forces in the presence of D-AAs is scarce.

This study aims to clarify whether exogenous D-AAs could inhibit the initial bacterial adhesion and to elucidate the interaction forces and energy mechanisms of bacterial adhesion by combining the use of XDLVO predictions and AFM. This work here has characterized the discrepancies of bacterial surface characteristics and the thermodynamic parameters over a range of D-tyrosine concentrations. Here, *Escherichia coli* (*E. coli*) and D-tyrosine were used as the model microbe and D-AAs, respectively. As a typical bacterium of microbial adhesion experiments, *E. coli* cannot produce and release D-AAs⁴²⁹⁻⁴³⁰ and D-tyrosine has potent activity towards biofilm disassembly.⁴²³ The results obtained from this study provide a better understanding of the role of D-tyrosine on bacterial adhesion from a thermodynamic perspective, which

may provide a new way to regulate biofilm formation by manipulating the content of D-AAs in natural or engineered systems.

Materials and Methods

Bacterial Growth and Surface Characteristics

Escherichia coli JM109 was provided by China General Microbiological Culture Collection Center and was used in this study as the test bacterium. Cells were cultured in a standard Luria-Bertani (LB) medium with different concentrations of D-tyrosine (Aladdin; 99%) (0, 10, 25, 50 μ M) at 37°C, 200 rpm, and for 18 h until stationary phase was reached, and then were collected by centrifugation at 5000 g for 15 min. L-tyrosine (Aladdin; 99%) (0, 10, 25, 50 μ M) was used as an additional control. The cells were washed twice using 10 mM KCl (the pH was unadjusted, ranging from 5.4 to 5.8) to remove any residual medium from the bacterial surface. Finally, the cells were resuspended in select solutions for cell surface characterization and adhesion experiments. To confirm the effect of exogenous D-tyrosine on bacterial cell adhesion behaviors, control experiments were conducted using the cells harvested from mineral medium (glucose, 5 g/L; (NH₄)₂SO₄, 2g/L; MgSO₄· 7H₂O, 0.2 g/L; K₂HPO₄, 4g/L; KH₂PO, 4.6 g/L; sodium citrate, 1 g/L; pH = 7.2) with different concentrations of L-

tyrosine or D-tyrosine (0, 10, 25, 50 μM) respectively. Each data point is composed of three independent samples.

Bacteria mass was described as the dry weight, and the optical density (OD_{600}) of the washed bacterial suspension was measured as absorbance by the spectrophotometer (UV-2000, Unic, Shanghai, China) at 600 nm in all the experiments. All chemical reagents in this study were of analytical grade.

Electrophoretic mobility (EPM) was measured by the ZetaSizer 3000HSA (Malvern, England) and repeated at least five times at 25°C. Zeta potential (ζ potential) was calculated in a 10 mM KCl solution via EPM using the Helmholtz-Smoluchowski equation.⁴³¹ EPS was extracted by the cation exchange resin technique (CER).⁴³² After filtrating through 0.22- μm cellulose acetate membranes, the supernatant was used as the EPS fraction for chemical analyses. Polysaccharides and proteins were determined by the anthrone-sulfuric³⁹³ and Lowery methods⁴³³, respectively. Glucose and bovine serum albumin were used as the standards. These processes were performed in duplicate and each data point is composed of three independent samples.

The hydrophilicity of bacteria was measured as the microbial adhesion to hydrocarbon (MATH) test (the percent of total cells partitioned into *n*-dodecane).³⁵⁰

⁴³⁴ In brief, 1 mL of *n*-dodecane (analysis grade) was added to 4 mL of a cell suspension, which was then mixed for 2 min with a vortex. The suspension was then

allowed to separate for 15 min at room temperature. The percentage of bacteria partitioning into the hydrocarbon phase was calculated after the optical density of the suspension in the water phase was measured at 600 nm. All experiments were conducted in triplicate.

The contact angle was calculated by a contact angle meter (JC2000C, Shanghai, China), which was used to evaluate interfacial tension and surface energy. Prior to the measurement, the prepared acetate cellulose membrane membranes were air-dried for 45 min. To measure contact angles of *E. coli*, the bacterial layer was prepared on a 0.22- μm acetate cellulose membrane by adding 10 mL of cell suspension ($\text{OD}_{600} = 1.0$), and then placed on a 1% agar plate for cell preservation before measurement. The contact angles were measured using the sessile drop technique with a drop of purified water ($\gamma^{LW} = 21.8$ and $\gamma^+ = \gamma^- = 25.5$ mJ/m^2), formamide ($\gamma^{LW} = 39.0$, $\gamma^+ = 2.3$ and $\gamma^- = 39.6$ mJ/m^2), and diiodomethane ($\gamma^{LW} = 50.8$ and $\gamma^+ = \gamma^- = 0$ mJ/m^2)⁴³⁵. Each measurement was made on at least ten droplets at different locations on the bacterial layer for each of the three liquids, which was used to calculate standard deviations. The other measurements are described in detail in the supplemental material.

Quartz Sand Treatment

Ultrapure quartz sand with a 1 mm diameter (Aladdin, $\geq 99\%$) was used as the collector surface for bacterial adherence. The sand was thoroughly immersed in 12 N HCl for at least 24 h, cleaned by deionized water, and then baked at 800°C for approximately 6 h to remove the organic substances on the surface. To increase the bacterial cells adhesion onto the quartz sands, the cleaned quartz sand was chemically modified with 4% (v/v) γ -aminopropyltriethoxysilane (APTES) (Aladdin; $\geq 99\%$) in acetone at 45°C for 24 h, then cleaned by soaking first in acetone, followed by a thorough rinsing with deionized water, and finally air-dried. Zeta potential of quartz sand was determined by an electrokinetic analyzer (Anton Paar SurPASS, Austria).

Cell adhesion and desorption experiments

The influence of D-tyrosine or L-tyrosine on cell adhesion to quartz sands was evaluated by batch adhesion experiments with *E. coli* harvested from growth media (LB and mineral medium) with different L-isomer or D-isomer tyrosine concentrations (0, 10, 25, 50 μM). The experiments were conducted by adding 10 g of sand into 50 mL glass bottles with 10 mL of cell solution, and then gently vibrating

with a shaker (8 rpm) for 3 h to reach equilibrium, based on the result of preliminary experiments.

The bacteria adhered on the collector surface irreversibly, and was washed by a 0.1 mM KCl solution after rinsing with the background solutions (10 mM KCl). The experiments were conducted with the washed quartz sands after the cell adhesion tests, and the sands were gently vibrated with shaker for 3 h to determine the desorption efficiency. The cell adhesion and desorption tests were conducted according to the methods provided in the SI.

AFM Measurements

Silicon wafers were used as the substrates for AFM measurements, and were treated with ultrapure water: hydrogen peroxide: ammonia water (1:3:1) for at least 15 min after cleaning with sonication in ultrapure water and ethanol, and were then immersed in a 25% sodium hydroxide solution for at least 24 h. After cleaning with ethanol and ultrapure water, the wafers were soaked in 1% APTES for 2 h to be silanized. The amino-functionalized wafers were cleaned by ultrapure water to remove the excess saline, and finally the silanized substrates were kept in 120°C for 15 min. Before and after making the AFM measurements on the bacteria, force measurements were made on a bacteria-free area of silicon wafers, to ensure that the tip had not been

contaminated by contacting the bacteria layer on the silica wafers. The spring constant (k) for the tips was 0.15 ± 0.02 nN/nm; tips were calibrated before each experiment by the equipment.

The cells used for AFM measurements were stirred in 2.5% v/v glutaraldehyde for 2 h at 4°C. The glutaraldehyde does not affect the physiochemical properties of the *E. coli* cells, but provides a method for ensuring no movement of the cells during measurements.⁴¹¹ Prior to the AFM experiments, a drop of the bacteria suspension (20 μ L) was deposited onto the silanized silicon slides and left to settle at room temperature for 20 min. The bacteria-coated slide was rinsed with sterile water to remove any weakly bounded bacteria and air dried before measuring the same day.

All AFM measurements were performed at room temperature using a scanning probe microscope (Veeco Instruments Inc., USA) with Si₃N₄ cantilevers (SDL-A, Bruker AXS Inc.). This microscope had a dimension icon controller and extender module. The tip elements are showed in the supplemental material. In this study, five cells were examined from each medium. And on each cell, 15 points were located to perform AFM measurements. AFM images were acquired by using the Scan Asyst Mode, while the force-distance curves were evaluated by tipping mode. The adhesion forces were calculated from the retraction curves which represented the sum of all interaction forces (specific and nonspecific) between the bacterial surface and the

silicon nitride tips. The specific and nonspecific forces were measured by the Poisson analysis of adhesion forces (MATLAB, Natick, MA, USA).⁴²⁷

Extended DLVO (XDLVO) Profiles

According to the XDLVO approach, the total energy of interaction (W^{TOT}) between spherical particles (bacteria) and an infinite planar surface can be calculated by the sum of electrostatic interactions (W^{EL}), Lifshitz-van der Waals interactions (W^{LW}), and Lewis acid-base interactions (W^{AB}).

$$W_{TOT} = W^{EL} + W^{AB} + W^{LW} \quad (3)$$

$$W^{LW} = \frac{2\pi\Delta G^{LW} R}{h} \quad (4)$$

$$W^{EL} = \pi\epsilon R(2\zeta_B\zeta_G \ln\left(\frac{1+e^{-\kappa h}}{1-e^{-\kappa h}}\right) + (\zeta_G^2 + \zeta_B^2) \ln(1-e^{-2\kappa h})) \quad (5)$$

$$W^{AB} = 2\pi R\lambda\Delta G^{AB} e^{-\frac{y_0-h}{\lambda}} \quad (6)$$

where, ζ_B and ζ_G are the zeta potential of bacteria surfaces (B) and quartz sands (G), respectively. Due to Born repulsion, y_0 , the minimum equilibrium cut-off distance between bacterial cells and the collector, equals 0.157 nm in previous work.⁴²⁴ R is the cell radius, and h is the separation distance between the cell and the solid surface. κ is defined as the Debye length or the "thickness" of the double layers and can be estimated by ionic strength and the concentration of background solution. λ is typically between 0.2~1 nm, and is used as 0.6 nm in this work, which is a

characteristic decay length of Lewis acid-base interactions in solution. The other parameters in these formulas have been described in supplemental material in details.

Statistical Analysis

In the figures and tables, data are presented along with error bars associated with one standard deviation. Statistical differences between mean values were analyzed using a student t test.

Results

Cell Adhesion and Desorption Tests

To evaluate the effect of D-tyrosine on the growth of *E. coli*, the bacteria cells cultivated from LB media with different concentrations of D-tyrosine (0, 10, 25, 50 μM) for at least 24 hours, and the biomass at different time point were determined by optical density. The growth curves indicated that D-tyrosine did not inhibit bacterial growth (Figure B.6, note: Figures B.6-B.9 are located in the SI at the end of Appendix B), which is consistent with previous report (Kolodkin-Gal et al. 2010).

The adhesion tests revealed changes in *E. coli* adhesion behavior over the range of D-tyrosine concentrations (Figure B.1). It is evident that the adhesion rates decreased sharply from 26.3% to 10.0% with an increase in the D-tyrosine

concentration from 0 to 25 μM . Above 25 μM D-tyrosine, there was no measurable cell adhesion (8.8%) (Figure B.1a). Therefore, the existence of D-tyrosine has an obvious effect on microbial adhesion ($p < 0.05$). Moreover, the desorption rate increased from 43% to 100% based on the adhered bacteria over the range of D-tyrosine concentrations (Figure B.1a); the amount of irreversibly adhered cells decreased from 14.7% to 0%. Nevertheless, there was no significant difference for adhesion and desorption efficiency among the cells grown in the presence of L-tyrosine with different concentrations (Figure B.1b). This result shows that D-tyrosine has a significant effect on bacterial adhesion ($p < 0.05$).

In order to identify whether there was any effect of exogenous D-AAS on cells in the LB broth, further experiments with *E. coli* cells harvested from mineral medium with D-tyrosine or L-tyrosine (0, 10, 25, 50 μM) were conducted (Figure B.7). The results indicated that D-tyrosine could affect microbial adhesion even in a chemically defined medium.

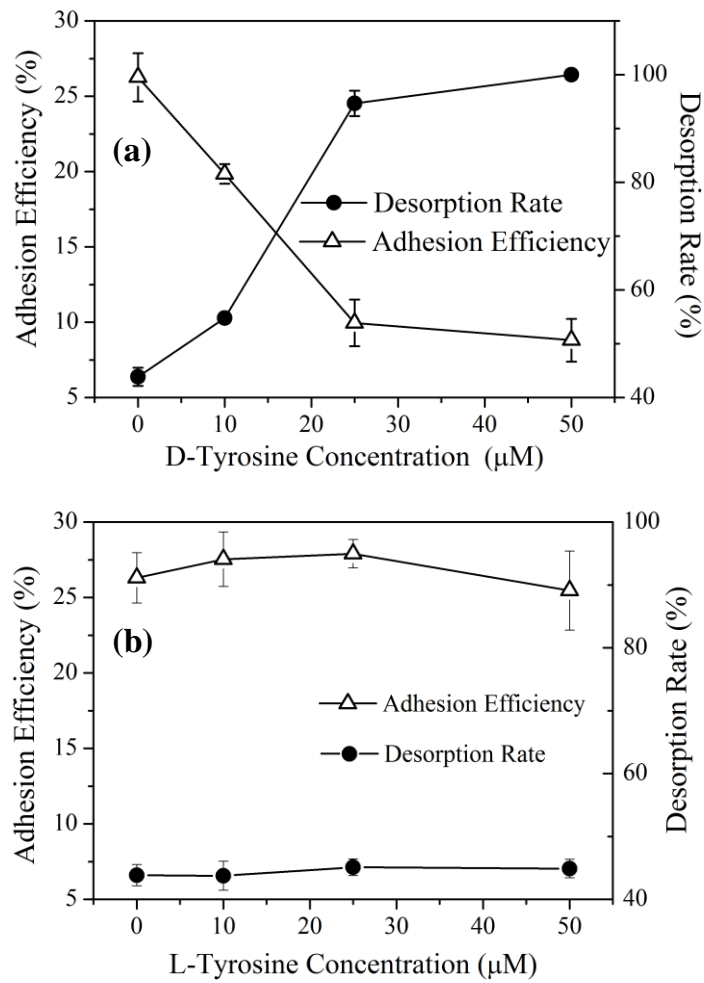


Figure B.1

Adhesion efficiency and desorption rate of *E. coli* onto a quartz collector surface, determined as a function of D-Tyrosine (a), and L-Tyrosine (b). Experiments were conducted at unadjusted pH (5.4-5.8), room temperature (25°C), and with bacteria cultivated from LB media with different concentrations of D-tyrosine. Error bars represent standard errors of the means.

The above results demonstrate that bacteria exposed to D-tyrosine exhibited poor adhesion ability. The bacterial adhesion is attributed to the concurrent existence of deposition, as well as irreversible and reversible adhesion. In this study, the deposition could be neglected since the desorption rate of bacteria with 50 μM D-tyrosine was nearly 100%. As to the bacteria without D-tyrosine, almost 40% of the adhered bacteria were detached under lower ionic strength solution, indicating that the bulk of the adhered microbes are reversibly bound. When cultivated at the high D-tyrosine concentration, the fraction of the reversibly adhered bacteria increased as the D-tyrosine concentration increased ($p < 0.05$), showing a higher reversibility for the cells (Figure B.1a).

Influence of D-tyrosine on Surface Properties of E. coli Cells

To better understand the effect of D-tyrosine on bacterial adhesion behavior, the extracellular polysaccharide and protein contents of bacteria were determined (Figure B.2). Compared with the cells that were not exposed to D-tyrosine, a decrease ($p < 0.05$) in protein was observed for the bacteria cultured with D-tyrosine. However there was only slight difference in protein of cells grown with different D-tyrosine concentrations. For polysaccharide it was less sensitive to changes ($p > 0.05$) with D-

tyrosine concentrations. This result indicated that D-tyrosine most likely inhibited protein secretion.

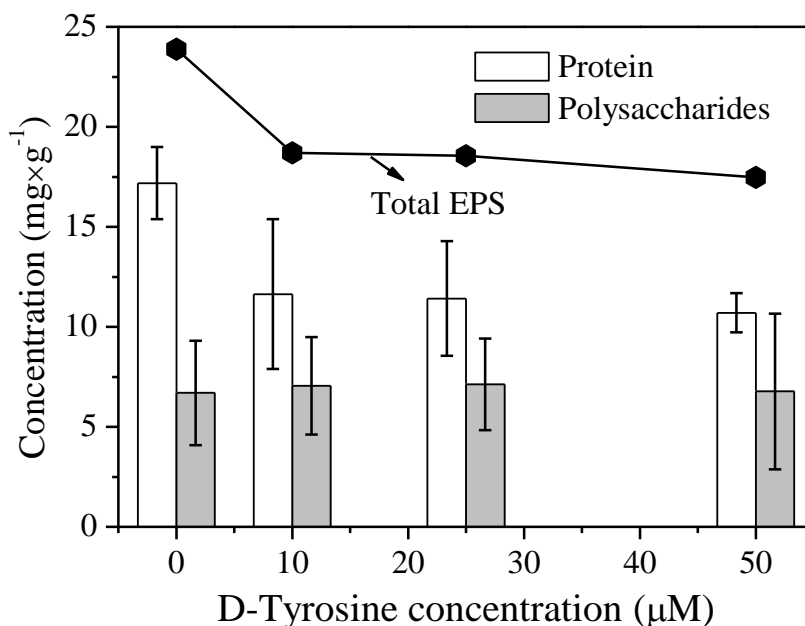


Figure B.2

The content of total EPS, polysaccharides, and proteins of the *E. coli* cells from LB media with different D-Tyrosine concentrations (0, 10, 25, 50 μM). Error bars represent standard errors of the means.

As indicated by the measured zeta potential (Figure B.3), all the *E. coli* cells used in this study were negatively charged, while the quartz sand modified with amino-silane was positively charged under the experimental conditions. The electrostatic interaction between bacteria and sand was attractive, which contributed to bacteria adhesion. Over the range of D-tyrosine concentrations, the absolute

magnitude of the cell zeta potential increased (from 30.0 mV to 43.6 mV) with the increase in D-tyrosine concentration.

The hydrophobicity of *E. coli* cells from experiments with different concentrations of D-tyrosine (Figure B.3) showed that the surface hydrophobicity decreased from 23.7% to approximately 12.0%, as the D-tyrosine concentration increased, which is consistent with zeta potential results. The result of relative hydrophobicity is also in consistency with that of water contact angles test (Figure B.8). The more negative surface potential denotes that the increased fractions of polar functional groups led to a more hydrophilic bacteria surface.⁴³⁶ In addition, the relative low EPS content was responsible for high hydrophilicity at high D-tyrosine concentrations.^{420, 437}

XDLVO Interaction Energy Profiles between E. coli cells and Sand

The XDLVO theory prediction was applied to evaluate the interaction energy between cells and the quartz sand (Figure B.4), which were consistent with the bacterial adhesion experimental data for *E. coli* cells. With an increase in D-tyrosine concentration, the height of the repulsive energy barrier between cells and the quartz sand exhibited a significant change ($p < 0.05$) (from 24.5 kT to 3328.4 kT). No energy barrier for microbial adhesion (i.e., completely favorable condition) in the absence of

D-tyrosine was observed. A higher energy barrier means a more stable suspension.

Hence, it was difficult for the bacteria exposed to D-tyrosine to attach to surfaces

In addition, secondary energy minima in the interaction energy predictions illustrate the desorption ability of microbial cells from collector surfaces.⁴³⁸ The values of the secondary energy minima and positions are summarized in Table B.2 (located in SI at the end of Appendix B). The percentage of bacteria (cultivated in 10 μM D-tyrosine) reversibly adhering on the collector was 11.5% when the depth of secondary energy minimum was -114.5 kT at the separation distance of 1.6 nm (Table B.2). However, when a secondary energy minimum of -54.7 kT existed at 2.9 nm, 9.4% of adhered cells were reversibly attached in 25 μM D-tyrosine. These results indicate that the shallower secondary energy minimum caused a decrease in the reversible attachment onto the surface and promoted the detachment from the surface.

As part of the total interaction energy, W^{AB} , W^{LW} and W^{EL} values for *E. coli* as a function of distance between bacteria and sands were determined (Figure B.5). The Lifshitz-van der Waals interactions (W^{LW}) were attractive and nearly identical, while the absolute values of attractive electrostatic interactions (W^{EL}) were variable with an increase in D-tyrosine concentration. However, Lewis acid-base interactions were attractive without D-tyrosine (favorable conditions for adhesion). With increasing D-tyrosine concentrations, Lewis acid-base interactions turned repulsive and the

absolute values increased. Therefore, the contribution of W^{AB} to the total energy was very significant.

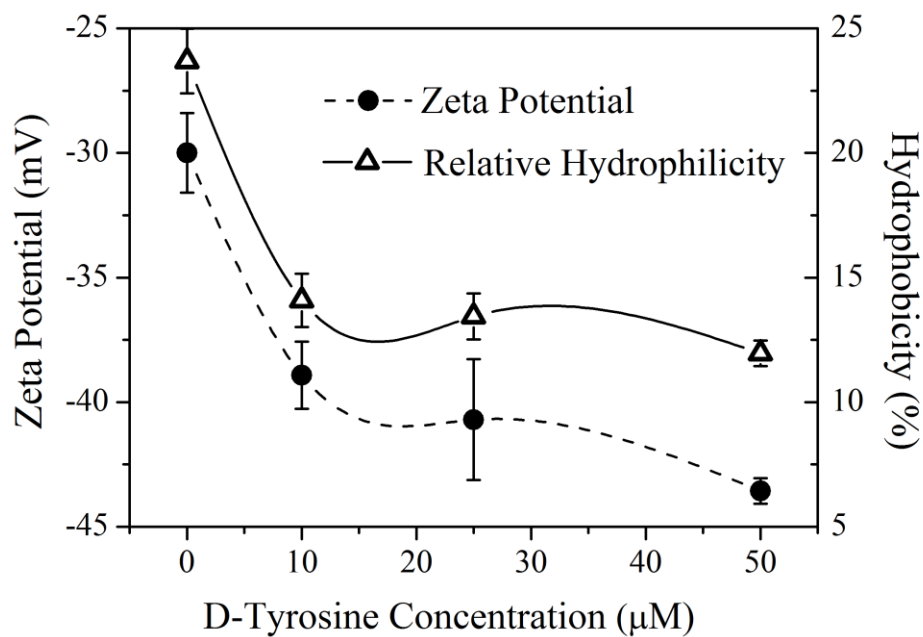


Figure B.3

The relative hydrophobicity and zeta potential values of *E. coli* cells as a function of D-Tyrosine concentration (0, 10, 25, 50 µM) in LB media. All experiments were conducted at unadjusted pH and room temperature. Error bars represent standard errors of the means.

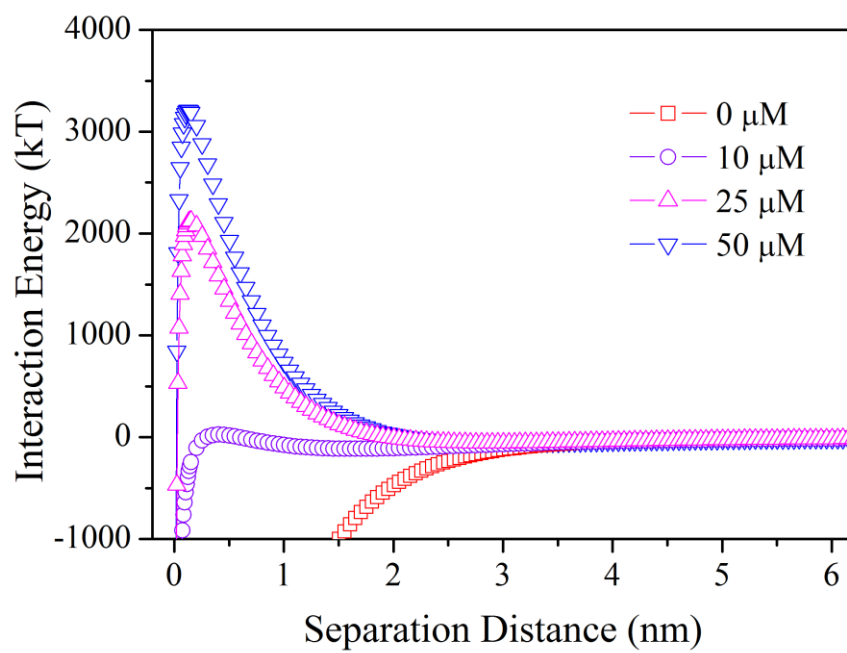


Figure B.4

Total interaction energy profiles as a function of separation distance for *E. coli* cells grown under a range of D-Tyrosine concentrations, suspended in 10 mM KCl.

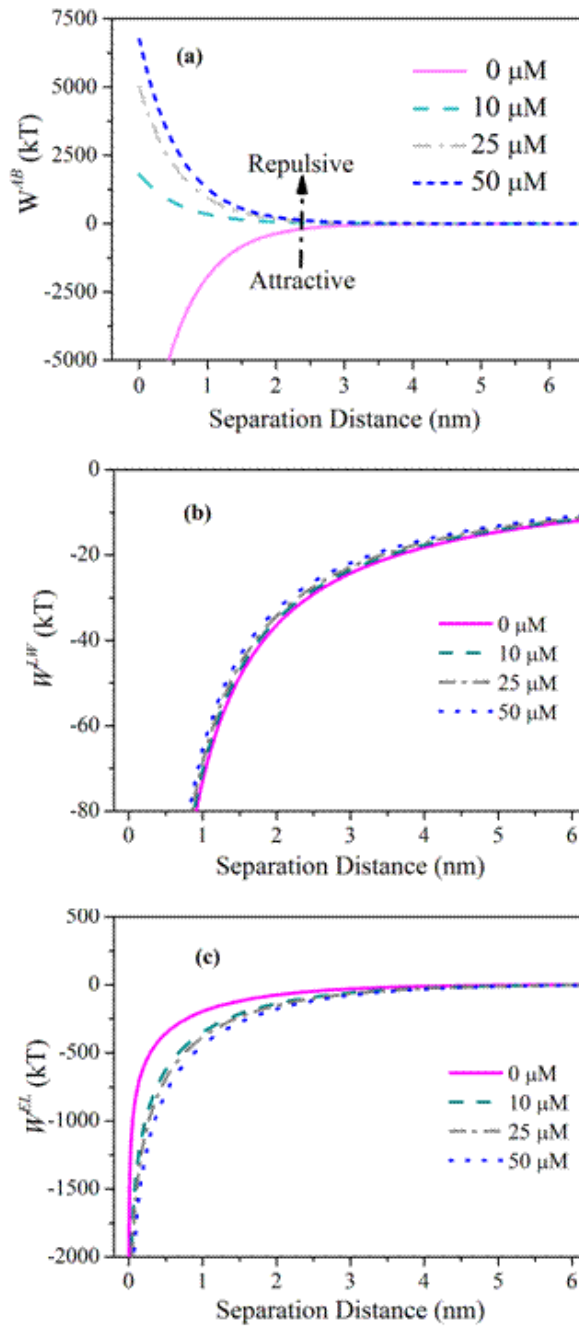


Figure B.5

Contribution of W^{AB} (a), W^{LW} (b) and W^{EL} (c) on the total interaction energy between *E. coli* cells and quartz sand exposed to different D-Tyrosine concentrations, which adhered on quartz sands in 10 mM KCl at uncontrolled pH values.

Probing the Adhesion Force with AFM

Since the Lewis acid-base interaction energy plays the most important role on inhibiting bacterial adhesion in the presence of D-tyrosine, it is indicated that the acid-base interaction including hydrophobic interaction and hydration effects, which are mainly electron-donor/electron-accepter interaction.⁴⁰⁵ The chemical bonds on the AFM tips are mainly O-H and Si-N, while the bonds on modified quartz surface O-H, Si-N, N-H, etc. The tips and modified quartz would form the similar bonds with the bacteria surface. Therefore, here we used AFM to quantitatively probe the adhesion force between bacteria and quartz sands. The shape and size of bacteria were assessed by AFM scans (see Figure B.9) and implied that D-tyrosine did not affect their morphology. In addition to topographic imaging, AFM force-distances were used to determine interactions between the silicon nitride probe and bacteria surface in the air. The retraction curves were variable, since the adhesion force or “liftoff” (the point where the tips break free of tip-sample interaction) was observed (Table B.1). The magnitude of the interaction forces was highly dependent on D-tyrosine concentration, which decreased from 61.8 nN to 28.1 nN. As shown in Table B.1, the adhesion force decreased sharply ($p < 0.05$) compared with that without D-tyrosine, while this adhesion force varied slightly ($p > 0.1$) in the presence of D-tyrosine.

The total separation energy is estimated as the total area of the attraction-force region in the retraction force by eq. 7 and these parameters obtained from the retraction curves are presented in Table B.1:

$$E_S = \sum_{i=1}^a IF_{s,i} = -\sum_{i=1}^a Ik_c d_{d,i} \quad (7)$$

in which, I is the distance (nm) moved by the cantilever in every interval, $F_{s,i}$ is the separation force, k_c is the spring constant (nN/nm) and the distance is $d_{d,i}$ (nm).

Table B.1 Results from the AFM force-distance curve over the range of D-Tyrosine concentrations

Parameters	0 μM	10 μM	25 μM	50 μM
Adhesion Force (nN)	61.8	40.2	33.5	28.1
Nonspecific Forces (nN)	-45.8	-40.5	-28.6	-17.5
Specific Forces (nN)	0.9	1.0	2.1	3.3
Separation Energy ($\times 10^{-18}$ J)	8479.2	3189.8	1452.8	1689.3
Hydrogen Bands Numbers	847919	318985	145275	168928

By using Poisson statistical analyses, nonspecific (i.e., Lifshitz-van der Waals force and electrostatic forces) and specific forces (i.e., Lewis acids-base interaction force) of the adhesion forces were quantified through linear regression (Table B.1).

The results illustrated that the nonspecific and specific forces decreased over the

range of D-tyrosine concentrations. The nonspecific forces were attractive for all conditions investigated, while the specific forces were repulsive for the cells cultured with D-tyrosine acids. On average, the nonspecific forces were stronger than the specific forces; meanwhile, 61.8% of nonspecific forces decreased and the specific forces increased from 0.9 to 3.3 nN.

The maximum energy of the original microbial cells was about 8500×10^{-18} J and the adhesion energy decreased sharply ($p < 0.05$) for the bacteria cultured in the presence of D-tyrosine (Table B.1). Consequently, the hydrogen bond numbers which equaled the adhesion energy divided by the value of *Gabbis* energy (10^{-20}) were reduced.⁴³⁹

Discussion

The experimental and theoretical results show that the interaction energies of bacterial cells changed significantly ($p < 0.05$) in the presence of D-tyrosine. These results also demonstrate the crucial role of D-tyrosine in inhibition of the initial bacterial adhesion.

Influence of Total Interaction Energy on Bacterial Adhesion Behavior

It has been recognized that a two-step mechanism of bacterial attachment to surfaces is involved in biofilm formation.⁴²⁷ The first step involves long-range nonspecific interactions such as Lifshitz-van der Waals and electrostatic interactions, as described by XDLVO theory. The second step is described as irreversible bacterial adhesion, due to much stronger specific short-range interactions (hydrogen bonds between cell and surface and/or EPS and surfaces, capillary forces, etc.) which could be interpreted as Lewis acid-base interactions (calculated in XDLVO theory) and polymer interactions.⁴⁴⁰

The total interaction energy for *E. coli* cells (Figure B.4) indicates that D-tyrosine had a negative contribution to bacterial adhesion and inhibited irreversible adhesion. This was confirmed by the adhesion and desorption tests (Figure B.1). Additionally, the depth of the secondary energy minima above the separation distances may determine the adhesion and desorption rates for cells. Reversible adhesion was reduced with the decrease of the depth of secondary energy minimum because of D-tyrosine concentration variations (see Table B.2).

The AFM measurement also indicated a decreased adhesion rate in the presence of D-tyrosine, which was consistent with above results. The quantification of specific and nonspecific forces revealed decreasing attractive nonspecific forces

performed the reversible adhesion, and the increasing specific forces inhabited the irreversible adhesion. This quantitative analysis enabled us to further understand the micro-scale mechanisms behind D-tyrosine-inhibited bacterial adhesion.

Contribution of W^{AB} , W^{LW} and W^{EL} to Bacterial Adhesion

The Hamaker constant, proportional to the Lifshitz-van der Waals interactions, is a parameter that describes the strength of the interaction between bacteria and surface. The discrepancy of effective Hamaker constants is nearly non-existent ($p > 0.1$) (see Table B.2), causing a slight decrease of the Lifshitz-van der Waals interaction energy with an increase of D-tyrosine. For the surface covered by layers that contain larger quantities water, the effective Hamaker constant was reduced,⁴⁴¹ which was consistent with the trend of cell surface hydrophobicity. Moreover, the intensity of the attractive Lifshitz-van der Waals interactions decayed slowly with the interaction distance and became zero for distances of about 10 nm (Figure B.5b). Furthermore, the zeta potential of bacterial cells increased ($p < 0.05$) (i.e., more negative) as D-tyrosine concentration increased, which should enhance the attractive electrostatic interaction force. However, with increasing D-tyrosine concentrations, the electrostatic interactions decay more slowly with the separation distance, due to the more negative zeta potentials (Figure B.5c). The resulting profile showed that the Lifshitz-van der

Waals interactions play a more important role than the electrostatic interactions in bacterial reversible adhesion, because the former are longer range.

Although W^{LW} and W^{EL} were identical and not sensitive to D-tyrosine concentration variations, the contribution of W^{AB} to the total interaction energy is flexible (Figure B.5). As the dominant interaction energy (Figure B.5a), W^{AB} interaction energy increased substantially ($p < 0.05$) with the increasing D-tyrosine concentration (over 0 μM), indicating that D-tyrosine reduced bacterial adhesion by preventing bacteria from approaching the surface at sufficiently close distances. The higher intensity of the Lewis acid-base interactions decays with longer interacting distances with the increasing D-tyrosine concentrations. After comprehensive analysis for those interaction energies, the cell surface hydrophilicity appears to be responsible for the change of energy barriers as well as primary and secondary energy minima observed for all the *E. coli* cells.

Influence of EPS on Adhesion Behavior

EPS are the bridge between the cell and collector surfaces to overcome the energy barrier, causing the bacteria to adhere to the surface irreversibly.^{405, 442} In our study, the EPS production decreased in the presence of D-tyrosine. Consequently, the reduction of EPS may directly cause decreased bacterial adhesion. A previous report

illustrated that high exopolymer production of *Sphingomonas paucimobilis* was quite beneficial to bacterial adhesion by overcoming the energy barrier of ~ 300 kT.⁴⁰⁵ The percentage of irreversibly adhered bacteria was 14.7% in 10 μ M D-tyrosine, whereas, for the bacteria in 25 and 50 μ M D-tyrosine, the energy barriers were much higher, and the irreversibly adhered bacteria were nonexistent (0.5% and 0%). This observed behavior is consistent with those reported previously on EPS.³⁷⁹

Role of Hydrogen Bonds in Adhesion Behavior

The hydrogen bonds are also important for the bacterial adhesion behaviors, and are mainly responsible for the Lewis base-acids interactions.⁴⁴¹ The results of cell surface hydrophobicity showed a strong electron donating potential with high γ^- and small electron acceptor ability (the value of γ^+ is almost 0) (data not shown), which was the same as quartz sand. The increased hydrophobic interactions (divided into Lifshitz-van der Waals and Lewis acid-base components), would be attributed to the stronger hydrogen bonding between bacterial surfaces and the experimental solutions with increasing D-tyrosine concentrations. This prevented bacterial adhesion. Additionally, the sand surface contains hydroxyl and amine groups that have the ability to donate and accept protons, respectively.⁴⁴³ Thus, a competition between the water and bacterial cells for hydrogen bond sites on the collector surface would occur. The

amide carbonyl oxygen found on the surface of the EPS acted as stronger electron donors for the hydroxyl groups on quartz sand, while the hydroxyl groups of the EPS offered sites for forming hydrogen bonds with amine groups on the quartz sand.⁴³⁷ This led to the preferential adhesion of bacteria onto the quartz sand.

With the decreasing amount of EPS, the reduction in hydrogen bonds (Table B.1) may be responsible for the poor bacterial adhesion. This result was consistent with the AFM analysis suggesting hydrogen bonds between the bacteria and quartz sand. Nearly 80% of the hydrogen bonds decreased with the increase in D-tyrosine concentrations from 0 to 50 μM . This provided evidence that hydrogen bonds were the key factors affecting bacterial adhesion.

Furthermore, a decrease in bacterial adhesion was also influenced by the detaching behavior demonstrated by AFM measurements. The forces measured by AFM were comprised of DLVO forces (Lifshitz-van der Waals and electrostatic interaction) and non-DLVO forces (Lewis acid-base interaction, steric interaction, etc.). The decrease in EPS excretion and Lifshitz-van-der Waals interactions will reduce the adhesion force (Table B.1). Consequently, bacteria on the surface tended to detach from quartz sand (Figure B.1). The experimental and theoretical results indicated that significant increases in hydrophilicity and decreases in hydrogen bond numbers (i.e., decreased EPS excretions) resulted in a significant decrease in the bacterial attachment efficiency.

Conclusions

In this study the effect of the exogenous amino acid D-tyrosine on initial bacterial adhesion was systematically investigated from a thermodynamic point of view. The total interaction energy increased with more D-tyrosine, and the contribution of Lewis acid-base interactions relative to the change in the total interaction energy was much greater than the overall nonspecific interactions. The hydrogen bond numbers and adhesion forces decreased with the increase in D-tyrosine concentrations. It was revealed that D-tyrosine contributed to the repulsive nature of the cell and ultimately led to the inhibition of bacterial adhesion

References

1. Xu, H.; Liu, Y., Reduced microbial attachment by D-amino acid-inhibited AI-2 and EPS production. *Water Research* **2011**, *45* (17), 5796-5804.
2. Hall-Stoodley, L.; Costerton, J. W.; Stoodley, P., Bacterial biofilms: from the Natural environment to infectious diseases. *Nature Reviews Microbiology* **2004**, *2* (2), 95-108.
3. Costerton, J. W.; Stewart, P. S.; Greenberg, E. P., Bacterial biofilms: A common cause of persistent infections. *Science* **1999**, *284* (5418), 1318-1322.
4. Ralebitso-Senior, T. K.; Senior, E.; Di Felice, R.; Jarvis, K., Waste gas biofiltration: Advances and limitations of current approaches in microbiology. *Environmental Science & Technology* **2012**, *46* (16), 8542-8573.
5. Rosche, B.; Li, X. Z.; Hauer, B.; Schmid, A.; Buehler, K., Microbial biofilms: a concept for industrial catalysis? *Trends in biotechnology* **2009**, *27* (11), 636-643.
6. Hori, K.; Matsumoto, S., Bacterial adhesion: From mechanism to control. *Biochemical Engineering Journal* **2010**, *48* (3), 424-434.
7. Xu, H.; Liu, Y., D-amino acid mitigated membrane biofouling and promoted biofilm detachment. *Journal of Membrane Science* **2011**, *376* (1-2), 266-274.
8. Flemming, H. C.; Wingender, J., The biofilm matrix. *Nature Reviews Microbiology* **2010**, *8* (9), 623-633.
9. Pope, P. B.; Totsika, M.; Aguirre de Carcer, D.; Schembri, M. A.; Morrison, M., Muramidases found in the foregut microbiome of the Tammar wallaby can direct cell aggregation and biofilm formation. *ISME J* **2011**, *5* (2), 341-350.
10. Lee, W. H.; Wahman, D. G.; Bishop, P. L.; Pressman, J. G., Free chlorine and monochloramine application to nitrifying biofilm: Comparison of biofilm penetration, activity, and viability. *Environmental Science & Technology* **2011**, *45* (4), 1412-1419.
11. Peulen, T. O.; Wilkinson, K. J., Diffusion of nanoparticles in a biofilm. *Environmental Science & Technology* **2011**, *45* (8), 3367-3373.

12. Razatos, A.; Ong, Y. L.; Sharma, M. M.; Georgiou, G., Molecular determinants of bacterial adhesion monitored by atomic force microscopy. *Proceedings of the National Academy of Sciences of the United States of America* **1998**, *95* (19), 11059-11064.
13. Nielsen, L.; Li, X.; Halverson, L. J., Cell–cell and cell–surface interactions mediated by cellulose and a novel exopolysaccharide contribute to *Pseudomonas putida* biofilm formation and fitness under water-limiting conditions. *Environmental Microbiology* **2011**, *13* (5), 1342-1356.
14. Lutterodt, G.; Basnet, M.; Foppen, J. W. A.; Uhlenbrook, S., The effect of surface characteristics on the transport of multiple *Escherichia coli* isolates in large scale columns of quartz sand. *Water Research* **2009**, *43* (3), 595-604.
15. Herzberg, M.; Elimelech, M., Physiology and genetic traits of reverse osmosis membrane biofilms: a case study with *Pseudomonas aeruginosa*. *ISME J* **2007**, *2* (2), 180-194.
16. Bos, R.; Mei, H. C.; Busscher, H. J., Physico-chemistry of initial microbial adhesive interactions–its mechanisms and methods for study. *FEMS microbiology reviews* **1999**, *23* (2), 179-230.
17. Sheng, G. P.; Yu, H. Q.; Li, X. Y., Extracellular polymeric substances (EPS) of microbial aggregates in biological wastewater treatment systems: A review. *Biotechnol. Adv.* **2010**, *28* (6), 882-894.
18. Harvey, R. W.; Metge, D. W.; Mohanram, A.; Gao, X.; Chorover, J., Differential effects of dissolved organic carbon upon re-entrainment and surface properties of groundwater bacteria and bacteria-sized microspheres during transport through a contaminated, sandy aquifer. *Environmental Science & Technology* **2011**, *45* (8), 3252-3259.
19. Terada, A.; Okuyama, K.; Nishikawa, M.; Tsuneda, S.; Hosomi, M., The effect of surface charge property on *Escherichia coli* initial adhesion and subsequent biofilm formation. *Biotechnology and Bioengineering* **2012**, *109* (7), 1745-1754.
20. Wang, L. L.; Wang, L. F.; Ren, X. M.; Ye, X. D.; Li, W. W.; Yuan, S. J.; Sun, M.; Sheng, G. P.; Yu, H. Q.; Wang, X. K., pH dependence of structure and surface properties of microbial EPS. *Environmental Science & Technology* **2012**, *46* (2), 737-744.

21. Sheng, G. P.; Yu, H. Q., Relationship between the extracellular polymeric substances and surface characteristics of *Rhodopseudomonas acidophila*. *Appl Microbiol Biotechnol* **2006**, 72 (1), 126-131.
22. Davies, D. G.; Parsek, M. R.; Pearson, J. P.; Iglewski, B. H.; Costerton, J.; Greenberg, E., The involvement of cell-to-cell signals in the development of a bacterial biofilm. *Science* **1998**, 280 (5361), 295-298.
23. McDougald, D.; Rice, S. A.; Barraud, N.; Steinberg, P. D.; Kjelleberg, S., Should we stay or should we go: Mechanisms and ecological consequences for biofilm dispersal. *Nature Reviews Microbiology* **2012**, 10 (1), 39-50.
24. Kolodkin-Gal, I.; Romero, D.; Cao, S.; Clardy, J.; Kolter, R.; Losick, R., D-amino acids trigger biofilm disassembly. *Science* **2010**, 328 (5978), 627-629.
25. Feriancikova, L.; Bardy, S. L.; Wang, L.; Li, J.; Xu, S., Effects of Outer Membrane Protein TolC on the Transport of *Escherichia coli* within Saturated Quartz Sands. *Environmental Science & Technology* **2013**, 47 (11), 5720-5728.
26. Chen, G.; Strevett, K. A., Impact of surface thermodynamics on bacterial transport. *Environmental Microbiology* **2001**, 3 (4), 237-245.
27. Chia, T. W. R.; Vu Tuan, N.; McMeekin, T.; Fegan, N.; Dykes, G. A., Stochasticity of bacterial attachment and Its predictability by the extended Derjaguin-Landau-Verwey-Overbeek theory. *Applied and environmental microbiology* **2011**, 77 (11), 3757-3764.
28. Gordesli, F. P.; Abu-Lail, N. I., Combined Poisson and Soft-Particle DLVO Analysis of the Specific and Nonspecific Adhesion Forces Measured between *L. monocytogenes* Grown at Various Temperatures and Silicon Nitride. *Environmental Science & Technology* **2012**, 46 (18), 10089-10098.
29. Volle, C. B.; Ferguson, M. A.; Aidala, K. E.; Spain, E. M.; Nunez, M. E., Quantitative changes in the elasticity and adhesive properties of *Escherichia coli* ZK1056 prey cells during predation by *Bdellovibrio bacteriovorus* 109J. *Langmuir* **2008**, 24 (15), 8102-8110.
30. Lam, H.; Oh, D. C.; Cava, F.; Takacs, C. N.; Clardy, J.; de Pedro, M. A.; Waldor, M. K., D-amino acids govern stationary phase cell wall remodeling in bacteria. *Science* **2009**, 325 (5947), 1552-1555.

31. Prigent-Combaret, C.; Prensier, G.; Le Thi, T. T.; Vidal, O.; Lejeune, P.; Dorel, C., Developmental pathway for biofilm formation in curli-producing *Escherichia coli* strains: role of flagella, curli and colanic acid. *Environmental Microbiology* **2000**, *2* (4), 450-464.
32. Nakatani, H.; Barber, J.; Forrester, J., Surface charges on chloroplast membranes as studied by particle electrophoresis. *Biochimica et Biophysica Acta (BBA)-Bioenergetics* **1978**, *504* (1), 215-225.
33. Sheng, G.-P.; Yu, H.-Q.; Wang, C.-M., FTIR-spectral analysis of two photosynthetic H-2-producing strains and their extracellular polymeric substances. *Appl Microbiol Biotechnol* **2006**, *73* (1), 204-210.
34. DuBois, M.; Gilles, K. A.; Hamilton, J. K.; Rebers, P. A.; Smith, F., Colorimetric method for determination of sugars and related substances. *Analytical Chemistry* **1956**, *28* (3), 350-356.
35. Lowry, O. H.; Rosebrough, N. J.; Farr, A. L.; Randall, R. J., Protein measurement with the Folin phenol reagent. *The Journal of Biological Chemistry* **1951**, *193* (1), 265-75.
36. Kim, H. N.; Hong, Y.; Lee, I.; Bradford, S. A.; Walker, S. L., Surface characteristics and adhesion behavior of *Escherichia coli* O157:H7: Role of extracellular macromolecules. *Biomacromolecules* **2009**, *10* (9), 2556-2564.
37. Tran, C. T. H.; Kondyurin, A.; Chrzanowski, W.; Bilek, M. M. M.; McKenzie, D. R., Influence of pH on yeast immobilization on polystyrene surfaces modified by energetic ion bombardment. *Colloids and Surfaces B: Biointerfaces* **2013**, *104* (0), 145-152.
38. Brant, J. A.; Childress, A. E., Assessing short-range membrane-colloid interactions using surface energetics. *Journal of Membrane Science* **2002**, *203* (1-2), 257-273.
39. Liu, X. M.; Sheng, G. P.; Yu, H. Q., DLVO approach to the flocculability of a photosynthetic H-2-producing bacterium, *Rhodospseudomonas acidophila*. *Environmental Science & Technology* **2007**, *41* (13), 4620-4625.

40. Chen, G.; Walker, S. L., Role of solution chemistry and ion valence on the adhesion kinetics of groundwater and marine bacteria. *Langmuir* **2007**, *23* (13), 7162-7169.
41. Liu, X. M.; Sheng, G. P.; Luo, H. W.; Zhang, F.; Yuan, S. J.; Xu, J.; Zeng, R. J.; Wu, J. G.; Yu, H. Q., Contribution of extracellular polymeric substances (EPS) to the sludge aggregation. *Environmental Science & Technology* **2010**, *44* (11), 4355-4360.
42. Wen, Z.; Stack, A. G.; Yongsheng, C., Interaction force measurement between *E. coli* cells and nanoparticles immobilized surfaces by using AFM. *Colloids and Surfaces B: Biointerfaces* **2011**, *82* (2), 316-324.
43. Dunne, W. M., Bacterial adhesion: seen any good biofilms lately? *Clinical microbiology reviews* **2002**, *15* (2), 155-166.
44. Hermansson, M., The DLVO theory in microbial adhesion. *Colloid Surf. B-Biointerfaces* **1999**, *14* (1-4), 105-119.
45. Azeredo, J.; Visser, J.; Oliveira, R., Exopolymers in bacterial adhesion: Interpretation in terms of DLVO and XDLVO theories. *Colloids and Surfaces B:Biointerfaces* **1999**, *14* (1-4), 141-148.
46. Tsuneda, S.; Aikawa, H.; Hayashi, H.; Yuasa, A.; Hirata, A., Extracellular polymeric substances responsible for bacterial adhesion onto solid surface. *Fems Microbiology Letters* **2003**, *223* (2), 287-292.
47. Hwang, G.; Lee, C. H.; Ahn, I. S.; Mhin, B. J., Analysis of the adhesion of *Pseudomonas putida* NCIB 9816-4 to a silica gel as a model soil using extended DLVO theory. *Journal of Hazardous Materials* **2010**, *179* (1-3), 983-988.

Supplemental Information for Appendix B: D-Amino Acids Inhibit Initial Bacterial Adhesion: Thermodynamic Evidence

Methods and Materials

Bacterial size

The size of bacteria was calculated using a scanning electron microscope (SEM, HITACHI S-570, Japan). The cells were fixed with 3.0% glutaraldehyde in 0.1 M phosphate buffer (pH 7.2), dehydrated with ethanol, silver-coated by a sputter, and observed in the SEM.

Bacterial preparation of Zeta potential

Zeta potential (ζ potential) of the bacteria (ZetaSizer 3000HSA (Malvern, England)) was determined using freshly harvested cells from the LB media with different concentrations of D-tyrosine (0, 10, 25, 50 μ M) and resuspended in 10 mM KCl (the pH of the solution was unadjusted (5.6-5.8) at an optical density of 0.2-0.25 measured at 600 nm with a spectrophotometer).

Cells Adhesion and Desorption Tests

Cells adhesion tests were conducted as previously reported³⁵⁰. The attachment efficiency (A , %) was calculated as:

$$A(\%) = \frac{C_0 - C_e}{C_0} \quad (S1)$$

where C_0 , C_e are the initial and final optical density, respectively.

Next the desorption rate (R , %) (OD_{600} of reversibly adhered bacteria divided by the value of OD_{600} for all the adhered bacteria) was calculated for each test by experimentally determined C_0' (OD_{600} before desorption tests in 0.1 mM KCl solution) and C_e' (OD_{600} after desorption tests in 0.1 mM KCl solution) as follows¹:

$$R = \frac{C_e' - C_0'}{C_0 - C_e} \times 100\% \quad (S2)$$

If adhesion of the cells was completely irreversible then $R = 0\%$, whereas if $R = 100\%$ adhesion was completely reversible. All the experiments were conducted for at least three times.

Equations and parameters of surface thermodynamics

The surface tension component and parameters of bacterial surface were calculated with eq. S3:

$$(1 + \cos \theta) \gamma_L = 2((\gamma_B^{LW} \gamma_L^{LW})^{1/2} + (\gamma_B^+ \gamma_L^-)^{1/2} + (\gamma_B^- \gamma_L^+)^{1/2}) \quad (S3)$$

where θ is the contact angle between the bacteria surface and the drop liquid and L represents the liquid used in the experiment. γ^+ and γ^- are the electron-acceptor and electron-donor parameters, respectively. The γ^+ , γ^- and γ^{LW} of bacteria could be determined by eq. S3.

The parameters for eq. 4 - 6 (shown in the manuscript) are listed here:

$$\Delta G^{LW} = 2 \sqrt{\gamma_L^{LW}} - \sqrt{\gamma_G^{LW}})(\sqrt{\gamma_B^{LW}} - \sqrt{\gamma_L^{LW}}) \quad (S4)$$

$$\Delta G^{AB} = 2\sqrt{\gamma_L^+}(\sqrt{\gamma_G^-} + \sqrt{\gamma_B^-} - \sqrt{\gamma_L^-}) + 2\sqrt{\gamma_L^-}(\sqrt{\gamma_G^+} + \sqrt{\gamma_B^+} - \sqrt{\gamma_L^+}) - 2(\sqrt{\gamma_G^+ \gamma_B^-} + \sqrt{\gamma_G^- \gamma_B^+}) \quad (S5)$$

Results

Table B.2 Total interaction energy profiles as a function of separation distance between *E. coli* JM109 cells and quartz sand

Parameters	0 μM	10 μM	25 μM	50 μM
Secondary Energy Minima Depth (kT)	(-) ^a	-114.5	-54.7	-54.1
Secondary Energy Minima Distance (nm)	(-) ^a	1.7	2.9	3.1
Closest Approach Distance (nm)	(-) ^a	0.6	2.0	2.2
Hamaker Constant (J)	3.3×10^{-21}	3.2×10^{-21}	3.1×10^{-21}	2.9×10^{-21}

(-)^a indicate the values that do not exist.

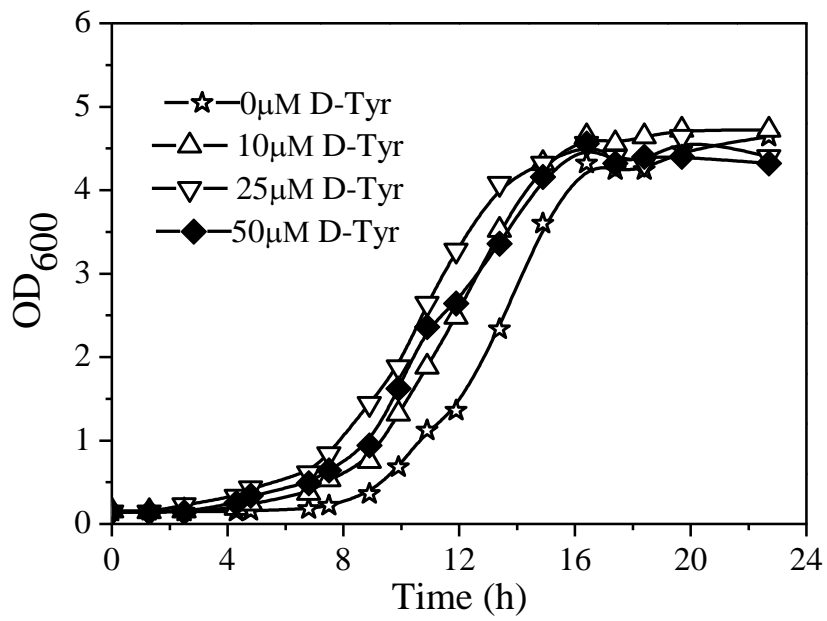


Figure B.6.

Growth curves of *E. coli* cells from LB media with different D-Tyrosine concentrations (0, 10, 25, 50 μM).

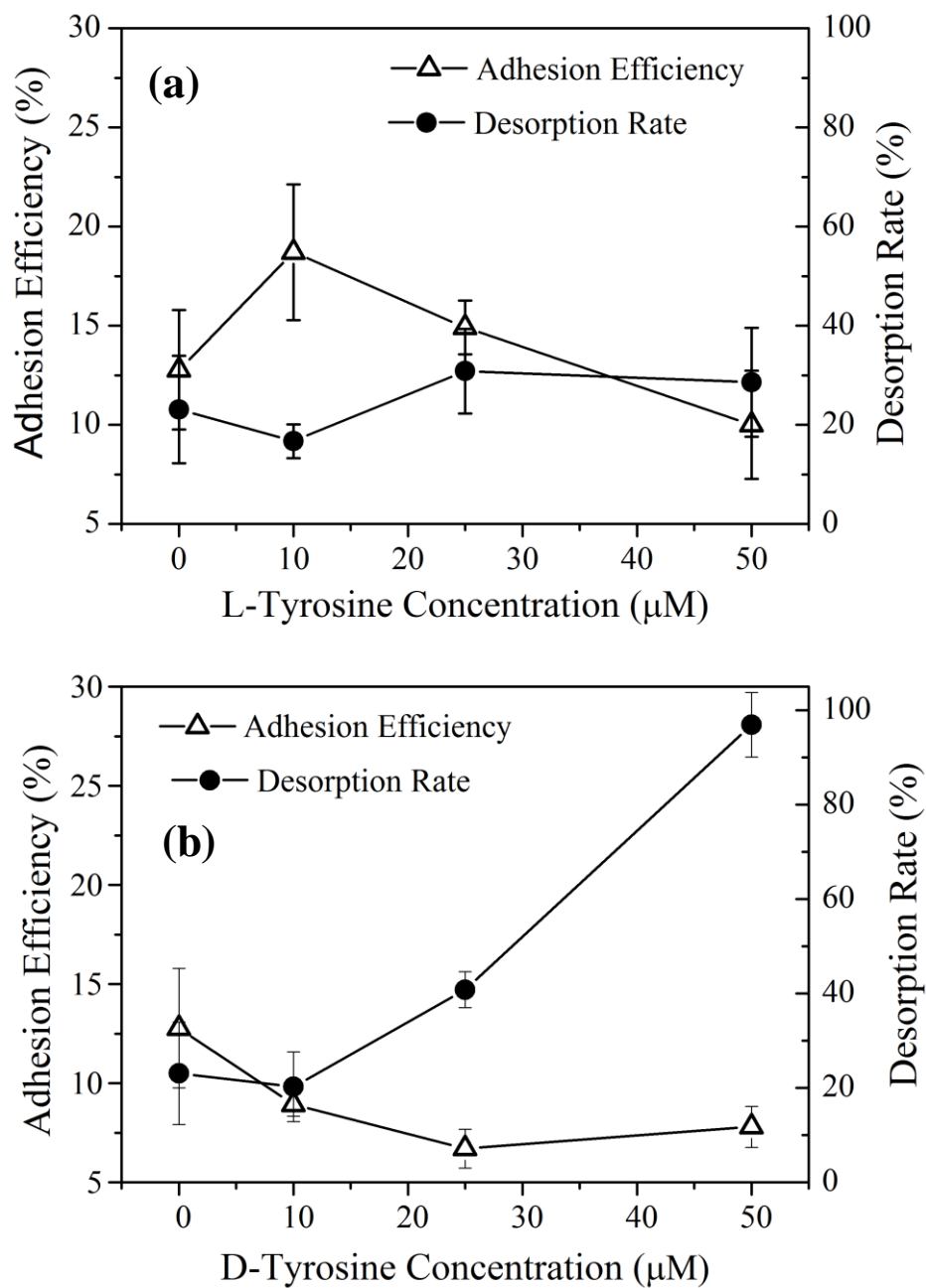


Figure B.7.

Adhesion and desorption efficiencies of *E. coli* onto and off of a quartz collector surface, determined as a function of D-Tyrosine (a), and L-Tyrosine (b). Experiments were conducted at unadjusted pH (5.6-5.8), and at room temperature (25°C); bacteria were cultivated from the bacterial minimal media. Error bars indicate one standard deviation.

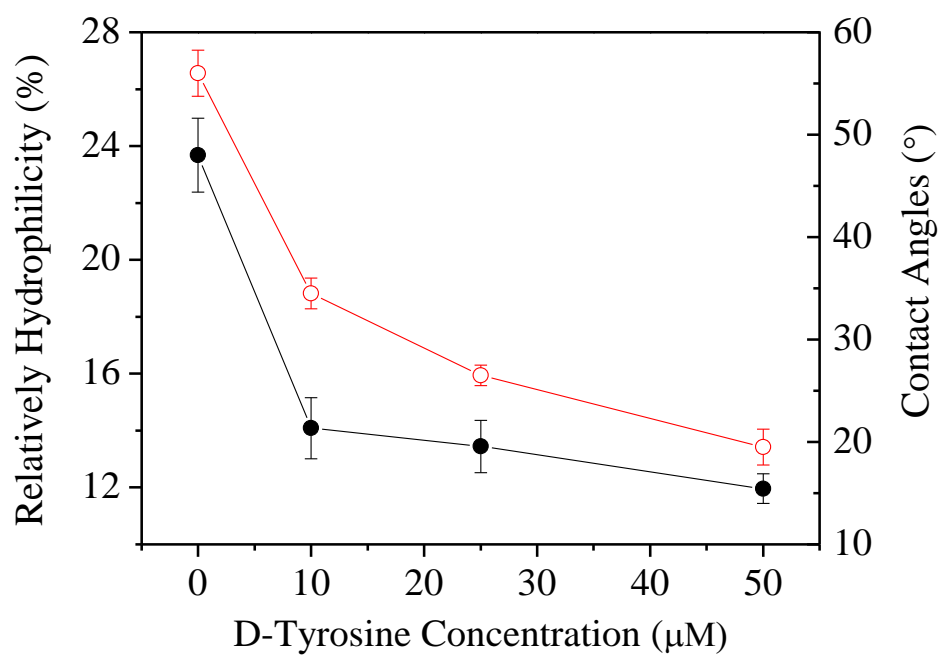


Figure B.8.

The relative hydrophobicity and contact angles of *E. coli* cells as a function of D-Tyrosine concentration.

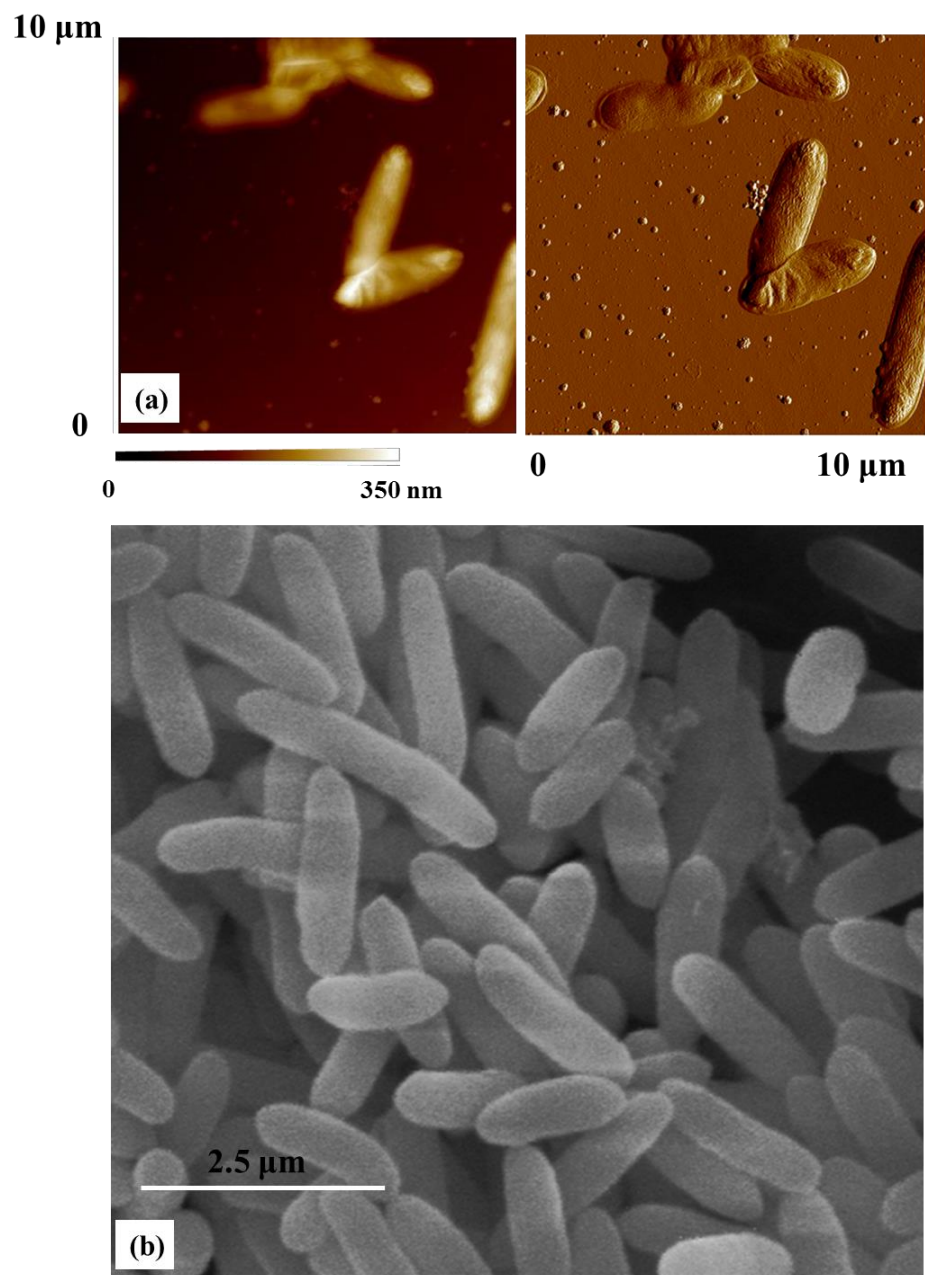


Figure B.9.

AFM topographical (left) and deflective (right) images are shown for (a) *E. coli* JM109 cells and (b) SEM images of *E. coli* JM109 cells.

References

1. Hentzer M, Teitzel GM, Balzer GJ, Heydorn A, Molin S, Givskov M, Parsek MR. 2001. Alginate overproduction affects *Pseudomonas aeruginosa* biofilm structure and function. *Journal of Bacteriology* 183: 5395-5401.